Effect of seizures on the cognitive and behavioral phenotypes of mouse models carrying the Scn1a gene mutation : implications for Dravet Syndrome

Ana Rita Salgueiro Pereira

UNIVERSITÉ CÔTE D'AZUR

Ecole Doctorale Sciences de la Vie et de la Santé
Unité de recherche : UMR 7275

Thèse de doctorat

Présentée en vue de l'obtention du
grade de docteur en Interactions Moléculaires et Cellulaires
de l'Université Côte d'Azur

par

Ana Rita Salgueiro Pereira

L'effet des crises épileptiques sur les fonctions cognitives et comportementales des modèles murins portant la mutation du gène *Scn1a*.

«Implications dans le Syndrome de Dravet »

Effect of seizures on the cognitive and behavioral phenotypes of mouse models carrying the Scn1a gene mutation.
"Implications for Dravet Syndrome"

Dirigée par *Hélène Marie, CR1, CNRS*
et codirigée par Ingrid Bethus, MCU, UNS

Soutenue le 7 avril 2017

Devant le jury composé de :

Docteur Ingrid BETHUS	Maitre de Conférences, Nice (UNS, IPMC)	**Co- Directrice de thèse**
Professeur René GARCIA	Professeur Universitaire, Nice (UNS,INT)	**Président de Jury**
Docteur Hélène MARIE	Chargé de Recherche, Valbonne (IPMC)	**Directrice de thèse**
Docteur Nadine RAVEL	Directeur de Recherche, Lyon (CRNL)	**Rapporteur**
Docteur Alfonso REPRESA	Directeur de Recherche, Marseille (INMED)	**Rapporteur**
Docteur Francesca SARGOLINI	Maitre de Conférences, HDR, Marseille (LNC)	**Examinateur**

UNIVERSITÉ CÔTE D'AZUR

Ecole Doctorale Sciences de la Vie et de la Santé
Unité de recherche : UMR 7275

Thèse de doctorat

Présentée en vue de l'obtention du
grade de docteur en Interactions Moléculaires et Cellulaires
de l'Université Côte d'Azur

par

Ana Rita Salgueiro Pereira

L'effet des crises épileptiques sur les fonctions cognitives et comportementales des modèles murins portant la mutation du gène *Scn1a*.

«Implications dans le Syndrome de Dravet »

Effect of seizures on the cognitive and behavioral phenotypes of mouse models carrying the Scn1a gene mutation.
"Implications for Dravet Syndrome"

Dirigée par *Hélène Marie, CR1, CNRS*
et codirigée par Ingrid Bethus, MCU, UNS

Soutenue le 7 avril 2017

Devant le jury composé de :

Docteur Ingrid BETHUS	Maitre de Conférences, Nice (UNS, IPMC)	**Co- Directrice de thèse**
Professeur René GARCIA	Professeur Universitaire, Nice (UNS,INT)	**Président de Jury**
Docteur Hélène MARIE	Chargé de Recherche, Valbonne (IPMC)	**Directrice de thèse**
Docteur Nadine RAVEL	Directeur de Recherche, Lyon (CRNL)	**Rapporteur**
Docteur Alfonso REPRESA	Directeur de Recherche, Marseille (INMED)	**Rapporteur**
Docteur Francesca SARGOLINI	Maitre de Conférences, HDR, Marseille (LNC)	**Examinateur**

DESIRE
Development & Epilepsy

Strategies for Innovative Research to
Improve Diagnosis, Prevention and Treatment
In Children with Difficult to Treat Epilepsy

This work is the result of a collaboration between Doctor Bethus/Doctor Marie (from Dr.Marie's team with expertise in behavior analysis and hippocampus slices electrophysiology) and Dr. Mantegazza's team (with expertise in sodium channels biology and genetic epilepsies' neuropathology and that contributed to the generation of the first Dravet Syndrome mouse model). This project was funded by the DESIRE Consortium, a 2013-2018 FP7-HEALTH funded European project focused on Development & Epilepsy - Strategies for Innovative Research to Improve Diagnosis, Prevention and Treatment In children with Difficulty to treat Epilepsy (http://epilepsydesireproject.eu/)

RÉSUMÉ

Les mutations du gène *SCN1A*, codant pour le canal sodique de type 1 potentiel-dépendant (Nav1.1), sont impliquées dans plusieurs formes d'épilepsie du nourrisson, comme le Syndrome de Dravet (SD), une épilepsie rare et pharmaco-résistante ou l'Epilepsie généralisée avec crises fébriles plus (GEFS+), une épilepsie plus légère. GEFS+ et SD sont associés à des crises épileptiques fébriles dès l'âge de 6 mois. Le SD constitue la forme la plus grave où l'on voit apparaitre des retards mentaux mais également des déficits moteurs, visuels, langagiers et mnésiques au cours de l'évolution de la maladie. L'impact des crises épileptiques au cours de la petite enfance sur ces déficits cognitifs n'est pas connu. Jusqu'à présent, le SD était considéré comme étant une encéphalopathie épileptique où les crises étaient les principales responsables du phénotype à l'âge adulte. Cependant, récemment, un rôle potentiel de la mutation dans les troubles cognitifs a été mis en évidence changeant a priori la définition de SD d'encéphalopathie épileptique à une canalopathie (Bender et al., 2013, 2016; Han et al., 2012a). Notre projet adresse la question suivante: Quel est le rôle des crises épileptiques répétées présentées par les enfants SD sur les fonctions cognitives à l'âge adulte? Pour cela nous avons utilisé un modèle murin de la maladie portant une mutation faux-sens du gène *Scn1a* (R1648H), et qui présente une pathologie très légère. Nous avons induit des crises épileptiques par hyperthermie à l'âge de 21 jours pendant 10 jours et testé les effets à long-terme sur ces animaux à l'âge adulte. Nos résultats révèlent que l'induction de crises épileptiques par hyperthermie induit une hyperactivité, des altérations dans les interactions sociales et des déficits en mémoire hippocampo-dépendante et cortex préfronto-dépendante. Ces modifications comportementales sont associées à des modifications de l'électrocorticogramme avec apparition de crises spontanées et à d'importantes modifications de l'excitabilité neuronale intrinsèque dans l'hippocampe. Même si le rôle possible du canal $Na_V1.1$ dans le dysfonctionnement neuronal et l'effet des crises répétées ne sont probablement pas mutuellement distinctes, l'induction de crises répétées à un jeune âge semble donc suffisante pour convertir un modèle léger portant la mutation du gène *Scn1a* en un modèle sévère. Ainsi nous avons mis en évidence que les crises épileptiques répétées pendant le développement ont un fort impact sur la fonction cérébrale et qu'il est donc capital de les prévenir afin de diminuer, voir de prévenir, ces déficits.

ABSTRACT

Sodium voltage-gated channel alpha subunit 1 (*SCN1A)* gene code for type-I voltage-gated sodium channels ($Na_V1.1$) in human and rodent central nervous systems. *SCN1A* mutations cause genetic epilepsies, as Generalized Epilepsy with Febrile Seizures plus (GEFS+), a mild epileptic syndrome, or Dravet Syndrome (DS), a rare, severe and drug-resistant epileptic encephalopathy (EE). DS children present multiform and intractable seizures starting in the first year of life and severe cognitive, social and neurological deficits that, according to the definition of EE, should be caused by the recurrent epileptic activity. Yet, there are currently two main hypotheses that could explain behavioral and cognitive outcome in DS children. The first hypothesis states that the Nav 1.1 mutation *per se* causes neuron network functional alterations responsible for behavioral outcome. Recent work in mice models of the disease supports this first hypothesis (Bender et al., 2013, 2016; Han et al., 2012a). The other hypothesis, supported by the classical definition of EE, is that the repeated seizures in early childhood cause the behavioral outcome. However, this second hypothesis currently lacks experimental and clinical support. Identification of the pathomechanisms responsible for disease progression is crucial for the development of efficient treatments. We therefore tested this second hypothesis. We studied the implication of repeated seizures during childhood to the later long-term modifications on cognitive/behavioral and epileptic phenotypes by submitting the *Scn1a* mouse model carrying the R1648H missense mutation and presenting mild phenotype to a protocol of repeated seizures induction by hyperthermia (10 days/one seizure per day). We observed that early life seizures can worsen the epileptic phenotype and induce cognitive/behavioral defects notably by inducing hyperactivity, sociability deficits and hippocampus- and prefrontal cortex-dependent memory deficits. These deficits are correlated with changes in the intrinsic neuronal excitability in the hippocampus without major cytoarchitecture changes or neuronal death.

Although the effect of $Na_V1.1$ dysfuntion in altering brain synchrony and the effect of repeated seizure activity in the young brain are not mutually exclusive, we thus conclude that epileptic seizures are sufficient to convert a *Scn1a* mouse model carrying a mild phenotype into a severe phenotype. This work points the necessity of treating the epileptic seizures for a better long-term outcome in DS patients.

Aos meus pais…

Porque esta conquista também é vossa.

AKNOWLEDGMENTS/REMERCIEMENTS/AGRADECIMENTOS

Il y a tellement de gens que je souhaite remercier pour ces $4_{1/2}$ merveilleuses années passées à l'IPMC. Je ne les oublierai jamais.

Premièrement à ma directrice de thèse, le docteur Hélène Marie d'avoir accepté que j'intègre son équipe lors de mon master alors qu'on ne s'est jamais vues. Merci pour toute la confiance dès le premier jour, merci de ne m'avoir jamais dit 'non' à ce que je demandais d'acheter ou faire et m'avoir poussée à aller toujours plus loin en m'encourageant à chaque avancée. Merci pour la liberté et autonomie que vous m'avez données dans la réalisation des expériences et dans les horaires de travail. Merci pour avoir permis que toutes les conditions de travail soient réunies pour la bonne réalisation de mon projet. Merci d'avoir été un exemple pour moi au niveau de ton organisation et efficacité. Je te l'ai déjà dit mais je n'ai jamais vu quelqu'un d'aussi efficace et j'espère le retenir de toi pour mon futur. Merci de m'avoir appris à faire de l'électrophysiologie sur tranches d'hippocampe, et pour toute ta patience. Merci pout toute ta précieuse aide dans les corrections des différents rapports au cours de ma thèse. Merci de t'être autant impliquée dans ce projet, pour moi et que je puisse avoir de bons résultats. Merci car tous tes enseignements ont contribué à me faire grandir scientifiquement. Merci.

Et premièrement à nouveau à ma co-directrice de thèse, le docteur Ingrid Bethus, merci pour avoir pleuré autant que moi le jour de mon départ en master. Merci d'avoir tout fait pour que je reste en thèse, car aujourd'hui je suis sûre que j'ai fait le bon choix. Merci de m'avoir transmis cette passion pour le comportement animal et la mémoire humaine. Tu sais qu'aujourd'hui je les aime autant que tu les aimes. Merci de m'avoir appris toutes les tâches comportementales, de m'avoir aidé à trouver et résoudre les problèmes et de m'avoir remplacée dans les expériences quand j'en ai eu besoin. Merci pour ton dévouement inconditionnel à notre projet et d'avoir célébrer chaque victoire avec moi. Et merci d'avoir été plus qu'une directrice de thèse une amie pour toute les fois où on s'est amusées ensemble au labo ou en congrès. Merci pour toute ta bienveillance et pour toutes les connaissances que tu m'as transmises. Merci, car avec Hélène vous avez contribué à me former scientifiquement et humainement. Merci.

Ma super équipe:

Paula, nunca te vou esquecer. Obrigada por tantos conselhos, sugestões e ensinamentos. Admiro a forma como descobres e exploras os resultados científicos que me fizeram compreende-los melhor. Lembrarei sempre o "é giro" que tanto te caracteriza. Obrigada por dedicares o teu tempo para fazeres as experiências para o meu projeto e por me transmitires um bocadinho da tua paixao pela electrofisiologia. Obrigado por me ensinares tao bem com os teus desenhos e por me transmitires a tua forma de fazer todas as coisas bem-feitas "bonitinhas". Obrigada minha querida, foste o meu maior e mais seguro porto de abrigo no laboratório. Obrigada porque muito mais do que cientificamente me soubeste proteger sempre emocionalmente. Foste a minha irmã mais velha e nunca te vou esquecer. Obrigada pela tua genuinidade e sinceridade. Obrigada porque foi tao bom poder falar em português todos os dias no laboratório.

Scherazad, my everyday friend. Thank you for being there always for me. I will never forget the long nights in the lab together listening to beautiful songs. Thank you for all the help with mice, the experiments, the documents, formations, deadlines and everything. Thank you for all the sharing: work, personal life and friendship. We grew together during these 3 years and I am very proud of us. But I am even more proud of you, and to have assisted to your change in being much stronger while keeping your sincerity and honesty. These years were so nice and I would love spending more years with you all in the lab.

Sebastian, thank you for all the help with the different experiments (electrophysiology, graph pad, cameras in Animex, while manipulating the very dangerous compound, survival curves ☺…etc). Thank you for so many times helping us while leaving your work for later. Thanks for all the advice, comments; help, critics and for always being honest…and for all the good times we had all together. You are such a nice person and your sense of humor has made our days better in the lab. You are the sun of the lab. I will miss us laughing all the time. You know that you changed us, making me and Scherazad say bad words and your main failure during these years was to make us more social, but still you tried hard (and if we didn't… want we can go…). It was ok, we had a lot of fun because our team was full of stories every day.

Xavier merci pour toute ton aide précieuse au cours de ces années. Merci pour toute l'aide avec les commandes et les manips que tu m'as fournie. Merci pour ton sens de l'humour et toutes tes histoires. Merci pour ta gentillesse au cours de ces 3 années.

Jacques même si on n'est pas amis et que tu nous le répètes sans cesse ou que j'ai perdu la gentillesse au cours de ma thèse ☺ je te remercie beaucoup pour tous les conseils, toutes les discussions et ta bienveillance. Je t'admire beaucoup scientifiquement. Même si tout ce qui bouge doit disparaitre de devant toi quand tu fais des manips, tu es quelqu'un de très gentil. Merci beaucoup et bonne chance bientôt co-chef d'équipe.

Marie-Lise, Préci, et Loïc merci pour les bons moments passés dans le bureau. Merci pour votre bonne humeur et pour votre sincérité. Merci pour tous les sourires et encouragements. Merci à chacun de vous d'avoir partagé un petit peu de soi et m'avoir fait sentir à la maison au long de ces années.

Martine et Marion merci d'avoir fait un petit peu partie de mon projet. Merci pour toute votre aide et dévouement dans la réalisation des expériences. Vous êtes de super étudiantes.

Ma deuxième équipe:

Massimo, merci pour tout l'échange scientifique. Je t'admire beaucoup scientifiquement. Merci de me faire confiance et de me transmettre ton savoir. Merci de toujours savoir répondre à mes questions avec autant de patience et précision. Tu es quelqu'un de très important dans le domaine et j'espère que tu feras avancer la recherche sur le Syndrome de Dravet et qu'un jour tu puisses trouver le remède pour les patients☺.

Marraine Sandrine, merci d'avoir accepté d'intégrer le rôle de ma marraine de thèse et de l'avoir aussi bien exécuter. Merci de m'avoir accompagnée et d'être toujours aussi présente. Merci de surtout au début m'avoir aidée à résoudre les problèmes avec le protocole d'induction de crises. Merci pour ta douceur, pour ta gentillesse et bienveillance. Merci avoir été là pour me protéger de tous mes encadrants ☺ mais au final tout s'est bien passé.

Marion et Jenny, merci sincèrement les filles pour toutes les souris, génotypage, primers…etc. Désolé de vous avoir autant embêtées, votre aide a été précieuse à cours de ma thèse.

Fabrice, tu es exceptionnellement organisé et bricoleur. Tout ce que tu fais a un rendu parfait**.** Je t'admire beaucoup. Merci pour toute ton aide et pour être toujours disponible.

Alexandre, merci de m'avoir aidée avec les expériences de patch-clamp. Merci pour ton sens de l'humour et ta gentillesse.

Pour le support:

Lucien, merci de t'occuper aussi bien de toutes mes souris à Animex sans jamais te plaindre. Merci pour les petits (grands) mots d'encouragements quand ce n'était pas toujours facile pour moi d'être

enfermée à Animex sans voir la lumière du jour. Après avoir badgé plus de 400 fois en 6 mois, on s'est habitués à se voir souvent. Merci!

Thomas Lorivel, merci infiniment pour toutes les discussions scientifiques et pour toutes les fois où tu as consacré ton temps à m'aider avec les infinis problèmes à Animex (caméra, lampes, ordinateur…etc). Merci pour tous les partages lors des repas, cafés etc. Merci.

Doctor Battaglia and Doctor Dravet for this amazing experience in Rome. Thank you very much for being so patient in explaining me all the clinical aspects of Dravet Syndrome and making me feel part of the team. Thank you for giving me the opportunity to see the Dravet patients. Thank you very much.

Ao maior suporte emocional:

Meu amor, Talvez já te tenha dito, faço questão de voltar a dizer o quanto foste importante nestes 4 anos e desde sempre. O facto de te seguir e vir para França acabou por ser benéfico em todos os sentidos. Obrigada por me incentivares a fazer o doutoramento mesmo quando sabíamos que ia ser difícil e desgastante. Obrigada por nunca te queixares e sempre me apoiares quanto tinha que fazer horários prolongados e trabalhar muitos fins-de-semana seguidos. Obrigada porque a nossa casa foi o meu porto de abrigo, aquele em que me sentia segura e protegida. O teu amor e carinho foram essenciais para mim. *"O amor move montanhas"*. O meu sucesso hoje é tambémo teu sucesso e espero que possamos partilha-los mutuamente por muito tempo.

Meus Pais queridos, obrigada por me ensinarem a pescar, e não me darem o peixe. Obrigada pelo dever do trabalho, responsibilidade e independência que sempre me incutiram desde pequena. Esse dever pertiu-me duante esta caminhada enfrentar as mais variadas adversidades com garra e sem nunca baixar os braços. E hoje essa caminhada moldada por bases solidas permitiu-me alcançar os meus objectivos e chegar mais longe. O meu sucesso dedico-o a vos pois é graças a vos. Obrigada por acreditarem em mim sem nunca questionarem ou criticarem as minhas escolhas. Obrigada pelo conforto, amor e segurança que me transmitem que se tornaram essenciais em moldar a minha personalidade. *"O amor move montanhas"*.

À minha família, por todo o apoio especialmente tia e sana vos sabeis o amor que nos une. Mais forte do que simples tia ou prima amo-vos como se fosseis mae e irmã. Obrigada por todo o suporte, por todo o amor. Mesmo quando passamos juntas por momentos difíceis, mais uma vez *"o amor move montanhas"*. Sabes que fiz tudo o que pude por ti mesmo se às vezes foi difícil com o trabalho. Minha avo Idalina querida, infelizmente hoje não estas aqui para ver a minha caminhada, no entanto sei que estarás para sempre a olhar por mim.

Dora e Abilio, por seres para mim como pais e me acolheres como filha. Obrigada por me amares tanto e me apoiares incondicionalmente nos mais diversos problemas. Obrigada por estares sempre presentes para nos ajudar e nos acompanhar. Obrigada por que foste essenciais na minha caminhada e o meu sucesso é também o vosso *"O amor move montanhas"*.

Minhas queridas amigas Eliana e Soraia, obrigada pelas longas noitadas passadas juntas. Por toda a vossa amizade, estarei sempre aqui para tudo o que precisareis. Vos sabeis o quanto sois especiais para mim. " a amizade certamente também move montanhas"

February 2017, Policlinico A. Gemmeli, Rome.

Doctor Charlotte Dravet and me

I am really glad to have been given the opportunity by Doctor Domenica Battaglia who welcomed me in the Pediatric Phychiatric service to assist to the patients' consultations with Doctor Charlotte Dravet. The experimental research is very pleasant but it only becomes gratefull when you see the reason of all your efforts. I will never forget those kids and the mix of suffering and hope in their parents' eyes.

TABLE OF CONTENTS

LIST OF TABLES

LIST OF FIGURES

LIST OF ABBREVIATIONS

AIS – Axon Initial Segment

Bp – Base pairs

CFC – Contextual fear conditioning

CNS – Central Nervous System

C57Bl/6-B6

DNA – Deoxyribonucleic acid

D – Day

DG – Dentate gyrus

DS – Dravet Syndrome

ECoG – Electrocorticogram

EEG - Electroencephalogram

fEPSP – field Excitatory Post Synaptic Potentials

FS – Febrile seizures episodes and Febrile Seizures disease

GEFS+ – Generalized epilepsy with febrile seizures plus

GTC- Generalized tonic-clonic

H – height

ILAE – International League Against Epilepsy

L – Length

LTP – Long-term potentiation

MWM – Morris Water Maze

Na_v 1.1 – Type-I voltage gated sodium channel

PCR– Polymerase chain reaction

PFC–Prefrontal córtex

Post-natal Day-P

PV– Parvalbumin

RH–R1648H

sEPSC – spontaneous Excitatory Post Synaptic Currents

sIPSC – spontaneous Inhibitory Post Synaptic Currents

***SCN1A* –** sodium voltage-gated channel alpha subunit 1

SCN1B – sodium voltage-gated channel beta subunit

SIH – Seizures induced by hyperthermia

SST – Somatostatin

SE–*Status Epilepticus*

W – Width

WT– Wild-type

129/SvJ-129

LIST OF DEFINITIONS

*Some concepts are defined in this list and marked in the text with a *.*

ELECTROENCEPHALOGRAPHY AND SEIZURES:

ICTAL ACTIVITY: Electroencephalogram recording during a seizure.

INTERICTAL ACTIVITY: EEG activity between 2 seizure events.

DELTA WAVES: Usually slow waves, but the highest in amplitude. Frequency <4Hz

THETA WAVES: Seen normally in young children, or high relaxation states in humans (Frequency 4-7 Hz). The theta frequency is the most prominent oscillation in the rat hippocampus when engaged in active motor behavior such as walking or exploratory sniffing, and also during REM (rapid eye movement) sleep.

GAMMA WAVES: Gamma rhythms are thought to represent binding of different populations of neurons together into a network for the purpose of carrying out a certain cognitive or motor function. Frequency 30–100Hz.

STATUS EPILEPTICUS: Seizures that last longer than 30 minutes.

GENERALIZED TONIC CLONIC SEIZURES: Seizures involving both hemispheres of the brain and presenting a clonic phase followed by a tonic phase. Also called "grand mal seizures".

GENETICS:

MOSAICISM: Two or more cell types that carry different genotypes.Mutatios that are not present in all cells of the same individual.

HAPLOINSUFFICIENCY: Caused by a loss-of-function mutation, in which only one functional copy of the wild type allele is not sufficient enough to express the wild type phenotype.

SPLICE MUTATIONS: Mutations that inserts, deletes or changes nucleotides at the boundary of an exon and an intron (splice site). This change can disrupt RNA splicing resulting in the loss of exons or the inclusion of introns and an altered protein-coding sequence.

NONSENSE/ TRUNCATION MUTATION: Mutations that prematurely stops the translation of messenger RNA resulting in a polypeptide chain that ends prematurely and a protein product that is truncated and incomplete and usually nonfunctional.

MISSENSE MUTATION: Point mutation where a single nucleotide is changed to cause substitution of a different amino acid**.**

HETEROZYGOSITY: Two different alleles for the same gene (in the case of our study one mutant allele - and one WT allele +).

DOMINANT INHERITANCE: In the heterozygotic cells where both alleles are present but only one allele is dominant, meaning responsible for the phenotype and transmitted to the progeny.

REVISION OF CONCEPTS

1.Role of prefrontal cortex and medial-temporal lobe in cognitive functions

1.THE PREFRONTAL CORTEX IN COGNITIVE FUNCTIONS

The prefrontal cortex (PFC) is involved in higher-level cognitive processes including planning, motor control, language, reasoning, decision–making grouped under the more general term of "executive functions", personality and social interaction (Kesner and Churchwell, 2011). Executive functions include the organization of the input from diverse sensory modalities, the maintenance of attention, the monitoring of information in working memory, and the coordination of goal-directed behaviors. From Baddeley's definition, working memory is characterized by a limited capacity system for maintaining and manipulating information and it underpins the capacity for complex and flexible cognition (Baddeley, 1996). Working memory requires attention processes for temporary maintenance of domain-specific information over a brief period of time in a form that is fragile and vulnerable to distractions (Fuster, 2004; Miller et al., 2014). Given all the cognitive functions for which the PFC participates, it is not surprising that the PFC also contributes to higher-order cognitive functions such as social cognition. The term social cognition can encompass any cognitive process engaged to understand and interpret the self, others, and the self-in-relation-to-others within the social environment. Human social interaction requires knowledge and recognition of mental states, beliefs, desires, intentions in peers that guide our own behavior (Fiske, 1993; Macrae and Bodenhausen, 2000).

2-THE MEDIAL-TEMPORAL LOBE IN COGNITIVE FUNCTION

The major breakthrough in neurology that helped the neurobiologists in defining the role of medial-temporal function came in 1957 from a medical report written by *Scoville and Milner, 1957* on the most famous neurological patient ever, Henry Molaison known by his initials H.M. This patient carried severe epileptic disease for several years. In an effort to alleviate his disease, the medial temporal lobe area (including hippocampi and parahippocampal girus) was removed, and the surgery could reduce considerably the seizure frequency. However, following the surgery H.M. patient became severely amnesic in

selective memory types. This patient had severe anterograde amnesia and a partial retrograde amnesia focus on episodic memory. The discovery of a "pure" memory deficit following a selective brain damage also addressed how memory is compartmentalized in the brain. Memory is the faculty of the brain by which information is encoded, stored, and retrieved. The time between memory acquisition and retrieval will dissociate between short-term and long-term memories: short time for working memory- memory-described in previous paragraph- (usually few seconds or minutes) and long-time for long-term memory (from hours to years) (Baddeley and Warrington, 1970). *Squire and Knowlton, 1995* defined a taxonomy of human long term memory that can be classified in explicit/declarative (involving episodic and semantic memory) and implicit/non-declarative memory (involving implicit learning as procedure, priming, conditioning) (Morris et al., 1986; O'Keefe et al., 1998) **(FIGURE 1)**.

Episodic memory characterizes episodes of personal life and its integration in a spatial and temporal context (Tulving, 2002). Semantic memories are those that we acquire by learning, like factual information and general knowledge. To distinguish between these two memories, it can be said that episodic memory requires recollection of a prior experience and semantic memory does not.

Non-declarative memory includes information that is acquired during skill learning, habit formation, emotional learning, and other knowledge that is expressed through performance rather than recollection. Non-declarative memory is dissociated into procedural memory (required for the execution of integrated procedures involved in both cognitive and motor skills : associated to striatum and cerebellum functions) (Knowlton et al., 1996; Nagao and Kitazawa, 2008), priming memory (memory dependent on the neocortex through which an initial exposure is expressed unconsciously by improved performance at a later time) and conditioning memory (associated to emotional learning that implicates the amygdala) (Adolphs et al., 2005).

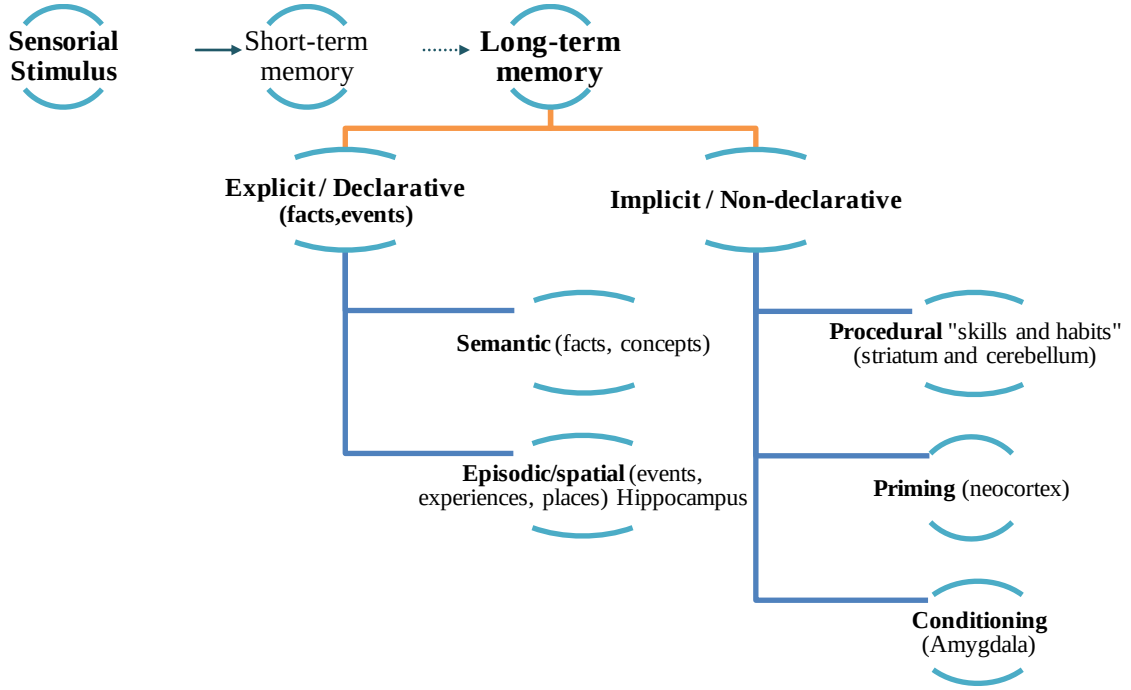

FIGURE 1. TAXONOMY OF HUMAN MEMORY (ADAPTED FROM SQUIRE AND KNOWLTON, 1995 FOR LONG TERM MEMORY AND ATKINSON AND SHIFFRIN, 1968 FOR SHORT TERM MEMORY)
When a sensorial stimuli is received it can be converted in a short-term memory within a reduced period of time (<60 minutes). It can then be transformed into long-term memory or not and last for hours, days or years. Two type of long term memory have been proposed: explicit and implicit memory.

3. HIPPOCAMPUS: ROLE, ORGANIZATION AND SYNAPTIC PLASTICITY

The hippocampal formation (including the entorhinal cortex and hippocampal system) has been implicated as the major structure in the encoding, storage and retrieval of declarative memory (Eichenbaum, 2001; Morris et al., 1986; Squire, 1992). Also, the hippocampus is highly implicated in spatial memory, which stores information regarding the location of physical objects in space, in other words, the spatial properties of the environment (Morris et al., 1986; O'Keefe et al., 1998).

The hippocampus is a complex structure of the brain located in the medial temporal lobe. It belongs to the limbic system, closely associated with the cerebral cortex. Humans and other mammals have two hippocampi, one in each side of the brain. The hippocampus contains two parts: the Ammons horn, which contains CA1, CA2, CA3 and CA4, and the dentate gyrus (DG) **(FIGURE 2)**.

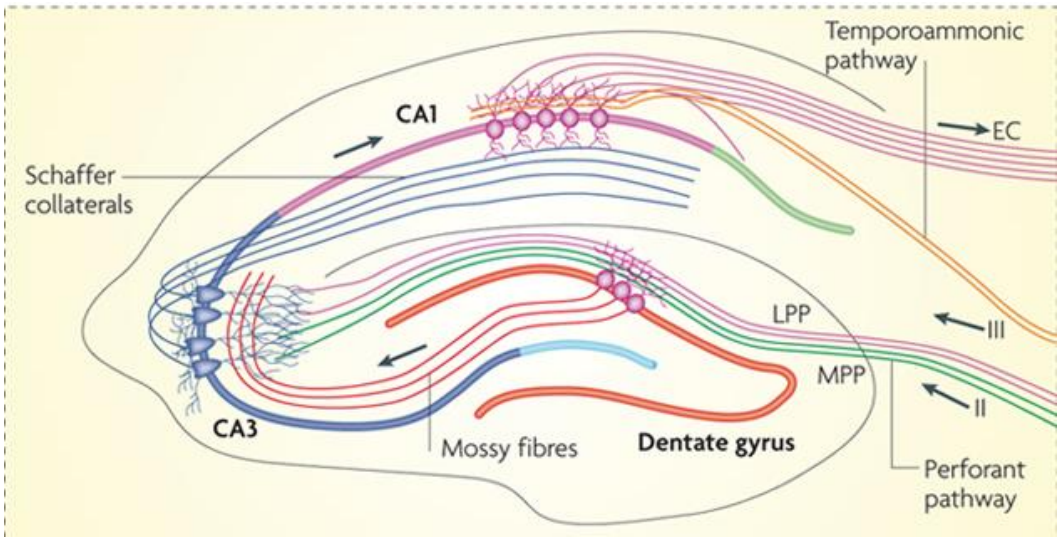

FIGURE 2. HIPPOCAMPUS STRUCTURAL ORGANIZATION IN MOUSE BRAIN.
The flow of information from the EC is largely unidirectional, with signals propagation trough a series of tightly packed cell layers, first to the dentate gyrus, then to the CA3 layer, then to the CA1 layer, then to the subinculum and then out of the hippocampus to the EC. Image from (Deng et al., 2010).

Synaptic plasticity plays an important role in neurochemical foundations of learning and memory. Hebb (1949) first said that memory formation is due to changes in the synaptic efficiency and that storage is made by cellular junctions that associate among them. In other words, synaptic plasticity is the ability of synapses between two neurons to change in strength, in response to the transmission of synaptic inputs (two active neurons at the same time strengthen their connection to ensure that future connections will be easier) (Purves, 2005). Long-term potentiation (LTP) reflects the strengthening of synapses and is believed to represent a major cellular mechanism at the basis of long term memory formation. LTP was first described using artificial stimulation by (Bliss and Lomo, 1973). *Whitlock et al., 2006* first observed a naturally-induced long-term potentiation in the hippocampus during a memory task in rats. LTP is now well admitted to represent a cellular correlate of long term memory.

The association between the hippocampus and epilepsy has been often described, notably in seizure generation, abnormal electrophysiological properties, abnormal oscillatory rhythms and cognitive abnormalities. The effect of frequent early life seizures and hippocampal-dependent cognition has been well studied in rodent models and support the view that epileptic discharges disrupt normal development of hippocampal networks (*reviewed in* Holmes, 2016). The hippocampus seems to be frequently involved in seizures, even if they are not generated there. Also, the relatively simple histological construction and lamellar organization of the hippocampus makes it a structure of choice for experimental and clinical studies of epilepsy.

4. Excitatory and inhibitory Balance in epilepsy: Role of interneurons

The brain balance is maintained through excitatory and inhibitory mechanisms handled by the main excitatory neurotransmitter glutamate counterbalanced by the main inhibitory neurotransmitter- γ-aminobutyric acid (GABA). The recurrent seizure activity is an electrographic hallmark of epilepsy, and consists in an excessive synchronous discharge of cerebral neurons, generated in one or more neuron populations. The electrical activity in the epileptic network is in general associated with a deficit in excitatory/inhibitory imbalance, which promotes neuronal hyperexcitability and hyper-synchronization, through an increase in excitatory neurotransmission or a decrease in inhibitory neurotransmission or both. Neurons are excitable cells that receive and transmit information trough electrical and chemical signals. Those electrical signals, received at the dendrites, generate action potentials at the axon initial segment (AIS) that are transmitted through the axon to the terminals. There, the synaptic boutons communicate with the other cells forming synapses. The structural organization of a neuron is represented in **Figure 3**. The work concerning the epileptic syndromes we will study here, focused mostly on two types of neurons: the excitatory neuron, releasing glutamate (eg hippocampal excitatory neurons described above) and the inhibitory interneuron releasing the neurotransmitter GABA.

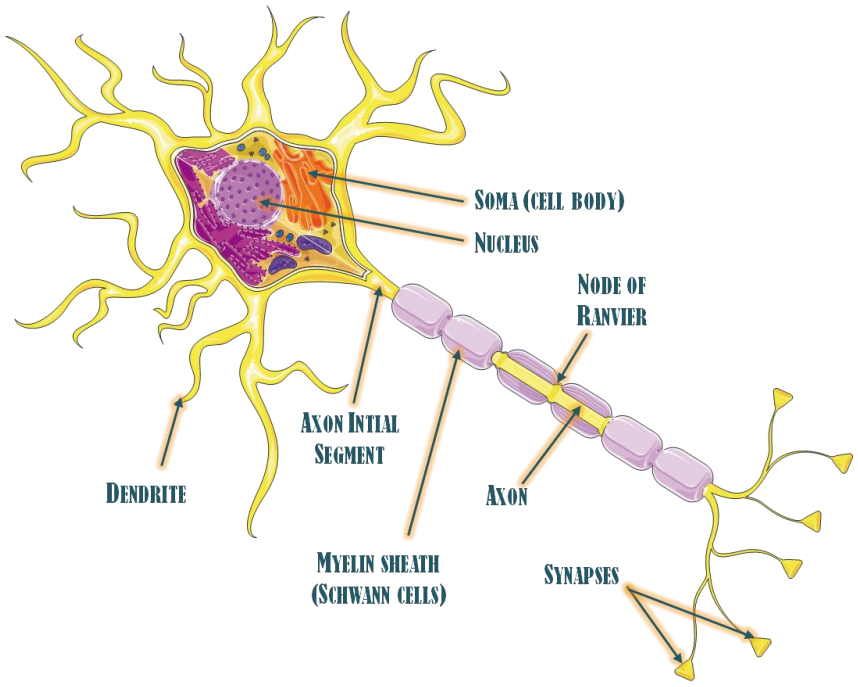

Figure 3. Structure of the neuron.

We will briefly describe the interneurons, a neuron type that is crucial for *Scn1a* mutant mouse models neurophysiopathology. Based on their network connectivity and intrinsic properties, the interneurons generate and control the rhythmic output of large populations of principal cells and other interneurons. In the central nervous system (CNS) they are primarily inhibitory, and use GABA or glycine as main neurotransmitters. They represent approximately 20-25% of cortical neurons and are highly diverse in morphology, connectivity, neurochemical and physiological properties (Kepecs and Fishell, 2014; Petilla Interneuron Nomenclature Group et al., 2008). **FIGURE 4** represents the described subtypes of interneurons in the brain.

The morphological appearance of interneurons is a source of important information regarding their specific role in a neuronal circuit. Using immunohistochemical tools, they can be marked by tagging the enzymes that synthesize GABA: GAD-65 and GAD-67. Various populations of interneurons were found to contain different peptides (e.i. somatostatin, cholecystokinin (CCK), calretinin, neuropeptide Y, parvalbumin, etc) **(FIGURE 4)** and these peptides gave the name to the interneuron subtypes. This has resulted in a neurochemical classification that is based on the cell-specific presence of these markers. Moreover, using electrophysiological tools, the interneurons have also been classified according to their firing properties and, for example, the terminology fast spiking PV+ basket cells combines electrophysiological, biochemical and morphological characteristics.

Several GABAergic cell types contribute to feedback circuits in the hippocampus. These include parvalbumin-positive (fast-spiking PV+) a major GABAergic type in contributing to the pathology in *Scn1a* mutant mouse models.

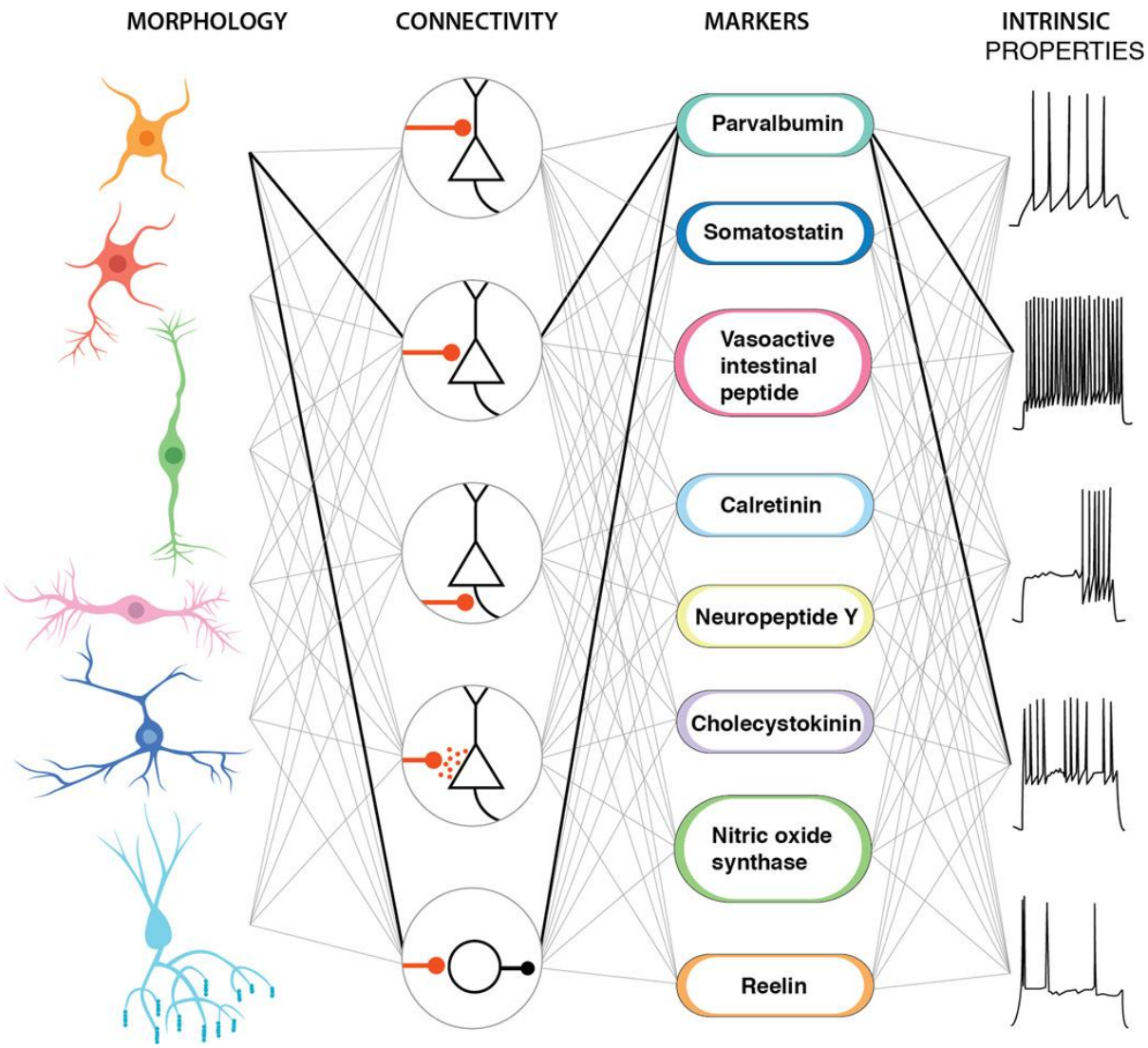

FIGURE 4. SCHEMATIC OF INTERNEURON DIVERSITY ACROSS THE BRAIN. FROM (KEPECS AND FISHELL, 2014).

They are mainly characterized according to morphology, type of connection, neuropeptide expressed and electrophysiological properties.

A 17th-century epileptic patient being restrained by another man is taken to see a priest to be blessed (in Madness (Porter, 2003).

Introduction

I- INTRODUCTION

Chapter 1- EPILEPSY AND GENETIC EPILEPSIES

1. HISTORICAL, DEFINITION AND EPIDEMIOLOGY.

Epilepsy is the most common neurological disorder affecting 65 million persons worldwide and 0.5–1.0% of children younger than 16 years old (Shinnar and Pellock, 2002; Thurman et al., 2011). The word epilepsy was derived from greek words that mean "seizure" or "attack" (Reynolds, 2002). The first known report of epilepsy was in a Babylonian medical report written 3000 years ago. The Babylonians described the seizures as invasions of the body by a particular evil spirit and characterized them similarly in what can be correlated with the seizures we know nowadays (Wilson and Reynolds, 1990). This supernatural view of the seizures has persisted until recently. In the 5th century, Hippocrates challenged this view by stating: *"I do not believe that the Sacred Disease is any more divine than any other disease but, on the contrary, has specific characteristics and a definite cause. Nevertheless because it is completely different from other diseases it has been regarded as a divine visitation by those who, being only human, view it with ignorance and astonishment... The brain is the seat of this disease, as it is of other very violent diseases"*. Interestingly, he already had some notions that the disease could be on the rise if not treated and become chronic and intractable, *"Moreover it can be cured no less than other diseases so long as it has not become inveterate and too powerful for the drugs which are given. When the malady becomes chronic, it becomes incurable* (Zanchin, 1992)*."* However Hippocrates's view of the supernatural disease was not taken into account until the 17th and 18th centuries. Thomas Wills, in 1961 first characterized epilepsy as a brain disorder (Willis and Pordage, 1681) and during the next two centuries very important debates took place to give rise to the first definitions of epilepsy in the 19th century. The works of Todd, influenced by Faraday and Jackson were very important in defining the electrical basis of seizures and in 1952, Hodgkin & Huxley (Hodgkin and Huxley, 1952) obtained the Nobel Prize for discoveries of the ionic basis of Todd's nervous polarity/force. Thanks to the development of genetics, molecular biology, neurophysiology, functional imaging

and numerous neurochemical techniques for exploring the concepts of excitation, inhibition, modulation, neurotransmission and synchronization, the 20th century conferred the most important advance in epilepsy and seizures research.

2. Classification of Seizures, Epilepsies and comorbidities

2.1 *Seizures Definition and Classification*

Epilepsy is characterized by the presence of epileptic seizures. They can be acutely provoked by head trauma or stroke (for example) or unprovoked as the result of a pathological condition. In 2014, the International League Against Epilepsy (ILAE) defined epilepsy as a "*disease of the brain enduring predisposition to generate epileptic seizures, and by the neurobiological, cognitive, psychological, and social consequences of this condition.*" An epileptic seizure is a *"transient occurrence of signs and/or symptoms due to abnormal excessive or synchronous neuronal activity in the brain"* (Fisher et al., 2014). The definition of epilepsy requires the occurrence of any of the following conditions: at least two unprovoked (or reflex) seizures occurring 24h apart, one unprovoked (or reflex) seizure and a probability of further seizures similar to the general recurrence risk (at least 60%) after two unprovoked seizures, occurring over the next 10 years, or a diagnosis of an epilepsy syndrome (Fisher et al., 2014).

Epileptic seizures arise from abnormal synchronization of neurons in the brain that disrupts normal patterns of neuronal signaling and results in electric discharges in the electroencephalogram (EEG). The brain hyperexcitability in epilepsy describes a general increase in response to a particular stimulus or enhanced tendency to generate repetitive synchronous neuronal discharges manifesting as a burst of population spikes. It is a very harmful disease leading to discrimination, misunderstanding, social stigma and the fear of living with a chronic unpredictable disease that can lead to loss of autonomy for daily activities.

Seizures are divided in focal or generalized seizures according to the brain structure involved in the seizure origin.

Focal (synonym=partial) seizures are those in which, in general, the first clinical and EEG alterations indicate initial activation of a system of neurons limited to a part of one cerebral hemisphere. The networks involved may be very discrete and highly localized or more broadly distributed within the hemisphere. Focal seizures are

classified primarily on the basis of whether or not consciousness is impaired during the attack (simple and complex respectively) and whether or not progression to generalized convulsions occurs. They are divided into motor and non motor focal seizures **(FIGURE 5)**.

Generalized (synonym = bilateral) seizure are those in which the first clinical changes indicate initial involvement of both hemispheres. Consciousness may be impaired and this impairment may be the initial manifestation. The ictal EEG patterns are initially bilateral and presumably reflect neuronal discharge, which is widespread in both hemispheres. Generalized seizures may be motor or absence seizures and vary considerably. Motor manifestations of generalized seizures are bilateral. Motor generalized seizures can be tonic-clonic (GTC) or (previously called '*grand mal' seizures*), and are characterized by bilateral symmetric tonic contraction and then bilateral clonic contraction of somatic muscles, usually associated with autonomic phenomena and loss of awareness. Alternatively generalized seizures can be purely tonic, purely atonic (sudden loss of muscle tone), purely myoclonic (sudden, brief (<100 ms), involuntary, single, or multiple contractions of muscles or muscle groups of variable topography (axial, proximal limb, distal)), myoclonic-atonic (clonic seizures that results in falls), pure myoclonic, clonic-tonic-clonic (one or a few jerks of limbs bilaterally, followed by a tonic-clonic seizure) and epileptic spasms. Absence generalized seizures (previously called '*petit mal' seizures*) are seizures characterized by a sudden onset, interruption of ongoing activities (a blank stare), and can be typical (brief loss of consciousness, normal EEG pattern), atypical (last longer than typical and can present irregular EEG pattern), myoclonic or characterized by eye-lid myoclonia (jerking of the eyelids at frequencies at least 3 per second, commonly with upward eye deviation) **(FIGURE 5)**. Generalized seizures may be primarily (if they are generalized from the onset) or secondarily generalized (if they are focal at the onset but progress to generalized) (Berg, 2016; Berg et al., 2010; Blume et al., 2001; Fisher et al., 2014).

Unclassified epileptic seizures or those with unknown onset are seizure types which cannot be classified because of inadequate or incomplete data **(FIGURE 5)**.

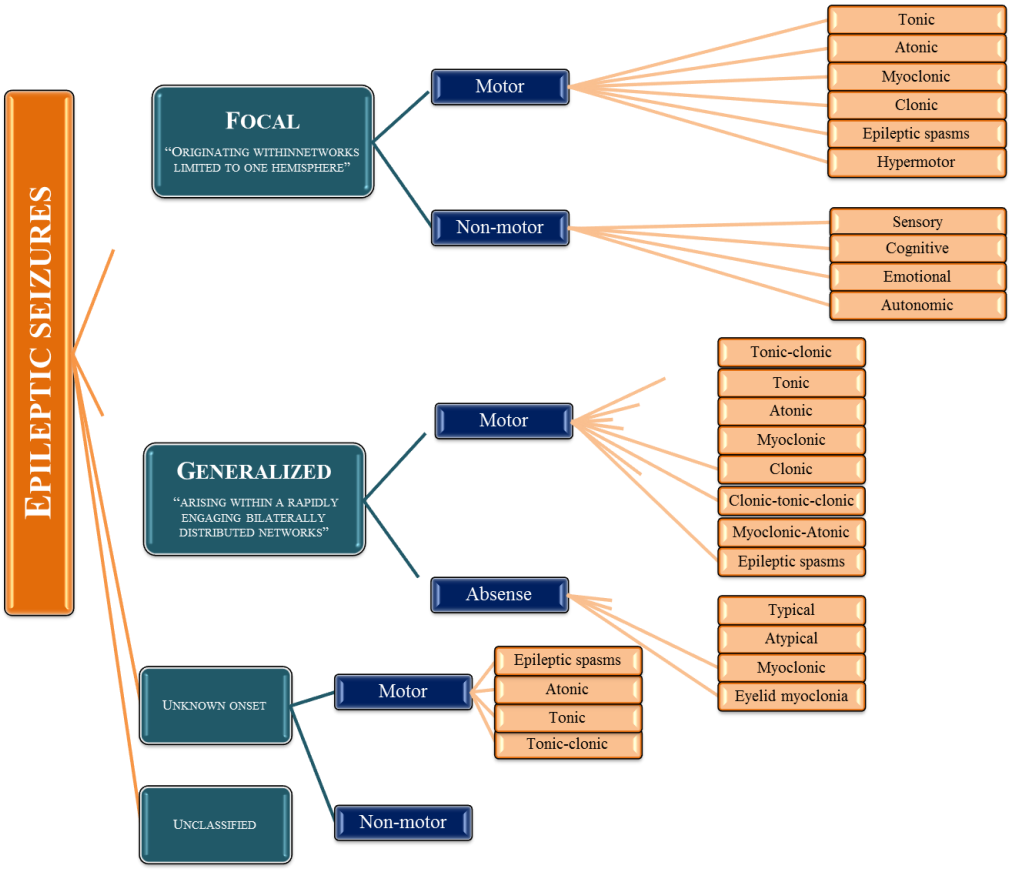

FIGURE 5. OPERATIONAL CLASSIFICATION OF SEIZURE TYPES BY THE INTERNATIONAL LEAGUE AGAINST EPILEPSY (FISHER ET AL., 2016).

The characterization of seizures types, origin and causes are the main focus of epilepsy care, due to their devastating effects on the quality of life and increasing stigmatism around the patients. Also, high epileptic activity confers a high risk of sudden death in epilepsy, so it has to be taken seriously into account.

2.2 *Co-morbidities in epilepsy*

A good seizures control remains the main challenge in epilepsy. However, the epilepsy-associated comorbidities are very disabling for patients and sometimes more than seizures. Co-morbidities in epilepsy are pathological conditions that usually follow the epileptic onset and are present in addition to epilepsy. They can precede epilepsy and in this case are causative of the epilepsy (i.e. brain infection, trauma). However, in the majority of the cases they are a consequence of epilepsy, and are caused by *1)* the negative effects of chronic epileptic abnormalities on brain development, *2)* the anti-epileptic drugs or *3)* an independent effect of the physiological disturbances that predispose the brain to seizures (Wei and Lee, 2015). Depression and anxiety are the

most common comorbidities in epilepsy, encountered in 1/3rd of epileptic patients and are mainly caused by anti-epileptic drugs (Sankar and Mazarati, 2012). In children between 4 and 15 years, additional co-morbidities have been reported in 40% of patients. The co-morbidities identified in epileptic children are: neurological (cognitive and language impairment, migraine and headache or sleep problems), psychological (autism spectrum disorder, attention-deficit and hyperactivity disorder, mood disorders, sociability problems) and physical (bone loss, immunological disturbances, body weight retardation and others). Among them, the most common are intellectual disabilities, speech and language difficulties or other specific cognitive disabilities (Holmes, 2015; Mula and Sander, 2016). Children with epilepsy have lower performances in school than children without epilepsy (Reilly et al., 2015) and their mental capacities tend to regress over time (Bailet and Turk, 2000). The children's immature brain seems to be more prone to a poor cognitive outcome due to several reasons. The young age at seizure onset, the effects of the chronic treatments with anti-epileptic drugs (AEDs) and the presence of a symptomatic cause or epileptic encephalopathy are all negatively contributing to abnormal cognitive or psychological development. However, whether poorly controlled epileptic activity is associated with progressive cognitive deterioration is still controversial, and this has been demonstrated only for some specific syndromes: mesial temporal lobe epilepsy and epileptic encephalopathies (*reviewed in* Avanzini et al., 2013).

2.2.1 Epileptic Encephalopathies

Epileptic encephalopathy (EE) carries the notion that *"the epileptic activity itself may contribute to severe cognitive and behavioral impairment above and beyond what might be expected from the underlying pathology alone (e.g., cortical malformation), and that these can worsen over time"* (Berg et al., 2010). EE are a group of heterogeneous brain disorders that occur in childhood and are characterized by pharmaco-resistance, focal and generalized seizures and severe cognitive and developmental delay often associated to premature death (Cross and Guerrini, 2013). The frequent and intense epileptic activity in young children interferes with normal brain development, induces delays in cognitive maturation and often cognitive regression. It can also have psychiatric and behavioral consequences. The different types of epileptic encephalopathies observed in children are listed in **TABLE 1.**

TABLE 1. LIST OF EPILEPTIC ENCEPHALOPATHIES ASSOCIATED TO NEONATAL PERIOD, INFANCY AND CHILDHOOD (ADAPTED FROM CROSS AND GUERRINI, 2013).

NEONATAL PERIOD	CHILDHOOD
Early myoclonic encephalopathy (EME)	Epileptic encephalopathy with continuous spike-and-wave during sleep (CSWS) (including Landau-Kleffner syndrome)
Ohtahara syndrome	Lennox-Gastaut syndrome
INFANCY	Other severe epileptic encephalopathies
Epilepsy of infancy with migrating focal seizures	Kozhevnikov-Rasmussen syndrome
West syndrome	Fever-induced refractory epileptic encephalopathy
Dravet syndrome	Hemiconvulsion-hemiplegia-epilepsy syndrome
Myoclonic encephalopathy in nonprogressive disorders	

Conversely, an important part of the concept of EE treatment is that amelioration of epileptiform activity will improve the developmental consequences of the disorder (Jehi et al., 2015). It has been observed that individuals with EEs who are successfully treated with medications or surgery, display improvements in cognitive function. This demonstrates that seizures and an abnormal EEG play an important role in cognitive outcome (Asarnow et al., 1997; Lee et al., 2014; Matsuzaka et al., 2001).

However, many, if not most, of these disorders are not solely associated with developmental or behavioral deterioration due to epileptiform activity. The term EE is currently being reviewed and debated, because it does not fit to all the EEs. In particular, whether Dravet Syndrome can be classified as an EE has been questioned recently, because development delay may occur in a period were seizures are not very frequent, so this suggests that this delay might have other underlying causes. In fact, the ILAE has recently proposed the new term "development encephalopathy" for particular EE cases (Scheffer et al., 2016).

2.3 *Etiology of epilepsy*

Etiology describes the origin or causation of a problem, in this case epilepsy. The new classification recognizes three types of causes: **1)** Genetic (idiopathic), **2)** Structural/Metabolic, and **3)** Unknown (Baxendale and Thompson, 2016; Berg et al., 2010). Genetic epilepsies (1) are those in which there is a known or presumed genetic defect(s) and seizures are the symptoms of the disease. In structural/metabolic epilepsies (2), seizures appear subsequent to brain condition (as stroke, trauma, infection,

poisoning. etc). This type of etiology might also have a genetic variation, but, it is the brain condition that interferes between the genetic cause and epilepsy. Unknown etiologies (3) are those that do not fit in the two previous characterizations, meaning that they are caused by non-identified factors. The majority of the gene in which mutations have been identified in epilepsy code for ion channels (Cossette, 2010). In my thesis, I will focus in the genetic epilepsies associated to *SCN1A* gene mutation that is the most commonly mutated gene in human epilepsies. Due to the high number of mutations identified to date in *SCN1A* gene (>900 different types), it has been referred to as a 'super culprit' gene (Lossin, 2009).

Chapter 2- GENETIC EPILEPSIES ASSOCIATED TO *SCN1A* GENE MUTATION

Voltage-gated sodium channels *(SCN)* genes code for voltage-gated sodium channels (Na_V). In the first part of this chapter, I will review the importance of voltage-gated channels in maintaining optimal neuronal excitability and introduce their different sub-types and molecular organization. In the second part, I will focus on the voltage-gated sodium channel alpha subunit 1 (*SCN1A)* gene and $Na_V1.1$ channel and the epileptic syndromes associated to this channel.

1. *SCN1A* GENE AND TYPE-I VOLTAGE GATED SODIUM CHANNEL

Excitation and electric signaling in the central nervous system involves the flow of ions (sodium, potassium, calcium and chloride) through ion channels. Voltage-gated ion channels underlie the electric properties of the neurons. They are membrane proteins with highly selective pores that can be in open or closed states according to the membrane electrical potential. Changes in membrane electrical potential induce modifications in channel conformation that allow ion transition between the extracellular and intracellular fluid - this property is called ion channel gating. Because these channels allow the ion flux down their electrochemical gradient in response to voltage-gating, they were called voltage-gated ion channels. There are three main types of voltage-gated ion channels with very conserved function similarities, but high selectivity for either sodium, potassium or calcium (Hille, 2001). They are composed by polytopic, transmembrane, pore forming and voltage-sensing α or α1 subunits (Catterall, 1995). The work of *Hodgkin and Huxley, 1952* was very important in the description of the action potential's propagation. Action potentials propagate by voltage-gated activation of Na+ channels that conduct sodium ions inside neurons and allow for activation of potassium-gated channels that reestablish membrane charges by carrying K^+ ions out of the cell **(FIGURE 6)**. The authors defined three characteristics of sodium channels: voltage-dependent activation, rapid inactivation and selective ion conductance.

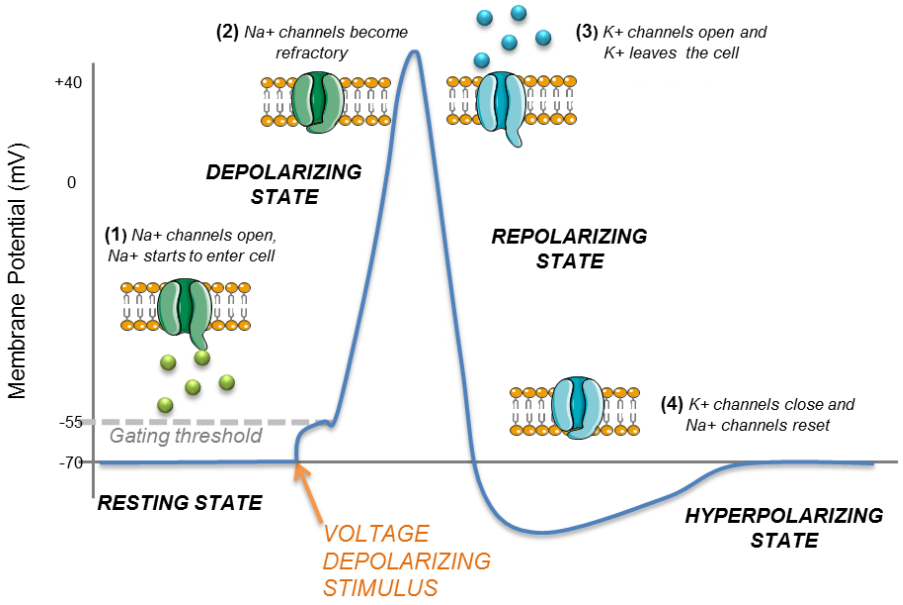

FIGURE 6. ACTION POTENTIAL INITIATION AND PROPAGATION IN NERVE CELLS.
When the voltage depolarizing stimulus arrives to the neuron (orange arrow), the voltage-gated sodium channels open allowing sodium ions to enter the cell (depolarizing state). The potassium (K^+) channels open allowing potassium ions to exit the cell while Na^+ channels became refractory (repolarizing state). After a period of hyperpolarization of the cell (hyperpolarizing state), the potential is normalized and the K^+ channels close.

The role of Na_V channels in initiating and propagating action potentials became clear by that time and further research characterized these channels at their molecular and functional levels. Na_V channels are composed by a large α subunit (260kDa) and smaller β subunits (30-40kDa) **(FIGURE 7)** (Lai and Jan, 2006). The α subunit is encoded by ten genes termed from *SCN1A* to *SCN11A* (Sodium Voltage-Gated Channel α Subunit 1-11). These genes code for nine Na_V and one sodium channel involved in salt sensing (*reviewed in* Mantegazza and Catterall, 2012). The genes encoding the nine Na_V, called $Na_V1.1$ to $Na_v1.9$, and their primary localization in human and rodent tissues are described in **TABLE 2**.

TABLE 2. VOLTAGE-GATED SODIUM CHANNELS SUBTYPES, ENCODING GENES AND LOCALIZATION IN PRIMARY TISSUE. REVIEWED IN (MANTEGAZZA AND CATTERALL, 2012)

Gene	Voltage-gated sodium channel type	Primary tissue
SCN1A	**$Na_V1.1$**	Central Nervous System
SCN2A	**$Na_V1.2$**	Central Nervous System
SCN3A	**$Na_V1.3$**	Central Nervous System
SCN4A	**$Na_V1.4$**	Skeletal Muscle
SCN5A	**$Na_V1.5$**	Heart
SCN8A	**$Na_V1.6$**	Central Nervous System
SCN9A	**$Na_V1.7$**	Peripheral nervous system
SCN10A	**$Na_V1.8$**	Peripheral nervous system
SCN11A	**$Na_V1.9$**	Peripheral nervous system

$Na_V1.1$, $Na_v1.2$, $Na_v1.3$ and $Na_v1.6$ are expressed in the central nervous system (CNS), while $Na_v1.7$, $Na_v1.8$, and Nav1.9 act mainly at the peripheral nervous system. $Na_v1.4$ is found in the skeletal muscle and $Na_v1.5$ is primary in the heart (Goldin, 1999). Less subtypes of Na_V β-subunits where identified (β_1, β_2, β_3, β_4) and are characterized according to the type of ligation they present with the α subunit (noncovalent or disulfide) (Morgan et al., 2000; Yu et al., 2003). The Na_V channel α-subunit consists of four domains (I–IV), with six transmembrane segments (S1–S6) each. The fourth transmembrane segment of each domain contains positively charged amino-acid residues in every third position that act as sensors for membrane depolarization and initiation of channel activation. The loop between S5-S6 segments form the selective pore domain through which sodium ions flow **(FIGURE 7).** One or more β-subunits, which are single transmembrane proteins with an extracellular immunoglobulin-like loop and an intracellular C terminus, co-assemble with the α-subunit and influence their functional properties. β2 and β4-subunits are covalently attached to the α-subunit while the β1 and β3-subunits are non-covalently attached (Messner and Catterall, 1985).

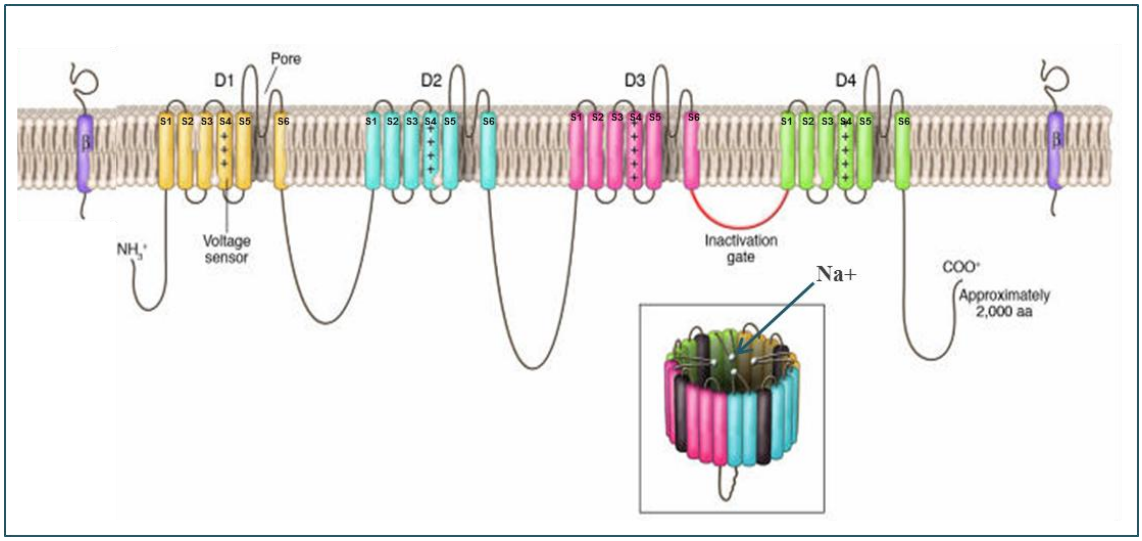

FIGURE 7. TRANSMEMBRANE ORGANIZATION OF Na_V SUBUNITS AND 3-D STRUCTURE.
Na_V α-subunits represent a single polypeptide that consists of four domains (D) (I–IV), with six transmembrane segments (S1–S6) each. The fourth transmembrane segment (S4) of each domain contains positively charged arginines (represented with + + + +) that are primarily responsible for voltage sensing, as well as the S5-pore loop-S6 region, which forms the pore domain through which sodium ions flow. The β subunits, β 1/3 and β 2/4, are single transmembrane proteins that co-assemble with the α subunit. Three-dimentional structure of sodium channel (adapted from (Meisler and Kearney, 2005)).

SCN1A codes for the $Na_v1.1$ channel and, along with the $Na_V1.2$, $Na_V1.3$ and $Na_V1.6$, it is primarily expressed in the CNS. As mutations in the *SCN1A* gene, and thus perturbations in the function of $Na_v1.1$, are strongly associated with epilepsy (Claes et al., 2001), work has been carried out to deeply examine its developmental expression profile. Na_V 1.1 expression becomes detectable at post-natal day (P) 7 in rats and around P10 in mice (Ogiwara et al., 2007) and at post-natal month one in humans (Cheah et al., 2013a). They are predominantly localized in the caudal region and spinal cord (Gong et al., 1999; Gordon et al., 1987; Ogiwara et al., 2007; Westenbroek et al., 1989). Previous studies in rodents showed that high $Na_V1.1$ expression was observed in the hippocampus, notably on the soma of DG cells and throughout the dentate hilus, in the stratum pyramidale of all hippocampal subfields, and within the stratum radiatum and statum oriens of the CA1 region. Strong expression was also observed within the layer V of the cortex and in the cerebellum (Westenbroek et al., 1989). Similar distribution of $Na_V1.1$ was found in human brain (Whitaker et al., 2001), indicating that the balance and distribution of this particular Na^+ channel is highly conserved and thus probably important for brain function. At the microscopic level, the $Na_V1.1$ was found primarily in cell bodies (Whitaker et al., 2001) and later, in depth analysis revealed a specific concentration of these channels at the axon initial segment (AIS) (proximal part of the axon, and the primary site for initiation of action potentials in neurons **(FIGURE 3)**

reviewed in (Kole and Stuart, 2012)) and in myelinated fibers, clustered at the nodes of Ranvier (Duflocq et al., 2008; Ogiwara et al., 2007). The creation of mouse models of $Na_V1.1$ mutations confirmed that the $Na_V1.1$ channels play an important role in the excitability of GABAergic interneurons (Ogiwara et al., 2007; Yu et al., 2006a) and confirmed concentrated localization of these channels at the AIS in fast-spiking parvalbumin basket cells (Hedrich et al., 2014) **(FIGURE 4)**.

Few $Na_V1.2$ mutations have been identified which are also causing epilepsy (Howell et al., 2015; Misra et al., 2008; Ogiwara et al., 2009). Although even less frequent, mutations in $Na_V1.3$, $Na_V1.6$ and $Na_V1.8$ were also reported in epilepsies (Estacion et al., 2014; Kambouris et al., 2016; Makinson et al., 2016; Malcolmson et al., 2016; Meisler et al., 2001; Vanoye et al., 2014). For the purpose of this thesis, the next sections will focus on $Na_V1.1$ channel-associated epileptic syndromes.

2. $Na_V1.1$ CHANNEL PHENOTYPIC/GENOTYPIC SPECTRUM

2.1 *A shared common feature: Febrile seizures*

It is described that around 5-12% of the children experience febrile seizures (FS) within the range of age 6-60 months with a peak at 2 years (Vestergaard and Christensen, 2009). FS are GTC seizures that happen in childhood associated to an increase in body temperature (~38,5ºC), without CNS infection. They occur in children without history of epilepsy or neurological dysfunction and might be due to a particular sensitivity to fever in the developing brain. It has been clearly demonstrated that there is an increased risk of FS incidence shortly after childhood vaccinations caused by vaccine-induced fever (Brown et al., 2007; Scheffer, 2015). **Simple FS** last usually less than 15 minutes, are generalized with often loss of consciousness, shakes, and movements in limbs on both sides of the body and do not occur more than once within a 24 hours period (Whelan et al., 2017). FS, first called benign but this term is not accepted anymore by the ILAE, is considered a self-limited condition different from epilepsy. **Complex FS** are classified in: 1) complex if they last between 15-30 minutes, happen more than once in a period of 24 hours and are focal or localized to a specific part of the brain or 2) febrile *status epilepticus (SE)* if they last more than 30 minutes (Whelan et al., 2017). FS plus (FS+) were considered as a simple FS that can occur more than once within a 24 hours period or that occur beyond the age of 6 (Grill and Ng, 2013). In terms of duration, the principal ictal* event (seizure) can be confused with the post-ictal events (tonic posture, eye deviation that last for some time post-seizure). So, basically, without EEG recording it is hard to delimitate the end of the seizure. The probability of recurrence after a simple FS is around 2%, while the probability is 2-3 times higher after a complex FS (Camfield and Camfield, 2015). These long-lasting/complex FS are better candidates to cause important modifications in the brain and epileptogenesis (Ellenberg and Nelson, 1978).

The mechanism by which FS are generated is unknown. Yet four theories have been proposed for FS generation: **1)** the neuronal hyperexcitability induced by the increased temperature (Fisher and Wu, 2002), possibly by acting directly on Na_V gating at the AIS (Thomas et al., 2009), **2)** the neuronal hyperexcitability caused by the release of inflammatory mediators during fever (eg.: Il-1β) (Alheim and Bartfai, 1998; Dubé et al., 2005), **3)** the neuronal hyperexcitability caused by brain alkalosis during high

ventilation in hyperthermic conditions (Aram and Lodge, 1987; Balestrino and Somjen, 1988; Schuchmann et al., 2006, 2011) or **4)** a result from inefficient thermoregulation (Feng et al., 2014; Richmond, 2003).

Among the many risk factors for FS, the genetic predisposition strongly confers the epidemiological link in many families (Baulac et al., 2004). *Mantegazza et al., 2005* identified a mild loss-of-function mutation in $Na_V1.1$ responsible for the familial FS condition. Very few children exhibit more than three FS during their childhood (*reviewed in* Camfield and Camfield, 2015), and there is little evidence for a correlation of FS in these children with long-lasting consequences like brain damage or cognitive problems (Sillanpää et al., 2011). Also, the incidence of FS does not indicate that epilepsy will develop (15% of the children have a febrile seizure event and do not develop epilepsy). FS are common to all diseases characterized by $Na_V1.1$ channel haploinsufficiency* thus it is considered that FS is a mild phenotypic consequence of the mutations in *SCN1A* gene.

2.2 *Epileptic syndromes associated to $Na_V1.1$ channel mutation: genetic and phenotypic variants.*

SCN1A gene mutations associated to $Na_V1.1$ loss of function cause a vast range of epilepsy syndromes in humans. The associated phenotypes range from simple FS as described in the previous part (Mantegazza et al., 2005), *en passant par* generalized epilepsy with febrile seizures plus (GEFS+), a mild epileptic syndrome with high phenotypic variability (Escayg et al., 2000a), to an extremely severe condition – Dravet Syndrome (DS) (Claes et al., 2001) **(FIGURE 8C)**. The diseases associated to the $Na_V1.1$ spectrum are categorized according to patient's phenotype (mainly to seizures history). The first identified mutation in the $Na_V1.1$ α-subunit was the *SCN1A*-R1648H missense mutation* in one large family presenting GEFS+ (Escayg et al., 2000a). Since then, more than 30 other missense mutations have been identified that cause GEFS+, a disease usually associated to the partial loss of the channel's function. Most displayed GEFS+ cases present autosomal-dominant transmission with high variability of phenotypes. Following the first *SCN1A* mutations that accounted for 10% of GEFS+ patients, a new report of *SCN1A* mutation was described in children presenting the sporadic severe myoclonic epilepsy in infants (SMEI) later called Dravet Syndrome (DS) (Claes et al., 2001). In SMEI children the mutations were *de novo* mutations since

none of the parents were affected. More than 80% of DS patients present *SCN1A* gene mutations and more than 900 different types had been described by 2013 (Parihar and Ganesh, 2013)(see also www.gzneurosci.com/scn1adatabase/). The types of mutation in DS are: 1) severe truncating mutations* (and less often splicing* or deletion* mutations) causing loss of $Na_V1.1$ function or 2) severe missense mutations that prevent the channel's expression or severely impair its function (Brunklaus et al., 2014). The duplication and deletion of sequences in the gene have also been pointed to impair the channel's function (Marini et al., 2009).

2.2.1 Type of mutations and their localization in the *SCN1A* gene.

FIGURE 8A&B represents some of the mutations found in GEFS+ and DS patients, respectively (but by now they are many more). In **FIGURE 8B** one can observe that the DS-causing missense mutations (green circles) are concentrated within the transmembrane segment where they probably prevent the channel's folding and function. In fact, a recent study on large cohort of Japanese DS patients showed that the missense mutations found in DS were in the majority concentrated at the S4 voltage sensor and pore loops (S5 and S6) (Ishii et al., 2016). It was described that disease phenotype is worse when there is a substantial change in the physicochemical properties of the amino acids as measured by the Grantham score (A formula for the difference between amino acids that correlate better with protein residues substitution frequencies: composition, polarity, and molecular volume) (Grantham, 1974).

The heritability of *SCN1A* is complex in GEFS+ and DS patients. The mutations reported for *SCN1A*-causing diseases were usually heterozygous as expected for a dominantly inherited disorder such as GEFS+ or with mutations that appears *de novo* as in DS. However, very interestingly, two new homozygous missense mutations of *SCN1A* gene were identified in 4 patients born from consanguineous parents (Brunklaus et al., 2015) and the phenotypic variability ranges from simple FS to DS. The heterozygous mutation in parents was conservative (preventing the channel from harboring functional changes) justifying why they remain unaffected. However, a change on both alleles had a cumulative and detrimental effect on the homozygous children. Basically, patients with heterozygous missense mutations can display a very mild phenotype if the mutation does not induce important conformational and functional

changes to the channel (mutation position and type of amino acid change), or very detrimental effects if it induces important modifications to the channel, justifying the heterogeneity of phenotypes in GEFS+ and DS patients.

Another important feature is the possibly out-dated notion that inherited mutations are associated to GEFS+ and *de novo* mutations are associated to DS. Indeed, a recent study reported *de novo* mutations in 7 patients with GEFS+ (Myers et al., 2017), again evidencing the importance of performing in depth genetic analysis in GEFS+ patients potentially carrying the de novo *SCN1A* gene mutations. In parallel, DS patients carrying inherited mutations were also observed and will be described it in the next paragraph (Depienne et al., 2006).

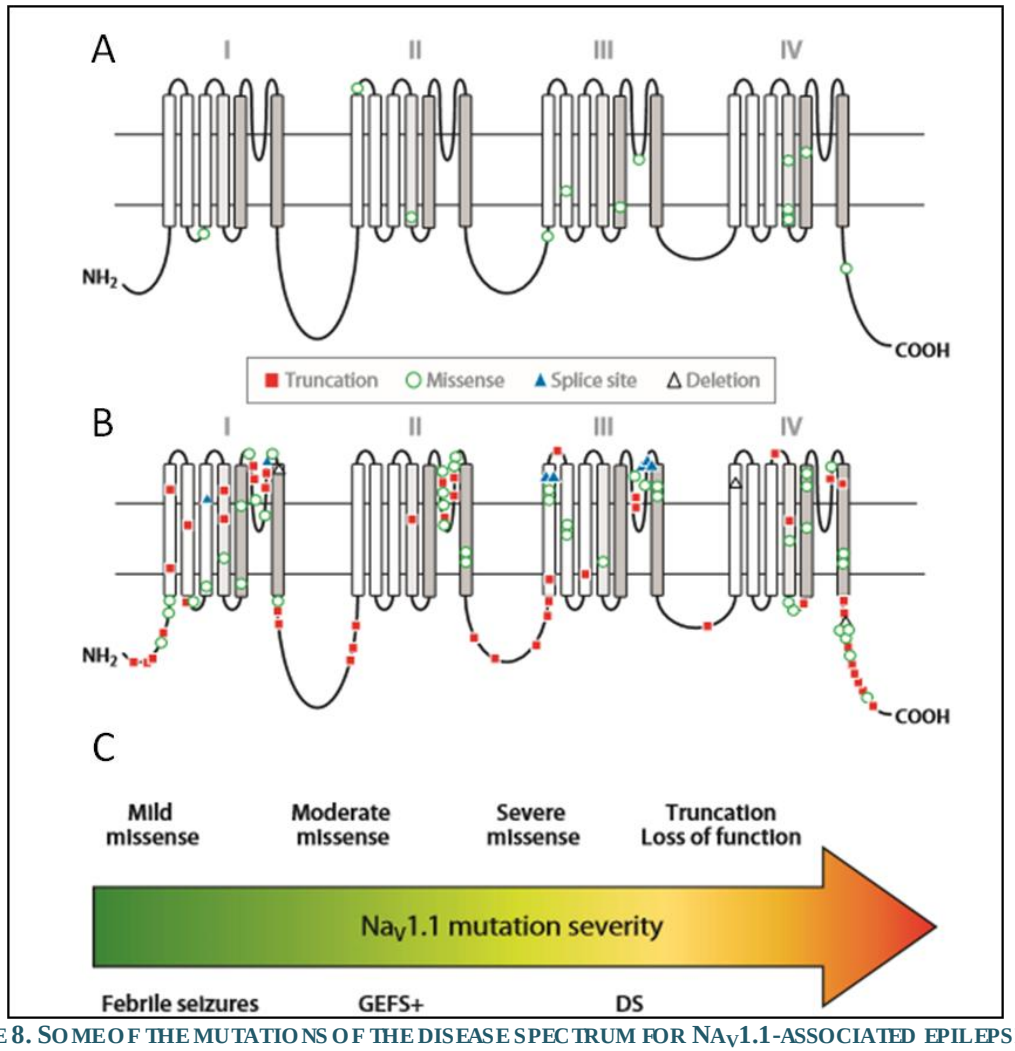

FIGURE 8. SOME OF THE MUTATIONS OF THE DISEASE SPECTRUM FOR $Na_V1.1$-ASSOCIATED EPILEPSIES. A: Mutations in $Na_V1.1$ channels in patients with generalized epilepsy with febrile seizures plus (GEFS+). B: Mutations in $Na_V1.1$ channels in patients with Dravet syndrome (DS). The loss-of-function hypothesis for $Na_V1.1$ genetic epilepsies (Mulley et al., 2005). C:Increasing severity of loss-of-function mutations of $Na_V1.1$ channels, noted above the arrow, causes progressively more severe epilepsy syndromes from familial febrile seizures to GEFS+and finally DS, noted below the arrow. *Adatped from* (Catterall, 2014).

2.2.2 Inherited transmission of *SCN1A*-DS mutations. The concept of mosaicism.

DS mutations are mainly *de novo* mutations meaning that they appear for the first time in a given child and it is not transmitted from the parents. Another important issue contributing to the phenotypic variability in *SCN1A* gene-related epilepsies (and other types of genetic diseases) is the mosaicism*, phenomenon in which the person can have more than one population of cells with different genotypes. First cases of mosaic mutations were reported in DS families in 2006 (Depienne et al., 2006; Gennaro et al., 2006; Marini et al., 2006, 2009) and it is now reported to account for 10% of all DS mutations (Depienne et al., 2010). These studies described many families in which the *SCN1A* mutation affected more than one sibling which led to genetic analysis of the parents. For example, a recent report showed a family with two affected DS children, and two unaffected parents. The in-depth genetic analyses of this family confirmed the diagnosis of affected father with mosaic DS-mutation (Tuncer et al., 2015). Mosaic parents of DS patients carry truncating mutations (Singh et al., 2001; Veggiotti et al., 2001) and present phenotypes associated to the GEFS+ spectrum (explained by the lower number of affected cells). *Depienne et al., 2010* reported 19 families (of which 6 had GEFS+ spectrum) with inherited DS in the progeny (9 truncating, 9 missense and 1 whole gene deletion mutation). The 6 families with GEFS+ were not mosaic, but there was one patient with DS in each family (Depienne et al., 2010). Mutations observed in DS patients were also previously reported in a GEFS+ families (Annesi et al., 2003; Escayg et al., 2000a). Therefore, truncating mutations cause DS in most of the cases if there is complete penetrance (not mosaic), and missense mutations can cause GEFS+ and DS according to the type of missense mutation and genetic modifiers. The authors therefore justify that DS disease can be at the severe end of the GEFS+ spectrum.

2.2.3 Phenotypic variability in GEFS+ and DS: genetic and environmental factors.

Genetic and environmental factors also contribute to phenotypic variability in families with extreme phenotype distributions. Almost all the mutations in GEFS+ are missense mutations (Claes et al., 2009) that usually do not lead to complete ablation of channel function (Sugawara et al., 2002). However, complete truncating mutation can

cause GEFS+ or DS in two sibling brothers, indicating that genetic/environmental factors play a crucial role (e.i. family 12 in (Depienne et al., 2010)). It is apparent that the variability of phenotypes cannot be exclusively justified by the *SCN1A* mutation type, as in the same family, patients with the same mutation can have different phenotype severities (as observed in mutations transmitted from mosaic parents). Moreover, the same study reported a DS patient carrying the mild R1648H missense mutation first identified in the GEFS+ family (Depienne et al., 2010; Escayg et al., 2000a). Several genes have been identified for their involvement as genetic modifiers (i.e. *Scn8a* in mice studies, SCN1B, SCN19, GABRG2 and CACNB4 in humans) (Gaily et al., 2013; Ohmori et al., 2008, 2013; Singh et al., 2009), possibly by compensating the $Na_V1.1$ loss of function (Hawkins et al., 2016).

All the reported genetic variables will be crucial determinants for the age of onset and the type/frequency of seizures that the patients present, and also in defining the outcome of the disease. The epileptic history of the patients in $Na_V1.1$ mutation phenotypic spectrum is crucial for a correct diagnosis. It is therefore safe to assume that the genotype ↔ phenotype correlation is not applicable to all the cases. According to this assumption, the diagnosis classification for a disease associated to the *SCN1A* mutation is given primarily according to the phenotypic spectrum, then taking into account the epileptic history (age at seizure onset, sensitivity to febrile seizures, type/duration of seizures and familial history of seizures) and the genetic profile (the type of mutation, the location in the gene, the genetic and environmental modifiers and the possibility of eventual mosaic caregivers). In the following section, an in-depth description about GEFS+ and DS diseases will be provided.

3. GENETIC EPILEPSY WITH FEBRILE SEIZURES PLUS (GEFS+)

3.1 *GEFS+ historical, definition and epidemiology*

GEFS+ is the most variable syndrome of the *SCN1A* gene mutations spectrum and its prevalence in the world is unknown to date, but hundreds of cases have been reported in the literature. It was first described in 1997 by *Scheffer and Berkovic*, when they observed important correlations between generalized epilepsy and FS within several families, but with markedly different severity. The phenotypic spectrum in the

families was large, from FS, FS+ to GEFS+, and the genetic transmission trough autossomic dominance was clear.

3.2 *The genetics of GEFS+*

GEFS+ disease is divided into type 1 and type 2. Type 1 GEFS+ is associated to a mutation in the Na_v ß1 subunit gene (*SCN1B*) and was first identified in 1998 (Wallace et al., 1998). Type 2 GEFS+ is associated to mutations in the *SCN1A* gene, and cited earlier (Escayg et al., 2000a). Mutations in *SCN2A*, *SCN9A*, *STX1B* and *GABRG2* have also been associated to GEFS+ (Meisler and Kearney, 2005). *Escayg et al., 2000a* found the first *SCN1A* mutations in GEFS+, in particular the R1648H missense mutation that was later also found in a patient with DS as mentioned earlier (Depienne et al., 2010). Nevertheless, genetic origin in the GEFS+ syndrome only accounts approximately for 10% of the cases (*reviewed* in (Lossin, 2009)), and the cause for the other 90% cases remain unknown.

GEFS+ has long been associated to missense inherited mutations; however, due to the complex heritability of the *SCN1A* in GEFS+, some exceptions appeared. In brief, not only heterozygous but also homozygous mutations have been observed (Brunklaus et al., 2015), not only missense mutations but also truncation mutations (mosaic or not) (Depienne et al., 2010; Singh et al., 2001; Veggiotti et al., 2001) and finally not only inherited mutations but also *de novo* mutations (Myers et al., 2017).

3.3 *Clinical characterization of GEFS+:epileptic history*

GEFS+ is a familial epilepsy syndrome where at least two family members have phenotypes consistent with the GEFS+ spectrum. The patients usually present a first FS at a variable range of ages (6 months-6 years) (Singh et al., 1999). The most common feature in GEFS+ is the presence of FS+ (febrile seizures that persist beyond the age of 6 years – until late childhood or adolescence) that tend to remit in adolescents when other seizure types take over. Patients with GEFS+ also present afebrile seizures within the range of FS (condition also considered as FS+) or after the period of FS remission (Scheffer and Berkovic, 1997; Singh et al., 1999). Both FS and FS+ may be associated with other seizure types. Often, GEFS+ also present GTC seizures, although focal seizures may occur and have been associated with more severe missense mutations and

poorer prognosis (Pineda-Trujillo et al., 2005; Sugawara et al., 2001). Because of the presence of focal seizures in some cases, the term was adapted to Genetic Epilepsy with Febrile Seizures plus (GEFS+) (Scheffer and Berkovic, 1997). In terms of generalized seizure types, absence seizures, myoclonic, atonic seizures, and myolonic-astatic are also observed in addition to GTC seizures (Scheffer and Berkovic, 1997; Singh et al., 1999). GEFS+ patients with a mild phenotype display normal cognition upon neurological examination and normal EEG. However, more severe GEFS+ cases can present generalized epileptiform abnormalities in a normal EEG background.

As far as we know, none had reported neuroimaging and neuropathological examinations in GEFS+ patients probably due to the generally positive long-term outcome in patients.

3.4 *Therapeutic strategy and long-term outcome*

The treatment is considered in the children if they have several individual episodes of FS. In the cases reported by *Scheffer and Berkovic, 1997*, most had febrile seizure onset in the first year of life and many had remittance of the seizures in the first or second decades, although some had seizures into adulthood. The treatment window and response can vary within the same family. It was reported that two GEFS+ mutations, that conferred a change in the $Na_V1.1$ folding were partially rescued by treatment with anti-epileptic drugs (Rusconi et al., 2007, 2009). This might be the cause of successful treatment response in mild cases of GEFS+. However, GEFS+ patients with more severe phenotypes can present pharmaco-resistance (Grant and Vazquez, 2005).

Long-term outcome in GEFS+ children is usually self-limited and favorable. Seizures tend to decrease and in general, patients do not develop cognitive and behavioral deficits (Scheffer and Berkovic, 1997). However, some cases have been reported to exhibit mild psychiatric (Mahoney et al., 2009; Osaka et al., 2007) or cognitive deficits (Myers et al., 2017). On one hand, seizure intensity and severity have been pointed to contribute to the behavioral and cognitive outcomes, but on the other hand, the mutation severity might also be involved. GEFS+ spectrum is comparable to DS spectrum (Singh et al., 2001), and it has been suggested that DS could be a severe end of GEFS+ spectrum.

4. DRAVET SYNDROME (DS)

4.1 *DS historical, Definition and Epidemiology*

Severe myoclonic epilepsy of infancy (SMEI) was first described in 1978 in a French medical journal by doctor Charlotte Dravet, psychiatrist at Marseille Hospital (Dravet, 1978). An increased evidence of common cases emerged from all around the world, but myoclonic seizures were not always present in these patients (Ogino et al., 1989; Yakoub et al., 1992). Also the disease was not limited to infants, because the epilepsy persisted in adults. The name of the disease was then adapted to Dravet Syndrome (DS) in 1989. DS is a rare and severe epileptic encephalopathy (Catarino et al., 2011) affecting around 1/30 000 patients in France (Yakoub et al., 1992) and 1/15 000 in the USA (Wu et al., 2015). The gender incidence is equivalent, except for DS caused by mutations in the *PCHD19* gene that affects a small percentage of females (Depienne et al., 2009).

The diagnosis for DS is based on a first febrile or prolonged afebrile clonic seizure occurring during the first year of life in a normally developed child who can have or not family history of FS. If the patient presents two seizures associated to an increase in body temperature and if at least one of these seizures lasts more than five minutes possibly evolving to *status epilepticus (SE)**, a diagnosis of DS is suspected and the genetic analysis is performed. Also, DS patients present sensitivity to fever and light.

DS represents the epilepsy type with highest mortality incidence that can occur at any age, but mainly in childhood. The exact mortality incidence was not homogenous in all the studies. However, it varies from 5% to 10% at early age. The main causes of death reported were the Sudden Unexpected Death in Epilepsy (SUDEP), *SE*, accident, infection or unknown causes. SUDEP is generally defined as the sudden, unexpected, witnessed or unwitnessed, nontraumatic, and non-drowning death in patients with epilepsy with or without evidence for a seizure, and excluding documented *SE*, in which postmortem examination does not reveal a structural or toxicologic cause for death (Nashef, 1997). Mechanisms involved in SUDEP seem to be correlated with sudden cardio-respiratory arrest and the main risk factor seems to be the high level of GTC seizures (Hesdorffer et al., 2011; Sowers et al., 2013). It confers the highest reported

cause of death in DS, a condition that occurs mostly during sleep, in children who did not show a recent aggravation of the disease and under controlled medication.

4.2 *The genetics of DS*

Since 2001, it is known that most of the DS cases are associated to *SCN1A* gene mutations (Claes et al., 2001). DS is the most severe disease of the $Na_V1.1$ mutation spectrum, with 80% of the patients harboring a mutation in the *SCN1A* gene. Some patients who remain negative in genetic analysis have deletions or chromosomal rearrangements involving *SCN1A*. Mutations in other genes have also rarely been associated with DS, especially *PCDH19* mutations (Depienne et al., 2009). *SCN1A* mutations arise usually *de novo*, but ~10% are inherited from mosaic parents, as described above (Gennaro et al., 2006).

4.3 *Clinical characterization of DS: Epileptic history*

Contrarily to GEFS+ that present a large spectrum of phenotypic severity, DS presents marked characteristics and a homogeneous phenotypic spectrum. The first febrile or afebrile seizure usually appears before the age of 1 year, within a range of ages from 2 to 12 months and the final diagnosis of DS disease is usually made between 2 and 3 years of age (Bureau and Dalla Bernardina, 2011). Some studies suggested a correlation between the age of the first seizure with the severity of the phenotype, i.e. lower ages of onset correlating with poorer prognosis (Cetica et al., 2017; Ragona et al., 2010). The disease progression can be divided in three phases: the febrile phase, the worsening phase and the stabilization phase. The first seizure is usually clonic, generalized or focal triggered by fever or body temperature elevation (after a bath or high physical activity) and lasts longer than a simple FS (>15 minutes). The first seizure might also be afebrile in some cases (Ragona et al., 2010), but this is still controversial (Nieto-Barrera et al., 2000). These seizures can evolve into *SE* (seizures lasting longer than 30 minutes) that occurs at least once in each patient (Chipaux et al., 2010). The *SE* can be febrile (usually in the first year of life – duration >30 minutes) and obduntation (non-convulsive) between 4-8 years of age – duration can last for days. Isolated cases of focal myoclonic jerks were observed to precede the GTC seizures in a few children

(Dravet et al., 2005; Oguni et al., 2001). At the onset (febrile period), patients usually experience an average of one seizure per month or even less.

Within the worsening seizure period, patients present multiple seizure types including: GTC seizures, generalized clonic seizures, myoclonic seizures, atypical absence seizures and simple and complex focal seizures (with or without secondary generalization). The end of the active period can vary from on child to another, usually until 3 years of life but sometimes extending up to 13 years of age. Later on, partial seizures, myoclonic seizures, atypical absenses and *SE* tend to disappear. GTC seizures persist, at least until reaching 25 years old when they tend to remit (Dravet, 2014). In adults, seizure-free periods of 1-5 years are low (>10%) (Akiyama et al., 2010; Jansen et al., 2006).

At the onset, the EEG of DS children has a normal background, during awake and sleeping states. During GTC seizures patients show typical EEG pattern, characterized by a transient postictal flattening, which is rapidly replaced by diffuse delta waves (Bureau and Dalla Bernardina, 2011) **(FIGURE 9)**.

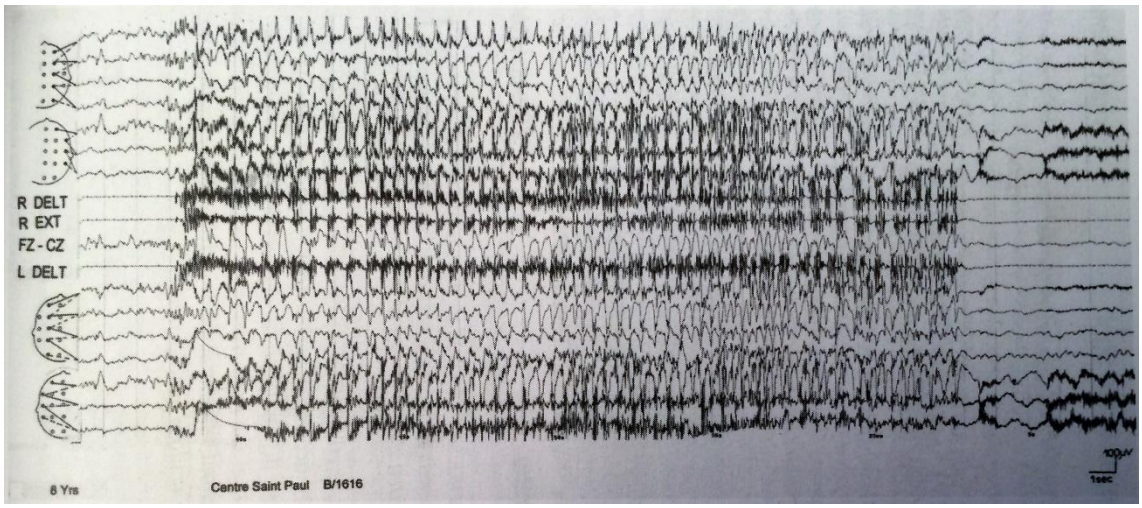

FIGURE 9. EEG TRACE OF A GENERALISED TONIC-CLONIC SEIZURE IN AN 8-YEAR OLD DS PATIENT. FROM (DRAVET AND GUERRINI, 2011) WITH JLE PUBLISHER AUTHORIZATION TO REPRODUCE.
At the onset of the seizure, a brief burst of fast activity correlated to muscle tonus (R DELT, R EXT, L DELT), the clonic jerks progressed to GTC seizure and, at the ictal end, it is possible to see the brief flattening followed by low voltage theta* activity.
R DELT = Right deltoid muscle, R EXT= right extensor muscle, L DELT = Left deltoid muscle

With the disease progression, the EEG activity can be maintained at normal background level during awake phases in some patients, while in the others the background activity can become slower and poorly organized with presence of alpha-rhythm, an increase in theta* activity and generalized or multifocal interictal spikes

(Bureau and Dalla Bernardina, 2011). During the night, the interictal* EEG is usually abnormal, due to the persistence of higher ictal* events during sleep.

4.4 *Neuroimaging and neuropathology*

There are not many studies about imaging or neuropathological studies in DS. No gross brain abnormalities using Magnetic Ressonance Imaging (MRI) or Computer Tomography (CT) have therefore been detected in the published studies. Only *Dalla Bernardina et al., 1982 and Dravet et al., 2005* reported a few cases presenting brain atrophy with increased white matter. In 2005, Dravet et al., reported that MRI changes were observed in 4 out of 35 DS patients carrying *SCN1A* mutations, with one presenting hippocampal atrophy and another cerebellar atrophy (Dravet et al., 2005). *Olivieri et al., 2016* analyzed a cohort of 20 patients, in which 4 patients presented either ventricular enlargement with corpus callosum thining, hippocampus atrophy, mild cerebellar atrophy or diffuse cortical atrophy. Neither seizures frequency, age at seizure onset, nor the mutation was correlated with the neuroanatomical abnormalities in these patients.

4.5 *Therapeutic strategy and long term outcome*

DS is an intractable disease characterized by high pharmaco-resistance. The first therapeutical goal in DS consists of reducing the seizures frequency (in particular long-lasting seizures - as *SE*) and to minimize the anti-epileptic drug toxicity. The second goal is to reduce the associated co-morbidities (*reviewed in* (Wirrell, 2016)).

During the first years of DS progression, the seizures are extremely resistant to all treatments available until now, and seizure-free patients have rarely been described even after passing the worst epileptic period (Jansen et al., 2006).

Na^+ channel blockers (carbamazepine, oxcarbazepine, phenytoin, lamotrigine) have been used mainly before the *SCN1A* mutation identification, but appeared to clearly exacerbate the seizure phenotype in DS patients (Ceulemans, 2011; Chipaux et al., 2010; Guerrini et al., 1998; Wang et al., 1996). It was then suggested to stop using them. Currently, first lines of treatments focus on benzodiazepines like clobazam, clonazepam, diazepan to increase GABAergic function and decrease brain excitability. Valproate is also used, but its mechanism of action is less specific including voltage-

gated sodium channel and NMDA receptors blocker and enhancer of GABAergic function.

Stiripentol is used as a second-line drug. Its use has clearly reduced the number of seizures including *SE* in patients, helping medical doctors to reduce the high mortality incidence caused by these prolonged seizures. Stiripentol is considered as the drug that, in combination with other drugs, has shown higher effectiveness in DS patients (Chiron et al., 2000; De Liso et al., 2016; Kassaï et al., 2008). It acts by increasing GABAergic function, but also increasing the effects of the other antiepileptic drugs on the GABAergic system (Fisher, 2011). Stiripentol is usually combined with topiramate that, as valproate, has a large spectrum of action (voltage-gated sodium channels and AMPA receptors blocker and enhancer of GABAergic function). In summary, the most common recent combined treatment comprises first of valproate with or without a benzodiazepine, and then of stiripentol with topiramate (Wirrell, 2016).

Yet, the seizures tend to be resistant even though multiple medications exhibit clinical evidence of efficacy (by reducing the number of seizures) in DS: stiripentol, valproic acid, clobazam, bromide and topiramate.

Two recent treatments are in development (cannabidiol and fenfluramine). Cannabidiol was highly mediatic in the press however the very few studies who evaluated its efficacy in DS patients showed low level of responsiveness to the drug (O'Connell et al., 2017; Press et al., 2015). A current study is being done to test its efficacy.

Fenfluramine is an agent that releases serotonin by disrupting vesicular storage and reversing serotonin transporter function, is actually on phase III of clinical trials, after showing remarkable efficacy in DS at low-dose concentration in seizures reduction (Ceulemans et al., 2016; Schoonjans et al., 2017). The effects of fenfluramide on cognition have not been assessed yet.

Alternative non-pharmacological treatments have been proposed to combine with the anti-epileptic drugs notably: vagus nerve stimulation and ketogenic diet. Vagus nerve stimulation have been effective in treating several forms of refractory pediatric epilepsy (Cersósimo et al., 2011). However, the studies done in DS patients were not very promising (Zamponi et al., 2011). Only very recently, a new study showed improvement in seizure frequency (>50% of patients reduced significantly the seizure frequency) with behavioral and cognitive ameliorations in 75% of a small cohort of

patients submitted to vagus nerve stimulation in combination with anti-epileptic drugs (Fulton et al., 2017). The studies using ketogenic diet in combination with anti-epileptic drugs have been much more beneficial for patients than vagus nerve stimulation. Several studies reported seizure reduction from 50 to 99% in patients (Caraballo et al., 2011; Korff et al., 2007), and even with improvement in behavioral phenotypes in some patients (Laux and Blackford, 2013; Nabbout et al., 2011)

Other alternative treatments as immunotherapy have been tried without reaching significant conclusions to date (Chabardès et al., 2002).

No published reports compared the effects of different anti-epileptic drug administration schedules for GTC seizures or *SE* in patients with DS. This could probably explain some worsening in the phenotypes, mainly in cases where Na^+ channel blockers are still being administrated.

Seizures importantly decrease the quality of life of DS patients and their relatives. In addition to seizures, important psychiatric, neurological and cognitive co-morbidities are present in DS patients. To improve the comorbidities in DS, several therapies are used notably, occupational and speech therapy, social work and others.

Chapter 3- BEHAVIORAL AND COGNITIVE: LONG-TERM OUTCOME IN DRAVET SYNDROME :

The long-term outcome in DS patients is always unfavorable. The development is normal in the first year of life (before the severe period of high seizures intensity) and children can have a normal life. They usually start walking at normal age but then tend to show progressive development delay and regress, becoming severely impaired. Among the psychiatric and behavioral abnormalities shown in DS patients, it is always hard to say which ones are consequences of the disease and which ones result as side effects of the anti-epileptic drugs. DS patients develop neurological, psychiatric and cognitive abnormalities.

1. NEUROLOGICAL ABNORMALITIES IN DRAVET SYNDROME

Neurological signs progressively appear in DS children. They are characterized by hypotonia, ataxia, pyramidal signs, interictal myoclonus and "crouch" gait. Hypotonia, meaning low muscle strength, is observed very early in DS children (around one year of age). Patients have difficulty to stand up correctly and exhibit orthopedic problems later on (Dalla Bernardina et al., 1982). In addition to muscle strength abnormalities, DS children have also altered coordination of muscle movements. Pyramidal signs are the results of the activity of pyramidal cells in the motor cortex. It is usually present as voluntary, discrete and skilled movements that are observed in DS children by spasticity or walking on tiptoes. The frequency of these events is not continuous and is more frequent after severe seizure episodes (Caraballo and Fejerman, 2006; Dalla Bernardina et al., 1982). In addition to the "voluntary" abnormal movements, the children also develop involuntary movements. Ataxia, the lack of muscle coordination, is reflected in DS children when they start walking, at around 12-18 months (sometimes delayed) (Dalla Bernardina et al., 1982; Dravet et al., 2005). These neurological signs are observed in the majority of the patients and were hypothetically correlated to a cerebellar co-factor in DS disease progression (Battaglia et al., 2013). Additional involuntary movements are the interictal myoclonus (myoclonic jerks that appear independently to seizure events) that are more frequent after intense seizure activity and transitory in patients. They appear as involuntary facial or limb movements (Nabbout et al., 2003). All these neurological signs and skeletal

abnormalities lead to a particular posture in DS patients. They usually maintain a normal or nearly normal gait in the first 5 years of age that then evolves into a “crouch” gait associated with skeletal misalignment in the lower limbs in the majority of patients after 13 years of age (Rilstone et al., 2012). This handicap is degenerative and irreversible prominently affecting all the motor skills which lead hence to the inability to realize the patient’s daily-life needs.

2. COGNITIVE DELAY AND REGRESSION IN DRAVET SYNDROME

Cognitive decline in DS has no specific age of onset. Visual functions seem to be primarily affected in DS children. Fine visuo-motor (i.e. object assembly, coding) and visuo-spatial (i.e. block design) skills through eye-hand coordination seem to be altered in the first year of life in children, even before the appearance of other cognitive symptoms and clinical confirmation of the syndrome (Battaglia et al., 2016; Chieffo et al., 2011a; Ricci et al., 2015; Wolff et al., 2006a). Moreover, language is delayed in DS patients. The reported studies classify language capacities in three levels (average speech, isolated words but not the ability to construct sentences and complete lack of speech). These speech incapacities directly impact the school level of DS children, and some with lower prognosis can not even attend the school (Caraballo and Fejerman, 2006; Fujiwara et al., 1992; Wolff et al., 2006a; Yakoub et al., 1992). Comparing to visual capacities, language seems to be more conserved or partially recover in late childhood in DS children (Chieffo et al., 2011b). However, *Acha et al.*, showed that visual processing was preserved in their cohort of 8-14 years old DS patients, while verbal information was more affected (Acha et al., 2015).

Memory function has not been as explored in DS study cases as behavioral phenotypes and visual skills, possibly due to the youth of patients. A study evaluating memory processing shows that verbal working memory was importantly impaired demonstrating, in the majority of DS children, an inability to integrate sensory serial events (Battaglia et al., 2013). This could also be correlated with the lack of visual and auditory attention demonstrated by the children, and other authors suggested a cerebellar role (Gottwald et al., 2003). However, as mentioned above, the PFC plays a crucial role in attention driven tasks (Clark et al., 2015), so alterations in the function of this structure in DS patients could also explain impairments in working memory tasks. Impaired executive function was reported in all the studies, which highlight an

important perturbation in the sequencing of activity plan (Acha et al., 2015; Chieffo et al., 2011a; Olivieri et al., 2016), again pointing to alterations in brain structures driving executive functions like the PFC.

Sleep disturbances can importantly affect the cognitive profile in DS children but have been more controversial. There are not many studies that had a look into the sleeping patterns of DS children. *Chieffo et al., 2011a* reported sleep problems in all 5 DS patients studied but did not specify the abnormalities observed. More recently, *Dhamija et al., 2014* observed non-REM sleep abnormalities typical of immature cortical synaptic activity but no changes in the sleeping architecture in their cohort. The many hypothetical reports about sleeping abnormalities in DS children can be possibly due to the intense seizure activity during the night, and that certainly affects the normal sleeping cycle during the night, but probably not inducing important architectural changes (Oguni et al., 2001). In sum, the major reports about cognitive dysfunctions in DS patients are about vision (visio-spatial, visio-motor), language, attention, working memory and executive functions, suggesting the role of PFC-mediated damage. Visuo-spatial impairments were also reported (Chieffo et al., 2011b) indicating that the hippocampus might be affected in these children.

3. PSYCHIATRIC/BEHAVIORAL ABNORMALITIES IN DRAVET SYNDROME

As mentioned above, attention deficits frequently appear during the second year of life and are reflected in the many neuropsychological tests performed by clinicians. Correlated to the lack of attention, DS patients show increased activity and stereotypies. Thus, their attention deficits and hyperactivity reflect the poor eye-contact and the social integration difficulties (Battaglia et al., 2013). Autistic traits are often observed in DS patients, like difficulty to establish eye-contact, no emotional reciprocity, difficulty to establish friendships and to deal with social rules (Chieffo et al., 2011a, 2011b; Villeneuve et al., 2014). However, while many authors reinforce the fact that DS children are not autistic but have severely impaired social contact (Li et al., 2011; Wolff et al., 2006a), others promote autistic traits in these children (Berkvens et al., 2015). Along the same line, DS patients tend to be repetitive in their activities and to have obsessive attitudes. During adolescence, some DS cases can display internalized behaviors : anxiety, depression or exhibit externalized behaviors: becoming aggressive, hyperactive and rule-breaking (Akiyama et al., 2010; Battaglia et al., 2013; Olivieri et

al., 2016). Excessive familiarity with strangers, and poor danger awareness was reported by *Villeneuve et al., 2014*. In adulthood, however, patients seem to be calmer, but still maintain their tendency to perseverate, difficulty to communicate and exhibit motor impairments that render them socially isolated. In summary, the main behavioral features in DS patients are characterized by hyperactivity and social isolation and in some cases internalized or externalized behaviors. In the studies that performed continuous behavioral and cognitive analysis through life, there was high evidence that the phenotype tends to get worse. In adulthood, fully independent patients have rarely been reported, but some can become only partially dependent (Akiyama et al., 2010).

Chapter 4- ANIMAL MODELS OF EPILEPSY AND SEIZURES CONSEQUENCES ON COGNITION

Several mouse and rat models of epilepsy have been developed and described in the literature. There are two types of models: *1)* models of acute or chronic seizure induction in a normal brain that does not indicate the presence of an epileptogenic condition and *2)* models that are associated with permanent "epileptic" disturbances (i.e. mice/rats carrying genetic mutations associated to epileptic phenotypes).

Although experimental studies using animal models are crucial to understand the physiopathology of epilepsy and develop anti-epileptic drugs, they also have many limitations. The seizure types in humans are very diverse, and some of them might be hard to reproduce in the rodent models. Accordingly, different epileptic syndromes are characterized by the typical seizures that the patients present. Although several mouse models seem to reflect human epilepsies, it is impossible to imagine that the mouse model will faithfully reflect all the aspects of the human epileptic syndrome (Guillemain et al., 2012). In addition, the genetic heterogeneity of backgrounds observed in human cohorts does not reflect the homogeneity of a particular group of animals with very little genetic variability, under controlled house conditions in the animal facility. Rodent models carrying genetic mutations found in epileptic patients are still one of the most accepted models by the epilepsy scientific community (Frankel, 2009; Guillemain et al., 2012). They usually fulfill three criteria, namely face validity (analogy to the human symptoms), construct validity (conceptual analogy to the cause of the disease) and predictive validity (specific response to treatments in patients). The rodent models of epilepsy have contributed to important advances and knowledge of human epilepsies and the associated comorbidities, contributing to the drug-therapy improvement and the more accuracy in the diagnosis.

1. MODELS OF RECURRENT SEIZURES AT EARLY-AGE ON THE DEVELOPING BRAIN AND THEIR CONSEQUENCES ON BEHAVIORAL AND COGNITIVE PHENOTYPES

1.1 *Hyperthermia-induced seizures: the model of febrile seizures, its epileptic and behavioral consequences*

As stated earlier, FS are convulsions associated with fever and are typically elicited by temperature higher than 38.5ºC in humans (Ellenberg and Nelson, 1978). Fever, an adaptive host defense response to viral and bacterial infections, and other inflammatory stimuli, relies on coordinated neuro-immune interactions between the periphery and the brain (Alheim and Bartfai, 1998). Yet, FS are not identical to hyperthermia-induced seizures, because febrile seizures occur in response to fever that triggers the release of pro-inflammatory cytokines (interleukin (IL)-1, IL-6 and tumour necrosis factor (TNF)-α) (Alheim and Bartfai, 1998). It was previously described that inducing fever in rodents, through injection of established pyrogenic agents (i.e. lypopolysacharide) to provoke an increase of body temperature of more than 1ºC (in an inflammation context) is almost impossible (Cartmell et al., 1999; Fewell and Wong, 2002; Heida and Pittman, 2005). However, while children present FS, they are also sensitive to hyperthermia in most cases. Moreover, FS and hyperthermic seizures share common mechanisms trough cytokines as mediators (i.e. Il-ß) (Dubé et al., 2005; Gatti et al., 2002).

The rat model of experimental FS was largely described in the literature (Baram et al., 1997; Bender et al., 2003; Dubé et al., 2005, 2012). Simple FS, lasting less than 15 minutes, are known to be self-limited, not causing brain damage and cognitive impairment (Berg and Shinnar, 1996). The effect of complex FS (lasting longer than 15minutes), however, is more controversial. Briefly, FS are induced in P10-11 rats and P14-15 mice by elevating the body temperature at a rate of 0.5ºC every 2 minutes using hot air. Seizures are usually triggered at an average of 41ºC. Animals are maintained in hyperthermia (40-42ºC) from the initial behavioral sign of a seizure (time 0) to a total duration of 15 minutes for simple FS or 30 minutes for complex FS. Neither type of FS induces neuronal death (Bender et al., 2003; Chang et al., 2003).

The occurrence of FS increases the probability of recurrent FS in children (Annegers et al., 1987) and in animal models (Dubé et al., 2010; McClelland et al.,

2011; Yagoubi et al., 2015). In animal models, the occurrence of further epileptic seizures and the reduced thresholds to chemically induced seizures after one prolonged FS episode indicate that FS lead to epileptogenesis in the immature brain (Dubé et al., 2010).

Many studies in rodents addressed the neuropathological consequences of FS. It was clearly showed that FS perturb the neuronal network of the hippocampus rending it hyperexcitable throughout life without cell loss (Bender et al., 2003; Dube et al., 2000; Dubé et al., 2010). However, fewer reports investigated the long-term effects of FS in cognition. This can be associated to the benign or self-limited effect of these seizures in young children and the controversies about their effects. One prolonged hyperthermic seizure (~25-30 minutes) was shown to cause memory deficits in the spatial Morris water maze test in rats, however the effects were usually moderate or transient (Dubé et al., 2009; Rajab et al., 2014; Yagoubi et al., 2015). Also, the results in animal models of FS are contradictory. Indeed, after one prolonged hyperthermic seizure (30 minutes) in rats, some authors showed alterations in hippocampus synaptic plasticity (increased LTP and reduced LTD) but no spatial memory deficits (Lemmens et al., 2009; Notenboom et al., 2010). Interestingly, one study in mice has shown an age-dependent effect of FS on cognition. While FS induced at P10 cause cognitive problems, when induced at P14 they cause an enhancement in hippocampal-dependent memory performance (Tao et al., 2016).

Simple episodes of hyperthermic seizures (5 minutes) have been induced chronically in rats (1, 3 and 9 episodes over 1, 3 and 3 days respectively) at P10 and the animals were tested for spatial memory at P35 and at P60. One simple FS did not change memory performance at P35 or at P60, however the animals who experienced 3 or 9 seizures, respectively exhibited memory deficits at P35 and those where maintained at P60 (adulthood) in the group which experienced 9 seizures, whereas it recovered in the group with 3 seizures (Xiong et al., 2014).

Thus it was concluded that one episode of brief hyperthermia-induced seizure (<15 minutes) does not cause memory deficits, but long-lasting or repeated episodes of these seizures seem to affect normal brain development. The behavioral results seem to indicate memory deficits caused by the seizures. Additional studies are however required to confirm these findings.

1.2 *Flurothyl-induced seizures: its epileptic and behavioral consequences*

Flurothyl, a $GABA_A$ antagonist, is a volatile chemoconvulsant that was previously used to induce seizures in severely depressed patients as an alternative to electroconvulsive therapy (Fink, 2014) and has been used to induce repeated seizures in rats and mice (Holmes et al., 1998). It is a good model for repeated seizure induction, due to the low mortality level and the rapid reestablishment of the animals following the seizure episode.

Flurothyl is infused into a plexiglass closed chamber usually at a rate of 20µL/min, until the seizure occurs. The number of induced seizures usually varies. *Holmes et al*, reports a seizure-induction protocol of a minimum of 25 seizures and a maximum of 100 seizures induced during 5-10 days (5 -8 seizures p/day) (Holmes et al., 1998). Seizures are induced at different ages from P1 to P70. A follow up study did not report spontaneous seizures following the protocol of flurothyl-induced seizures in neonatal rats (Holmes, 2009). However, recently, *Kadiyala et al. 2016*, induced seizures for 1, 5 and 8 days, at 7 weeks of age in C57BL/6 mice and observed the appearance of spontaneous seizures. The authors report that one single seizure does not induce the appearance of subsequent GTC seizures, 5 seizures and 8 seizures induced subsequent GTC seizures in 28% and 95% of mice respectively. These spontaneous seizures in remitted within 1 month (Kadiyala et al., 2016)

At the neuronal network level, repeated flurothyl-induced seizures lead to persistent decreases in GABA currents in the hippocampus and neocortex (Isaeva et al., 2009, 2010, 2013), enhanced short-term plasticity and LTP alterations (Hernan et al., 2013; Isaeva et al., 2013; Karnam et al., 2009a).

The effects of single or chronic induction of seizures by flurothyl during early life on cognition were also evaluated. One single flurothyl-induced seizure at P6 does not induce cognitive changes in rats in adulthood (Bo et al., 2004). *Karnam et al., 200*9a induced seizures from P0 to P10 and P15 to P25 (5seizures/day and 50 seizures in total) and the animals were tested for spatial memory 2 weeks following seizures. The authors observed that neonatal seizures impaired spatial memory with no differences between age of induction. Other studies used the following protocols: from P1 to P10 (7-8 seizures p/day:75 seizures in total), from P15-P37 (4-5 seizures p/day:100 seizures in total) or from P7-P11 (3 seizures p/day:15 seizures) and

behavioral testing was usually conducted 2 to 3 weeks following the seizures (P40). All the protocols above induced cognitive impairment in the different behavioral tasks tested (mainly spatial and working memory deficits) (Karnam et al., 2009b, 2009a; Kleen et al., 2011; Nishimura et al., 2011; Zhou et al., 2007). When tested at P90, almost 80 days following recurrent seizures induction from P0 to P9 (5seizures p/day – total of 50 seizures) no behavioral changes were observed in seizure-induced rats (Huang et al., 1999).

Together, the data on flurothyl induced-seizures indicate that recurrent neonatal seizures (more than 15 seizures, and usually more than one seizure per day) induce cognitive defects in adulthood, with no difference between the ages at induction in childhood (P0-P10 or P15-P37), but that seizures induced in adulthood seem to be reversible long-time after seizures induction.

The long-term effects of repeated seizures on the otherwise normally developing brain are still controversial. While it is clear that they increase epileptogenesis and alter neuronal circuits, their effects on cognition are not consistent. The majority of the studies suggest hippocampus-dependent memory deficits even though these effects seem to be transient or moderate.

2. ANIMAL MODELS HARBORING THE *SCN1A* MUTATION

2.1 *Using animal models of Scn1a mutation*

The first *Scn1a*$^{+/-}$ mutant mouse was created by (Yu et al., 2006a). This model carries a *Scn1a* knock-out (KO) gene mutation obtained by target deletion of the last coding exon of the *Scn1a* gene (encodes the domain 4 (D4) downstream of the segment 3 (S3) and the cytoplasmic tail). Following this model, other models of DS pathology have been created (Miller et al., 2014; Ogiwara et al., 2007; Tsai et al., 2015) and two models of GEFS+ have also been developed in 2010 and carry missense mutations (Martin et al., 2010a; Mashimo et al., 2010) **(TABLE 3)**. To more intensively describe the neurophysiopathology and address specific neuronal populations in specific brain areas, several conditional mouse models have been developed and are described in the bottom part of **TABLE 3**.

TABLE 3. *SCN1A* MUTANT MOUSE/RAT MODELS (TYPE OF MUTATION, LOCATION, ASSOCIATED DISEASE).

SPECIE	MODEL	TYPE OF MUTATION		POSITION IN THE PROTEIN/GENE	PHENOTYPE	AUTHORS
Constitutional Models						
Mouse	*Scn1a*$^{+/-}$	truncation	KO	D4 : S3	DS	Yu et al. 2006
Mouse	*Scn1a*$^{RX/+}$	nonsense	KI-R1407X	D3 S5:S6 linker	DS	Ogiwara et al. 2007
Mouse	*Scn1a*$^{RH/+}$	missense	KI-R1648H	D4:S4	GEFS+	Martin et al. 2010
Rat	*Scn1a*$^{NH/NH}$	missense	KI-N1417H	D3 S5:S6 linker	GEFS+	Mashimo et al. 2010
Mouse	*Scn1a*$^{E1099X/+}$	nonsense	KO-E1099X	D2:D3 linker	DS	Tsai et al. 2015
Mouse	*Scn1a*$^{+/-}$	truncation	KO	Exon 1 replaced by selection cassette	DS	Miller,2014
Conditional Models						
Mouse	*Scn1a*$^{fl\text{-}A1783V\text{-}Cre/+}$	missense	*Scn1a* KI-A1783V	D4:S6	DS	Jackson Laboratory (Unpublished, 2005)
Mouse	*Scn1a*$^{fl\text{-}Dlx\text{-}Cre/+}$	truncation	*Scn1a* KO ~50% reduction forebrain interneurons	Exon 25	DS	Cheah et al. 2012
Mouse	*Scn1a*$^{fl\text{-}Ppp1r2\text{-}Cre/+}$	truncation	*Scn1a* KO in forebrain PV+ interneurons (incomplete)	Exon 1	Mild DS	Dutton, 2013
Mouse	*Scn1a*$^{fl\text{-}Emx1\text{-}Cre/+}$	truncation	*Scn1a* KO in excitatory neurons		No	
Mouse	*Scn1a*$^{fl\text{-}PV\text{-}Cre\text{-}Tg/+}$	truncation	Tg ablation in PV+ interneurons (higher deletion)	Exon 7	DS	Ogiwara et al. 2013
Mouse	*Scn1a*$^{fl\text{-}PV\text{-}Cre\text{-}KI/+}$	truncation	*Scn1a* KO in PV+ interneurons (incomplete)		Mild DS	
Mouse	*Scn1a*$^{fl\text{-}VGAT\text{-}Cre/+}$	truncation	*Scn1a* KO in global interneurons		Severe DS	
Mouse	*Scn1a*$^{fl\text{-}Emx1\text{-}Cre/+}$	truncation	*Scn1a* KO in global excitatory neurons		No	
Mouse	*Scn1a*$^{fl\text{-}Emx1\text{-}VGAT\text{-}Cre/+}$	truncation	*Scn1a* KO in global excitatory and inhibitory neurons		DS	
Mouse	*Scn1a*$^{fl\text{-}SST\text{-}Cre/+}$	truncation	*Scn1a* KO in SST interneurons (incomplete)	Exon 25		Rubintein et al.2015

2.2 *Impaired neuronal inhibition in Scn1a mouse models: Role of interneurons*

The creation of the *Scn1a*$^{+/-}$ KO model by (Yu et al., 2006a), was very important to better understand the neurophysiopathology in DS. The KO mutation caused the reduction of $Na_V1.1$ staining by half in heterozygous animals and to 100% in homozygous animals. Homozygous mutant mice (*Scn1a*$^{-/-}$) showed severe ataxia, seizures beginning at day 9 (coinciding with the beginning of the channel's expression) and died by day 15 (Yu et al., 2006a), showing that $Na_V1.1$ is essential for life. The $Na_V1.1$ staining was observed in pyramidal neurons and inhibitory interneurons in the hippocampus but also in other brain areas. Using electrophysiogical tools, they showed that the $Na_V1.1$ driven sodium current of the hippocampus pyramidal cells was lower than 10%, while it corresponded to approximately 75% in the interneurons. Moreover, the number of interneurons was unaltered (anti-GAD antibody staining), and most of

them where positive for $Na_V1.1$ in WT mice. The authors clearly illustrated a substantial decrease in sodium current levels of interneurons in the *Scn1a*$^{+/-}$ and *Scn1a*$^{-/-}$ mutant mice, correlated with a decrease in firing frequency (as seen by decreased number of action potentials for a given current injection) in those interneurons. The results confirmed that $Na_V1.1$ haploinsufficiency caused brain excitability rather than inhibition. The excitability was thus associated to a loss of inhibition mediated by interneurons, which suffered a massive $Na_V1.1$ reduction. The excitability and sodium currents in pyramidal cells were unaffected in *Scn1a*$^{+/-}$ mice (Yu et al., 2006a). This study was a major discovery for the field because: *1)* *Scn1a*$^{+/-}$ mice had striking phenotypic similarities to human DS pathology that varies according to the genetic background (as observed in humans), Thus, this model could be used in pre-clinical investigation of pharmacological treatments; and *2)* the electrophysiological studies allowed the extrapolation of the cause of excitability and epileptic activity in DS patients based on the interneuron physiopathology. In sum, $Na_V1.1$ are preferentially expressed in GABAergic neurons, although a small fraction was observed in the excitatory cells and this suggests that DS disease is caused by a loss of GABAergic-driven inhibition.

With the creation of other *Scn1*a mutant mouse models, these results were further confirmed (Martin et al., 2010a; Ogiwara et al., 2007). While further investigating the consequences of $Na_V1.1$ reduction of function in the *Scn1a*$^{RH/+}$ mouse model (KI-missense mutation), *Hedrich et al., 2014* showed that in addition to previously reported reduction in Na+ current in the cortex, there was reduction in the sodium current of GABAergic thalamus and hippocampus characterized by a deficit in action potential firing at the AIS (Hedrich et al., 2014). Using the *Scn1a*$^{+/-}$ mice, *Kalume et al. 2007* observed that the firing rates of Purkinje neurons (a class of GABAergic cells in the cerebellum) from mutant ($^{-/-}$ and $^{+/-}$) mice were substantially reduced, as seen previously in the hippocampus (Yu et al., 2006a), an alteration that could be responsible for ataxia observed in these mice. Later, the same authors reported reduced Na^+ currents and action potential firing in GABAergic neurons of the reticular nucleus of the thalamus potentially related with the sleep abnormalities observed in the *Scn1a*$^{+/-}$ mice and reported in the same study (Kalume et al., 2015).

The *Scn1a*-KI mouse model created by *Ogiwara et al., 2007* showed that Nav1.1 is primarily localized at the AIS, axons, and soma of parvalbumin (PV+) interneurons in the developing neocortex and hippocampus.

In 2012, *Cheah and her collaborators*, created a conditional mouse model with the specific ablation of $Na_V1.1$ in the forebrain and observed that the mice had a severe DS-like phenotype similar to the *Scn1a*$^{+/-}$KO mouse created before by the same laboratory (Cheah et al., 2012; Yu et al., 2006a).

While the studies with the KO mouse evaluated the effect of the specific deletion on spontaneous seizures frequency and survival rate, the *Scn1a*$^{RH/+}$ (model of GEFS+) was used to evaluate the seizure susceptibility that characterized the model because these mice do not otherwise present enough spontaneous seizures and the mortality is inexistent. *Dutton et al. 2013* suggested that the phenotype could be due to a specific type of interneurons and studied the different contributions of the excitatory and inhibitory neurons. They showed that, in the hippocampus and neocortex, 69% of $Na_V1.1$ immunoreactive neurons were also positive for PV. In contrast, 13% and 5% of $Na_V1.1$ positive cells in the hippocampus and neocortex, respectively, were found to co-localize with excitatory cells. Next, they reduced the expression of *Scn1a* in either a subset of interneurons (mainly PV interneurons) or excitatory cells by using conditional ablation of *Scn1a* gene in mice and observed that the reduction in interneurons of the neocortex and hippocampus was sufficient to reduce thresholds to induced-seizures, whereas thresholds were unaltered following inactivation in excitatory cells (Dutton et al., 2013).

Ogiwara et al., 2013, using the DS mouse model, showed that $Na_V1.1$ haploinsufficiency in excitatory and inhibitory neurons are both involved in the pathology of DS. By using three conditional mouse models that had the conditional ablation of Nav1.1 specifically in forebrain interneurons, excitatory neurons or both, they observed that: 1) the ablation of $Na_V1.1$ specifically in excitatory neurons did not change the phenotype; 2) the ablation of the $Na_V1.1$ channel in the interneurons but not in the excitatory neurons caused a more severe phenotype (higher lethality and spontaneous seizures) than observed before in the constitutive *Scn1a*-KI mouse model; 3) but the severe lethality was rescued in the model by additional Nav1.1 deletion in excitatory neurons. Completing the results, the two major subtypes of interneurons in layer V of the neocortex, PV+-expressing and somatostatin (SST)-expressing, had impaired excitability, resulting in desinhibition of the cortical network (Tai et al., 2014). An important role of the impaired GABAergic ininhition in the DG in the *Scn1a*$^{E1099X/+}$ DS mouse model have been proposed recently by *Tsai et al., 2015*. They also showed that the $Na_V1.1$ staining is decreased in the DG at post-natal week 3, but not in CA1 or

CA3 areas, suggesting that the hippocampus gating might be primarily affected in these models in the critic epileptic period (Tsai et al., 2015).

All together, the studies using animal models indicate that the neuronal cause for DS is a widespread loss of sodium currents in the inhibitory GABAergic neurons. The ablation of $Na_V1.1$ in the forebrain is sufficient to cause the disease and while different interneuron types have been implicated (Purkinje neurons, reticular nucleus of the thalamus or SST, PV+ interneurons were consensually reported to play a major role in DS pathology.

2.3 *Strain and age dependent - phenotypic severity: mortality, seizure frequency and electrophysiological properties.*

As described in the previous part, the creation of the first *Scn1a*$^{+/-}$ mutant mice (model of DS), revealed high dependency of the genetic strain to the severity of the phenotype, as observed in DS patients. (Yu et al., 2006a). They observed that the mortality was very high in *Scn1a*$^{+/-}$ mutant mice in pure C57BL/6 background and almost inexistant in the 129/SvJ genetic background **(FIGURE 10B)**, and that the mice in the mixed 129:B6 hybrid background from F2 and F3 generations had an intermediate phenotype **(FIGURE 10A)**. Showing striking correlation with mortality the spontaneous seizures were not observed in *Scn1a*$^{+/-}$ mutants in the 129 genetic background, but frequent in the hybrid 129:B6 and very frequent C57BL/6 backgrounds (Yu et al., 2006a). Thus, the *Scn1a*$^{+/-}$ mutation induced a severe DS-like phenotype in mouse models with B6 background and a mild phenotype (cannot be considered DS) in the 129 background, possibly by compensatory genetic modifications. These results were further confirmed in other DS mouse models (Miller et al., 2014; Ogiwara et al., 2013; Tsai et al., 2015). In 2009, *Oakley and his colleagues* showed that the *Scn1a*$^{+/-}$ mutant mice in pure B6 background were sensitive to seizures-induced by hyperthermia (SIH), a phenomenon largely described in DS patients (Dravet et al., 2005). They saw that no P17-18 *Scn1a*$^{+/-}$ had SIH, but practically all P20-22 and P30-46 *Scn1a*$^{+/-}$ mice had myoclonic seizures followed by generalized seizures caused by elevated core body temperature. The seizure susceptibility and severity was worse in the P30-46 mice (Oakley et al., 2009a) **(FIGURE 10C)**. In 2013, *Cheah et al.*, interestingly showed that the timing at increase in $Na_V1.1$ channel staining correlated with the decrease in $Na_V1.3$, corresponds to the critical period of spontaneous seizure generation in *Scn1a*$^{+/-}$ channels

(around P20) **(FIGURE 10D)**. The fact that the inefficient $Na_V1.1$ activity is not able to take over the role of $Na_V1.3$ can be responsible for the brain hyperexcitability in these mice. The same correlation was found in humans and corresponds to 5 months, the average of seizure onset in DS the patients **(FIGURE 10E)** (Cheah et al., 2013a). Spontaneous seizures start around P20-P21 in *Scn1a*$^{+/-}$ mice in pure B6 background (Kalume et al., 2013; Yu et al., 2006a). In the electrocorticogram (ECoG) recordings for spontaneous seizures in *Scn1a*$^{+/-}$ mice, studied in *Kalume et al., 2013* the animals presented an average of spontaneous seizures per day that varied from 3 for animals who survived to 9 in animals who died following the intense seizure activity. They confirmed a striking correlation between high seizure activity and death in those mice, and a critical period of higher incidence of death from P23 to P27 (Cheah et al., 2013b). *Mistry et al., 2014* showed that preserved hippocampus sodium current density in GABAergic interneurons contributes to the milder phenotype of *Scn1a*$^{+/-}$ 129 mutant mice. Also they reinforced the observations made first by *Ogiwara et al., 2013*, showing that excitatory pyramidal neurons contribute to severity of phenotype in *Scn1a*$^{+/-}$ mutant mice. They observed an increase in the Na^+ current in hippocampal pyramidal cells that was age-dependent, and correlated with the higher spontaneous seizure activity in the *Scn1a* $^{+/-}$ 129:B6 mutant mice (Mistry et al., 2014). Later, it was demonstrated that *Scn1a* $^{+/-}$ 129 mice had a higher threshold for SIH, fewer myoclonic seizures when compared to *Scn1a* $^{+/-}$ B6 mice, similar to patients with GEFS+. Consistent with this mild phenotype, *Scn1a*$^{+/-}$ 129 mice had higher sodium currents in inhibitory GABAergic neurons, indicating less impaired excitability of those neurons (Rubinstein et al., 2015a). Concerning the *Scn1a*-RH mouse model created by *Martin et al. 2010*, the authors observed that all the homozygous *Scn1a*$^{RH/RH}$ mice die by P25 following high frequency of spontaneous seizures while the heterozygous and WT mice presented the same survival proportion. The ECoG recordings for spontaneous seizures in the heterozygous *Scn1a*$^{RH/+}$ were done between 3-5 months and only few spontaneous seizures were observed. However, they presented lower threshold for hyperthermia and flurothyl-induced seizures when compared to WT controls (Martin et al., 2010a).

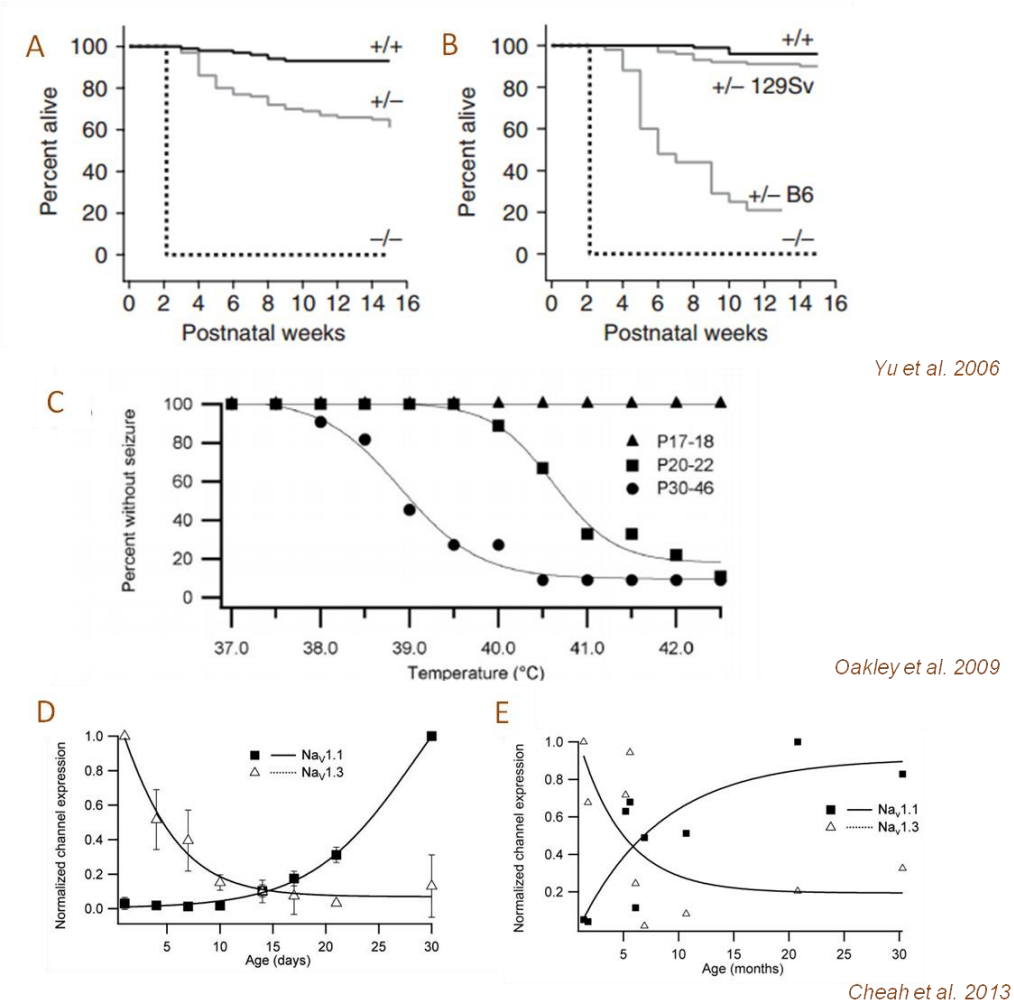

FIGURE 10. SURVIVAL, EPILEPTIC PHENOTYPE AND TIMING FOR NA_V EXPRESSION IN THE BRAIN. Survival percentage according to the genetic background in *Scn1a*$^{+/-}$ mutant mice (**A**-mixed 129:B6 background, **B**-129 and B6 backgrounds) and age-dependent seizure susceptibility (**C**). Expression of sodium channel proteins in developing mouse cerebral cortex (**D**).Expression of sodium channel proteins in developing human cerebral cortex (**E**). From (Cheah et al., 2013b; Oakley et al., 2009b; Yu et al., 2006a).

All together, these studies showed a highly phenotypic correlation to the genetic background confirmed by the severity of the phenotype, and also, an age-dependent seizure susceptibility in the *Scn1a*$^{+/-}$ mutant mice.

2.4 *Behavioral/cognitive phenotypes in mouse models of Scn1a gene mutation*

The *Scn1a* mouse models have striking similarities to human diseases GEFS+ and DS. They show sensitivity to SIH, spontaneous seizures and high mortality as observed in DS patients. It was important to confirm if *Scn1a* mutant mice presented behavioral abnormalities.

2.4.1 DS mouse model

The first behavioral observation in *Scn1a* mice was done in *Yu et al., 2006* when they observed dramatic behavioral abnormalities in homozygous *Scn1a*$^{-/-}$ mice' prior to death (in the 3 genetic backgrounds:129; B6 and 129:B6) . From P9 the homozygous mice started showing progressive epileptic seizures phenotype and could easily be distinguished from the *Scn1a*$^{+/-}$ heterozygous and the WT mice. They develop severe ataxia, with limb tremors, side-to-side swaying and complete loss of postural control. The time to recover their righting reflex (between back and up-side position) was significantly higher in *Scn1a*$^{-/-}$ mice, they were progressively immobile and did not feed themselves leading to death by P15 (Yu et al., 2006b) **(TABLE 4)**. In a later study, ataxic phenotype was confirmed in *Scn1a*$^{-/-}$ mice further by impaired gait, coordination and motor reflexes when compared to the *Scn1a*$^{+/-}$ and WT mice (Kalume et al., 2007a). These findings reported on young *Scn1a*$^{-/-}$ mice **(TABLE 4)** were correlated with the low firing rates of cerebellar Purkinje neurons, as mentioned earlier. Interestingly, the *Scn1a*$^{+/-}$ had a similar phenotype to WT mice at this age. The same ataxia profile was observed in the homozygous *Scn1a*$^{RX/RX}$ mice (Ogiwara et al., 2007).

TABLE 4. BEHAVIORAL ABNORMALITIES OBSERVED IN YOUNG *SCN1A*$^{-/-}$ HOMOZYGOUS MICE.

Mouse model		From P9-P16		Authors
		observation	results	
Scn1a+/- (129,B6,129:B6)	Yu et al. 2006	Righting Reflex	*Scn1a*$^{-/-}$: **Impaired** *Scn1a*$^{+/-}$:Normal	Yu et al. 2006
		Ataxia, limb tremors, side-to-side swaying and complete loss of postural control	*Scn1a*$^{-/-}$: **Impaired** *Scn1a*$^{+/-}$:Normal	
		Auto-feeding	*Scn1a*$^{-/-}$: **Impaired** *Scn1a*$^{+/-}$:Normal	
Mouse model		**From P13-P21**		**Authors**
		observation	**results**	
Scn1a+/- (129:B6)	Yu et al. 2006	Gait	*Scn1a*$^{-/-}$: **Impaired** *Scn1a*$^{+/-}$:Normal	Kalume et al, 2007
		Cordination	*Scn1a*$^{-/-}$: **Impaired** *Scn1a*$^{+/-}$:Normal	
		Motor reflexes	*Scn1a*$^{-/-}$: **Impaired** *Scn1a*$^{+/-}$:Normal	

In 2012, Han and his collaborators conducted a battery of behavioral and cognitive tasks using the *Scn1a*$^{+/-}$ mutant mice in the pure B6 background at adulth age. As illustrated in **FIGURE 10B**, the percentage of survival of these mice at 12 weeks is

20%. The animals were tested between 2 and 8 months of age. The authors reported profound behavioral and cognitive alterations in these animals (Han et al., 2012b) **(TABLE 5)**. *Scn1a*$^{+/-}$ mice were hyperactive, anxious and presented stereotyped behavior when compared to the WT littermates. They also reported important autistic-like traits as social interaction deficits and social avoidance. To ensure that social deficits were not correlated to olfactory perception, they conducted different tests. Using olfactory tests, they showed that, while food perception and preference was not changed, they clearly avoid social and aversive odors. Hippocampus-dependent memory was assessed using the Barnes maze and contextual-fear conditioning (CFC) tests. The contextual-fear and spatial memories were impaired **(TABLE 5)**. A reduction in $Na_V1.1$ staining was confirmed in the *Scn1a*$^{+/-}$ animals in the medial prefrontal cortex, motor cortex, sensory cortex, parietal cortex and hippocampus CA1 region (Han et al., 2012b). Using electrophysiological recordings, they reported a deficit in GABAergic transmission, observed by a decrease in spontaneous inhibitory post-synaptic current frequency (sIPSC), and an increase in spontaneous excitatory post-synaptic current (sEPSC) in pyramidal cells of the CA1 region of the hippocampus and prefrontal cortex. The synaptic functions, measured with the miniature IPSP and EPSP, were unaltered.

TABLE 5. BEHAVIORAL AND COGNITIVE ALTERATIONS IN SCN1A$^{+/-}$ MUTANT MICE IN PURE B6 BACKGROUND. REPORTED BY HAN ET AL.2012.

Mouse model	From 2-8 months of age			Authors
	Test	Results	Main conclusion	
Scn1a+/- (B6) *Yu et al. 2006*	Open field	***Scn1a*$^{+/-}$:** ↑ Distance travelled ↓Time in the center	***Scn1a*$^{+/-}$:** ↑ activity ↑ anxiety ↑ stereotyped behaviour	*Han et al, 2012*
	Stereotyped behaviour	***Scn1a*$^{+/-}$:** ↑ time self grooming ↑ circling behaviour		
	Nesting behaviour	***Scn1a*$^{+/-}$:** ↓ nest-building ability		
	Elevated plus maze	***Scn1a*$^{+/-}$:** ↓ entries in open arms ↓ time in open arms		
	Tree-chamber social preference	***Scn1a*$^{+/-}$:** ↓ Sociability ↓ Social Novelty	***Scn1a*$^{+/-}$:** ↓ social behaviour ↔ Agressivity	
	Open field social interaction	***Scn1a*$^{+/-}$:** ↓ interaction with the stranger		
	Reciprocal interaction	***Scn1a*$^{+/-}$:** ↓ agresive interactions ↓ non-agresive interactions ↑ immobilization		
	Olfactory discrimination	***Scn1a*$^{+/-}$:** ↔ preference for food odor ↓ social odor preference (male/female) ↔ avoidance of aversive/stressing odor (fox)	***Scn1a*$^{+/-}$:** ↔ Odor perception ↓ preference for social odors ↔ avoidance of stressfull odor	
	Olfactory habituation/dishabituation	***Scn1a*$^{+/-}$:** ↑ aversion to novel odors; ↓ preferencefor social odor ↔ preference for food odor		
	Novel Object Recognition	***Scn1a*$^{+/-}$:** ↔ preference for the novel object	***Scn1a*$^{+/-}$:** ↔ novel object recogntion ↓ hippocampus-dependent memory function.	
	Barnes circular maze	***Scn1a*$^{+/-}$:** ↓ spatial learning ↓ spatial memory		
	Contextual fear-conditioning	***Scn1a*$^{+/-}$:** ↓ freezing 30 min and 24 h after the shock		

Ito et al, 2013 also tested the DS mouse model *Scn1a*$^{RX/+}$ created by (Ogiwara et al., 2007). Similar to the previous study (Han et al, 2012), the *Scn1a*$^{RX/+}$ in pure B6 background showed hyperactivity that normalized after habituation, normal anxiety profile, hippocampus-dependent memory deficits, and social interaction problems. They reported also, olfactory problems and normal motor coordination (Ito et al., 2013) **(TABLE 6)**.

To go further in the study, *Han et al. 2012* also conducted behavioral tasks to test the conditional *Scn1a*$^{fl\text{-}Dlx\text{-}Cre/+}$ created by (Cheah et al., 2012) that has the specific

deletion of $Na_V1.1$ in forebrain interneurons (represented in **TABLE 3**). The *Scn1a*$^{fl\text{-}Dlx\text{-}Cre/+}$ mice with conditional $Na_V1.1$ reduction showed similar behavior compared to the *Scn1a*$^{+/-}$ with ubiquitous $Na_V1.1$ ablation indicating that the GABAergic interneuronopathy was responsible for the behavioral alterations observed. Using low-dose clonazepan (enhancer of GABAergic transmission), they clearly rescued the social deficits and the contextual fear conditioning impairment observed in the *Scn1a*$^{+/-}$ mutant mice, without changing the hyperactive phenotype.

TABLE 6. BEHAVIORAL ABNORMALITIES OBSERVED IN *SCN1A*$^{RX/+}$ MICE IN ITO ET AL. 2013

Mouse model	From 2-7 months of age			Authors
	Test	Results	Main conclusion	
Scn1a$^{RX/+}$ (B6) *Ogiwara et. 2007*	**Home cage behavior**	***Scn1a***$^{RX/+}$**:** ↓ Distance travelled ↓ Rearing ↑ Grooming	***Scn1a***$^{+/-}$**:** ↑ novelty-associated activity ↔ Activity after habituation ↑ or ↔ anxiety	*Ito et al, 2013*
	Open field	***Scn1a***$^{RX/+}$**:** ↑ Distance tavelled (1st 10 min.) ↔ Distance travelled (10-30min.) ↓ Time in the center		
	Dark/light	***Scn1a***$^{RX/+}$**:** ↑ Number of entries ↔ Time in the light side		
	Elevated plus maze	***Scn1a***$^{+/-}$**:** ↑ time in open arms ↑ distance travelled		
	Three-chamber social interaction	***Scn1a***$^{RX/+}$**:** ↓ Sociability ↓ Social Novelty	***Scn1a***$^{+/-}$**:** ↓ social behavior	
	Reciprocal interaction	***Scn1a***$^{RX/+}$**:** ↓ Sociability (same age/genotype stranger mice) ↔ Sociability (younger mice)		
	Buried food	***Scn1a***$^{RX/+}$**:** ↑ latency to find the food.	***Scn1a***$^{RX/+}$**:** ↓ Olfactory sense	
	BarnesMaze	***Scn1a***$^{RX/+}$**:** ↓ spatial learning ↓ spatial memory ↓ reversal learning	***Scn1a***$^{RX/+}$**:** ↓ hippocampus-dependent memory	
	Rotarod and footprint	***Scn1a***$^{RX/+}$**:** ↑ latency to fall ↔ Paw coordination	***Scn1a***$^{RX/+}$**:** ↔ Locomotor ability	

Although sleep disorders are still controversial in DS patients and are mainly attributed to side effects of anti-epileptic drugs, *Kalume et al., 2015* showed sleep abnormalities (reduced delta wave power, reduced sleep spindles, increased brief wakes, and numerous interictal spikes in Non-Rapid-Eye-Movement sleep) in the *Scn1a*+/- DS mice in pure B6 background without drug treatment. With electrophysiological tools, they attributed those abnormalities to the GABAergic interneurons of the reticular nucleus of the thalamus. In line with the previous findings, *Rubinstein et al. 2015* recently published a work in which they dissected the contribution of two subclasses of interneurons affected in *Scn1a*$^{+/-}$ DS model :the PV^{+} and SST^{+} interneurons (Tai et al., 2014) to the behavioral abnormalities observed by *Han et al., 2012b*. They used conditional mice with specific ablation of the *Scn1a* gene in the PV+, SST+ or both and investigated the behavioral effects. Selective deletion of $Na_V1.1$ in PV+ or SST+-expressing interneurons increases susceptibility to thermally-induced seizures, with a higher contribution of the PV+, and the deletion of both recapitulates the phenotype observed in the *Scn1a*$^{+/-}$ mutant mice. They also observed that the reduced excitability of PV-expressing neurons caused social interaction deficits, whereas impaired excitability of SST-expressing neurons resulted in hyperactivity. Deletion in both PV and SST interneurons impaired long-term spatial memory in context-dependent fear conditioning, but was not sufficient to recapitulate the full extent of the cognitive impairment observed in the *Scn1a*$^{+/-}$ mice by *Han et al. 2012* (Rubinstein et al., 2015b).

The most recent published study was done to test the behavioral effects caused by the genetic background in *Scn1a*$^{+/-}$ mice. As described earlier, the *Scn1a*$^{+/-}$ mutant mice in the 129 pure background did not develop spontaneous seizure activity nor premature death (Yu et al., 2006b) **(FIGURE 10A)**. Rubinstein and her colleagues showed that the *Scn1a*$^{+/-}$ in 129 background have higher threshold for hyperthermia-induced seizures, increased inhibitory Na+ currents in the hippocampus and preserved contextual-fear conditioning, when compared to the severe DS model in the B6 background (Rubinstein et al., 2015c). Thus, the phenotypic severity is clearly affected by the genetic background.

In conclusion, as shown in this section, the *Scn1a*$^{+/-}$ mutant mice in B6 background present striking similarities to the human DS disease (Han et al., 2012a; Ito et al., 2013; Kalume et al., 2015; Oakley et al., 2009; Rubinstein et al., 2015b; Yu et al., 2006b) in terms of spontaneous seizure activity and important behavior and cognitive

abnormalities, while the same mutant in 129 background has a mild phenotype comparable to GEFS+ patients (Rubinstein et al., 2015c; Yu et al., 2006a).

2.4.2 GEFS+ mouse model

The analysis of the behavioral phenotype in GEFS+ mouse models is more recent (Ohmori et al., 2014; Papale et al., 2013; Sawyer et al., 2016). The GEFS+ mouse model carrying the human R1648H mutation was developed by *Martin et al., 2010a*. This mutation was found in a large family of GEFS+ disease (Escayg et al., 2000a) and in one DS patient (Depienne et al., 2010).

The *Scn1a*$^{RH/+}$ mutant mice display a mild phenotype comparable to what is observed in GEFS+ patients. Sleep abnormalities, characterized by increased wakefulness and reduced non-rapid eye movement (NREM) and rapid eye movement (REM) sleep amounts during the dark phase, were reported in these mice at 3-4 months of age (Papale et al., 2013). Recently, Sawyer et al, had done a behavioral characterization of the *Scn1a*$^{RH/+}$ model and reported very mild behavioral abnormalities when compared to WT controls. They observed that the *Scn1a*$^{RH/+}$ mice have an increase in activity in the openfield and slightly impaired spatial object recognition memory and social interaction. They also reported an increase in the cued-fear conditioning and decreased sensory gating (Sawyer et al., 2016). The behavioral tests performed in the *Scn1a*$^{RH/+}$ model are summarized in **TABLE 7**.

TABLE 7. BEHAVIORAL CHARACTERIZATION OF THE *SCN1A*$^{RH/+}$ MICE BY SAWYER ET AL. 2016

Mouse model	From 3-4 months of age			Authors
	Test	Results	Main conclusion	
Scn1a$^{RH/+}$ (B6) *Martin et al. 2010*	**Openfield**	***Scn1a***$^{RH/+}$**:** ↑ Distance travelled ↑ Average speed ↔ Time in the center	***Scn1a***$^{RH/+}$**:** ↑ activity ↔ anxiety	*Sawyer et al., 2016*
	Object Recognition	***Scn1a***$^{RH/+}$**:** ↔ preference for novel object	***Scn1a***$^{RH/+}$**:** ⇔ preference for novel object	
	Spatial object Recognition	***Scn1a***$^{RH/+}$**:** ↓ preference for displaced object	***Scn1a***$^{RH/+}$**:** Spatial recognition slightly impaired	
	Contextual fear Conditioning	***Scn1a***$^{RH/+}$**:** ↔ contextual fear memory	***Scn1a***$^{RH/+}$**:** ↔ contextual fear memory ↑ cued fear memory ↓ pre-pulse inhibition	
	Cued-fear conditioning	***Scn1a***$^{RH/+}$**:** ↑ cued fear memory		
	Startle	***Scn1a***$^{RH/+}$**:** ↓ pre-pulse inhibition		
	Predator odor exposure	***Scn1a***$^{RH/+}$**:** ↔ aversive odor avoidance	***Scn1a***$^{RH/+}$**:** ↔ Olfactory funtion	
	olfactory discrimination	***Scn1a***$^{RH/+}$**:** ↔ Olfactory discrimination		
	Visual Cliff avoidance	***Scn1a***$^{RH/+}$**:** ↓ avoidance	***Scn1a***$^{RH/+}$**:** Normal visual function	
	Visual test	↔ visual capacities		
	Social Interaction	***Scn1a***$^{RH/+}$**:** ↔ Social interaction ↓ social novelty	***Scn1a***$^{RH/+}$**:** ↔ Social interaction (slightly affected)	
	Matting calls	***Scn1a***$^{RH/+}$**:** ↔ mating calls		

A rat carrying the homozygous *Scn1a* N1417H missense mutation in the third pore of the Na_V channel, induced by gene-driven N-ethyl-N-nitrosourea mutagenesis (never observed in patients), was also generated (Mashimo et al., 2010). Homozygous mutations are lethal in all the mouse models of *Scn1a* mutation without exception, but this rat model survived normally. In humans, homozygous mutations have been reported recently only in one patient with GEFS+ and one patient with DS (Brunklaus et al., 2015). The electrophysiological studies in the *Scn1a*$^{NH/NH}$ rat model showed a decreased inhibition in the GABAergic interneurons of the hippocampus. Also similar to the previous models, they are sensitive to hyperthermia-induced seizures (Mashimo et al., 2010). However, the authors did not observe spontaneous seizures using EEG recordings from 5 weeks of age, suggestive of the mild phenotype carried by the model. The behavioral analysis showed that the rats present a slight increase in activity in the openfield and poorer spatial learning than the control WT. However, the anxiety level is normal in the elevated plus maze, the sociability skills are preserved and they reach the

same level of performance in the last day of spatial learning as the controls. The behavioral skills are only mildly affected in the rats (Ohmori et al., 2014) **(TABLE 8)**.

TABLE 8. BEHAVIORAL CHARACTERIZATION OF THE *SCN1A*$^{NH/NH}$ RAT BY OHMORI ET AL. 2014.

RAT model	From 5-8 weeks of age			Authors
	Test	Results	Main conclusion	
Scn1a$^{NH/NH}$ *Mashimo et. 2010*	**Repetitive self-grooming**	***Scn1a*$^{NH/NH}$:** ↑ Grooming	***Scn1a*$^{NH/NH}$:** ↑ Activity ↑ Anxiety ↔ Anxiety	*Ohmori et al., 2014*
	Open field	***Scn1a*$^{NH/NH}$:** ↑ Distance tavelled ↓ Time in the center		
	Elevated plus maze	***Scn1a*$^{NH/NH}$:** ↔ time in open arms		
	Three-chamber social interaction	***Scn1a*$^{NH/NH}$:** ↔ Sociability ↔ Social Novelty	***Scn1a*$^{NH/NH}$:** ↔ Sociability	
	BarnesMaze	***Scn1a*$^{NH/NH}$:** ↓ spatial learning	***Scn1a*$^{NH/NH}$:** ↓ spatial learning	
	Rotarod	***Scn1a*$^{NH/NH}$:** ↔ latency to fall - constant rotarod ↓ latency to fall - accelerated	***Scn1a*$^{NH/NH}$:** preserved mototr skills	

As expected, the two GEFS+ models (*Scn1a*$^{RH/+}$ and *Scn1a*$^{NH/NH}$) show very mild behavioral and cognitive abnormalities, as expected from animals with no mortality, low or inexistent seizure activity and mild mutations that do not severely impair the channels function. Compared to the *Scn1a*$^{+/-}$ mice in the B6 background (model of DS and severe phenotype), GEFS+ models offer a good opportunity to investigate the role of epileptic activity in cognitive and neurobiological outcomes presented by DS patients (see Chapter 5 below).

The studies in animal models in the past 10 years have helped to clarify the physiopathology behind the *SCN1A*-related diseases and confer an excellent tool to investigate potential therapeutic strategies for patients.

Chapter 5- SEIZURES AND COGNITIVE PHENOTYPE IN DS: EPILEPTIC ENCEPHALOPATHY OR CHANNELOPATHY?

While early-life seizures are the most striking feature of DS, the most debilitating consequences of the disease are often the associated cognitive and behavioral impairments. DS was classified as an EE; however there is still an ongoing debate about the variables affecting phenotype in these children. The concept of EE has recently been adapted to "*the epileptic activity itself may contribute to severe cognitive and behavioral impairment above and beyond what might be expected from the underlying pathology alone".* Consequently, suppressing the seizures might have benefic effects in improving cognition and behavioral abnormalities (Berg et al., 2010).

1. CAN SEIZURE SEVERITY BE CORRELATED WITH COGNITIVE/BEHAVIORAL OUTCOME IN DS PATIENTS?

Evidence from different epileptic syndromes suggests that seizure frequency and early age at onset could be crucial for cognitive delay. The main reason is that the immature brains are most sensitive to seizures and are certainly less able to develop a functional reserve capacity to cope with subsequent decline (*reviewed in* Hermann et al., 2002). Also, the hypothesis that *"seizures beget seizures"* have been formulated in the basis of the occurrence of brain function modifications following seizures and consequently each seizure increases the risk for further seizures (Gowers, 1881). However, this theory is still controversial (Allen Hauser and Lee, 2002; Ben-Ari et al., 2008; Karoly et al., 2017).

It is possible but not clear that the *SCN1A* mutation confers a particular epileptic profile in patients with DS. Nevertheless, the several seizure types inducing EEG abnormalities (ictal and post ictal), the age at onset and duration of the seizures observed in patients, the large therapeutic window applied and the high genotypic variability of the *SCN1A* gene spectrum associated with the infinite possible genetic and environmental modifiers accounting for the phenotypic variability, give rise to an unclassifiable range of inconsistent outcomes.

Clinical studies have reported families carrying *SCN1A* gene mutations, where amongst affected patients, those who had lower seizures number had normal cognition, while those with intractable seizures were cognitively impaired (Guerrini et al., 2010;

Suls et al., 2010; Takayama et al., 2014) The age at seizure onset and the duration of the seizures events seemed also to correlate with the worst outcomes in some cases (Acha et al., 2015; Cetica et al., 2017; Wolff et al., 2006a). Moreover, it has been hypothesized that more complex seizures, as myoclonic seizures, focal seizures, absence seizures and prolonged *SE* could be responsible by worsening the phenotype (Ragona et al., 2011a). *Chipaux and collaborators* observed three unusual cases of *SE*. In these patients the long-lasting *SE* (2, 7 and 12 hours respectively), clearly caused persistent and severe cognitive and motor deterioration following the event (Chipaux et al., 2010).

Yet, adding to the debate, many clinical studies failed to correlate the seizure profile with the cognitive outcome and the reduction of seizures seems to not ameliorate the phenotype (Akiyama et al., 2010, 2012; Nabbout et al., 2013; Riva et al., 2009; Villeneuve et al., 2014). Some authors argue that the neurological signs observed in patients (i.e. ataxia, crouching gait) can hardly be explained by the epileptic activity and that mutations in *PCDH19* do not cause this motor neuropathy. They better correlate them to the channel dysfunction at the motor neuron axon initial segment (Duflocq et al., 2008; Gitiaux et al., 2016). *Guerrini and Striano, 2016* argued that this motor impairment might have a complex origin, which also includes ataxia, in line with evidence that *SCN1A* is also expressed in basal ganglia and cerebellar Purkinje neurons. In addition, a possible detrimental effect of a high seizure frequency and multiple anticonvulsants treatment should be taken into account (Guerrini and Striano, 2016).

Despite the fact that seizures reduction did not ameliorate the phenotypes, there are very few "seizure-free" patients in response to therapy. Very few patients were reported. One study reported a case carrying the *SCN1A de novo* truncation mutation, and presenting a normal cognitive and developmental phenotype in adulthood after considerable reduction of seizures events after the age of 4 years old (Buoni et al., 2006). Another case presenting a *de novo* frameshit mutation in a patient presenting refractory seizures until 5 years of age and who presented mild cognitive impairment at 2 years of age showed normal cognitive functions by 10 years of age (Jiang et al., 2016).

With the exception of few truncation mutations found in patients presenting a mild phenotype (as described previously), the most impacting mutations for the $Na_V1.1$ function have been found in DS patients (Brunklaus et al., 2014). However, not many studies have correlated the severity of the mutation with the cognitive outcome. The presence of mosaicism and genetic modifiers make the correlations difficult to make.

Ricci et al, 2015 showed that visual functions can be affected shortly after seizure onset in DS patients, even before the diagnosis and the strong epileptic period. They reported that the language functions are more preserved in these children, and suggest a possible role of the $Na_V1.1$ haploinsufficiency in impairing these primitive functions (Ricci et al., 2015). However, in this study only one patient (out of 5) had a confirmed *SCN1A* mutation and had a rare late cognitive impairment appearance. Nevertheless, the visual impairment was otherwise reported in the majority of DS patients. *Passamonti et al,* 2015 reported one family carrying a splicing inherited mutation in the *SCN1A* gene and a large heterogeneity of epileptic and neuropsychological phenotypes (from non-affected to DS). All the affected patients (having epileptic history) shared common visual problems, and one of the non affected patients (never had a seizure, but carrying the mutation) had also mild visual problems (Passamonti et al., 2015). Opposite observations (higher impairment in language than visual function in DS patients) have also been reported by *Acha et al., 2015*, where they correlate the worst epileptic phenotypes to the poorer cognitive outcomes.

To date, all these clinical observations provide controversy as to the origins of the behavioral and cognitive deficits in DS. It would have been ideal to test whether children have entirely normal cognitive skills before seizure onset to clarify this issue. However, there are methodological limitations in planning prospective studies that would unequivocally demonstrate complete integrity of early development. Studying more simple/controlled models is crucial to understand the epileptic/cognitive and genetic/cognitive correlations in DS patients.

2. DO $NA_V1.1$ DYSFUNCTIONAL MICE SUPPORT THE CHANNELOPATHY THEORY?

The induction of repeated early-life seizures in the normal rodent brain have suggested the appearance of important neuronal rearrangements and behavioral modifications in those animals (*reviewed in* Barry and Holmes, 2016). These studies suggest that seizures can induce long-lasting changes in an otherwise normally developing brain.

Interestingly, the identical $Na_V1.1$ truncation mutation is present in the B6 and 129 mice, however they present very different behavioral phenotypes. The DS mouse model in the B6 background has striking similarities with the human DS disease, however the same mutation in 129 background induce a mild phenotype (Rubinstein et

al., 2015c; Yu et al., 2006b). *Han et al, 2012* and *Ito et al, 2013* submitted the *Scn1a*$^{+/-}$ mice in B6 background to a battery of behavioral tasks and observed important behavior and cognitive impairment. Unfortunately, the behavioral deficits observed in these mice cannot be dissociated from the negative impact of the strong recurrent epileptic activity that these mice present throughout life. *Han et al.*, rescued the phenotype by treating the animals with GABAergic enhancer at low-dose to avoid sedation (Han et al., 2012b), and suggested that the disease was a pure consequence of the network dysfunction caused by $Na_V1.1$ haploinsufficiency.

In addition, there is now evidence in mice that the mutation of the sodium channel can result in cognitive deficits independent of seizures. *Bender et al, 2013* used an siRNA approach to knockdown $Na_V1.1$ channels selectively in the basal forebrain region, were they could target a learning and memory network while avoiding the generation of spontaneous seizures. They showed that the reduction of $Na_V1.1$ expression, without epileptic seizures in the medial septum and diagonal band of Broca lead to a dysregulation of hippocampal oscillations in association with a spatial memory deficit (Bender et al., 2013). Using the same technique, they later confirmed that $Na_V1.1$ dysfunction impairs fast- and burst- firing properties of neurons *in vivo* altering brain rhythms by decreasing theta frequency during a working memory task (Bender et al., 2016).

These studies therefore strongly support the notion that $Na_V1.1$ dysfunction *per se* can alter neuronal networks and associated brain oscillations and thus affect memory performance in DS. However these rodent models, in which the investigator can control the majority of the variables, do not account for the DS phenotypic and genetic variability and do not represent all the phenotypic spectrum present in patients. These experiments need further confirmation.

It is clear that the genetic predisposition lead to seizures. However, it is not clear whether the comorbidities present in DS are pure consequence of epilepsy, whether both epileptic and cognitive phenotypes are pure consequences of the genetic defect or whether both the genetic defect and the epileptic activity build the resulting outcome. Thus, whether DS should be considered as an EE or a channelopathy remains an outstanding question that needs to be resolved.

PROBLEMATIC AND OBJECTIVES

II- PROBLEMATIC AND OBJECTIVES

Clinical studies failed to correlate the epileptic severity with the cognitive outcome in DS (Battaglia et al., 2016; Chieffo et al., 2011b; Ragona et al., 2011a; Riva et al., 2009; Suls et al., 2010). On another hand, genotype-phenotype correlations are blurred by the occurrence of genetic and environmental modifiers and the presence of genetic mosaicism.

Experimental studies, using *Scn1a* mutant mice, push the fact that the mutation *per se* can be responsible for the long-term behavioral and cognitive outcome in DS patients, challenging its definition as an EE. Yet, it was shown that recurrent seizures in the first weeks of life result in considerable cognitive impairment in adolescent or adult rodents (Holmes, 2009).

In this controversial context, we designed a study to investigate the effect of seizures in the worsening of cognitive/behavioral phenotypes in mouse lines carrying the *Scn1a* gene mutation, an issue that had not yet been addressed. Our goal was to investigate if seizures in early life in DS and GEFS+ mutant mice can cause the developmental delay and cognitive regression observed in DS patients. Answering this question is crucial to adapt the definition of DS (as an EE or not) and for the development of adequate treatments in DS and other EEs.

To do so, we used *Scn1a* mutant mice carrying mild phenotypes (no mortality and no spontaneous seizures). We first tested if the mutation *per se* could alter the behavioral and cognitive phenotypes. We then chronically induced seizures using hyperthermia for 10 days at post-natal day 21 and evaluated the long-term effects on:

1) The evolution of the epileptic activity after the seizures induction protocol using EcoG recordings, and understand if *"seizures beget seizures"*;
2) The long-term structural modifications in adulthood (P60) by analyzing neuronal mortality using immunohistochemical analysis;
3) The long-term functional modifications in the hippocampus at later age (P60) using field and patch-clamp electrophysiological recordings;
4) The cognitive and behavioral effects at later age (P60) using different behavioral and cognitive tasks.

Material and Methods

III- MATERIAL AND METHODS

1. ANIMAL MODELS , BREEDING AND HOUSING CONDITIONS

1.1 *Scn1a*$^{+/-}$ (*Na*$_V$*1.1 knock-out): Dravet Syndrome's mouse model:*

The *Scn1a*$^{+/-}$ mice, model of Dravet Syndrome, and created by (Yu et al., 2006a) was used initially in this study. Summarizing, the *Scn1a*$^{+/-}$ mouse was obtained by disruption of the last coding exon of the gene that encodes for the Na_V 1.1 channel (*Scn1a* gene) with a replacement-type construct. This exon encodes for the domain IV of the channel downstream of the S3 segment of the cytoplasmic tail. The mouse line was generated from stem cell clones and the founding chimeric male was bred to 129/SvJ females in order to generate congenic *Scn1a*$^{+/-}$-129 SvJ mice. The line was then backcrossed in 129 SvJ background for more than 12 generations. After receiving the mutant males we crossed them with 129/SvJ females (Envigo, France) and used the litters obtained (results chapter 1). After observing a very low breeding performance we created a mixed 129/SvJ:C57BL/6 line in order to increase the number of animals to use in the experiments. We backcrossed the *Scn1a*$^{+/-}$ mutant mouse in 129 SvJ background with C57BL/6J females (Charles River, France) and used the F1 generation that were hybrid and 50% 129/SvJ: 50% C57BL/6J (Results Chapter 1 and 5).

1.2 *Scn1a*$^{RH/+}$ (*Na*$_V$ *1.1 knock-in): GEFS+ mouse model*

The knock-in GEFS+ mouse model harboring the human *SCN1A*-R1648H mutation was used in this study. This specific mutation was identified in a large and one of the first families with GEFS+ disease (Escayg et al., 2000a). This model was generated as described previously by *Martin et al., 2010b*. The targeting vector containing the human *SCN1A*-R1648H mutation was knocked-in into the exon 26 of the mouse *Scn1a* gene. The mutation resulted in the replacement of the arginine residue with a histidine residue at the position 1648 of the gene (voltage sensor of domain 4). The B6 - *Scn1a*$^{RH/+}$ heterozygous mutant male, maintained in C57BL/6J background for more than 10 generations was backcrossed with a 129/SvJ female. The F1 generation of the hybrid mixed 129/SvJxC57BL/6J background mice was used for this study (results chapter 3, 4).

1.3 *Housing conditions*

All experiments were done according to policies on the care and use of laboratory animals of European Communities Council Directive (2010/63). The protocols we approved by the French Research Ministry following evaluation by a specialized ethics committee (protocol number NCE/2014-216). All efforts were made to minimize animal suffering and reduce the number of animals used. The animals were housed under controlled laboratory conditions with a 12-h dark light cycle, a temperature of 22 ± 2°C and 55±10% humidity. Mice had free access to standard rodent diet and tap water. The number of animals per cage was maintained at 6 ± 1 containing the four test groups.

2. EXPERIMENTAL TIMELINE

To study the effect of early life seizures induced by hyperthermia on the phenotype of mouse models with *Scn1a* mutation, we organized the experimental approach as shown in **TABLE 9**. From postnatal day 8 (P8) the animals were identified and genotyped. At P21, after weaning, we induced seizures by hyperthermia (SIH) once a day for 10 days. Following the protocol of SIH 4 different cohorts of animals were prepared for: 1) Video electrocortigram (ECoG) recordings; 2) behavioral analysis; 3) electrophysiological recordings and 4) Immunohistochemistry staining. For ECoG recordings, electrophysiological recordings and immunohistochemistry males and females were used, however for behavioral studies, only males were studied to avoid hormonal interference. One cohort of animals was implanted with electrocortigram electrods immediately following the end of the SIH protocol and recorded from P34 to P90 to analyze the presence of spontaneous seizures. In parallel, SIH was also induced in three other cohorts of animals, which were allowed to age in the stabulation room before being tested at P60 (adulthood) **(TABLE 9)**.

TABLE 9. EXPERIMENTAL TIMETABLE.
Sequence of experiments from P8 to P90. All groups went through identification and genotyping, then SIH protocol followed by: either ECoG recordings (from P32 to P90), behavioral analysis, electrophysiological recordings or immunohistochemistry staining.

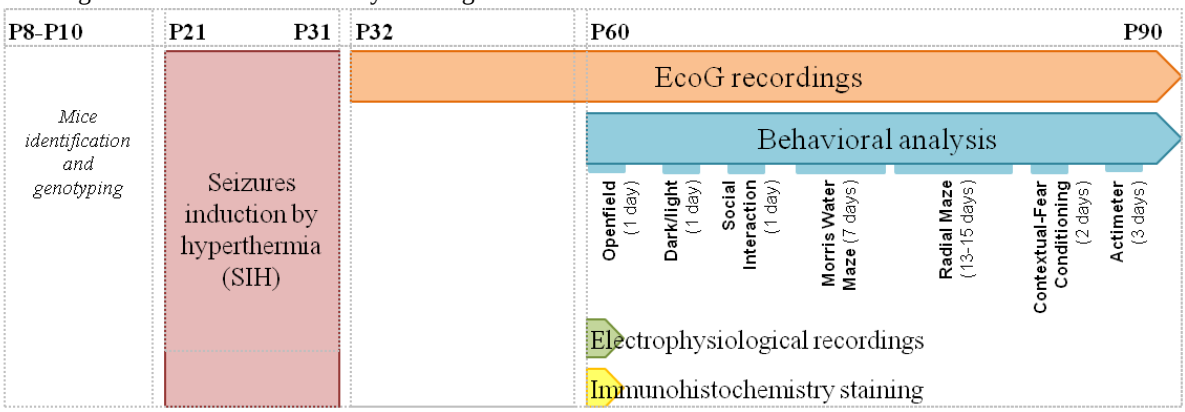

2.1 *Genotyping*

2.1.1 DNA extraction

Genotyping for mutation screening in the offspring was performed using DNA obtained from tail biopsies acquired when the animals were identified (between P8-P10). Tail biopsies were digested overnight at 56ºC and gentled shaking with lysis buffer (50 mM Tris-HCl pH 8, 100 mM EDTA pH 8, 100 mM NaCl 1% SDS) and proteinase K (10 mg/ML). After overnight incubation, samples were centrifuged for 10 minutes at 15000 g to get rid of undigested tissues and supernatants were transferred into new eppendorf tubes. To lyse cells and access genomic DNA, saturated NaCl was added to samples and incubated for 10 minutes on a rocking platform. Samples were then centrifuged for 10 minutes at 15000g at 4ºC to get rid of cell debris. Supernatants were transferred into new eppendorf tubes and DNA was precipitated with 2-propanol. After centrifugation for 10 minutes at 15000g, the pellet was washed with 70% Ethanol. After air drying the pellet, DNA was resuspended in TE buffer (100 mM Tris-HCl pH 7,5 and 1 mM EDTA). pThe DNA concentration of each sample was quantified by spectrophotometry (A260 and A280) and stored at - 20ºC.

2.1.2 DNA amplification

For PCR analysis, DNA was placed in PCR tubes and used as template for amplification by adding the Master Mix solution (each primer (presented on **TABLE 10**), ddH_2O, Buffer 5X, dNTPS and Taq Polymerase). 268, 269 and 316 primers amplify mutated $Na_V1.1$ fragment from the *Scn1a*$^{+/-}$ mouse model, while 38S and 39S amplify mutated $Na_V1.1$ fragment fom the *Scn1a*$^{RH/+}$ mouse model. All the primers were used at 10 µM concentration. For the *Scn1a*$^{+/-}$ mouse the following polymerase-chain reaction (PCR) was used : denaturation of the DNA at 95ºC for 2 min, followed by 30 cycles of amplification: 95ºC for 30 sec, 67ºC for 30 sec, 72ºC for 45 sec and a final extension step at 72ºC for 7 min. The PCR-specific primers used are presented in (**TABLE 10**). For the Ki mouse model the PCR was done with minor modifications: 94ºC for 2 min, followed by 30 cycles of amplification: 94ºC for 30 sec, 56ºC for 30 sec, 72ºC for 45 sec and a final extension step at 72ºC for 7 min. Immediately following this reaction 1µl was taken to a second reaction and mixed with ddH_20, oligomers, DNA polymerase, primer 39S and buffer to prepare for DNA sequencing (the mutant fragment is usually obtained after EcoR1 cutting, but this reaction never worked in our hands so the entire fragment surrounding the mutation had to be sequenced systematically). The PCR reaction was the following: 96ºC for 1 min, followed by 30 cycles of amplification: 96ºC for 30 sec, 50ºC for 30 sec, 60ºC for 150 sec. The sequencing was done in a platform in the institute. .

TABLE 10. PRIMERS USED FOR DNA AMPLIFICATION IN *SCN1A* MOUSE LINES.

Mouse line	Primer	Sequence 5'→3'
Scn1a$^{RH/+}$ KI (GEFS+)	38S	TTGATGACTTCTTCACTGATTGAT
	39S	ACCAGGAAGGATATGATGATGTA
Scn1a$^{+/-}$ KO (DS)	268	CGAATCCAGATGGAAGAGCGGTTCATGGTC
	269	ACAAGCTGTCATGGACATTGTCAGGTCAGT
	316	TGGCGCTCGATGTTCAGCCCAAGC

2.1.3 DNA revelation and sequencing

For *Scn1a*$^{+/-}$ mouse model, PCR products were visualized on a 1.5% agarose gel containing 2% of ethidium bromide to confirm the presence of DNA from the mutated mouse models. To allow band size estimation, 100 bp DNA ladder was added, as

demonstrated in (**FIGURE 11)**. Gel was run for 20 minutes at 100 volts in an electrophoresis bath containing 1x Tris-Acetate-EDTA (TAE) buffer and then placed under UV light for band visualization. **FIGURE 11A** shows a typical progeny genotyping containing bands for mutant and WT mice. WT mice presents one single band of 291 base pair (bp) that corresponds to non-mutant amplified band (lanes 2,4), while *Scn1a*$^{+/-}$ heterozygous mice exhibits two bands, one of 261bp (control band) and one at 141 bp that corresponds to the mutant band (lanes 1,3,5). *Scn1a*$^{+/+}$ positive (+/+) littermates were used as controls (WT mice). After DNA sequencing the files were analysed and we searched for the mutation at around base number 130. WT animals present the sequence GAATCCTACG, while mutant animals have the sequence GAATYCTACR as illustrated in **FIGURE 11B**.

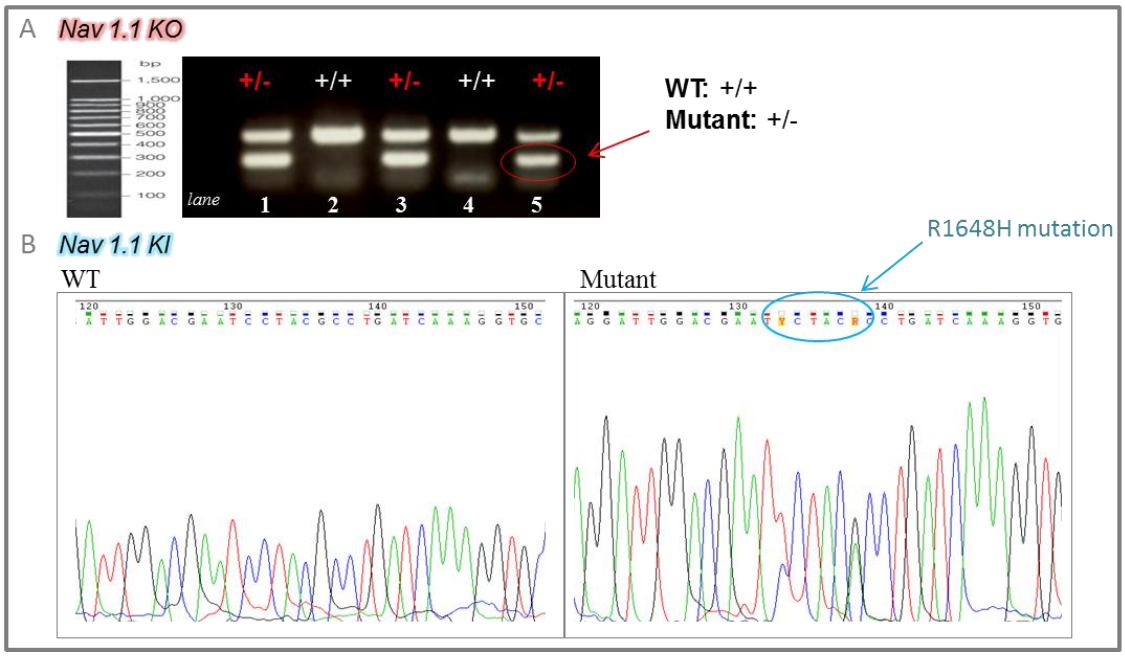

FIGURE 11. GENOTYPING REVELATION.
A: Agarose gel contaning Na_V 1.1 KO progeny. WT animals are illustrated in white (+/+) and mutants in red (+/-). **B:** DNA sequencing of the Na_v 1.1 KI progeny. On the left an example of the WT mouse and on the right the presence of the R1648H mutation surrounded by the blue circle.

2.2 *Repeated Seizures induction*

2.2.1 Seizures induction by hyperthermia

Acute seizure induction by hyperthermia (SIH) have been described previously (Oakley et al., 2009a). We optimized and developed a protocol of chronic SIH. SIH protocol started at P21 (weaning time), once a day for 10 days. The time at which seizures were induced during the day was randomized as well as the order for mice having the seizure. SIH protocol was done as described previously for acute hyperthermia induced seizures with minor modifications (Cheah et al., 2012). The mouse was placed in an incubator (Dominique Dutscher, France) (width *(w)* 23cm, length *(l)* 20cm, height *(h)* 20cm) and allowed to acclimatize for 10 minutes. The core body temperature was continuously monitored with a rectal temperature probe (type RET-4, Physitemp Instruments, Inc, USA) controlled by a temperature controller (type TCAT-2, Physitemp Instruments, Inc, USA). The temperature was increased 0.5°C every 2 minutes, until a seizure appearance or a maximum temperature of 42° was reached. The animal was then removed from the incubator and the temperature was decreased to 37°C before returning the mouse to the home cage. For mice having a seizure, the temperature threshold and behavioral characterization were noted. WT and *Scn1a*$^{RH/+}$ mice were submitted to the protocol but only mutant animals had short-lasting seizures (< 1 minute) at this temperature. Seizures were systematically video recorded to allow off line analysis. WT and *Scn1a*$^{RH/+}$ control animals followed the same handling protocol but the temperature of the incubator was maintained at room temperature.

2.2.2 Seizures induction by flurothyl

As an internal control, a convulsant known to perturb the GABAergic system was used to induce seizures in WT and *Scn1a*$^{RH/+}$ animals. Flurothyl (Bis 2,2,2-trifluoroethyl ether) (Sigma-Aldrich) induced seizures were described previously (Holmes et al., 1998). Animals were placed in a transparent plexiglas box (15 cm W, 10 cm L, 12 cm H). Liquid flurothyl was delivered using a syringe pump injector at a rate

of 10 µl/min and allowed to volatilize. The animals were removed after the appearance of a generalized tonic clonic seizure. The latency to seizure was quantified.

2.2.3 Behavioral characterization of seizures

The seizure characterization is important in order to fathom which brain areas are involved in the seizure development. According to different methods of seizure induction, the behavioral consequence in rodents will be different. SIH and Flurothyl-induced seizures show common sequence and seizure type than seizures with limbic origin (Hashimoto et al., 2006; Liautard et al., 2013). The origin of clonic seizures (grade 1-4 **TABLE 11**) happens in the forebrain. The rapid and synchronized forelimb clonus usually accompanied by head nodding indicates the activation of zones beyond the limbic system (Velíšková et al., 2005). Following the forelimb clonus a tonic component appears and the mouse loose balance having a twist of the body (failing) but a rapid effort to get back happens (grade 5 **TABLE 11**). This phase indicates the spreading of the seizure from the forebrain to brainstem. Seizures usually quickly develop to more complex seizures called generalized tonic-clonic (GTC) seizures. The GTC seizures that provoke the loss of consciousness announce the involvement of the brainstem areas (grade 6 **TABLE 11**) (Browning, 1985). This seizure event is characterized by wild run or jump with failing, followed by a tonic phase characterized by tonic flexion presenting forelimb and hind limb extension (most severe part of the seizure and sometimes culminating in death (grade 7 **TABLE 11**)) and finally long-lasting clonus in all limbs. During all the GTC seizure phase the mouse doesn't show efforts to regain balance. After passing all the steps if the seizure completely develops, the mouse regains the upright position.

TABLE 11. SEIZURES SEVERITY SCORING ADAPTED FOR SEIZURES WITH LIMBIC ORIGIN (ADAPTED FROM VELISKOVA, 2007).

SEIZURE SEVERITY SCORING

Seizures with origin in limbic structures (Veliskova, 2006)

1	Abnormal behavior (freezing, staring, orientation problems)
2	Head nodding
3	Isolated myoclonic jerks
4	Fully developped bilateral forelimb clonus
5	Forelimb clonus with a tonic component (rearing) and twist of the body (failing)
6	Generalized tonic clonic seizures: 1) with a supressed tonic phase (loss of postural control with wild running and rapid movements in all limbs) or 2) fully developped with running, wild jumping, lying on the side with hindlimb extension
7	Death

2.3 *Electrocorticogram recordings*

After SIH protocol, the mice were implanted with ECoG electrods. The electrods' implantation and ECoG monitoring was done by Dr. Fabrice Duprat and Dr. Ingrid Bethus.

2.3.1 Electrods implantation

The animals were anesthetized with ketamine (11.25 mg/kg) *Virbac/* xylasine (7.5 mg/kg) (*Rompun 2%*). After being placed in the stereotaxic support, ocular gel (Dexpanthénol , Bausch Lomb) was put into the mouse's eyes to protect them from drying. The animals were maintained at 37ºC core body temperature for all the procedure duration. The head's hair was removed using depilatory cream. An incising was done to access the scull and a local anesthetic was applied under the exposed area (Lidocaïne 21,33 mg/ml, Xylovet). The skin was cleared using clippers. The bregma position was measured in order to then calculate the distance of the wholes to it (Antero-posterior; Lateral). Fives holes were made (diameter 0.95 mm) using a screw

driver (one placed in each hemisphere as recording electrodes and one placed above the cerebellum as ground reference). The coordinates for the recording electrodes were:

- electrode 1: AP : 0.0 mm / Lat : + 3 mm;
- electrode 2 : AP : - 3.5 mm / Lat : +3 mm;
- electrode 3: AP : 0.0 mm / Lat : - 3 mm;
- electrode 4 : AP : - 3.5 mm / Lat : -3 mm;
- Reference electrode: AP : -6.0 mm / Lat : ±0.2 mm.

The screws connected to the wires (Bilaney, Plastics One) were placed in the holes. The screws were fixed to the skull with a resin (Super Bond, Sun Medical) and the electrodes were placed in the connector and enveloped with dental cement (Dentalon, Phymep) forming the hat above the mouse's head. The mice were surveyed until the recovering from anesthesia and then placed in their home cages with an anti-inflammatory in the drinking-water (Ketofen 0.04 mg/mL of water).

2.3.2 Video Electrocorticogram recordings

After recovering from surgery, the animals were allowed to rest for 2 days. They were individualized in the appropriate recording cages and connected to an amplifier (Animal Bio Amp, AD Instruments) for ECoG recording. Each mouse was connected to the amplifier through a cable and a swivel to allow the mouse to freely move in the cage. The amplifiers were connected to an acquisition system (PowerLab 16/35, AD nstruments) that converted the analogic signal into a numeric signal recorded, and anlysed with the software (Labchart 8, ADInstruments). The system was equipped with 16 amplifiers that connected 16 electrodes, which allowed us to record simultaneously 4 mice with 4 recorded channels per mouse **(FIGURE 12)**. Four infrared cameras (Day&Night, Ganz) were connected and synchronized to the ECoG leading to the analysis of the ECoG seizures and behavioral seizures, simultaneously. The animals were recorded for 2 months in regular windows of 3-days periods.

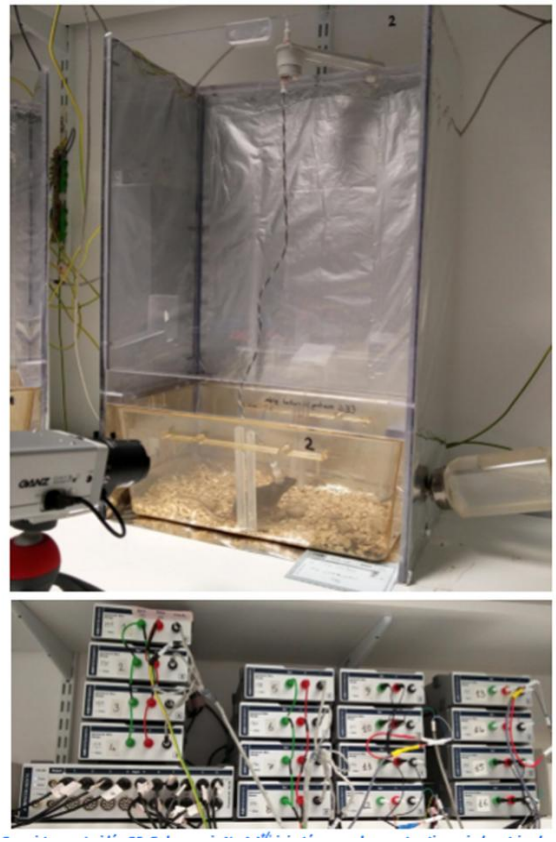

FIGURE 12. ECOG RECODINGS SYSTEM.
Top Figure: Recording cage.The mouse is connected to the signal collecting cable that has a rotator that allows the animal to freely move. Bottom figure: 16 amplifiers allowed the recording of 8 mice simultaneously. *Photo from Doctor Lavigne PhD manuscript*.

2.3.3 Signal analysis

The recordings were analyzed with Labchart 8 (AD Instruments). ECoG traces were screened manually to identify the signal with a typical seizure pattern, and the generalized tonic-clonic seizure was confirmed by watching the corresponding video. We quantified the seizures' frequency (number of seizures divided by time recorded) and their durations. All values were normalized to 24h in order to be compared.

2.4 *Electrophysiological recordings in the hippocampus*

Acute transverse hippocampal slices (350 µm thick for field recodings and 250 µm thick for whole cell recordings) were obtained from mice 60-70 days of age. Animals were first anaesthetized with isoflurane and killed in accordance with the European Communities Council Directive (80/609/EEC). Slices were cut on a vibratome (Microm HM600V, Thermo Scientific) in ice-cold dissecting solution containing (in mM): 234 sucrose, 2.5 KCl, 0.5 $CaCl_2$, 10 $MgCl_2$, 26 $NaHCO_3$, 1.25

NaH_2PO_4 and 11 D-glucose, oxygenated with 95% O_2 and 5% CO_2, pH 7.4. Slices were first incubated, for 60 min at 37°C, in an artificial CSF (aCSF) solution containing (in mM): 119 NaCl, 2.5 KCl, 1.25 NaH_2PO_4, 26 $NaHCO_3$, 1.3 $MgSO_4$, 2.5 $CaCl_2$ and 11 D-glucose, oxygenated with 95% O_2 and 5% CO_2, pH 7.4. Slices were used after recovering for another 30 min at room temperature. For all experiments, slices were perfused with the oxygenated aCSF at 31 ± 1 °C. fEPSPs were recorded in the stratum radiatum of the CA1 region using a glass electrode (RE) (filled with 1 M NaCl, 10 mM HEPES, pH 7.4) and the stimuli (30% of maximal fEPSP) were delivered to the Schaeffer Collateral pathway by a monopolar glass electrode (SE) (filled with ACSF) **(FIGURE 13A)**. Whole-cell recordings were made using borosilicate glass pipettes of 3–6 MΩ resistance containing (in mM) K-gluconate 120, KCl 15, $MgCl_2$ 2, EGTA 0.2, HEPES 10, QX-314 1.5, P-Creatine 20, GTP 0.2, Na_2-ATP 2, leupeptin 0.1 and adjusted to pH 7.3 with KOH and osmolarity between 290 and 300 mOsm. Slices were visualized on an upright microscope with IR-DIC illumination and epi-fluorescence (Scientifica, Ltd). After a tight seal (>1 GΩ) on the cell body of the selected neuron was obtained, whole-cell patch clamp configuration was established, and cells were left to stabilize for 2-3 min before recordings began.). The recordings were performed using a Multiclamp 700B (Molecular Devices) amplifier, under the control of pClamp10 software (Molecular Devices).

2.4.1 Field potential recordings

LTP was induced using a high-frequency stimulation protocol (HFS) protocol with one pulse of 100 Hz or 4 pulses of 100Hz spaced by 5 minutes inter-stimulus interval (ISI). For LTP analysis, the first third of the fEPSP slope **(FIGURE 13B)** was calculated in baseline condition (20 minutes prior to induction protocol delivery and for 45-60 minutes post-induction). The average baseline value was normalized to 100% and all values of the experiment were normalized to this baseline average (one minute bins).

The paired-pulse ratio (PPR) was obtained by stimulating the Schaeffer collateral consecutively within a short-period of time. The PPR (P_2/P_1) was expressed as the peak amplitude of the second response (P_2) relative to that of the first response (P_1) at different ISI (150ms, 200ms, 250ms, 300ms, 350ms, 400ms, 450ms) **(FIGURE 13C)**. Experiments were pooled per condition and presented as mean±s.e.m.

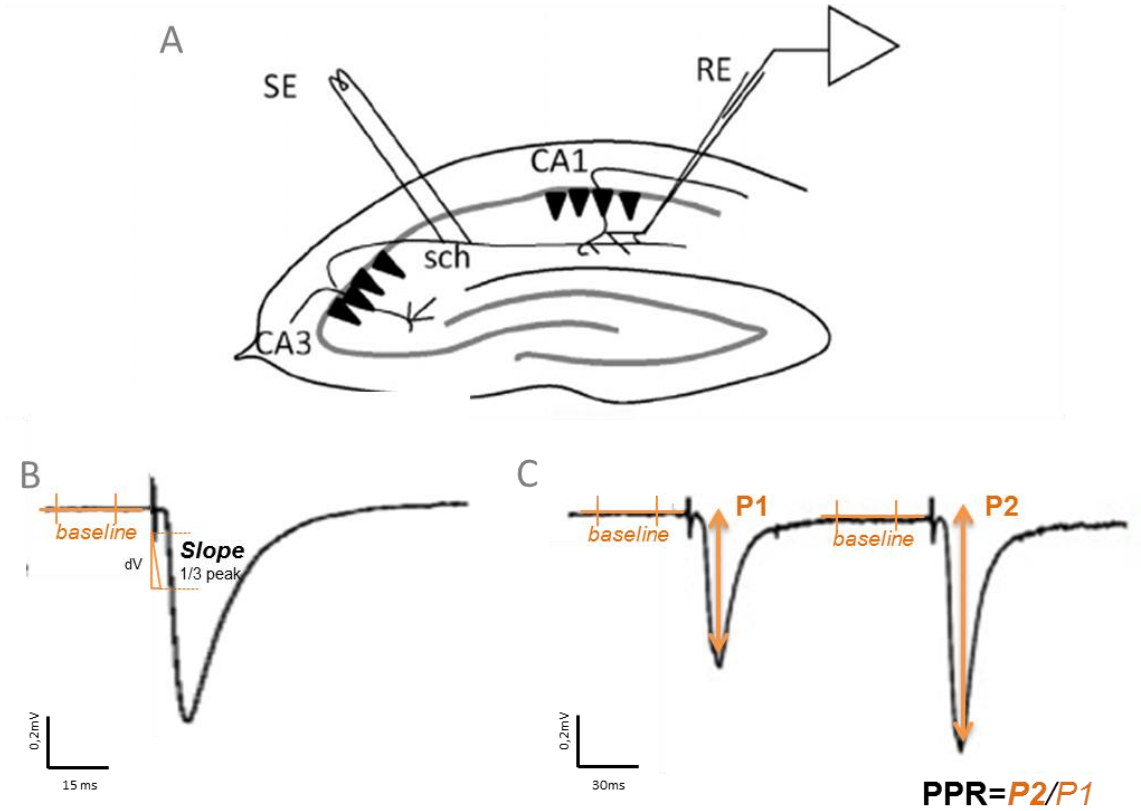

FIGURE 13. FIELD EXCITATORY POST-SYNAPTIC POTENTIALS IN THE HIPPOCAMPUS.
A: Coronal hippocampus slice. The SE (stimulation electrode) stimulates at the sch (Schaeffer collateral) and the signal is recorded by the RE (recording electrode) in the CA1 pyramidal neurons. **B:** the fEPSPs for baseline and post-LTP induction are calculated as slope (represented in orange) placed at 1/3 of the peak amplitude of the response. **C:** The PPR are calculated as the ratio between the peak amplitude 2 and the peak amplitude 1.

2.4.2 Patch-clamp recordings (performed by Doctor Pousinha)

Current-clamp recordings were performed on CA1 pyramidal neurons or on dentate gyrus (DG) granule cells. The resting (Vm) membrane potential was first measured in the absence of any spontaneous firing, and only cells with Vm more negative than -55mV were considered. To study the relationship between firing frequency and current input, we first adjusted the membrane potential of CA1 pyramidal neurons at Vh=-70 mV and of DG granule cells at Vh=-60 mV and then injected pulses of increased intensity in steps of 20 pA (from 0 to 400 pA, 1 s duration).

2.5 *Immunohistochemical analysis in brain slices*

After SIH, the mice from all the groups were collected at P60 for later immunohistochemical analysis. We fixed the brains with trans-cardiac perfusion of and shipped the brains to our collaborators. All the immunohistochemical analysis on these brains was done by Dr. Carolina Frassoni (team leader) and Dr. Cristina Regondi (researcher) in Instituto Carlo Besta in Milan.

2.5.1 Intracardiac paraformaldeyde perfusion

At 2 months of age the mice were anaesthetized with 11.25 mg/kg ketamine/7.5 mg/kg xylasine of body weight administered intraperitoneally, and then transcardially perfused with 4% paraformaldehyde in 0.1M phosphate buffer (PB), pH 7.2, using a peristaltic pump. The brains were removed from the skull, immersed overnight in 4% paraformaldehyde in PB and then transferred to 0.1M PB in 0.001 NaN_3.

2.5.2 Antibody staining

The brains were removed from the skull, immersed in 4% PFA in PB for 1 day, cut into 50-µm-thick serial coronal sections in a Vibratome VT1000S (Leica, Heidelberg, Germany), stored in PB and processed for immunohistochemistry. Selected free-floating vibratome sections were incubated overnight at 4°C using the following anti-neuronal nuclei (NeuN, 1:3000, Chemicon, Temecula, CA, USA) primary antibody, in accordance with the standard immunoperoxidase protocol (Moroni et al., 2008). After several rinses in PBS, the sections were incubated in biotinylated goat anti-rabbit IgG (Vector Laboratories, Burlingame, CA, USA) diluted 1:200 in 1% NGS in PBS. The avidin-biotin-peroxidase protocol (ABC; Vector) was followed, with 3, 3'-diaminobenzidine tetrahydrochloride (DAB; Sigma) being used as chromogen. For cytoarchitectonic analysis, selected sections were stained with Cresyl violet (2%). Finally, the sections were mounted, dehydrated, and coverslipped with DPX (BDH, Poole, Dorset, EN).

2.6 *Behavioral analysis*

A battery of behavioral tasks was done to assess behavioral abnormalities (anxiety, locomotor activity, sociability) and cognitive function (hippocampus and prefrontal cortex memory). For *Scn1a*$^{+/-}$ mice, model of DS, only control WT and mutant mice in one cohort of animals were tested. For *Scn1a*$^{RH/+}$ mice the four groups of animals (WT control, WT submitted to hyperthermia, *Scn1a*$^{RH/+}$ control and *Scn1a*$^{RH/+}$ with SIH) were obtained. We ran four cohorts of animals that we pooled. The order of the memory tasks was counterbalanced between cohorts (Morris water maze-radial maze-contextual fear conditioning; radial maze- Morris water maze-contextual fear conditioning or Morris water maze- contextual fear conditioning- radial maze). The openfield, dark/light and social interaction tests were always done at the beginning of the test battery to avoid handling/habituation interferences and the placement for 72 consecutive hours in the actimeter was always done at the end of the testing to prevent animal isolation-associated stress. For all the behavioral tasks'analysis the experimenter was blind to genotype.

2.6.1 Openfield test

- Apparatus

Hall, 1934 first described the openfield test (OF) to study emotionality in rats. Nowadays, it is largely used to study novel environment exploration, general locomotor activity, and provide an initial screen for anxiety-related behavior in rodents. The reaction to novelty was assessed by studying the anxiety, locomotor activity and stereotyped behaviors as previously described (Crawley et al., 1992). The apparatus consisted in a white and opaque quadratic arena *(40cm L (length) x40cm W (width) x30 cm H (height))* **(FIGURE 14)**. An imaginary central area *(20cm Lx 20W)* and a peripheral area *(30 cm L, 10 cm W)* were defined to study anxiety-like behavior. The light intensity was set at 300 lux.

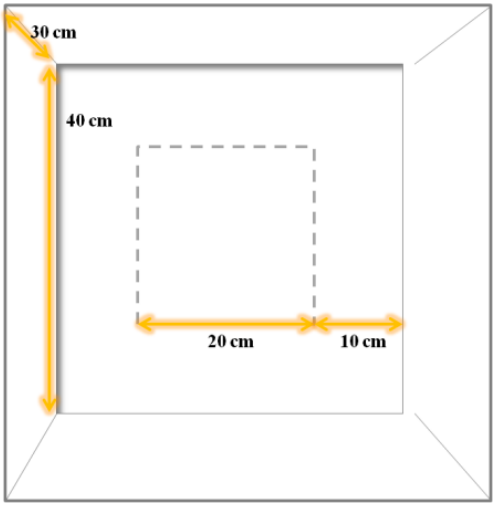

FIGURE 14. OPENFIELD APPARATUS.

- Procedure

The mouse was placed in the center of the arena and allowed to explore for 10 minutes. The apparatus was cleaned with 70% ethanol and rinsed with water between each animal. The trajectory of the animals was video recorded and tracked with ANYmaze software (Stoelting, Wood Dale, Il). The total distance travelled and average speeds were counted as measures of locomotor activity. The distance travelled in the center (anxious area) was divided by the total distance travelled to assess anxiety level. To evaluate stereotyped behaviors, the number of rearing episodes were scored manually, while the circling behavior was scored automatically by the video tracking software (ANYmaze software (Stoelting, Wood Dale, Il)). A complete 360-degree turn of nose angle with respect to the body center was counted as one circling event.

2.6.2 Dark↔light exploration test

- Apparatus:

The dark↔light paradigm has been extensively used for testing anxiolytic properties of drugs in rodents (Crawley and Goodwin, 1980; Holmes et al., 2003). The apparatus consisted of a white and black cage separated in two compartments (light and dark) by a partition, which had a small opening at floor level. The dark/closed compartment was made with black opaque walls (less anxious) cover by an opaque top and a light/open compartment was made with white walls and was light exposed (more

anxious). The total dimensions of the box were *42 cm L, 18 cm W, 29 cm H*, while the light compartment represents *28 cm L* and the black compartment *14 cm L* **(FIGURE 15)**. The opening that allowed dark↔light transitions was *7cm L* and *5 cm H*. The open side was illuminated by 300 lux light intensity.

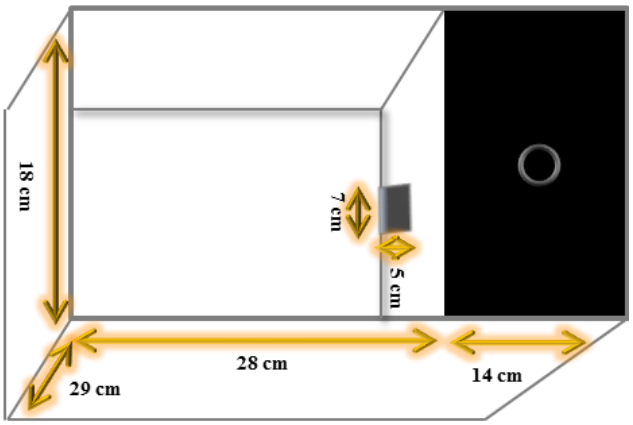

FIGURE 15. DARK↔LIGHT BOX APPARATUS.

- Procedure

The animals were released in the center of the light compartment and allowed to explore the entire apparatus, notably entering and exiting the dark compartment for a period of 5 minutes. The apparatus was cleaned with 70% ethanol and rinsed with water between each animal. The dark compartment represents the protected area while the light compartment represents the unprotected area. The test mouse has to deal with the conflict of explore the bright area or be safe in the protected area. The time spent (seconds) in the light compartment and the number of dark↔light transitions represent a measure of anxiety and were counted manually.

2.6.3 Three-chamber social interaction

- Apparatus

Sociability and social novelty tests were performed as described previously with minor modifications (Moy, 2004). The three-chamber apparatus consisted in a rectangular non-transparent plexiglass box *(60cm L x30 cm W)*. Two dividing walls were made with clear plexiglass containing one circular opening each *(4 cm diameter)* to allow the mouse to assess each chamber. Each chamber was *20 cm L, 30 cm W, 22*

cm H **(FIGURE 16)**. Light intensity was adjusted to 3.5 lux and the apparatus was cleaned with 70% ethanol and water between each mouse. The wire cages were *11 cm H*, with a bottom diameter of *10.5 cm* and bars spaced by *1cm* (Galaxy Cup, Spectrum Diversified Designs, Inc, Streetsboro, OH).

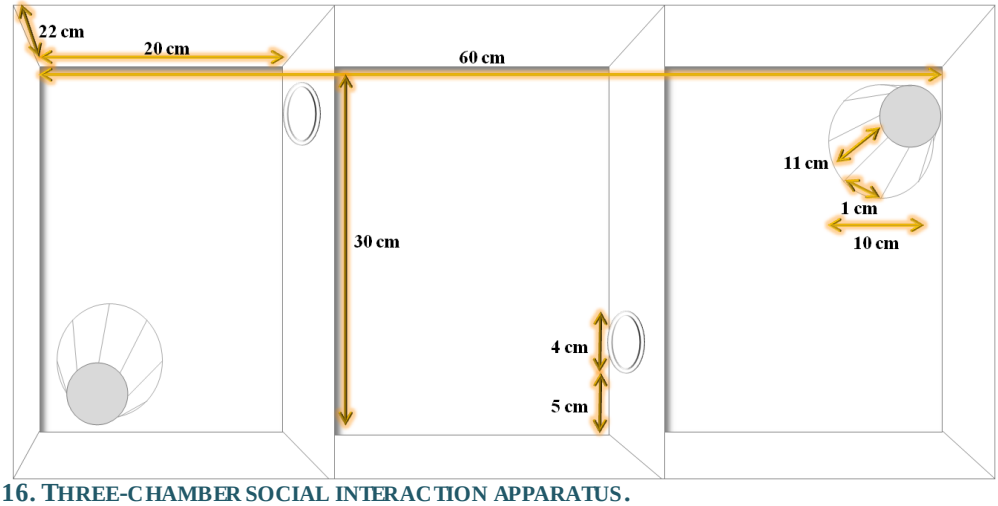

FIGURE 16. THREE-CHAMBER SOCIAL INTERACTION APPARATUS.

- Procedure

The test consisted in three phases: **1)** Habituation, **2)** Sociability test and **3)** Social Novelty test. All the stages were recorded using a camera to allow offline analysis. In the habituation phase the test mouse was placed in the empty box for 10 minutes, with the doors open in order to freely explore the 3 chambers and acclimated to the environment. The time spent in each chamber, the distance travelled and the average speed were measured using ANYmaze tracking software (Stoelting, Wood Dale, Il). After the habituation period, the test mouse was restrained in the central chamber for the time of the preparation of the next step. An unfamiliar mice (same strain/same age/same gender) (M) was enclosed in the round wire cup, which allowed sensory but not physical contact and placed in one of the side chambers and another empty wire cage (EC) was placed in the opposite side chamber. Emplacements of the unfamiliar stranger mouse cage and empty cage were counterbalanced between animals to avoid chamber side preferences. A weighted bottle was placed on top of the wire cages to avoid climbing from the test mouse. The test mouse was then allowed to explore for a 10-minute session. After the sociability stage, the test mouse was again blocked in the central chamber. For the last phase (the social novelty phase), a novel unfamiliar mouse

(nM) was placed in the cage that was previously empty. The doors were open and the test mouse had now the opportunity to choose between the familiar mouse (fM) (previously seen in the sociability phase) or the nM. The time spent interacting with/exploring the cages (distance between the test mouse and the cage less than 2cm) and also the time spent and the number of entries in each chamber was measured for the sociability and social novelty phases.

2.6.4 Morris water maze

- Apparatus:

The Morris Water Maze paradigm (MWM) was widely described for testing spatial learning and memory (Morris 1981, Morris 1984). The apparatus consisted in a circular tank *(90 cm diameter)* filled with opaque water (temperature 25°C±1). An escape platform *(8cm diameter)* was submerged 1.0 cm below the water surface. Extramaze cues were placed in the walls surrounding the maze to allow the animals to create a spatial map and find the platform. Light intensity was set at 30 lux. Animals were placed in the testing room 30 minutes prior to experiment in order to acclimatize.

- Procedure

The testing consisted in 3 phases: **1)** Cue task training (2 days) **2)** Spatial learning training (4 days) and **3)** Long-term reference memory-probe test (1 day) **(FIGURE 17)**. For the cue task and spatial trainings, all the animals received 4 trials/day with a maximum trial duration of 90 seconds (+30 seconds on the platform at the end of each trial) and an inter-trial interval of 10 minutes. For each trial, the animals were gently placed in the water facing the sidewalls in a different cardinal point (NWSE) and randomized between animals and training days. If the animal did not find the platform within the trial it was gently guided to it. All the trials were video recorded and tracked using ANYmaze software (Stoelting, Wood Dale, IL).

1) Cued task training: Cued task was done prior to spatial learning training to notice visual and motor problems and to accustom the mice to the testing rule (find the platform to escape). A visible object was placed on top of the platform and the maze was surrounded by opaque curtains. The mice were allowed to find the visible platform

for 2 consecutive days with 4 trials per day. If the animal did not find the platform within the trial it was gently guided to it. The platform emplacement was changed every day. The escape latency, average speed and distance travelled were recorded.

2) Spatial Training: For the spatial learning, the curtains and the object on top of the platform were removed. The animals could guide their learning to find the hidden and invisible platform based on the extramaze cues. If the animal did not find the platform within the trial it was gently guided to it. The escape latency for each trial was analysed.

3) Probe: A probe trial was run, 24 hours after training completion to assess the strength of the memory for the platform location. The platform was removed and the test mouse was allowed to search for it for 60s. The time spent in each quadrant (target, left, right and opposite) were recorded. An imaginary zone was draw around the platform –"platform zone" with 24cm diameter (3 x the platform diameter), and the number of crosses in the "platform zone" were counted.

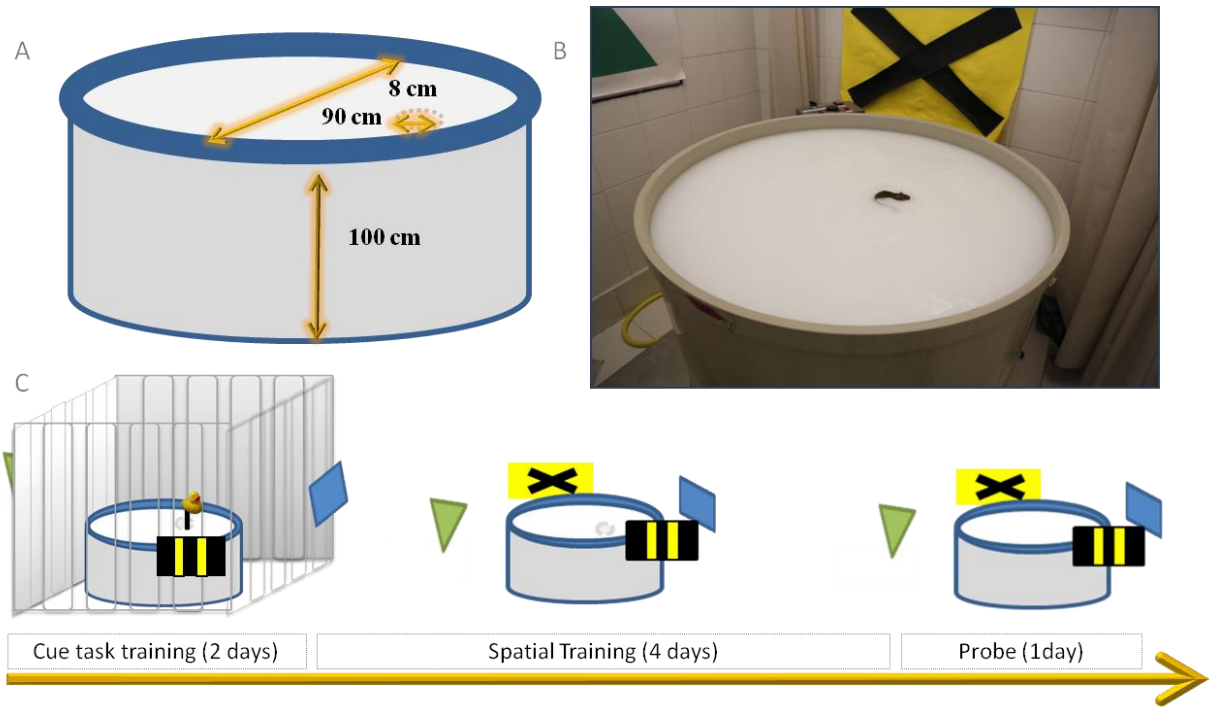

FIGURE 17. MORRIS WATER MAZE APPARATUS AND PROTOCOL TIMELINE.
A: Morris water maze apparatus. **B:** GEFS+ mouse trying to find the hidden platform. **C:** Scheduling of the task: the animals went trough two days of cue task, followed by 4 days of spatial learning (4 trials per day) and a probe day. Each day represents a 24 hours delay between them (D1 to D7). D= day

2.6.5 Contextual-Fear conditioning

The hippocampus plays an important role in the representation of contextual information in the contextual-fear conditioning paradigm) (Phillips and LeDoux, 1992). In this test, the mice are placed in a conditioning chamber and receive pairings of a conditioned stimulus (contextual chamber) and an aversive unconditioned stimulus (an electric foot-shock). After a time delay, the mice are re-exposed to the same conditioning chamber without receiving any shock and the freezing response observed in the mice expresses the memory association between the contextual stimulus and the foot-shock.

- Apparatus:

The CFC apparatus consisted in a cubic box *(25cm L x25cm W, 25cm H)* with black methacrylate walls, a transparent frond door and a metallic floor with bars spaced by 0,6 cm. The floor was connected to the electric shock generator and a control unit of signal amplification (Startel and Fear System, BIOSEB Allcat Instruments, France). The 3 shocks delivered in the conditioning phase had duration of 2 seconds and an intensity of 0.7mA. The light intensity was maintained at 5lux for all the procedure duration. The signal generated by animal's movement was analyzed using the automatic freezing software Panlab V1.3 (BIOSEB Allcat Instruments, France). All the experiments were video recorded using a camera connected to the top of the chamber. The chamber was cleaned between animals with 70% ethanol, water and finally wiped with paper towels.

- Procedure

The experiment was done in two days: 1) conditioning **(D1)**, 2) retrieval **(D2)** as illustrated in **FIGURE 18.**

1) Condtioning**:** The mouse was placed in the conditioning box. After exploring for 2 minutes, the first shock was delivered, followed by the two other shocks, at an inter-stimulus interval of 1 minute. One minute after the last shock, the mouse was returned to his home cage. The animal's activity was recorded.

2) Test**:** Twenty-four hours after the conditioning, the animal was placed in the CFC box (same context as in the previous fear conditioning) for 5 minutes and no shocks were delivered.

PROCEDURE	CONDITIONING	TEST
DAY	1	2
DURATION (MINUTES)	5	
INTER-TRIAL INTERVAL (HOURS)	24	
NUMBER OF SHOCKS ↙ (2 seconds duration)	3	-

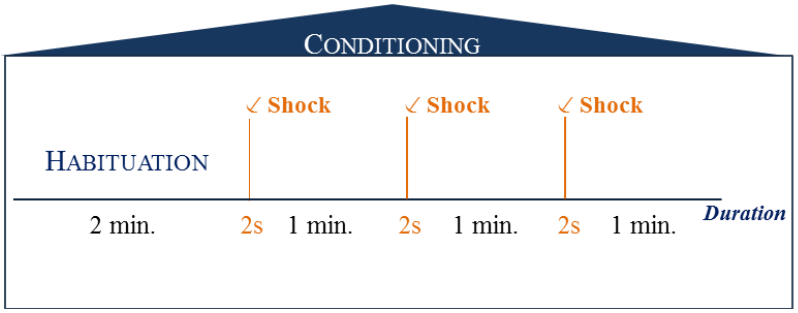

FIGURE 18. CONTEXTUAL FEAR CONDITIONING PROCEDURE.
Top table: The description of the protocol timeline. At day 1 the animals went trough the conditioning phase. Here, after a period of 2 minutes of habituation the animals (as seen in the scheme in the **bottom**) received 3 shocks with a duration of 2 seconds and spaced by 1 minute inter-stimulus interval.

The activity generated by the testing mice in the box (high and low activities and freezing) was recorded using the floor sensors and the video recording. The cumulated freezing time (s) was measured across the time.

2.6.6 Eight-arm radial maze

The radial maze was developed by *Olton and Samuelson, 1976* and is used to test working memory in rodents The protocol used in this study was adapted from (Etchamendy et al., 2003) and based in a win-shift strategy to discriminate between two arms-choice.

- Apparatus:

The apparatus consisted in a black plexiglass 8-arm radial maze (Viewpoint, Lyon, France). The maze was placed in an infrared floor and connected to a video recording camera and tracking software (Videotrack/Viewpoint). Distal and proximal extramaze cues were placed respectively on the walls of the room and above the infrared floor (between the arms). The central platform *(diameter of 24 cm)* and 8 arms *(35cm L, 5cm W, 2cm H)* which project radially outward were elevated 8 cm above the floor (see diagram **FIGURE 19**). Each arm had a transparent Plexiglass door, placed between the end of the arm and the central area that could be open and closed according to the protocol. A metallic and weighted food cup was placed at the end of each arm and maintained there for all the protocol. The maze was cleaned with water between each trial and light intensity was set at 3.5 lux. The procedure was divided in 2 phases: habituation (3 days) and training (n days until reach the criterion). For the whole protocol course the animals were food deprivated to motivate the mice in getting the food reward. Chocoloops ® (1/6 of the cereal ring) were used as food reward.

1) Food deprivation: Food deprivation started one day before the first day of the protocol. Daily feeding was adapted to maintain the level of 90% of the initial body weight. Water was provided *ad libitum*.

2) Habituation: In the habituation phase the test mouse was placed in the center of the maze, with the 8 doors opened and allowed to explore the entire maze. The bait was initially available throughout the maze, but was gradually restricted to the food cup. Three food rewards (**1** – **1** – **1**) were placed in all the arms at day one, two rewards at day 2 (0 – 1 – **1**) and 1 reward at day 3 (0 – 0 – **1**) placed only in the food cup to incentive the mouse to go to the end of the arm (see **FIGURE 19**)

3) Training: The protocol for the training was based in a win-shift strategy. We presented a sequence of 7 pairs of arms that was changed every day. The animal was placed in the center platform with all the arms closed for 30s. A first baited arm was opened while the other 7 arms were closed. After this first forced choice, the mouse had to return to the center for another 30s. For trial 2, the old arm and a new consecutive or non-consecutive (never more than 90° angle between the 2 arms) were open at the same time, allowing the choice between two arms of the maze. The previous (old) arm was this time unbaited while the new one was baited. When the animal went to an incorrect arm this one was immediately closed after returning to the center to avoid perseverance

errors. If his first choice is the correct arm, the two arms were immediately closed after returning to the center and the trial is ended. The animal had to wait 30s before the next trial. The protocol was repeated for 6 more trials for a total of 8 trials per day. The animal had to retain the rule that if, in a given arm, it won the reward, it had to shift the other one. The sequence was changed every day and the training was stopped when the control animals reached the criterion of having an average of 75% of correct choices for 2 consecutive days (5.25 correct choices out of 7).

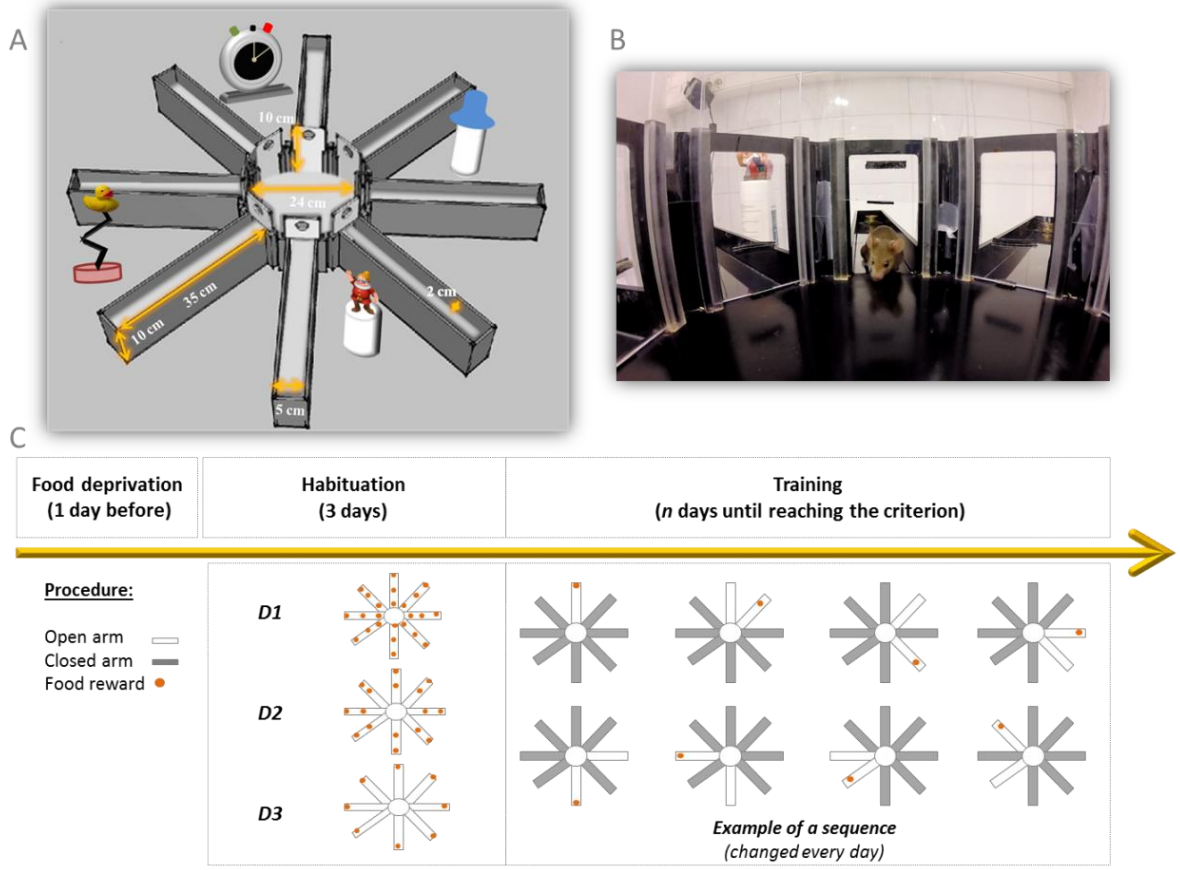

FIGURE 19. RADIAL MAZE DIAGRAM AND PROTOCOL TIMELINE
A: Radial maze apparatus and proximal and distal cues. **B:** Mouse returning to the center after having collected the reward from the arm. **C:** Protocol timeline. Food deprivation started one day before habituation. Then the animals went through habituation for 3 days with the 8 arms open (white arms),and food was distributed across the arms from D1 to D3 as illustrated in the diagram. Following habituation the training started until the criterion was reached. Each training day had 8 trials, with the sequence of open arms changed everyday (an example of a sequence is illustarted in the figure).

2.6.7 Actimeter

We placed the animals in the actimeter (Imetronic Apparatus, Pessac, France) for 3 consecutive days (72 hours). The animals had free access to food and water and a 12 hours light cycle. The actimeter box (*20 cm L, 11 cm W, and 18 cm H* - **FIGURE 20**)

was equipped with infrared sensors to detect locomotor activity (horizontal and vertical) and an infrared plane to detect rearing. The data was collected by bins of 30 minutes.

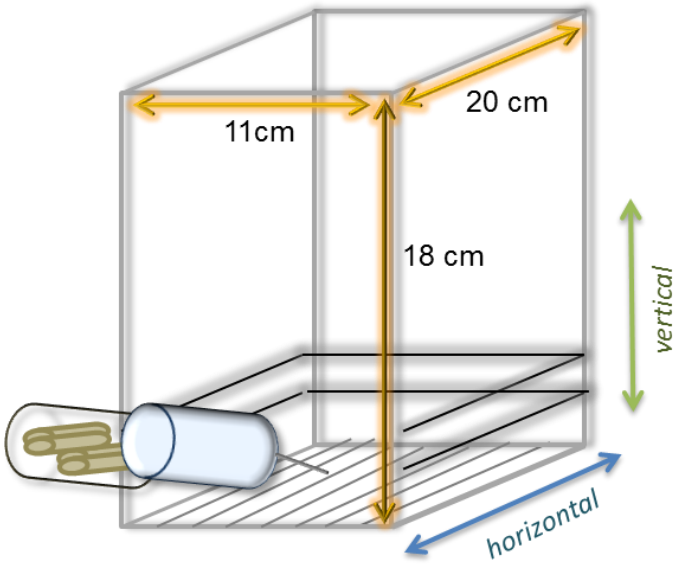

FIGURE 20. ACTIMETER DIMENSIONS.

3. THERAPEUTIC EFFECT OF DRUG X IN DECREASING THE SPONTANEOUS SEIZURES FREQUENCY IN *SCN1A*$^{+/-}$ MOUSE MODEL

3.1 *Drug X administration*

The *Scn1a*$^{+/-}$ -B6-129 mice were used for this study and the treatment started at P21. Drug X (name cannot be disclosed) was prepared at a concentration of 15 mg/kg in 5% DMSO and 95% PBS. Drug X was intraperitoneally administrated at a volume of 5.5 ml/kg once a day for 5 days (in parallel to the SIH protocol).

3.2 *Protocol of seizure induced by hyperthermia and monitoring*

Six hours after drug X administration, DS mice were submitted to the SIH protocol in order to increase the spontaneous seizure frequency. The protocol was repeated for 5 consecutive days. The threshold temperature for seizure induction and the seizure severity were measured. The animals were then grouped by 2 and video recorded to analyze the presence of spontaneous seizures. The seizures were detected with custom-made software designed by ULLO society (la Joliette) for this experiment.

4. STATISTICAL ANALYSIS

All the data analysis was obtained and analyzed blind to genotype. Statistical analyses were performed with GraphPad Prism V6.01 (La Jolla, CA 92037 USA). The normality of the data distribution was verified with Shapiro-Wilk's test.

Differences between groups were measured using two-tailed t-test, one way analysis of variance (ANOVA), two-way ANOVA (Genotype x Treatment) or repeated measures ANOVA in the protocol of consecutive dependent variables (i.e. Training days/time x Group (genotype-treatment)). The ANOVA was followed by Tukey's (3 or more comparisions) or Sidak's (2 comparisions) post hoc test. The one-sample t-test was used to compare the time spent in the target zone and the chance level (25%) and also to compare training performance and the chance level in the radial maze training (chance level = 3.5 correct choice). Survival curves were compared with Log-rank (Mantel-Cox) test and the analysis of the data concerning the SIH protocol was done with Kruskal-Wallis test. Details of each value and statistical test used are described in the statistic tables (VIII-1,0,VIII-3,VIII-4,VIII-5 page 185). Error bars represent s.e.m. Null hypotheses were rejected at the 0.05 level. Statistical significances are represented by the following P-values in all figures: * $p<0.05$; ** $p<0.01$; ***, $p<0.001$; ****$p<0.0001$ and n=number of animals, n=number of fields for field electrophysiology recordings, n=number of cells for patch clamp recordings.

Results

IV- RESULTS

Chapter 1- PHENOTYPIC CHARACTERIZATION OF *SCN1A*$^{+/-}$ (DS MODEL)

1. *SCN1A*$^{+/-}$ (DS MOUSE MODEL) IN 129 BACKGROUND (*SCN1A*$^{+/-}$-129)

The *Scn1a*$^{+/-}$-129 mouse, model of DS, is characterized as described previously, with high variability of phenotypes according to the genetic background (Yu et al., 2006a). Because of that, the model we chose preferentially was the *Scn1a*$^{+/-}$ in 129/SvJ background, which present the mild phenotype (high survival and no spontaneous seizures). We first wanted to see if the *Scn1a*$^{+/-}$ mutation *per se* affects the behavioral phenotype. With the first littermates obtained, we behaviorally characterized the control WT and mutant animals (this chapter). After getting the first results we could not get enough animals to continue and validate the experiments. We decided to start breeding the mutant line in a different background in order to increase the reproducibility. We crossed the *Scn1a*$^{+/-}$-129 male with a C57BL/6 female to get the F1 generation of a 50% B6:129 mice and increase the colony (results presented in the 2nd part of this chapter).

1.1 *The Scn1a*$^{+/-}$ *mouse in 129 background show normal spatial learning and memory in the Morris water maze task*

We submitted the *Scn1a*$^{+/-}$-129 mice and littermate controls to the MWM task. One of the most described cognitive perturbation in DS patients is the inability to integrate visual-motor and visual-spatial information (Chieffo et al., 2011a; Ragona et al., 2011b; Wolff et al., 2006a). It is believed that the visual function is affected before the cognitive problems. In the cue task phase, ran to decipher visual and motor problems the two groups showed a significant decrease in latency to find the platform from day D1 to D2 with no difference in the average between the groups (RM-two way ANOVA, main effect of Day). These first results allowed us to conclude that the *Scn1a*$^{+/-}$-129 had no major visual or motor dysfunctions. Following the cue task, the cue above the platform was removed and the animals had to learn the hidden platform location based on the spatial extra-maze cues. The *Scn1a*$^{+/-}$-129 mice and the WT controls showed no amelioration in learning performance from D1 to D2. However, the

latency significantly decreased from D2 to D3 **(FIGURE 21)**. After D2, we could conclude that this amelioration indicated that the two groups learnt the platform emplacement (RM-two way ANOVA, main effect of Day). In line with the learning curve results, when removed the platform 24 hours following the training end, the two groups of mice persisted higher than chance in searching the platform in the target quadrant (where the hidden platform has been positioned during training) than in the other 3 quadrants (left, target, right, opposite) **(FIGURE 21)**. The RM-two way ANOVA showed a Quadrant x Genotype interaction with a significant main effect of quadrant, and the Sidak's post-hoc analysis revealed a better performance of the *Scn1a*$^{+/-}$-129 mice than the WT mice in the probe test because the persistence of the *Scn1a*$^{+/-}$-129 mice in the 60s probe is mainly focused in the target quadrant (presence in target quadrant is significantly higher than in the 3 other quadrants: left, right, opposite) while the WT animals could not significantly discriminate between the left and target quadrants. With these results, we concluded that the spatial learning was preserved in the *Scn1a*$^{+/-}$-129 mice and that both groups remembered the platform emplacement though in the probe test, the memory strength was higher in *Scn1a*$^{+/-}$-129 mice.

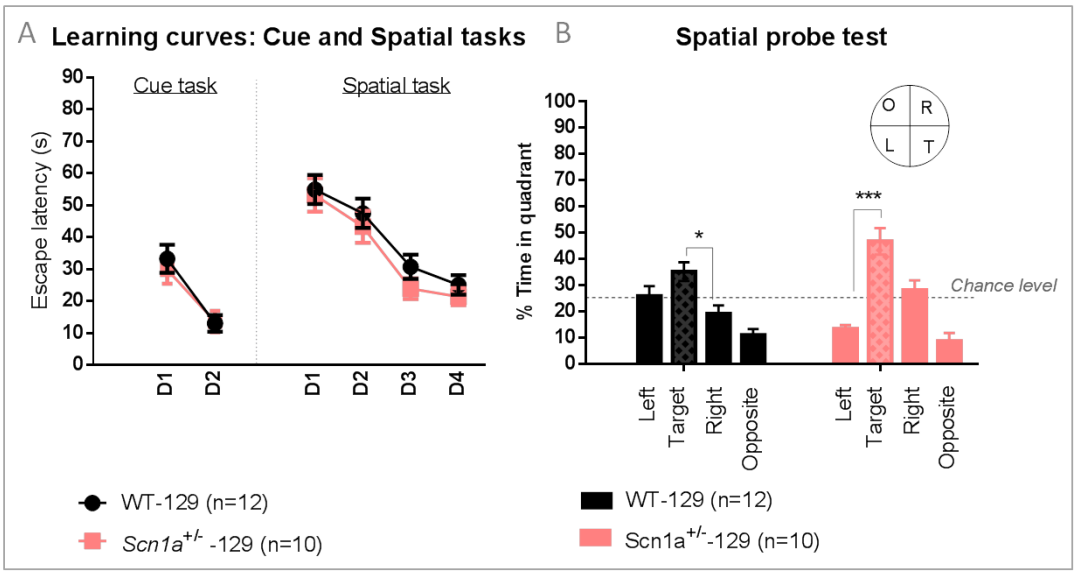

FIGURE 21. *SCN1A*$^{+/-}$ MICE IN 129 BACKGROUND SHOW PRESERVED SPATIAL LEARNING AND MEMORY IN THE MWM TASK.

A: Latency to findthe platform in the cue task (days 1&2) and training (days 1-4). **B:** Percentage of presence in the four quadrants (left, target, right, opposite) in the probe test, 24 hours after the training ended. *p<0.05; ***p<0.001, n=number of animals

1.2 *The Scn1a$^{+/-}$ mouse in the 129 background show normal contextual-fear conditioning*

The *Scn1a*$^{+/-}$-129 mice were submitted to the CFC using two different protocols. In the conditioning phase, the first group of animals received one shock. Twenty-four hours after the conditioning, the animals were placed in the conditioning context without receiving any shock. The freezing percentage was measured and was lower than published control animals of the same background (Rubinstein et al., 2015a), so we decided to increase the number of shocks in the next group of animals to ensure that the low freezing could not be causative of masked differences between the groups. The next group of mice received three shocks. We did not see differences in the freezing percentage between the groups **(FIGURE 22)**. Although the number of animals was low, the *Scn1a*$^{+/-}$ mutation does not seem to alter contextual fear memory.

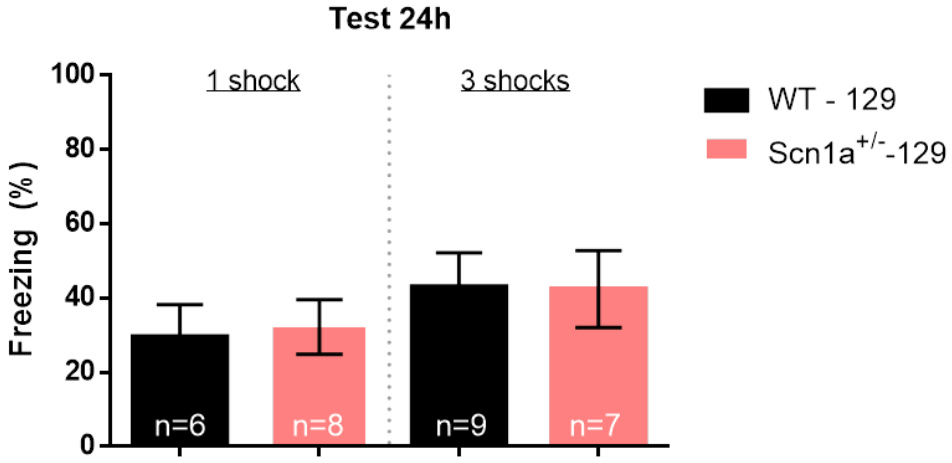

FIGURE 22. THE *SCN1A*$^{+/-}$ AND WT LITTERMATES SHOW SIMILAR FREEZING PERCENTAGE AFTER 1 SHOCK OR 3 SHOCKS IN THE CFC.
We run 2 different pilot experiments: the first with one conditioning shock (left side of the graph) and the second with 3 conditiong shocks (right side of the graph). n=number of animals

In sum, we could not observe differences in any of the hippocampus-dependent memory tasks tested (MWM and CFC). We cannot yet make major conclusions concerning the data due to the low number of animals and the poor performance of the control WT animals in the tasks. To validate our hypothesis that the mutation itself cannot affect the cognitive performance more animals would have been required. Although this *Scn1a*$^{+/-}$-129 mouse model was ideal due to its mild phenotype (characterized by high survival and low spontaneous seizures frequency) the low breeding rate did not allow us to pursue the experiments with this model. In the next

paragraphs I will present the first preliminary results we obtained in this model. We therefore decided to cross the *Scn1a*$^{+/-}$-129 mutant mouse with a C57BL/6J female and use the F1 generation of the *Scn1a*$^{+/-}$ B6:129 mice (50% B6, 50% 129). In the next paragraphs, I will present the results obtained with this *Scn1a*$^{+/-}$ B6:129 mice.

2. *SCN1A*$^{+/-}$ (DS MOUSE MODEL) IN B6:129 BACKGROUND

The *Scn1a*$^{+/-}$ -B6:129 showed 100% survival from P0 to P90 if not submitted to SIH (data not shown). We continued our investigation about the effect of the mutation *per se* in affecting the phenotype. As the number of animals was sufficient, we ran different behavioral and cognitive tasks.

2.1 *The Scn1a*$^{+/-}$*-B6:129 mouse display normal activity in the openfield*

After 10 minutes in the openfield, the automatic analysis allowed to us to evaluate some parameters. For locomotor activity, the distance travelled and average speeds were measured. The *Scn1a*$^{+/-}$-B6:129 mice had the same locomotor profile as the WT-control **(FIGURE 23A&B)** suggesting that the mutation *per se* did not cause changes in this parameter. The anxiety level was quantified by counting the time the test mouse spent in the center of the openfield. The two groups spent similar time in the center, suggesting again no changes in the anxiety profile induced by the mutation **(FIGURE 23 C)**.

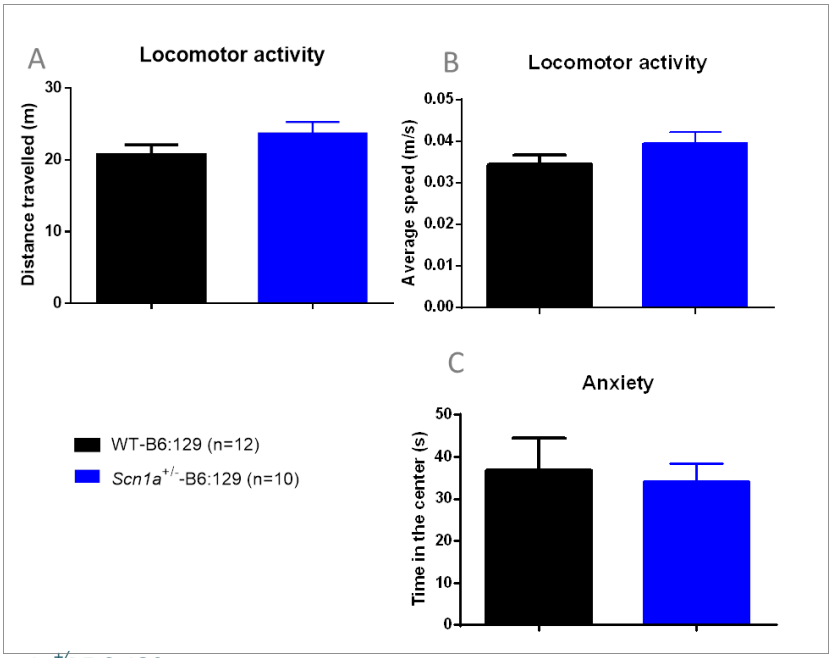

FIGURE 23. *SCN1A*$^{+/-}$-B6:129 MICE HAVE NORMAL ACTIVITY AND ANXIETY IN THE OPENFIELD.
A: Distance travelled (m) in the openfield. **B:** Average speed (m/s). **C:** Time in the center area of the openfield. n=number of animals.

2.2 *The Scn1a*$^{+/-}$*-B6:129 have normal circadian rhythm and activity*

The activity of *Scn1a*$^{+/-}$-B6:129 mice was normal in the openfield. However it was previously reported that mice carrying the *Scn1a* mutation in the pure C57BL/6 background had sleep disturbances and exhibited increased activity (Han et al., 2012a; Ito et al., 2013; Papale et al., 2013). To further confirm our results from the open field and study the circadian rhythm and activity in the *Scn1a*$^{+/-}$-B6:129 mice, we placed the animals in the actimeter for 72 consecutive hours.

The RM-two way ANOVA revealed a significant main effect of Time for both horizontal and vertical activities. This is clear in **FIGURE 24A&B** as the WT and *Scn1a*$^{+/-}$-B6:129 mice present a preserved circadian cycle with low activity during the light/resting phase and high activity during the dark/active phase, but no differences between them were pointed by the post-hoc analysis. The increased activity reported in previous studies (Han et al., 2012a; Ito et al., 2013; Papale et al., 2013), was not observed in the *Scn1a*$^{+/-}$-B6:129, thus indicating that the mutation *per se* is not responsible for the hyperactivity in the model.

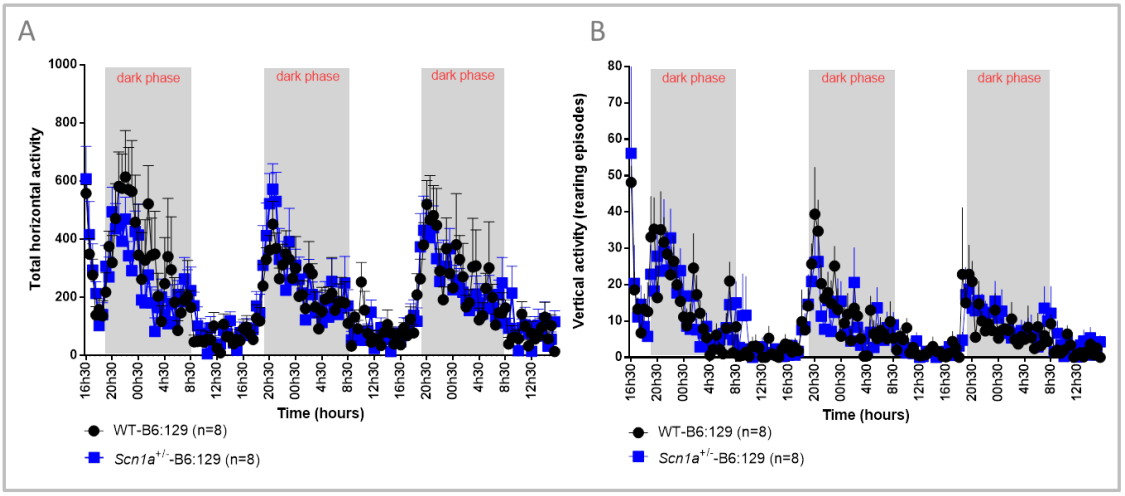

FIGURE 24. *SCN1A*$^{+/-}$-B6:129 MICE HAVE NORMAL CIRCADIAN ACTIVITY IN THE ACTIMETER.
A: Total horizontal activity for 72 consecutive hours. **B:** Total vertical activity (rearing episodes) for 72 consecutive hours. The timeline in gray represents the dark phase (20h00 to 8h00). n=number of animals.

2.3 *The Scn1a*$^{+/-}$*-B6:129 mouse have preserved social interaction skills*

Social interaction skills are affected in Dravet Syndrome patients (Berkvens et al., 2015; Olivieri et al., 2016). Also *Han et al., 2012b* and *Ito et al., 2013* reported severe social skill perturbations in *Scn1a*$^{+/-}$ mouse model in the pure C57BL/6 background, which exhibits a severe phenotype (high mortality, high spontaneous seizures frequency). One day after the openfield test, the mice were tested for social interaction skills in the three-chambered test. Before starting, the habituation trial was run in order to detect if there was a preference for one of the chambers that could interfere with the results. The two groups explored equally the two chambers (1 and 2) being slightly longer time in the center (RM-Two way ANOVA, main Chamber effect) **(FIGURE 25 C)**. Confirming normal locomotor activity, the WT and mutant animals presented similar average speed and distance travelled during the habituation phase **(FIGURE 25 A&B)**. In the sociability phase, the test mouse had to choose between an unfamiliar mouse and the empty cage. A normal mouse is expected to interact preferentially with the mouse than with the empty cage, though the WT showed an important preference for the mouse, none of the groups significantly discriminate between the two **(FIGURE 25D)** (RM-Two-way ANOVA, the Genotype effect is very close to reach statistical significance but did not, and there is no Cage effect). We would need to increase the number of animals to understand if the test was working for the

controls. In the next phase however, the two way ANOVA revealed a significant main effect of cage and Tuckey's post-hoc analysis showed that the two groups displayed higher preference for the new mouse than the familiar mouse as expected **(FIGURE 25E)**. We see that the empty cage and the mouse are not significantly discriminated, anticipating sociability problems in the Na_v 1.1 KO mice, however as the control animals did not significantly discriminate the two cages very well, it does not allow us to conclude for the impairment. A 2nd cohort of animals would allow us to conclude about the validity of the test. In the second phase, both groups preferred the social novelty than the social familiarity suggesting normal sociability skills in the *Scn1a*$^{+/-}$-B6:129 mice.

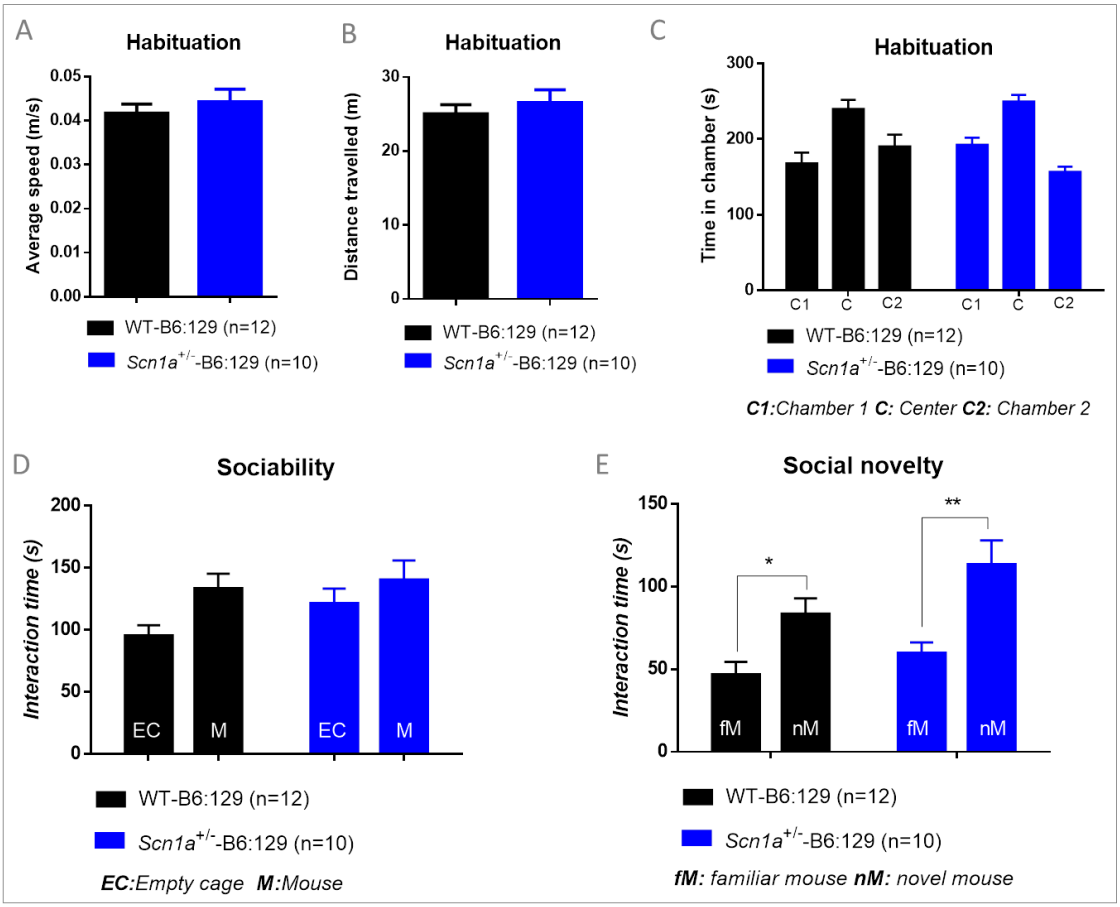

FIGURE 25. *SCN1A*$^{+/-}$-B6:129 MICE SHOW NORMAL ACTIVITY IN THE HABITUATION PHASE (A&B). THE SOCIAL PREFERENCE WAS NOT STRONG IN THE SOCIABILITY PHASE FOR THE WT AND *SCN1A*$^{+/-}$-B6:129 MICE, BUT REACHED SIGNIFICANCE FOR THE SOCIAL NOVELTY PREFERENCE IN THE SECOND PHASE (D)

A,B&C Habituation phase: **A:** Average speed (m/s). **B:** Distance travelled (m). **C:** Time in the 3 chambers (s). **D:** Sociability phase: interaction time with the empty cage (EC) or the mouse (M). **E:** Social novelty phase: time interacting with the familiar mouse (fM) or the novel mouse (nM). *p<0.05; **<0.01;n=number of animals

2.4 *The Scn1a$^{+/-}$-B6:129 express normal spatial memory*

In this *Scn1a$^{+/-}$*-B6:129 mouse model, we went further in the behavior characterization and assessed spatial memory in the MWM as described earlier. The results illustrated in **FIGURE 26** demonstrate that mice carrying the *Scn1a$^{+/-}$* gene mutation in the B6:129 background exhibit normal spatial learning and memory. In the cue task, as we had observed for the 129/SvJ background, the two groups significantly decreased their latencies from cue task D1 to cue task D2 being in the last day at a latency lower than 5 seconds (RM-Two way ANOVA, main effect of cue task day). Similarly, the training for spatial memory was achieved with success by the two groups of animals (RM-Two way ANOVA, main effect of training day) **(FIGURE 26 A)**. A significant increase in performance was observed from training D1 to D2, suggesting that the two groups learnt the platform location. Twenty-four hours after the end of the training, the platform was removed and the long-term memory strength was measured. Considering that the WT and *Scn1a$^{+/-}$* mice swam persistently in the target quadrant **(FIGURE 26B RIGHT)** where the hidden platform was normally located (higher than chance), it was interesting to see that while the WT animals significantly discriminate the target quadrant the *Scn1a$^{+/-}$* mice did not show a preference between target and right quadrants (RM-Two way ANOVA, main effect of quadrant) **(FIGURE 26B RIGHT)**. The same number of platform zone crosses again confirmed that both groups had preserved spatial learning and memory in the MWM task **(FIGURE 26B LEFT)**.

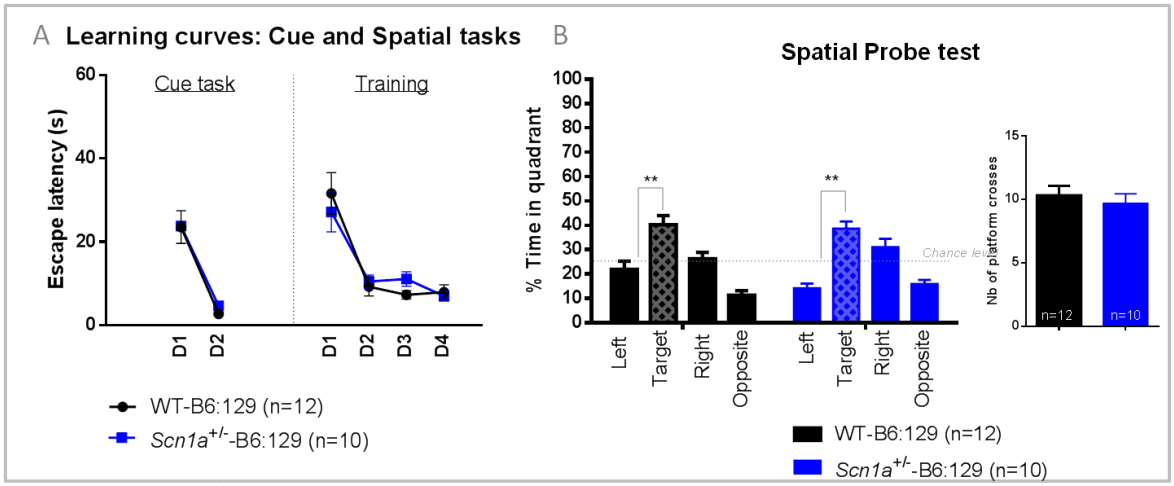

FIGURE 26. *SCN1A$^{+/-}$*-B6:129 DISPLAY NORMAL LEARNING AND MEMORY IN THE MWM TASK.
A: Average of the four trials latencies to find the platform in the cue task and training. In the cue task, the platform is visible, while in the training the platform is hidden. **B (left):** 24 hours after training completion the platform is removed and the persistance in the four quandrants of the MWM is measured. The target quadrant (where the platform was located) is highlited with a different pattern. The persistence in the target quadrant is compared to chance level (gray line) **B (right):** Number of crosses in the enlarged platform zone were measured. **p<0.01;n=number of animals.

2.5 *The Scn1a$^{+/-}$-B6:129 display normal contextual-fear memory*

The contextual fear conditioning was done in order to confirm that hippocampus-dependent memories are preserved in the *Scn1a*$^{+/-}$ model. Twenty-four hours after receiving three electric shocks, the animals were placed in the conditioning context. The total freezing time over the 5 minutes of testing was counted and, as shown in **FIGURE 27**, the two groups exhibited similar freezing behaviors, suggesting that the contextual-fear memory is preserved.

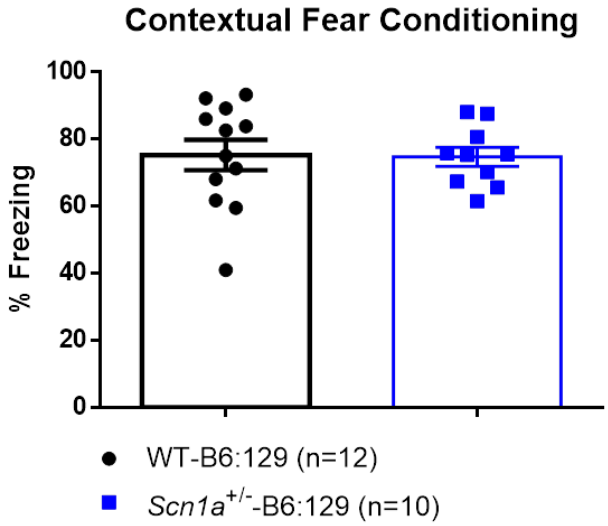

FIGURE 27. THE *SCN1A*$^{+/-}$-B6:129 MICE HAVE NORMAL CONTEXTUAL-FEAR MEMORY.
Freezing percentage showed during the 5 minutes test, 24 hours after the conditioning when replaced in the same context. N=number of animals.

Combining the two behavioral tasks that assessed hippocampus function, we conclude that the heterozygous $Na_V1.1$ loss of function cannot *per se* affect spatial memory.

2.6 *The Scn1a$^{+/-}$-B6:129 show normal working memory*

DS patients were previously reported to display important working memory deficits (Chieffo et al., 2011a; Ragona et al., 2011b). After food deprivation, we trained the animals to learn the working memory rule in the radial maze. There were 7 trials per day and the learning criterion was achieved when the animals had 75% of correct choices (5.25) for two consecutive days. The RM-Two way ANOVA showed a significant main effect of training day but no Training Day x genotype interaction. The

Sidak's post-hoc analysis confirmed that the mutation *per se* was not inducing differences between the 2 genotypes. The number of correct choices analysis showed that the WT control animals passed the criterion at training D12 and the mutant animals at training D11. Similarly, the WT controls behaved better than chance level from D8 to the end while mutant animals were already better than chance at D7 **(FIGURE 28)**. This indicates that all mice learned the 8-arm radial maze rule, and that the mutants with heterozygous loss of *Scn1a* gene showed no deficits in working memory compared with WT mice.

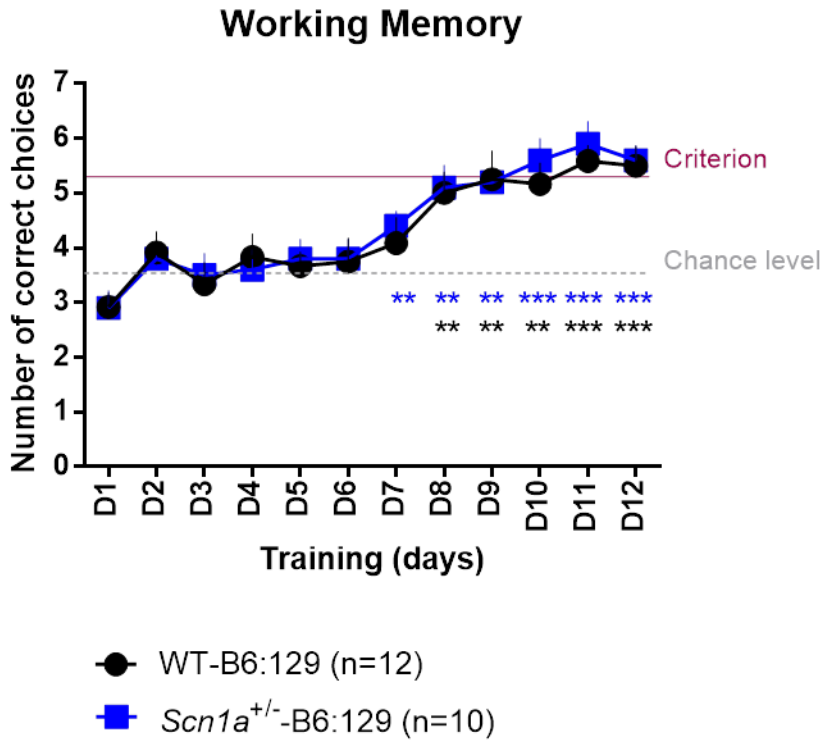

FIGURE 28. WT AND *SCN1A*$^{+/-}$-B6:129 MICE SHOWED PRESERVED WORKING MEMORY IN THE EIGHT-ARM RADIAL MAZE.
The animals were trained in the radial maze to learn the working memory rule for n training days until the criterion was reached. The chance level was 3.5 correct choices (gray line) and the criterion was 5.25 correct choices (burgundy line). The controls reached the criterion at training day 11. The statistical difference from chance level is represented. **p<0.01;***p<0.001; D=training day, n=number of animals

All together the data on the *Scn1a*$^{+/-}$ (DS mouse model) in the mixed B6:129 background indicates that DS mice present a similar cognitive phenotype to the WT, strongly suggesting that the cognitive impairment is not related to the mutation *per se*.

Chapter 2- SEIZURES INDUCTION BY HYPERTHERMIA (SIH) IN *SCN1A*$^{+/-}$-B6:129 AND *SCN1A*$^{RH/+}$-129:B6 MOUSE MODELS

We wanted to induce seizures using hyperthermia at early age (developing brain) in *Scn1a*$^{+/-}$ mutant mice to study the long-term effects in adulthood. The first febrile seizure in Dravet patients occur at around 4-6 months of age (Chieffo et al., 2011a), and in *Scn1a*$^{+/-}$ mutant mice with pure C57BL/6 background at P10 (Yu et al., 2006a). It has been described previously that rat brain development at P10-15 might correspond to the age at which human infants are most susceptible to febrile seizures (Dobbing and Sands, 1973). The corresponding age of the mouse brain is not clear (Andreollo et al., 2012; Quinn, 2005; Romijn et al., 1991) but the data tend more to the hypothesis that a rodent at P15 corresponds to one year of age in humans. As WT pups present SIH from P11-17 we wanted to use animals elder than this age to avoid WT animals submitted to hyperthermia to have seizures (Hjeresen and Diaz, 1988).

SIH have been acutely induced in *Scn1a* mutant models (Cheah et al., 2012; Martin et al., 2010b; Oakley et al., 2009a; Sawyer et al., 2016), but never chronically. We were therefore confronted with an important range of optimizations to the protocol. Our first question concerned the number of seizures that we should induce in the mice. Dravet patients can have more than 30 seizures for a period of 1 month in average but can have more than one seizure *per day* (Takayama et al., 2014). We first decided to induce 2 seizures *per day* for 10 days. The high level of mortality, rapidly persuade us to decrease the number of seizures previously established. We thus decided to induce only one seizure *per day* for 10 days. The next troubles concerned the technical method employed. Previous SIH were provoked using a red lamp heating, in a transparent cylinder and the temperature was controlled by a mouse rectal probe connected to a thermocouple (Oakley et al., 2009a). With the chronicity of the protocol, the mice suffered from some injuries caused by the red lamp (i.e. burning of the tail and ears) and we had to adapt the protocol by using a small incubator to cause hyperthermia. Following all these adaptions we started the SIH protocol.

1. *SCN1A*$^{+/-}$-B6:129 PRESENT HIGH SEIZURE SEVERITY AND HIGH MORTALITY DURING THE 10-DAYS PROTOCOL OF SEIZURES INDUCTION.

After confirming that the heterozygous loss of function of the *Scn1a* gene did not seem to induce cognitive problems in this genetic background, our next goal was to induce seizures by hyperthermia in this model. We observed that the survival percentage of the *Scn1a*$^{+/-}$-B6:129 mice was 100% at post natal week 16 (data not shown). We induced one seizure per day by hyperthermia for 10 days. The percentage of mice alive after 10 days was 100% for control non-hyperthermia animals (WT-B6:129 control and *Scn1a*$^{+/-}$-B6:129 control) (this animals underwent the same handling procedure but no hyperthermia), 72.72% in WT-B6:129 animals submitted to hyperthermia (WT B6:129 HYP) (WT mice, submitted to hyperthermia but did not present seizures) and 36.76% for *Scn1a*$^{+/-}$-B6:129 mice **(FIGURE 29 A).** All the *Scn1a*$^{+/-}$ mice presented seizures when submitted to hyperthermia and the seizures last usually lower than 1 minute (short-lasting or simple hyperthermic seizures). The temperature required to induce seizures at protocol day 1 (41.17±0.106ºC), **FIGURE 29 B**, was higher than reported previously in mouse models with the same mutation (*Scn1a*$^{+/-}$-129, *Scn1a*$^{+/-}$-B6, *Scn1a*$^{+/-}$-129:B6) (Kalume et al., 2007a; Oakley et al., 2009a; Rubinstein et al., 2015a). When increasing the temperature to induce seizures in the incubator, the animals were immediately removed after the appearance of the first behavioral signs of a seizure (i.e. staring, head nodding and myoclonic jerks (grade 1-4) see **TABLE 11** in material and methods). At D1 the majority of the animals presented a clonic seizure with a tonic component characterized by forelimb clonus with rearing and failing that indicates forebrain activation and the beginning of the seizures spreading from forebrain to brainstem. On the following days, the seizure severity significantly increased to GTC seizures indicating that the seizure had reached the brainstem, and was maintained at the same level for the following days **(FIGURE 29C)**.

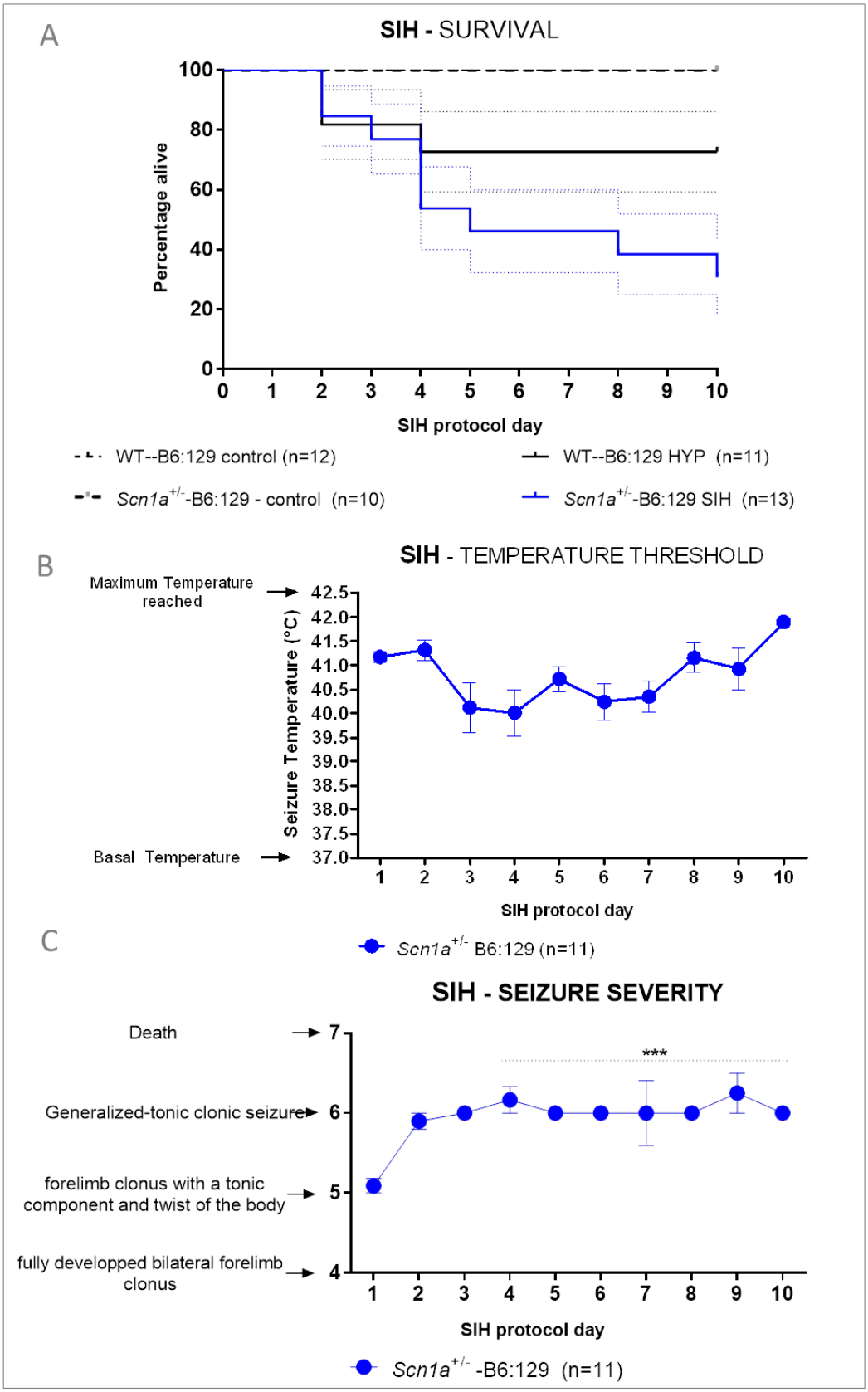

FIGURE 29. SEIZURES INDUCTION BY HYPERTHERMIA IN *SCN1A*$^{+/-}$ -B6:129 MICE.
A: Survival plot of $Na_v1.1$ mutant mice in B6:129 genetic background, shown as the percentage of live mice at each day of the SIH protocol.. **B:** Temperature treshold for the appeareance of the 1st behavioral sign of a seizure. **C:** Caracterization of the seizure severity according to the scale adapted for seizures with a limbic origin. n=number of animals, ***p<0.001

Due to the high level of mortality observed by *Scn1a*$^{+/-}$ mouse in B6:129 background after SIH, we could not obtain a sufficient number of mice to perform behavioral tasks to test the effect of seizures on cognitive phenotype. As previously described, the $Na_V1.1$ channel phenotypic spectrum is large and while truncating mutations are usually associated to the most severe phenotypes as DS, missense mutations are described to confer the higher variability of the spectrum (Volkers et al., 2011). Although missense mutations have been found preferentially in GEFS+ patients they also cause DS (Escayg and Goldin, 2010), i.e. the R1648H missense mutation that was originally found in two families with GEFS+ spectrum (Escayg et al., 2000a) was present in one DS patient (Depienne et al., 2010). Thus, the R1648H mutation had clinical relevance in GEFS+ and DS diseases.

We then decided to use the KI *Scn1a*$^{RH/+}$ mouse, model of GEFS+, having the heterozygous R1648H missense mutation (available in the laboratory). It was a good alternative because, the *Scn1a*$^{RH/+}$ mouse, created by *Martin et al., 2010* present a mild phenotype and almost no spontaneous seizures in the described pure C57BL/6 background. Moreover, these mice are sensitive to SIH so we could induce our protocol as previously done in the *Scn1a*$^{+/-}$ mutant. Similar to *Scn1a*$^{+/-}$ mouse, (KO model) the homozygous mutation is lethal in the *Scn1a*$^{-/-}$ mice. The *Scn1a*$^{RH/+}$ model was available in the pure C57BL/6 in the laboratory. To maintain the mixed background as in the previous *Scn1a*$^{+/-}$ line, the *Scn1a*$^{RH/+}$ male in the pure C57BL/6 background was crossed with a 129/SvJ WT female and all the experiments were continued in this *Scn1a*$^{RH/+}$-129:B6 model.

2. SIH PROTOCOL IN *SCN1A*$^{RH/+}$-129:B6 MOUSE

The SIH protocol was successful in the *Scn1a*$^{RH/+}$ mutant. As described previously in material and methods, there are 4 groups in this study. The WT and *Scn1a*$^{RH/+}$ control groups that underwent the same handling protocol but without hyperthermia were used to evaluate the effect of the *Scn1a*$^{RH/+}$ mutation *per se*. The WT HYP mice were WT littermates that were submitted to the hyperthermia protocol (up to 42°C) but did not display seizures and were used to evaluate the effect of hyperthermia *per se* when compared to WT control animals. Finally the *Scn1a*$^{RH/+}$ SIH group was analysed to evaluate the effect of the seizures in the mutant mice. At SIH protocol day 10 the percentage of *Scn1a*$^{RH/+}$-129:B6 mice alive was 65.07%, while 92.06% for WT-

129:B6 HYP and 100% for WT-129:B6 and *Scn1a*$^{RH/+}$-129:B6 control animals **(FIGURE 30A)**. The *Scn1a*$^{RH/+}$ mice presented seizures when submitted to hyperthermia and the seizures last usually lower than 1 minute (short-lasting or simple hyperthermic seizures). The temperature threshold to induce seizure at day 1 was 41.63±0.04 and significantly increased at day 2 and 3 indicating an adaptive compensation in response of the SIH. Passed day 3, the animals returned to temperature thresholds similar to day 1 for the following days **(FIGURE 30 B)**. The seizure severity started at grade 5 for the first day, meaning that the animals were having forelimb clonus with a tonic component (rearing) and twist of the body (failing) – seizure with origin in the forebrain but spreading to brainstem. The severity was increasing across the days **(FIGURE 30 C)**. By day 4, the majority of the animals were displaying GTC seizures (grade 6) indicating that the seizure was involving to the brainstem structures **(FIGURE 30 C)**.

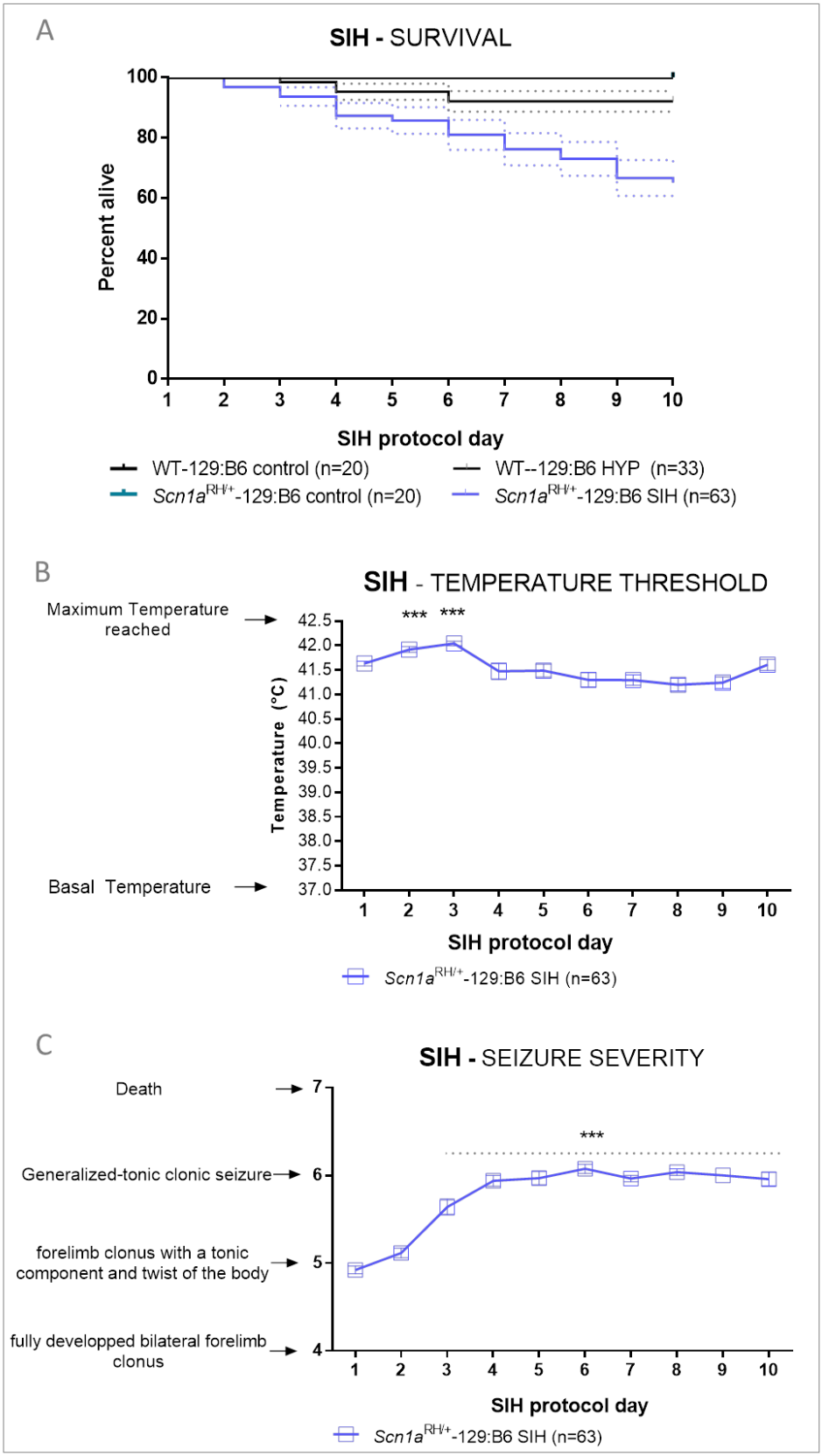

FIGURE 30. SEIZURES INDUCTION BY HYPERTHERMIA (SIH) IN *SCN1A*$^{RH/+}$-129:B6 MICE.

A: Percentage of mice alive during the 10-days of seizures induction by hyperthermia. **B:** Temperature treshold for the appeareance of the 1st behavioral sign of a seizure. *C:* Characterization of the seizure severity according to the scale adapted for seizures that resultt from the disruption of the GABAergic system. n=number of animals, ***p<0.001

Chapter 3- LONG-TERM EFFECTS OF THE 10-DAYS SEIZURES INDUCTION BY HYPERTHERMIA PROTOCOL IN *SCN1A*$^{RH/+}$-129:B6 MICE.

Due to the reasonable reproduction and resistance of the *Scn1a*$^{RH/+}$ -129:B6 mouse (GEFS+ model) to the SIH, we decided to pursue our research using this mutant mouse and thus answer our main question i.e if seizures can worsen epileptic and cognitive phenotypes in mouse models carrying the *Scn1a* gene mutation.

1. SIH WORSEN THE EPILEPTIC PHENOTYPE IN *SCN1A*$^{RH/+}$-129:B6 MUTANT MOUSE

It was previously reported that *Scn1a*$^{RH/+}$ in C57BL/6J background present very low level of spontaneous seizure activity (Martin et al., 2010b). We wanted to test if it was the case for our animals that should exhibit even milder phenotype introduced by the 129/SvJ background, as previously reported for other *Scn1a* mutants (Rubinstein et al., 2015a; Yu et al., 2006a). For this we induced seizures by hyperthermia for 10 days on the *Scn1a*$^{RH/+}$-129:B6 mice, as reported in the previous chapter. The animals were implanted with the 5 ECoG electrodes **(FIGURE 31A)** on the day following the last day of the protocol. Two days after the surgery, the animals were connected to the ECoG recording cables and recorded in time windows of three days during 2 months. The analysis of the ECoG signal was done simply by quantifying the number of GTC spontaneous seizures as illustrated in **FIGURE 31B**. We are conscious that a more profound analysis of the signal would a revealed more events and we plan to perform this analysis in due course.

FIGURE 31C shows the results obtained. We did not observe any spontaneous GTC seizure in the *Scn1a*$^{RH/+}$-129:B6 control mice during the period tested. It is possible that they exhibited more subtle ECoG alterations that we did not observe using our analysis method. However, it was clear that the SIH increased seizure frequency in the mutant animals. We observed the appearance of 0.5 to 1 seizure in average per day and per animal. We thus conclude that by inducing seizures for 10 days in the *Scn1a*$^{RH/+}$-129:B6 model that normally presented no (or very low) epileptic history, we could convert its phenotype into a severe epileptic model.

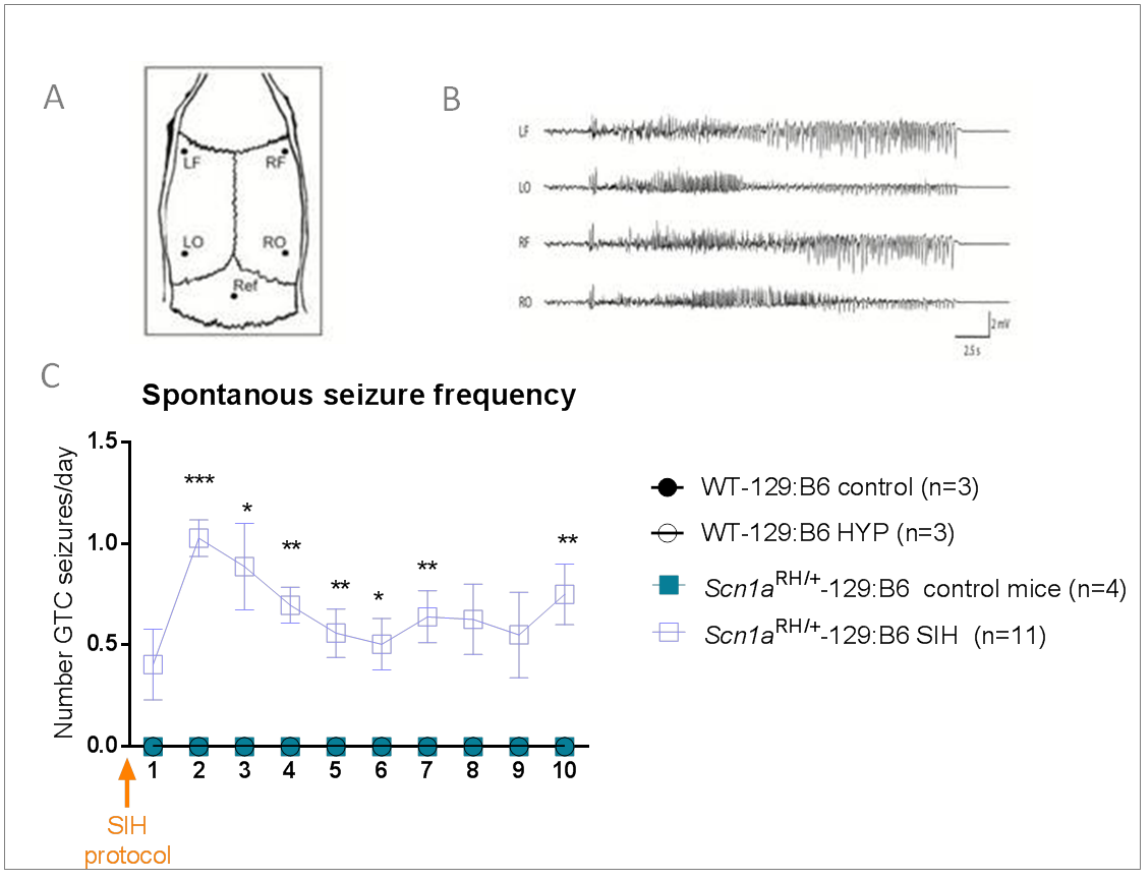

FIGURE 31. SIH PROTOCOL WORSENS THE EPILEPTIC PHENOTYPE IN *SCN1A*$^{RH/+}$-129:B6 MUTANT MICE. **A:** Position of the elctrods implantation. **B:** ECoG signal showing a spontaneous GTC seizure, scale bars 2mV, 2.5s. **C:** Spontaneous seizures frequency recorded two days following the last day of SIH (represented with the orange arrow) in *Scn1a*$^{RH/+}$-129:B6 mice after 10 days of SIH compared to control WT-129:B6 and *Scn1a*$^{RH/+}$-129:B6 and WT-129:B6 HYP mice. LF (Feft frontal), RF (right frontal), LO (Left occipital) RO (right occipital), Ref: Reference electrode. N=number of animals.

2. CELLULAR AND MOLECULAR ALTERATIONS IN HIPPOCAMPUS AFTER SIH IN *SCN1A*$^{RH/+}$-129:B6 MOUSE MODEL

After successfully inducing the protocol of SIH, we wanted to first understand if important cellular and molecular rearrangements had occurred during the post-SIH resting time.

2.1 *Cytoarchitecture is preserved after seizures in Scn1a*$^{RH/+}$ *mice in the hippocampus*

We first explored if seizures could induce neuronal damage and important cytoarchitecture changes. We induced seizures using the SIH protocol as described previously and allowed the animals to rest until they reached P60. The brains were then fixed, sliced and stained with Nissl and NeuN antibodies to evaluate neuronal integrity

and organization. The hippocampal formation receives the major excitatory input from the entorhinal cortex via the perforant path to primarily terminate in the dentate gyrus. Dentate axons, the mossy fibers, project to the CA3 region and from there the Schaffer collaterals convey the processed input to the CA1 area. Thus, the dentate gyrus operates as a gate at the entrance to the hippocampus, filtering incoming excitation from the entorhinal cortex (Acsády and Káli, 2007; Henze et al., 2002). In other *Scn1a* mouse models the hippocampus has been shown to participate in the seizure onset (Liautard et al., 2013; Ohno et al., 2011) and it is also of major importance in memory processing (Neves et al., 2008). Therefore, it is conceivable to speculate that seizures induction in a mouse model carrying a *Scn1a*$^{RH/+}$ mutation causes cellular alterations within the hippocampus. However, the neuropathological evaluations (Nissl and NeuN staining) showed no major cytoarchitecture modifications in the hippocampus of *Scn1a*$^{RH/+}$-129:B6 mice after the protocol of seizure induction.

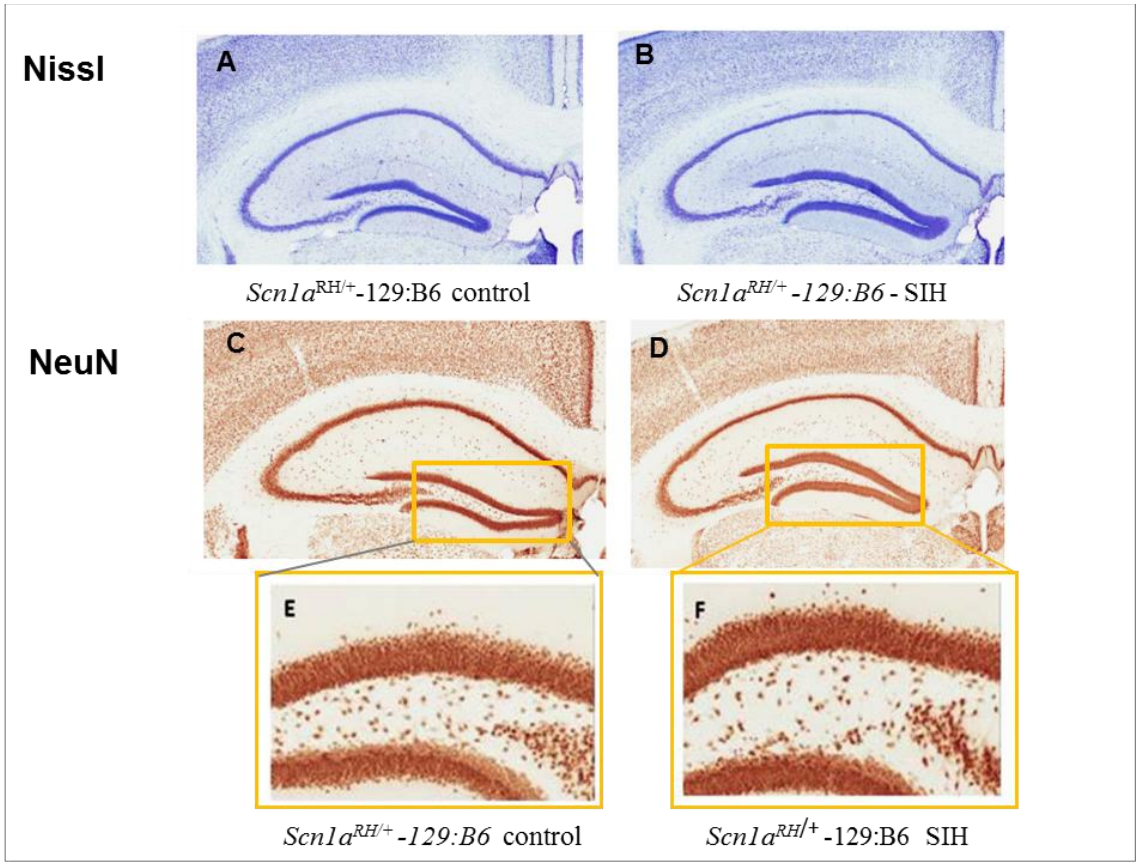

FIGURE 32. SIH DO NOT INDUCE IMPORTANT CYTOARCHITECTURE CHANGES IN THE HIPPOCAMPUS IN *SCN1A*$^{RH/+}$*-129:B6* MUTANT MICE.

A,B: Photomicrographs illustrating Nissl staining in *Scn1a*$^{RH/+}$-129:B6 control and SIH mice. **C,D**: NeuN immunolabelling in *Scn1a*$^{RH/+}$-129:B6 control and SIH mice and amplified to the dentate gyrus in **E,F**.

In conclusion, the seizures did not induce gross cytoarchitecture changes in the hippocampus in the *Scn1a*$^{RH/+}$129:B6, suggesting that the SIH did not induce major neuronal death unlike other models of epilepsy (kainite, pilocarpine) (Kang et al., 2015; Kim et al., 2011, 2015; Wang et al., 2015). The results are therefore in line with what was observed in the *Scn1a*$^{+/-}$ mouse model in pure C57BL/6 background that present high spontaneous seizure activity but no neuronal death (Yu et al., 2006a).

2.2 *Long-term synaptic plasticity is maintained but not short-term synaptic plasticity in the CA1 region of the hippocampus after SIH in Scn1a*$^{RH/+}$*129:B6 mice*

Long-term potentiation (LTP) has been described to underlie the synaptic basis of learning and memory in the hippocampus (Bliss and Collingridge, 1993; Morris et al., 1986; Whitlock et al., 2006). We tested whether the SIH protocol affected the ability of the CA1 neurons of the hippocampus to potentiate and maintain an LTP after a strong stimulus. After inducing seizures at P21, we sacrificed the animals at P60 and evaluated their synaptic properties in hippocampal slices. **FIGURE 33A** shows LTP of the field excitatory post-synaptic potentials recorded at the CA3 to CA1 synapse. After obtaining a stable baseline, averaged at 100%, a pulse of 100 Hz/1s was given to induce an LTP. The immediate response (1st 2 minutes), reflecting post-tetanic potentiation, was significantly increased in *Scn1a*$^{RH/+}$-129:B6 mice submitted to SIH when compared to the 3 control groups. LTP was maintained after 60 minutes post-induction. The four groups showed similar LTPs with no changes in the LTP averages when measured during the last 15 minutes of the recording **(FIGURE 33B)**. However, using this induction protocol (1 pulse at 100Hz/1s), the LTP obtained was not very strong (~115% in control WT-129:B6 animals). We thus decided to induce LTP with a stronger protocol (4 pulses of 100Hz/1s with 5 minutes inter stimulus interval (ISI)) to see if all the groups could equally respond to a stronger stimulus. As shown in **FIGURE 33C&D,** the LTP was higher (~150% in control WT-129:B6 animals) as compared to **FIGURE 33A&B** with the stronger protocol. Yet, also with this protocol, all the groups displayed the same average LTP of fEPSP in the last 15 minutes of the recording. The increase in the immediate response (post-tetanic potentiation) after LTP induction was not observed this time, possibly due to the saturation after 20 minutes of the 1st induction pulse. As alterations in post-tetanic potentiation is generally due to functional alterations at the

pre-synapse (Balakrishnan et al., 2010; Colino et al., 2002; Voronin, 1982), we decided to also study paired-pulse facilitation, a measure of pre-synaptic plasticity (Zucker and Regehr, 2002). The fEPSP were evoked at different short ISI in order to study the pre-synaptic release facilitation. As expected, the PPR (quantified as the peak amplitude of the 2nd response divided by the 1st) decreases with the increase of the ISI in all groups. Interestingly, we observed an increase in the PPR at different ISI (150, 250, 300, 350, 400 ms) suggesting that SIH in *Scn1a*$^{RH/+}$-129:B6 mice might alter the release probability of the presynaptic neuron.

With these data we can conclude that SIH does not affect the LTP in CA1. We planned to test the LTP in the dentate gyrus (DG) that acts as first gatekeeper of the hippocampus (Acsády and Káli, 2007; Amaral et al., 2007; Treves et al., 2008), and has been stressed to have major importance in epiloptogenesis studies (*reviewed in* Dudek and Sutula, 2007). Also, *Cheah et al., 2012* and *Tsai et al., 2015* reported a higher reduction of Na_V 1.1 protein in the DG than in CA1 or CA3 areas of the hippocampus in *Scn1a* mutant mice, and altered functional an structural properties of the DG region of the hippocampus (Tsai et al., 2015). According to previous results from the laboratory, reliable induction of LTP in the DG requires blocking the inhibitory function (Houeland et al., 2010). We could indeed obtain LTP in the DG using the GABAergic blocker picrotoxin (data not shown). Yet, this poised a conceptual problem regarding its use in the context of the *Scn1a* gene mice. Indeed, Nav 1.1 channel's mutations mainly affect GABAergic neurons (Yu et al., 2006a), and the . It would thus have been more appropriate to avoid blocking GABAergic function during the study of this mouse model. Unfortunately, we could not obtain LTP in WT mice without picrotoxin leading us to give up on this experiment (data not shown).

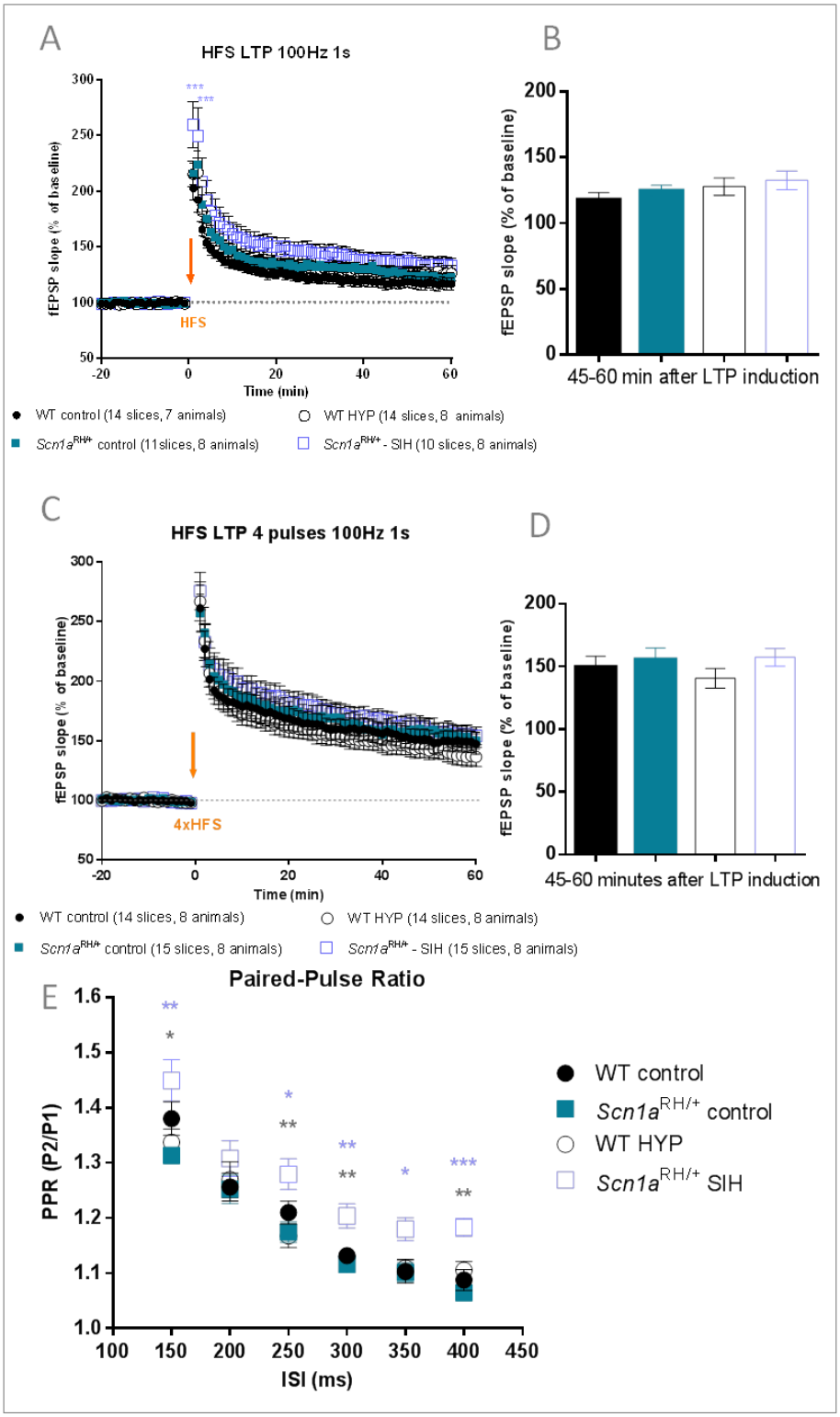

FIGURE 33. SHORT-TERM PRE-SYNAPTIC BUT NOT LONG-TERM POST-SYNAPTIC PLASTICITY IN CA1 REGION OF THE HIPPOCAMPUS IS ALTERED IN *SCN1A*$^{RH/+}$129:B6 MICE.

Long-term plasticity : **A,B:** LTP of fEPSP induced with one pulse of high-frequency stimulation at 100Hz/1s (orange arrow). **B:** Average of the last 15 minutes as % of baseline, from 45 minutes to 60 after LTP induction. **C:** LTP of fEPSP indcued with four pulses of high-frequency stimulation at 100Hz/1s with 5 min ISI (orange arrow). **D:** Average of the last 15 minutes as % of baseline, from 45 minutes to 60 after LTP induction. E: Short-term pre-synaptic plasticity. **E:** Paired-pulse ratio (P2/P1) at different inter-stimulus intervals. Statistical significance is represented in violet for difference between *Scn1a*$^{RH/+}$ control and SIH mice and in black for differences between *Scn1a*$^{RH/+}$ SIH mice and WT-HYP. * p<0.05; **p<0.01; ***p<0.001

2.3 *Scn1a*$^{RH/+}$ mice show an increase in firing frequency in granular cells in the dentate gyrus but not in CA1 pyramidal neurons after SIH

Field recordings of synaptic plasticity revealed the presence of modifications in short-term plasticity in CA1 area of the hippocampus. In addition previous studies in mouse models with *Scn1a* gene mutation had reported changes in DG granule cell's properties (Tsai et al., 2015). In collaboration with Dr Pousinha, we thus decided to pursue the analysis of DG granule cells and CA1 pyramidal neurons by whole cell current clamp recordings. We first examined their passive and intrinsic excitability properties. The intrinsic excitability, as measured by the frequency of APs at a given current injection, of CA1 pyramidal neurons from *Scn1a*$^{RH/+}$ SIH was slightly increased, though not statistically different, when compared to the other groups **(FIGURE 34A)**. By contrast, DG granule neurons from *Scn1a*$^{RH/+}$ SIH were strongly hyperexcitable **(FIGURE 34B)**, than DG granule neurons from the other control groups. Importantly, neither the mutation itself (compare WT control and *Scn1a*$^{RH/+}$ control) nor the hyperthermia induction (compare WT control and WT-HYP) affected, per se, the intrinsic excitability properties of the two neuron populations **(FIGURE 34)**. Other membrane properties including resting membrane potential and membrane resistance did not significantly differ between genotypes/treatments in both CA1 and DG hippocampus regions (Statistic Table chapter VIII-3 page 190).

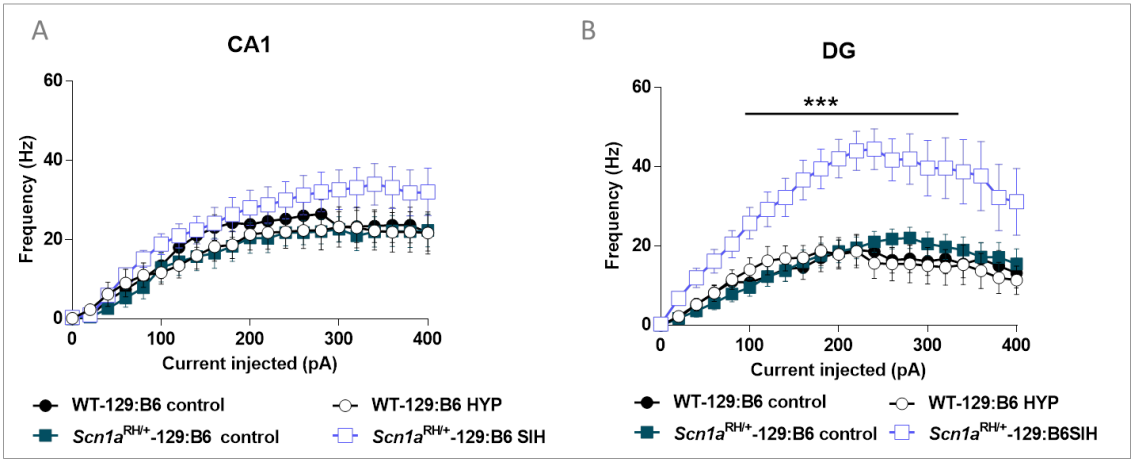

FIGURE 34. FIRING FREQUENCY OF EXCITATORY NEURONS IN THE DG BUT NOT IN THE CA1 IS INCREASED IN THE *SCN1A*$^{RH/+}$-129:B6 MICE SUBMITTED TO SIH.

Firing Frequency measured as the number of action potentials per second (Hz) when neurons were depolarized by increasing current steps (20pA steps with 1s duration) in CA1 **A** and DG **B**. n= number of animals, ***p<0.001.

3. SEIZURES INDUCED BY HYPERTHERMIA INDUCE LONG-LASTING CHANGES IN THE BEHAVIORAL AND COGNITIVE PHENOTYPES IN *SCN1A*$^{RH/+}$-129:B6 MICE.

As for the immunohistochemistry and electrophysiology analysis, another group of animals submitted or not to SIH at P21 went through a battery of behavioral tasks at P60. The order of the behavioral tasks was counterbalanced between cohorts of animals, except for openfield, social interaction and dark-light tests that were done at the beginning and for the analysis of activity in the actimeter that was done at the end.

3.1 *Scn1a*$^{RH/+}$*-129:B6 mice with SIH have a novelty-associated increase in activity in the openfield and stereotyped behavior without changes in anxiety.*

Previously, *Scn1a* mutation's carrying lines were reported to exhibit a novelty-associated increase in activity (Han et al., 2012a; Ito et al., 2013; Purcell et al., 2013; Sawyer et al., 2016). We placed the 4 groups in the openfield. The parameters analyzed to evaluate locomotor activity were the speed of travelling and the distance travelled. The two-way ANOVA of the distance travelled and average speed in the openfield (treatment x genotype) revealed a significant main effect of genotype and treatment and a significant interaction between treatment and genotype (all the statistical values are described in the chapter VIII-page 185). Tuckey's post hoc analysis showed that the WT-129:B6 (control and HYP) and *Scn1a*$^{RH/+}$-129:B6 control mice travelled similar distances and at similar average speed. *Scn1a*$^{RH/+}$-129:B6 mutants submitted to the SIH protocol travelled a greater total distance and travelled at a higher average speed than the 3 other groups **FIGURE 35A&B**. We could assume that the *Scn1a*$^{RH/+}$ mutation *per se* does not induce novelty-associated locomotor changes, however, after chronic seizure induction by hyperthermia at early-age, the *Scn1a*$^{RH/+}$-129:B6 was hyperactive when exposed to a novel environment (illustrated in the track-plot report

FIGURE 35. SCN1ARH/+ -129:B6 SIH HAVE A NOVELTY associated increase in activity and stereotyped behavior.**D)**

We wanted to go further in the analysis and we observed that the hyperactive mice had some repetitive behaviors. We counted the number of rotations of the animal's body and the number of rearing episodes in the period tested. The ANOVA showed a main effect of genotype and treatment for both measures with an interaction between

treatment x genotype for the number of rearing episodes but not for the rotations of the animal's body. The post-hoc analysis (Tuckey's) indicated that the WT-129:B6, *Scn1a*$^{RH/+}$-129:B6 control mice and WT-129:B6 HYP displayed similar number of these events, however the *Scn1a*$^{RH/+}$-129:B6 mice submitted to SIH had exacerbated number of rotations of the animal's body and rearings **(FIGURE 35E&F)**. These two measures are associated to stereotyped behavior.

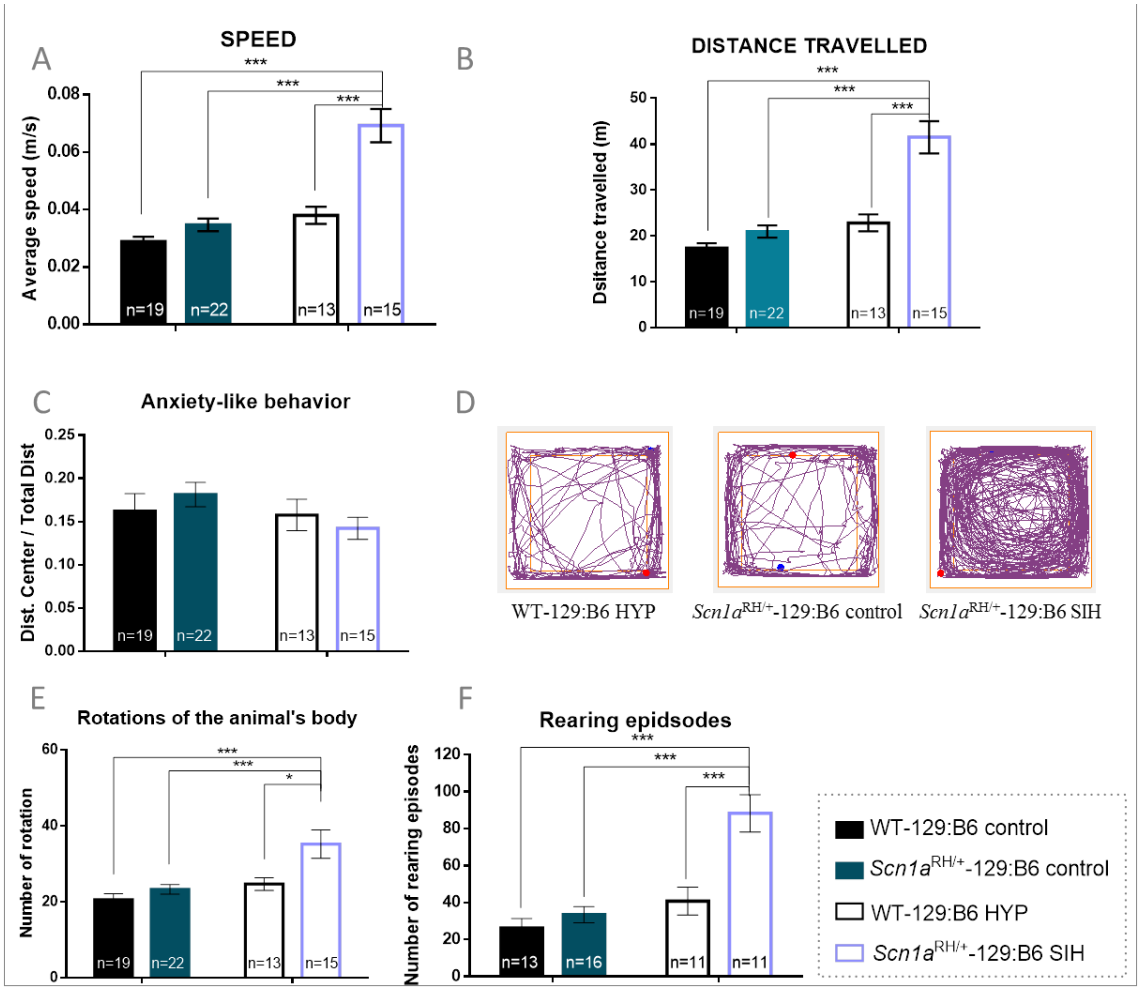

FIGURE 35. *SCN1A*$^{RH/+}$ -129:B6 SIH HAVE A NOVELTY ASSOCIATED INCREASE IN ACTIVITY AND STEREOTYPED BEHAVIOR.

The animals were placed in the openfield for 10 minutes. **A, B**- Locomotor activity. **A:** average speed (m/s) and **B:** Distance travelled (m) caracterize the locomotor activity of the 4 groups. **C:** Anxiety measured as the distance travelled in the center dicided by the total distance travelled. **D:** Track plots of the locomotor activity of a WT-129:B6 HYP, a *Scn1a*$^{RH/+}$-129:B6 control and a *Scn1a*$^{RH/+}$-129:B6 SIH mice during the 10 minutes in the openfield. **E, F** Measures of stereotyped behavior: **E:** Rotations of the animals body (counted when the animal complete a 180° turn) and **F:** Number of rearing episodes. The legend presented on the bottom right is for all the graphs. n=number of animals, *p<0.05,***p<0.001.

The openfield can be used as a first screen for anxiety in rodents however it should be complemented with other paradigms (Prut and Belzung, 2003). This measure can easily be obtained by quantifying the time spent in the center or the latency to first entry in the center. However, the important changes in locomotion induce a bias in this measure, proposing a decrease in anxiety in the *Scn1a*$^{RH/+}$-129:B6 mice submitted to SIH (data not shown). Another accepted measure for anxiety in the openfield is ratio: distance travelled in the center divided by the total distance travelled. We observed that all the groups had the same ratio of center exploration. This measure indicated that the SIH did not induce anxiety in the *Scn1a*$^{RH/+}$-129:B6 mice **(FIGURE 35C)** and all groups behaved equally. To complete the findings about anxiety obtained in the openfield we ran a trial: the dark↔light box (used to study anxiety in rodents). **FIGURE 36** shows the time spent in the light compartment – more anxiogenic **(A)** and the number of entries in the same compartment **(B)**. The Two-way ANOVA revealed a significant interaction between the treatment and genotype with a main effect of treatment for the number of entries in the light zone but not for the time in the light zone. The post hoc analysis show no differences between the groups for the time spent in the anxious light zone, but a difference between the WT-129:B6 and WT-129:B6 HYP in the number of entries. These results again suggest that there is no increase in anxiety caused by the seizures, even if this test is not very convincible due to the very low time spent by the WT-129:B6 control mice in the light side (lower than 10 %) possibly due to the high light intensity used in the test and the large variability inside the groups as seen in the dot-plot graphs.

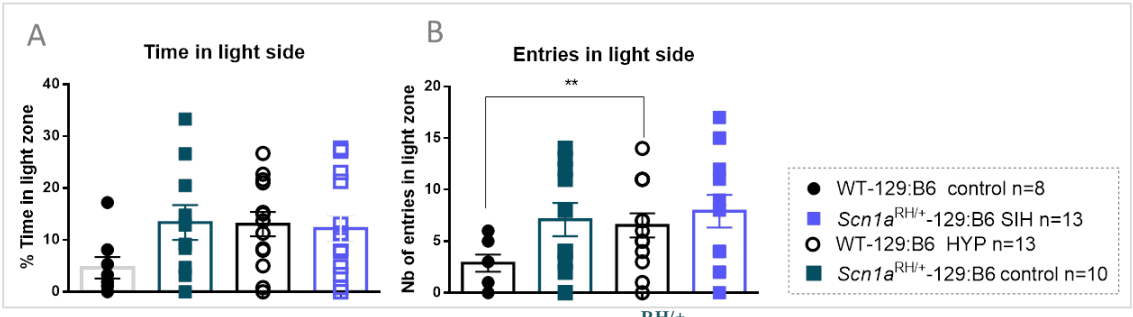

FIGURE 36. THE SIH DOES NOT INDUCE ANXIETY IN *SCN1A*$^{RH/+}$-129:B6 MUTANTS.
A: time in the light side of the dark↔light box. **B:** Number of entries in the light side of the dark↔light box. n=numer of animals. **p<0.01.

We could conclude that by confronting the 4 four groups to a novel and stressful environment, the WT-129:B6, WT-129:B6 HYP and *Scn1a*$^{RH/+}$-129:B6 control mice

behave at the same level indicating that the mutation *per se* or the hyperthermia *per se* do not affect the novelty reaction, while, the 10-days of SIH clearly changed the reaction to novelty in *Scn1a*$^{RH/+}$-129:B6 mice as demonstrated by a clear increase in activity, exacerbated stereotyped behavior but no changes in anxiety.

3.2 *The novelty-associated hyperactivity normalizes after habituation in the actimeter in Scn1a$^{RH/+}$-129:B6 SIH mice.*

Our first worry concerning the hyperactivity induced by the SIH was: is it associated to novelty or maintained chronically as home cage behavior? As we could not record the animals in their home cages, we placed them in the actimeter for 72 hours. The sensors in the actimeter give the parameters represented in **FIGURE 37**. The measures are represented in bins of 30 minutes period (**A&B**) and 12 hours period (**C**).

The animals were placed at 7 pm at day 1 and removed 3 days later. In **FIGURE 37A** the horizontal activity measures the activity on the actimeter's floor (movements at the back + movements in the front + number of crosses) of the 4 groups of animals. RM-two way ANOVA revealed a significant interaction (genotype-treatment x time) with a main effect of time but not genotype-treatment. This main effect is observed with the clear circadian cycle observed by the four groups. As the WT-129:B6 animals, the *Scn1a*$^{RH/+}$-129:B6 control and *Scn1a*$^{RH/+}$ -129:B6 SIH showed low activity during the light/resting phase and higher activity during the dark/active phase with no differences between the groups at any bin of time (pot-hoc analysis show no differences between the groups). The vertical activity, measuring the number of rearing episodes also represents a measure of activity and it is illustrated in **FIGURE 37A&B.** The RM-Two-way ANOVA of the vertical activity showed a significant main effect of time (as previously) but also of genotype-treatment and a significant interaction between the two. The four groups again showed a normal circadian cycle with low activity during the resting-light phase and high activity during the active-dark phase, confirming that neither the mutation nor the seizures induce important changes in the circadian cycle. Tuckey's post-hoc analysis showed a significant increase in the vertical activity for the *Scn1a*$^{RH/+}$-129:B6 SIH when compared to the 3 control groups during the first 12 hours in the actimeter (1st day and night). This activity tended to normalize and became similar to the controls for the following hours **(FIGURE 37B),** even if for 3 time points during the active phase this activity remained significantly increased. In **FIGURE 37C** the vertical activity is pooled in time bins of 12 hours and again we can see that the SIH significantly increases significantly the activity in the *Scn1a*$^{RH/+}$-129:B6 group but not the mutation *per se* (no differences between the WT-129:B6 control and *Scn1a*$^{RH/+}$-129:B6 control). Yet, this increase in activity is temporary and normalizes within 24

hours, indicating that the hyperactivity in *Scn1a*$^{RH/+}$-129:B6 with SIH is most probably associated to novelty.

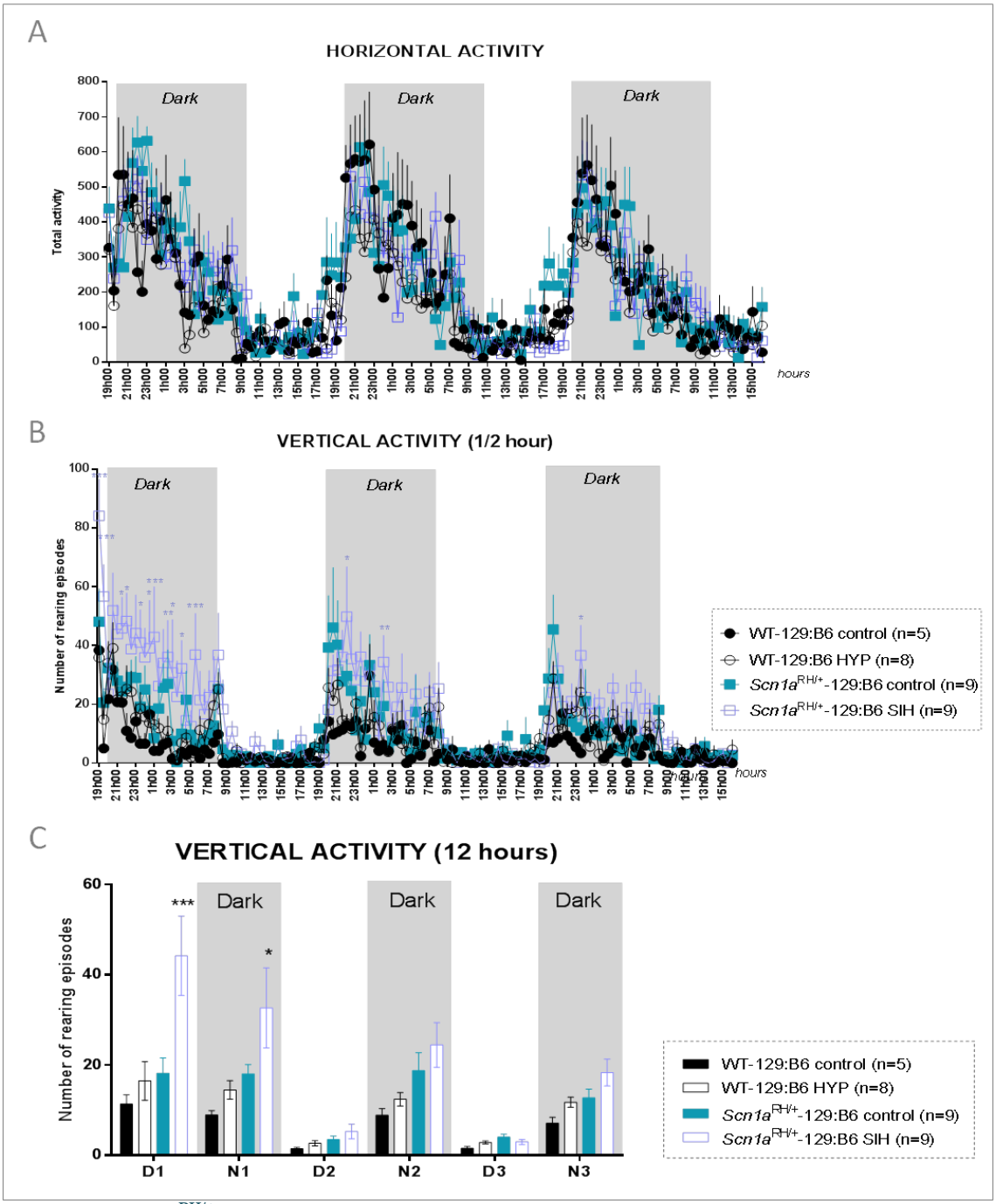

FIGURE 37. *SCN1A*$^{RH/+}$-129:B6 MUTANT MICE EXHIBIT A NOVELTY-ASSOCIATED INCREASE IN REARING ACTIVITY IN THE ACTIMETER.

A: Total horizontal activity (sum of the activity at the front + back + front-back crosses) scored for 69 consecutive hours (data showed by half-an-hour periods). B: Total vertical activity (number of rearing episodes) for 69 consecutive hours (data showed by half-an-hour periods). C: Total vertical activity (number of rearing episodes) for 69 consecutive hours (data pooled by 12-hour periods). Statistical significance is shown in violet when the *Scn1a*$^{RH/+}$-129:B6 SIH mice are different that *Scn1a*$^{RH/+}$-129:B6 control mice and WT-129:B6 HYP mice. *p<0.05, **p<0.01, ***p<0.001, n=number of animals.

3.3 *Scn1a*$^{RH/+}$*-129:B6 SIH mice show impaired social interaction ability in the three-chamber social interaction test.*

The autistic-like phenotype of *Scn1a* mutation's carrying mouse lines with severe phenotypes has been stressed previously (Han et al., 2012a; Ito et al., 2013). We then asked if the seizures could affect the sociability skills. The four groups were tested in the three chamber test.

We first ran a 10-minutes habituation trial, in which the animals were placed in the central chamber and had to explore the two side chambers. This trial was crucial in order to detect chamber preferences and acclimatize the animals to the testing apparatus. All groups explored equally the two-side chambers **FIGURE 38A,** but the two-way ANOVA of distance travelled and speed in this phase showed a significant main effect of treatment and genotype and a significant interaction between them. The post-hoc analysis (Tuckey's) highlighted that the *Scn1a*$^{RH/+}$-129:B6 SIH mice travelled significantly longer and at higher speed than the 3 other groups, confirming again the novelty-associated increase in activity seen in the openfield and actimeter. This increase in activity normalized and was comparable to other groups' level during the sociability and social novelty phases (data not shown, statistic values in the chapter VIII-page 185).

The sociability phase consisted in the choice between and empty wire cage or a wire cage containing a stranger mouse. We analyzed the social interaction with a RM-two way ANOVA and it revealed a significant main effect of the cage chosen for exploration by the test mouse. The post hoc analysis (Sidak's) indicated that the WT-129:B6 control, WT-129:B6 HYP and *Scn1a*$^{RH/+}$-129:B6 control mice interacted significantly longer with the M than with the EC, demonstrating preserved sociability skills. However, *Scn1a*$^{RH/+}$-129:B6 with SIH had no preference between the EC and the M, demonstrating a perturbation in the sociability skills after SIH **(FIGURE 38D)**. In the social novelty phase, again the analysis revealed a significant main effect of the cage, and the post-hoc analysis showed that the WT-129:B6, WT-129:B6 HYP and the *Scn1a*$^{RH/+}$-129:B6 control interacted significantly longer with the nM as expected. For *Scn1a*$^{RH/+}$-129:B6 mice with SIH, the time exploring the nM and the fM was equivalent, showing no preference between the nM **(FIGURE 38E)**. These results of the two phases demonstrate that the social skills were importantly affected after experiencing early life seizures in this mouse model. All together these results show that seizures in infancy can promote long-lasting alterations in social skills during adulthood.

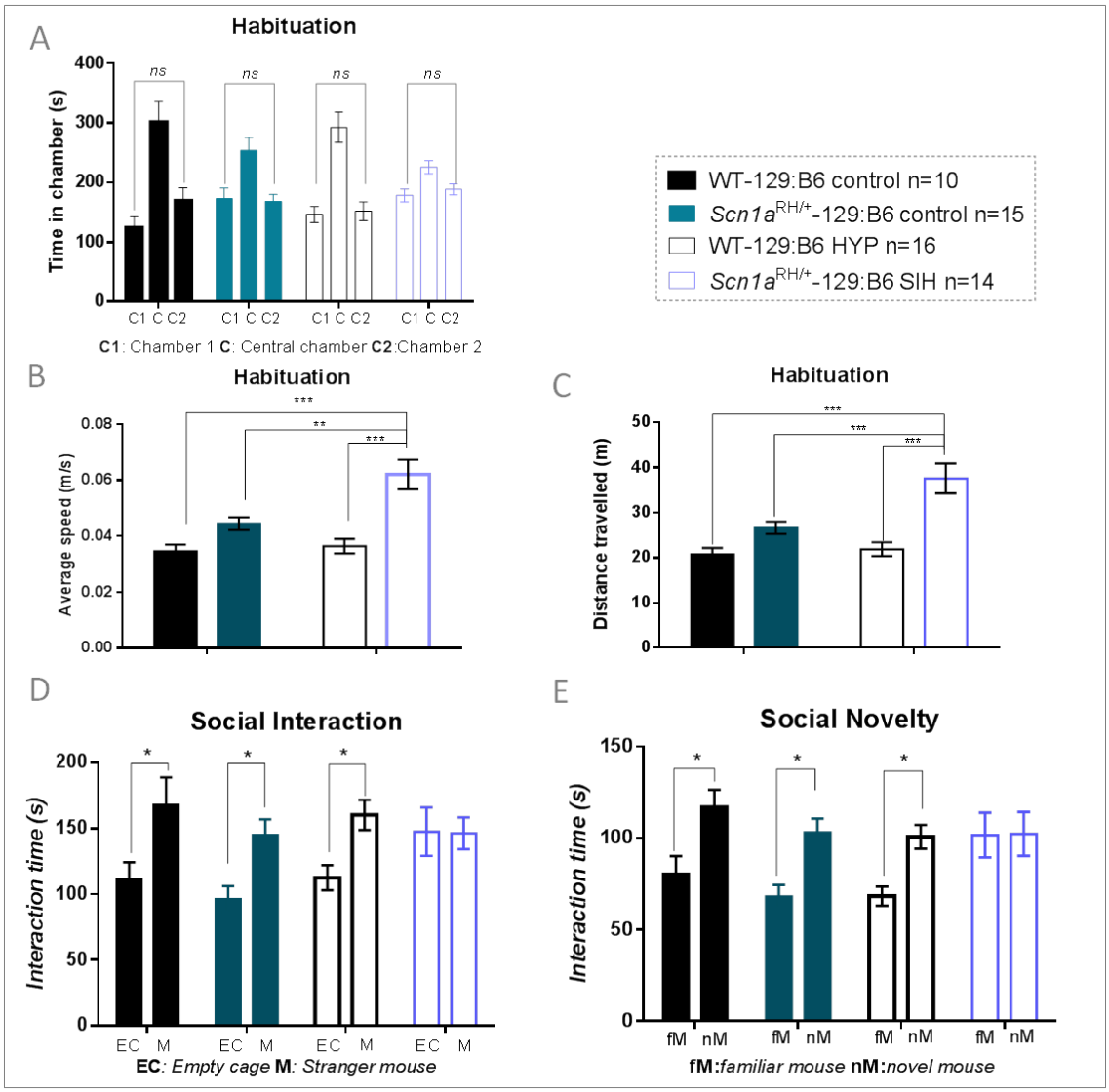

FIGURE 38. SIH IMPAIRS SOCIABILITY IN *SCN1A*$^{RH/+}$-129:B6 MICE.

A, B & C: Habituation phase. A: Time spent by the test mouse in each empty chamber (C1- chamber 1, C-center, C2- chamber 2). B: Average speed (m/s) during habituation phase. C: Distance travelled (m) during habituation phase. D: Sociability phase. Time spent by the test mouse interacting with the empty cage (EC) or the stranger mouse (M). E: Social novelty phase. Time spent by the test mouse interacting with the familiar mouse (fM) or the novel mouse (nM). *p<0.05, **p<0.01, ***p<0.001, n=number of animals. The bar legend is common for all the figures.

3.4 *Scn1a*$^{RH/+}$*-129:B6 mice with SIH have impaired learning and memory in the Morris water maze task.*

Mental retardation is a main consequence of DS disease progression (Olivieri et al., 2016; Ragona et al., 2011b). We observed alteration in neuronal function in the hippocampus so it was important to test the memory functions **(FIGURE 33 ; FIGURE 34)** dependent on this structure. We submitted the control and hyperthermia/SIH mice to a protocol of spatial learning and memory in the MWM apparatus. This test was divided in two phases: the cue task to confirm no visual and motor impairment and the spatial

task (4 training days and a 24h probe) to test learning and long-term memory. *Scn1a*$^{RH/+}$-129:B6 SIH mice were initially impaired having higher latency to approach a visible platform at cue task D1, but reached the same level of performance as *Scn1a*$^{RH/+}$-129:B6 control and WT groups by cue task D2. All groups significantly decreased the latency to find the visible platform from D1 to D2 (RM-ANOVA with significant main effect of Cue task day and Group), being all at an average of escape latency lower than 10 seconds **(FIGURE 39A)**. The increased latency to find the cued/visible platform at D1 was associated to a significant increase in the distance travelled by the *Scn1a*$^{RH/+}$-129:B6 SIH mice **(TABLE 13)** with a decrease in the average speed when compared to the WT-129:B6 HYP but not to the *Scn1a*$^{RH/+}$-129:B6 control mice **(TABLE 12)**, so we could not say that the higher latency was justified by motor problems in the SIH submitted mice. We did not observe the novelty-associated increase in locomotion in the MWM (as in the openfield and actimeter) possibly of the water be something that they never experience before, and probably they do not know how to react and try to escape. This first observation indicated that even if the *Scn1a*$^{RH/+}$-129:B6 SIH mice took longer time to understand the rule (D1), by the end of the cue task they equalize to the other groups latency's and prove that they did not have sensorimotor problems that could impede the animals to perform the MWM task. Only one animal of the *Scn1a*$^{RH/+}$-129:B6 SIH group that never escape by him self to the platform was removed from the study.

The spatial training proceeded by removing the cue from the platform and opening the curtains to expose the visual cues. The RM-two way ANOVA revealed a significant main effect of training day and group, the group x training day interaction did not, however, quite reach significance. The tuckey's post-hoc analysis showed that at training D1 the *Scn1a*$^{RH/+}$-129:B6 SIH mice showed higher escape latency than the 3 control groups **(FIGURE 39A)**. However, it is important to note that, as described in the material and methods, each training day results in the average of 4 trials. We could believe that in training 1 the *Scn1a*$^{RH/+}$-129:B6 SIH group started from a higher latency than the 3 other groups justifying why they never equalized their performance. However, on trial 1 of training day 1 all 4 groups had the same latency to find the platform suggesting that the *Scn1a*$^{RH/+}$-129:B6 SIH had a similar behavior as the other groups and that the within-day learning was not as good in this group as the 3 control groups **(FIGURE 39B).**

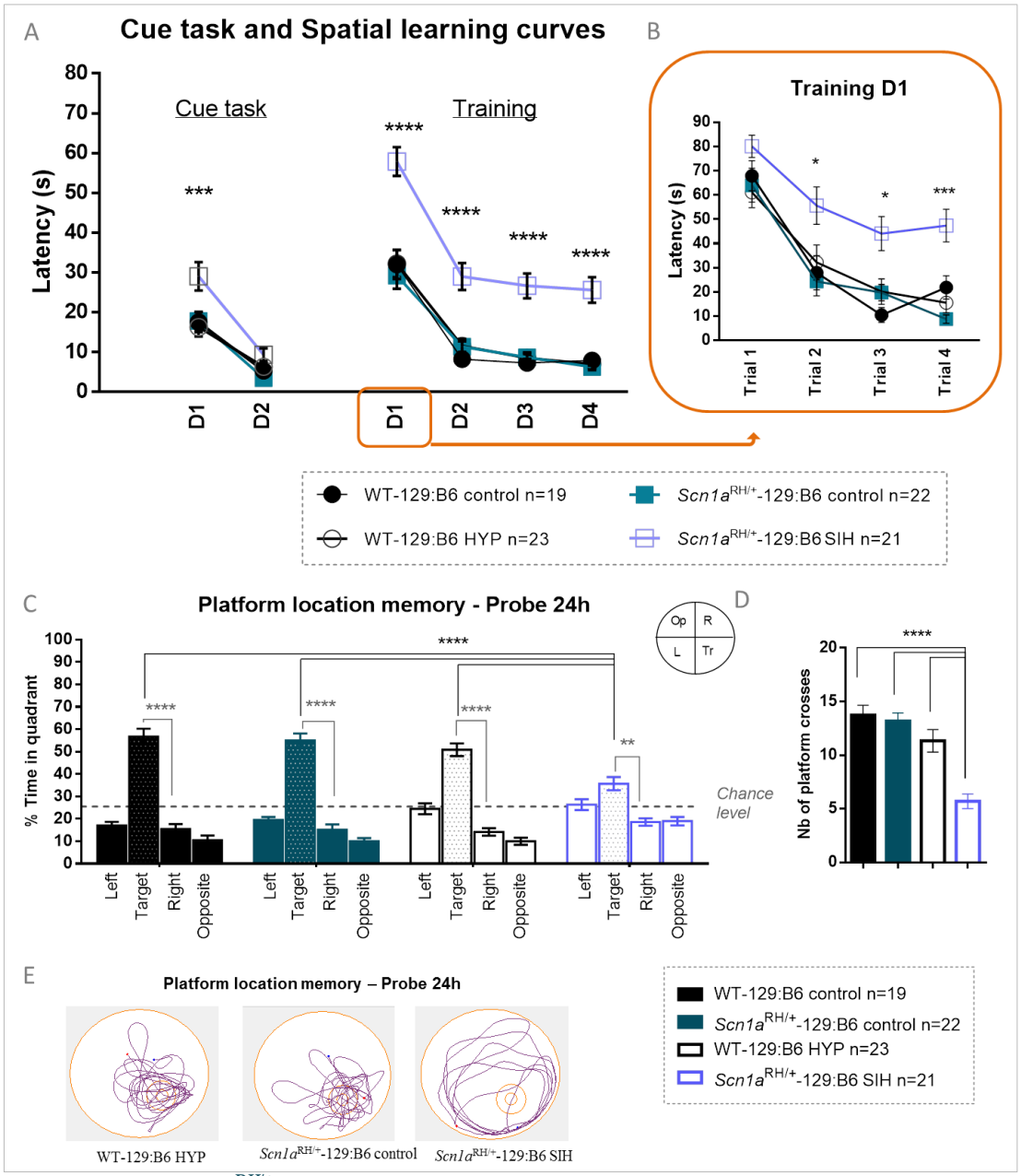

FIGURE 39. THE *SCN1A*$^{RH/+}$-129:B6 SUBMITTED TO SIH DISPLAY IMPAIRED SPATIAL LEARNING AND MEMORY IN THE MWM TASK.

A: Each cue task and training day represents the average of the four trials latencies to find the platform. In the cue task, the platform is visible, while in the training the platform is hidden. **B:** representation of the four trials of the spatial training day 1. **C:** 24 hours after training completion the platform is removed and the proportion of time spent searching each of the four quadrants of the pool during 60 sec of swimming in the absence of the hidden platform is reported. The target quadrant (where the platform was located) is highlited with a different pattern. The persistence in the target quadrant is compared to chance level (considered at 25%) (dotted line) **D (right):** Number of crosses in the enlarged platform zone (the smaller orange circle represents the platform in the track plots while the bigger circle is the enlarged zone **E**) were measured. *p<0.05, ***p<0.001, ****p<0.0001;n=number of animals.

TABLE 12. AVERAGE SPEED (M/S) IN THE MWM FOR CUE TASK AND SPATIAL LEARNINGS.
Mean±S.E.M of the swim speed across the cue task and training days by the 4 groups. Statistical significance is represented in the last column of the table. The 3 control groups did not differ in any day so we represented the statistics when the *Scn1a*$^{RH/+}$-129:B6 SIH mice (column in bold) are significantly different than the WT-HYP or *Scn1a*$^{RH/+}$-129:B6 control groups. *p<0.05, **p<0.01, ***p<0.001.

		WT-129:B6 control	WT-129:B6 HYP	*Scn1a*$^{RH/+}$-129:B6 control	*Scn1a*$^{RH/+}$-129:B6 SIH	Statistical significance
		Mean ± S.E.M				*Scn1a*$^{RH/+}$-129:B6 SIH *vs. :*
Cue task D1	Swim speed (m/s)	0,127± 0,006	0,133± 0,006	0,131± 0,006	**0,104± 0,006**	WT-HYP - **; *Scn1a*$^{RH/+}$ control-*
Cue task D2		0,145±0,009	0,137±0,009	0,138±0,008	**0,120±0,007**	-
Training D1		0,173 ±0,006	0,163±0,007	0,1572±0,006	**0,1914±0,006**	WT HYP - *; *Scn1a*$^{RH/+}$ control - **
Training D2		0,1398±0,007	0,144±0,008	0,1388±0,006	**0,1673±0,006**	*Scn1a*$^{RH/+}$ control - *
Training D3		0,1196±0,007	0,149±0,008	0,1390±0,007	**0,1699±0,006**	*Scn1a*$^{RH/+}$ control - **
Training D4		0,1254±0,007	0,1415±0,008	0,1298±0,007	**0,1735±0,006**	WT HYP - **; *Scn1a*$^{RH/+}$ control - ***

TABLE 13. DISTANCE TRAVELLED (M) IN MWM FOR CUE TASK AND SPATIAL LEARNING TRAINING DAYS.
Mean±S.E.M of the distance travelled across the cue task and training days by the 4 groups. Statistical significance is represented in the last column of the table. The 3 control groups did not differ in any day so we represented the statistics when the *Scn1a*$^{RH/+}$-129:B6 SIH mice (column in bold) are significantly different than the WT-HYP or *Scn1a*$^{RH/+}$-129:B6 control groups. *p<0.05, ***p<0.001

		WT-129:B6 control	WT-129:B6 HYP	*Scn1a*$^{RH/+}$-129:B6 control	*Scn1a*$^{RH/+}$-129:B6 SIH	Statistical significance
		Mean ± S.E.M				*Scn1a*$^{RH/+}$SIH *vs*:
Cue task D1	Distance travelled (m)	2,970±0,496	2,644±0,447	2,653±0,374	**4,338±0,654**	WT-HYP - *; *Scn1a*$^{RH/+}$ control - *
Cue task D2		1,223±0,206	1,073±0,203	0,558±0,075	**1,715±0,398**	-
Training D1		6,460±0,793	6,231±0,698	5,556±0,682	**11,689±0,837**	WT-HYP - ***; *Scn1a*$^{RH/+}$ control - ***
Training D2		1,315±0,163	2,066±0,364	1,921±0,276	**6,102±0,752**	WT-HYP - ***; *Scn1a*$^{RH/+}$ control - ***
Training D3		1,139±0,204	1,603±0,246	1,435±0,222	**5,877±0,736**	WT-HYP - ***; *Scn1a*$^{RH/+}$ control - ***
Training D4		1,295±0,283	1,220±0,212	1,025±0,171	**5,142±0,740**	WT-HYP - ***; *Scn1a*$^{RH/+}$ control - ***

The post-hoc analysis also showed that all the groups significantly decreased their latencies to find the platform from training D1 to D2, and then maintained their performance levels (D2-D4). Even if this indicate that all the groups understood that there was an escape rule to follow, the latency to escape was significantly higher in the *Scn1a*$^{RH/+}$-129:B6 SIH mice **(FIGURE 39A)** during the 4 training days. In addition, we

see in **FIGURE 39A** that by training D4 the WT-129:B6 control, WT-129:B6 HYP and *Scn1a*$^{RH/+}$-129:B6 control had an escape latency lower than 10 seconds as seen in the cue task D2, while the *Scn1a*$^{RH/+}$-129:B6 SIH did not (like they had a cue task D2). The poorer performance of the *Scn1a*$^{RH/+}$-129:B6 SIH mice is unlikely to be due to effects on motor function as the swim speed was significantly increased when compared to the *Scn1a*$^{RH/+}$-129:B6 control mice for all the training days and to WT-129:B6 HYP at D1 and D4 **(TABLE 12)**. The distance travelled was also increased during all the training days **(TABLE 13)**.

Twenty-four hours after training completion, we ran a probe trial to test the strength of the long-term memory when removing the platform, as explained previously. The one sample t-test comparing the percentage of time in the target zone, where the platform was located, to the chance level (25%) indicated that all the groups persisted longer than chance in this quadrant; By contrast, the *Scn1a*$^{RH/+}$-129:B6 SIH persisted lower time in this quadrant than the other 3 groups **(FIGURE 39C)** (RM-ANOVA main effect of Quadrant and significant Group (treatment-genotype) x Quadrant interaction). The post-hoc analysis of within group quadrant persistence revealed that the WT-129:B6 and *Scn1a*$^{RH/+}$-129:B6 controls persist significantly higher in the target quadrant than in the other 3 quadrants (left, right and opposite). By contrast, the *Scn1a*$^{RH/+}$-129:B6 SIH mice did not significantly discriminate between the target and left quadrants. In addition, we counted the number of crosses in the platform zone area. The two-way ANOVA revealed a significant Genotype x Treatment interaction with main effects of Genotype and Treatment. We observed that the number of crosses in the platform zone was significantly decreased in the *Scn1a*$^{RH/+}$-129:B6 SIH mice compared to the other groups **(FIGURE 39D)**. The tracking plots of the probe trial illustrated in **FIGURE 39E** clearly indicate that the *Scn1a*$^{RH/+}$-129:B6 SIH are less precise in remembering the previous emplacement of the spatial platform.

We conclude that, although *Scn1a*$^{RH/+}$ SIH mice showed a learning improvement in the latency to find the platform from training D1 to D2, they show poorer learning performance (within days and across days) and memory strength (long-term memory) than the control WT-129:B6 and *Scn1a*$^{RH/+}$-129:B6 and the WT-129:B6 HYP. Accordingly, the results suggest that SIH protocol in the mutant mice also induce perturbations in hippocampal learning and memory during adulthood.

3.5 *Scn1a*$^{RH/+}$-129:B6 mice show decreased contextual-fear conditioning

On the first day of the CFC the animals were placed in the conditioning box. After 2 minutes of habituation to the box, 3 consecutive shocks with 60s interval were delivered. **FIGURE 40A** illustrates the freezing percentage during the 5 minutes of conditioning. The RM-two way ANOVA (Genotype x Treatment) showed a significant main effect of genotype but not of treatment. The *Scn1a*$^{RH/+}$-129:B6 mutation seemed to decrease the freezing percentage in the control and SIH mice when compared to the controls. This decrease did not reach statistical significance when doing the post-hoc analysis **(FIGURE 40A)**. Twenty-four hours later, the mice were placed in the conditioning box, but this time without receiving any shock. The RM-two way ANOVA revealed a significant main effect of Genotype and Treatment but no significant interaction between the 2. Considering this conditioning phase, it is interesting to see that, in the test phase, the *Scn1a*$^{RH/+}$-129:B6 control mice show reduced contextual-fear memory that is excacerbated in the SIH mice, but did not reach statistical significance. Nevertheless, this difference was not statistically significant when compared to the WT-129:B6 control and WT-129:B6 HYP respectively, and between them (*Scn1a*$^{RH/+}$-129:B6 control *vs.* SIH) **(FIGURE 40B)**. By analyzing the results, we cannot assume perturbations in the contextual-fear conditioning for the *Scn1a*$^{RH/+}$-129:B6 SIH because the mutation *per se* seems to decrease the freezing response to fear, in the conditioning and test phases.

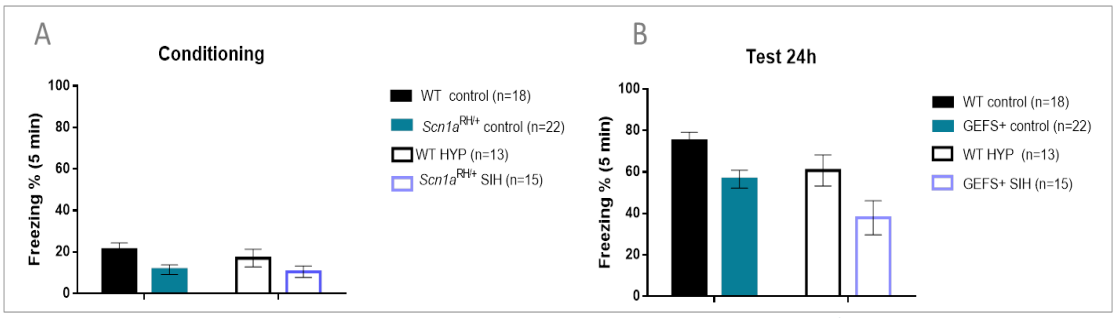

FIGURE 40. CONTEXTUAL FEAR CONDITIONING IS NOT CHANGED IN *SCN1A*$^{RH/+}$-129:B6 MICE.
A: Freezing time (%) during the 5 minutes' conditioning. **B:** Freezing time (%) during the 5 minutes of testing, 24 hours after the conditioning. n=number of animals

3.6 *Scn1a*$^{RH/+}$*-129:B6 mice with SIH show an impairment in working memory.*

Short-term memory associated with attention deficits has been observed in DS children at an early age (Villeneuve et al., 2014). To test this type of memory, we set up a protocol to test working memory in an 8-arm radial maze, a test dependent of the pre-frontal cortex. The protocol consisted in a choice between 2 arms (one rewarded and one non-rewarded) in a sequence of 7 consecutive trials that was changed every day. The training was continued until the control WT mice reached the criterion level, meaning more that 75% correct choices (5.25) for 2 consecutive days. Chance level was considered as 50% correct choices (3.5).

The first main observation we had was that the WT-129:B6 control, WT-129:B6 HYP and *Scn1a*$^{RH/+}$-129:B6 control mice reached the criterion for two consecutive days at training days D9 and D10 when the *Scn1a*$^{RH/+}$-129:B6 SIH never did. The RM two-way ANOVA revealed an interaction (training day x Group) with main effect of Training day and Group. The post-hoc analysis indicated that at training D9 and D10 the 3 control groups had higher number of correct arm choices than the *Scn1a*$^{RH/+}$-129:B6 SIH mice **(FIGURE 41A)**.

Also, the three control groups performed significantly higher than chance for the 2 last days of training. The RM two-way ANOVA revealed an interaction (training day x Group) with main effect of Training day and Group. Considering the chance level, using one sample t-test comparing to 3.5 correct choices, we observed that the 3 control groups were importantly better than chance from D8 until the end of the protocol. Considering the *Scn1a*$^{RH/+}$-129:B6 with SIH, we observed that they were slightly better than chance at training D8 and D10 but not at D9. This suggested that this group might have started to learn the rule but with lower performance than the 3 control groups and never reached the criterion for the 10 days tested.

Once again, the poor learning capacity of *Scn1a*$^{RH/+}$-129:B6 with SIH was apparent in this task, Indeed, for the same training duration, this group they had never reached the criterion and their better performance than chance was not consistent, meaning than their choices were mainly random during the protocol. Working memory was therefore also clearly affected in the *Scn1a*$^{RH/+}$-129:B6 mice after submission to early-life seizures.

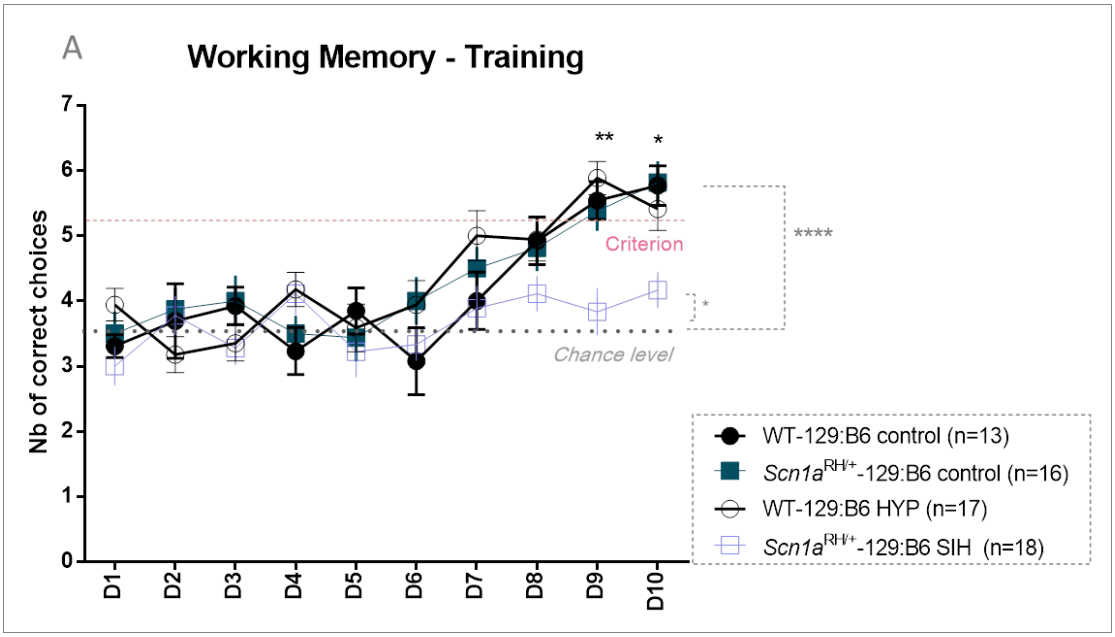

FIGURE 41. *SCN1A*$^{RH/+}$-129:B6 MUTANT MICE SUBMITTED TO SIH EXHIBIT AN IMPAIRMENT IN WORKING MEMORY.

A: Number of correct choices per day during the working memory training. The pink dotted line represents the criterion corresponding to 75% of 7 correct choices (5.25). Gray dotted line at chance level corresponds to 50% of 7 choices (3.5). Statistical significance is represented with black stars for differences between the *Scn1a*$^{RH/+}$-129:B6 SIH group and the 3 other control groups. Gray stars and associated dotted traces correspond to the statistical significance between groups and the chance level. N=number of animal, *p<0.05, **p<0.01 and p<0.001.

Together, these results allow us to conclude that the learning and memory abilities of the hippocampus and the pre-frontal cortex are disrupted after experiencing epileptic activity in *Scn1a*$^{RH/+}$-129:B6 mice.

Chapter 4- IS THE *SCN1A* MUTATION IMPLICATED IN THE BEHAVIORAL/COGNITIVE EFFECTS CAUSED BY SEIZURES? ROLE OF FLUROTHYL-INDUCED SEIZURES.

After observing important changes induced by the SIH in the mutant *Scn1a*$^{RH/+}$ mice, many questions rose up. Notably, *is the genetic background (i.e. Scn1a gene mutation) necessary for early life seizure-induced cognitive impairments? Or could early life seizures alone produce the same effect in WT animals?* We could not test this question using the SIH protocol because the WT-129:B6 animals that were submitted to hyperthermia never presented seizures. However, we organized another experiment that could answer this question. We submitted to WT-129:B6 and *Scn1a*$^{RH/+}$-129:B6 mice to a protocol that could induce seizures in the two genotypes, using flurothyl (a convulsant known to act on GABAergic functions and used previously in the *Scn1a*$^{RH/+}$ mice (Martin et al., 2007, 2010b)). The WT-129:B6 group was first submitted to hyperthermia to ensure that the effect that we observed in the *Scn1a*$^{RH/+}$ SIH (hyperthermia + seizures) was not an effect of seizures and exacerbated by the brain consequences of hyperthermia. This group was called WT-129:B6-HYP-FLU. The *Scn1a*$^{RH/+}$-129:B6 FLU (*Scn1a*$^{RH/+}$ with seizures induced by flurothyl) was not submitted to hyperthermia because it would have developed additional seizures with the increase in temperature. This chapter of results only presents very preliminary data. These experiments were done in the end of my PhD when we had a very important lack in breeding performance amplified by the fact that the 129/SvJ females (mothers of the *Scn1a*$^{RH/+}$-129:B6 mutant line) were not available commercially. We only obtained 5 WT-129:B6-HYP and 6 *Scn1a*$^{RH/+}$ -129:B6 FLU males to test for behavior.

1. FLUROTHYL-INDUCED SEIZURES PRODUCE HIGHER MORTALITY IN THE SCN1ARH/+-129:B6 MICE THAN IN THE WT-129:B6.

Our first worry was about the mortality that the seizures-induced by flurothyl would cause. We induced seizures with flurothyl for 10 days from P21 to mimick as closely as possible the SIH protocol. As one can see in **FIGURE 42** 88.23% of the WT-129:B6 HYP-FLU survived comparing to only 61.53% for *Scn1a*$^{RH/+}$-129:B6 FLU. The log-rank (Mantel-Cox) test for curve comparison indicated that the survival curves were not significantly different.

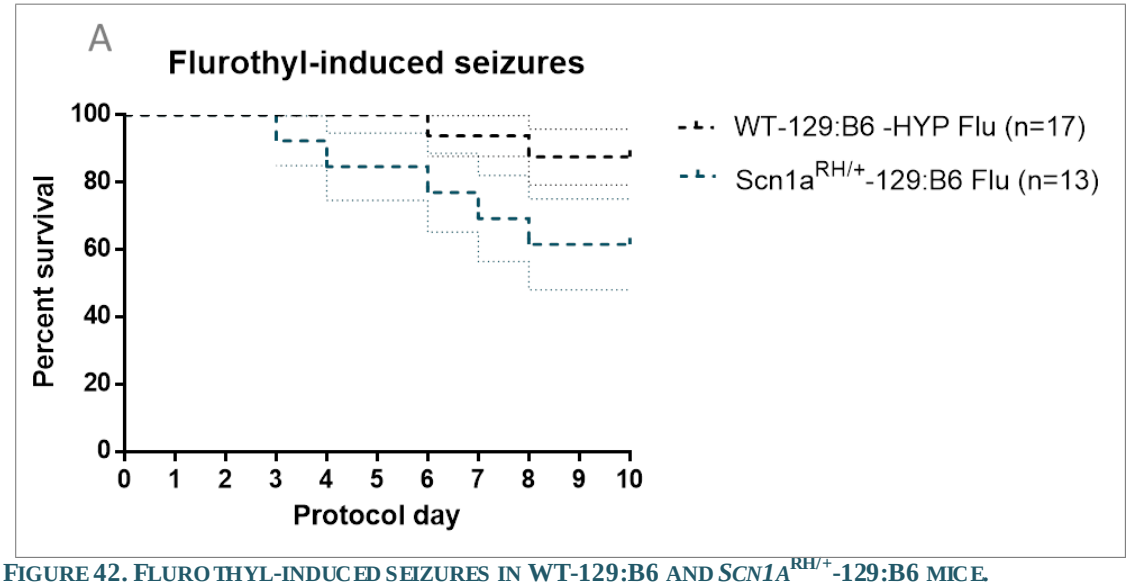

FIGURE 42. FLUROTHYL-INDUCED SEIZURES IN WT-129:B6 AND *SCN1A*$^{RH/+}$-129:B6 MICE.
A: Percentage alive of WT-129:B6-HYP-FLU and *Scn1a*$^{RH/+}$-129:B6 FLU during the 10-days of sezure induction.

Even if the number of mice tested was very limited, we ran 3 behavioral tasks to see if major behavioral effects were appearing at P60 after P21 flurothyl-induced seizures. We did not apply statistical analysis to the data because the number of animals was very limited. We ran the openfield, social interaction test and MWM. **FIGURE 43** shows the data obtained in the 3 tasks. In **FIGURE 43-1** the average speed, distance travelled and ratio distance travelled in the center/total distance in the openfield are presented. The average speed and distance travelled seem to be increased in the *Scn1a*$^{RH/+}$-129:B6 FlU but not in the WT-129:B6-HYP FLU when compared to the WT-129:B6-HYP controls. For the anxiety measure (ratio between the distance travelled in the center and the total distance travelled) the 3 groups seem to have similar ratio. For the social interaction task, the WT-129:B6 HYP mice clearly prefer the mouse than the empty cage as shown in the previous chapter. The WT-129:B6-HYP-FLU mice seem to prefer the mouse than the empty cage as well and the *Scn1a*$^{RH/+}$-129:B6 FLU explore the two equally. For the social novelty phase, the exploration difference between the nM and the fM was higher in the WT-129:B6 HYP than in the *Scn1a*$^{RH/+}$-129:B6 FLU.

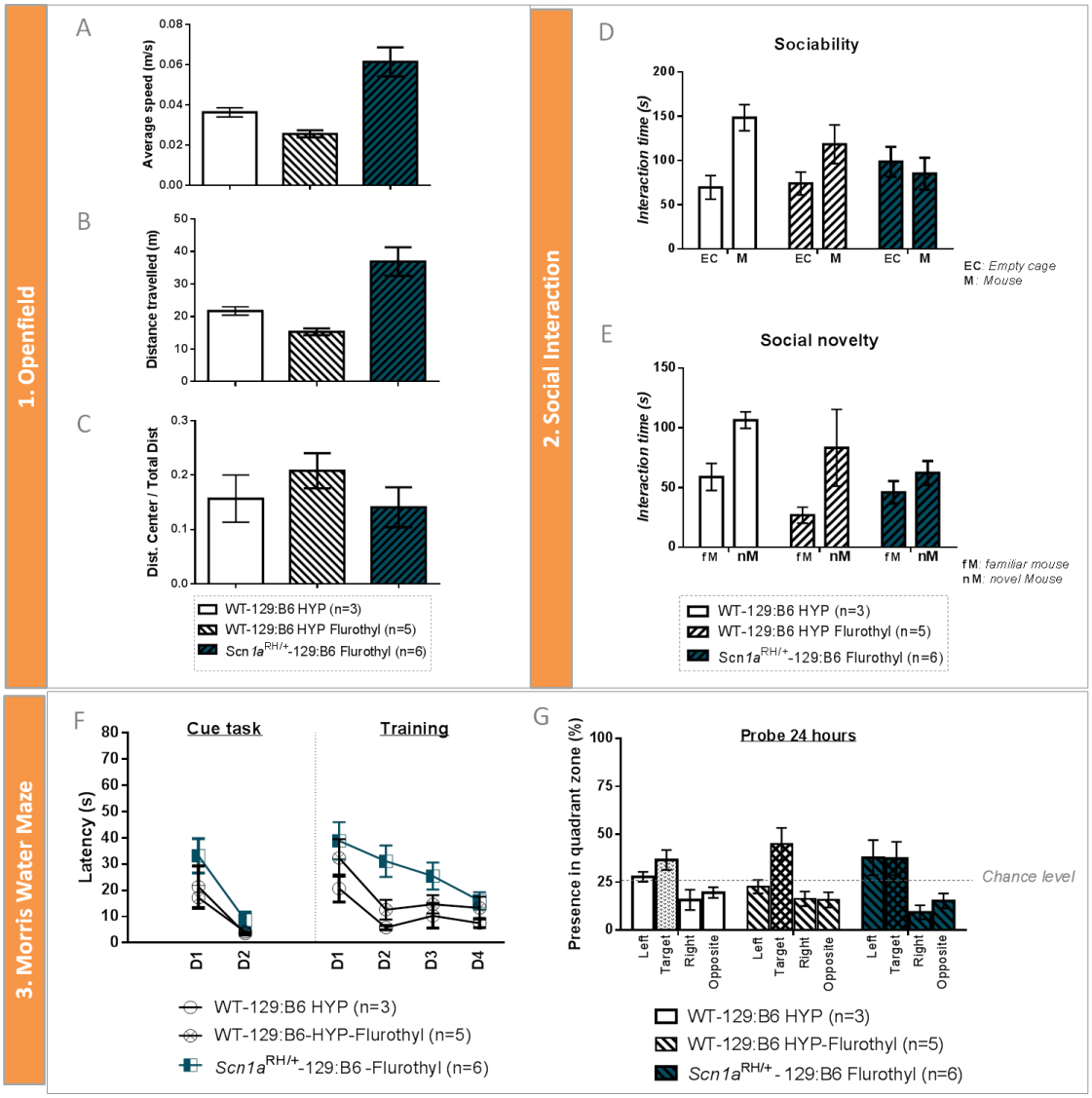

FIGURE 43. BEHAVIORAL/COGNITIVE TASKS IN SEIZURES-INDUCED WITH FLUROTHYL ANIMALS.
1.Openfield. **A:** Average speed (m/s). **B:** Distance travelled (m). **C:** Ratio distance in the center/total distance travelled. **2.**Three-chamber social Interaction. **D:**Social interaction. **E:** Social novelty. **3.** Morris water maze. **F:**Cue task and spatial learning latencies. **G:** Probe retrieval memory. n=number of animals.

For the MWM task, the cue task is equivalent for the groups, even if at D1 the *Scn1a*$^{RH/+}$ FLU seem to have higher latency to escape to the platform. The spatial learning curve indicates that the 3 groups decrease their latencies across the training days. However from D1 to D2 the learning improvements appear to be more important in the WT groups. Following the training, the probe task indicated that the WT-HYP FLU persisted longer in the target quadrant than the other groups. The poor performance of the WT HYP is due to the low number of animals, as we already demonstrated previously the ability of this group in remembering the platform location. The *Scn1a*$^{RH/+}$ FLU group did not seem to really discriminate between the left and target quadrants.

We cannot yet make hard conclusions from this very preliminary data. However, all together, it seems that the flurothyl-induced seizures affect more importantly the *Scn1a*$^{RH/+}$ mutant animals than the WT animals.

Chapter 5- COLLABORATIVE WORK USING *SCN1A*$^{+/-}$B6:129 (DS) MOUSE MODEL (DOCTOR INNA SLUTSKY, UNIVERSITY OF TEL AVIV, ISRAEL)

In collaboration with Doctor Inna Slutsky, professor and principal investigator at the University of Tel Aviv, Israel, we benefited from the SIH protocol we had previously set up to run a pharmacological trial to try to reduce the epileptic phenotype in DS mice (*Scn1a*$^{+/-}$ mouse model) (mixed B6:129 background). For intellectual property reasons, I am unable to disclose the name of the drug studied and will therefore call it X in this chapter.

1. DRUG X DECREASE THE MORTALITY OF *SCN1A*$^{+/-}$B6:129 MOUSE BUT NOT THE SPONTANEOUS GTC SEIZURE FREQUENCY

The drug injection started at P21 and delivered one time per day (10 AM) during 5 days In the first day of injection, 6 hours later, we started the SIH protocol for 5 days to increase the phenotype severity and have a more challenging number of spontaneous seizures (very low otherwise). The SIH protocol induced high mortality in the *Scn1a*$^{+/-}$ B6:129 vehicle mice. However, the high mortality was prevented by the drug in the treated animals **(FIGURE 44A)**. The log-rank (Mantel-Cox) test to compare survival curves indicated a significant difference between the curves.

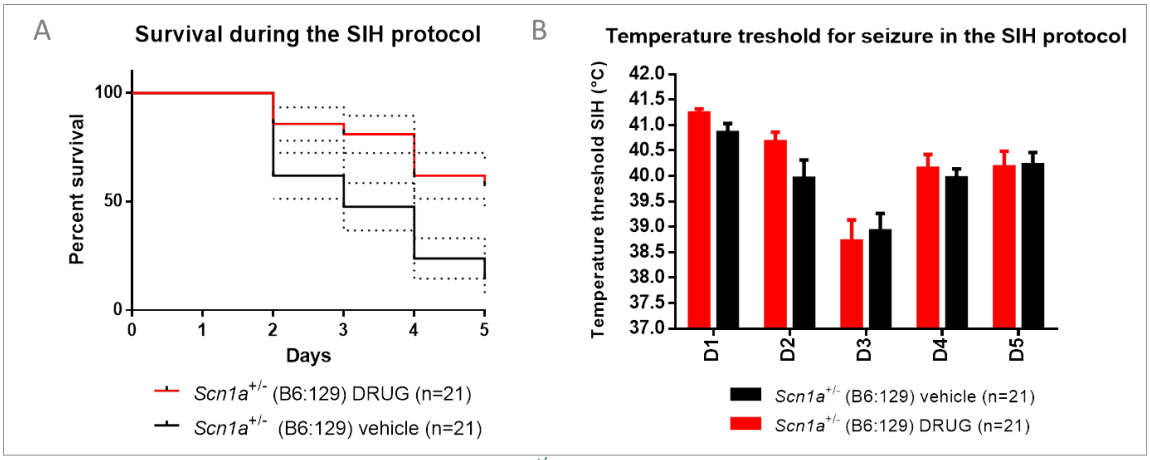

FIGURE 44. DRUG X ADMINISTRATION IN *SCN1A*$^{+/-}$B6:129 MOUSE DECREASES THE MORTALITY DURING THE SIH PROTOCOL BUT NOT THE SPONTANEOUS SEIZURE FREQUENCY.
A: Percentage of vehicle and drug-treated *Scn1a*$^{+/-}$B6:129 alive during the SIH protocol. **B:** Temperature threshold required to induce seizures by hyperthermia during the 5-days of the protocol.

The RM-two way ANOVA of the temperature threshold to induce the seizure revealed a significant main effect of protocol day, as one can see the temperature reaches the minimum level at induction D3, but no differences were observed between the groups **(FIGURE 44B)**.

We video-recorded the spontaneous seizures during all the SIH protocol days. The animals were individualized and placed above an infrared floor connected to a camera fixed on the ceiling. Using a C++ custom made software, designed by ULLO SAS (la Rochelle, France) for this experiment, the number of seizures was automatically counted and divided by bins of 12 hours-periods and per animal (day and night; defined as D and N respectively). The RM-Two way ANOVA revealed a significant main effect of Day and Treatment but no Treatment x Day interaction. No differences were detected by the post-hoc analysis for the number of spontaneous GTCs seizures across the days **(FIGURE 45)**.

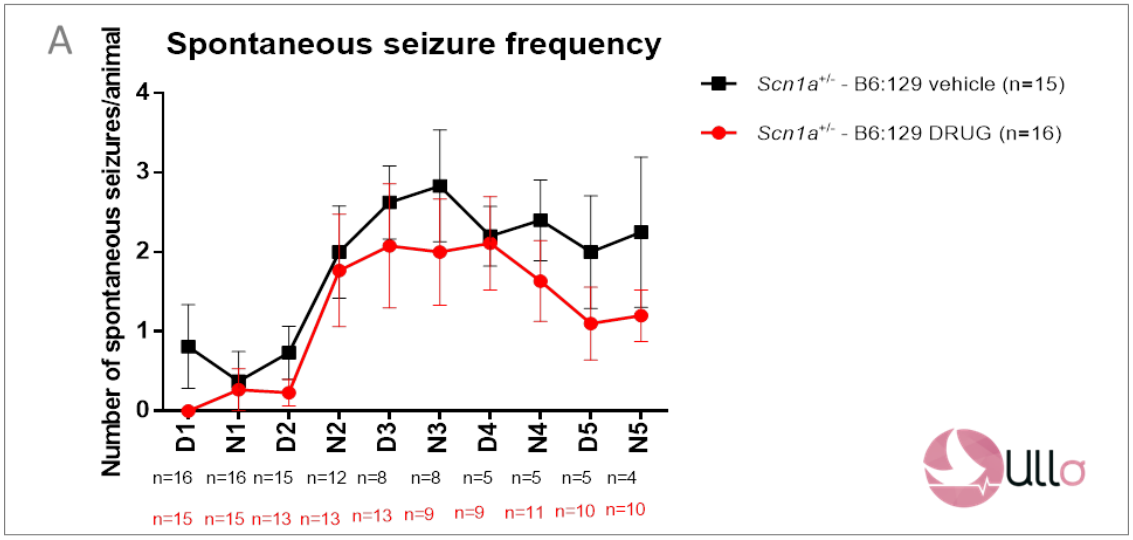

FIGURE 45. SPONTANEOUS SEIZURE ACTIVITY DURING THE 5 DAYS OF SIH WITH OR WITHOUT DRUG TREATMENT IN *SCN1A*$^{+/-}$B6:129 MICE.

A: Numer of generalized tonic-clonic seizures from D1 to N5 (day and night respectively). n=number of animals. Seizures were detected with a custom made software designed by ULLO SAS (La Rochelle, France).

The treatment clearly reduces the mortality in the *Scn1a*$^{+/-}$B6:129 mice, however the numbers of seizures seem to stay at the vehicle level and no differences in the temperature threshold were also observed.

Discussion

V- DISCUSSION

Identifying the cause of the cognitive and behavioral comorbidities in DS remains a major challenge for the field. While some studies investigated the role of $Na_V1.1$ dysfunction in neuronal networks and behavior, none had yet studied the role of epileptic activity on *Scn1a* mutant mouse models. In this study, we wanted to understand the role of epileptic activity on behavioral and cognitive phenotypes in *Scn1a* mouse models. To address this question, we used mouse models carrying *Scn1a* mutations and presenting mild epileptic phenotypes. We used the *Scn1a*$^{+/-}$, model of DS, in two genetic backgrounds (129 and B6-129) and observed that the mutation *per se* does not impact cognition in these models. We then tested the *Scn1a*$^{RH/+}$, model of GEFS+, and confirmed that the mutation *per se* does not change the behavioral and cognitive phenotypes in the model. We submitted the *Scn1a*$^{RH/+}$ mice to the SIH protocol during early life, once a day for 10 days, and observed a worsening in the epileptic phenotype with the appearance of spontaneous seizures. In adulthood, the *Scn1a*$^{RH/+}$ mice submitted to SIH displayed an increase in activity, sociability impairment and hippocampus and prefrontal cortex-dependent memory problems. Our study thus demonstrates that hyperthermic seizures can change a mild GEFS+ mouse model into a severe DS mouse model.

1. THE *SCN1A*$^{+/-}$ MUTATION *PER SE* IS NOT RESPONSIBLE FOR THE COGNITIVE AND BEHAVIORAL PHENOTYPE OBSERVED IN DS PATIENTS.

The *SCN1A* gene mutations are associated with a vast range of phenotypic severity progressing from GEFS+ to DS. GEFS+ patients usually present missense mutations and DS patients present missense and truncating mutations. While in GEFS+ the missense mutations cause the partial loss of the $Na_V1.1$ function, in DS patients these mutations severely impair or cause the complete loss of channel function. There are many exceptions to this generality as described in the introduction (I-Chapter 2-2.2), and the modifications introduced by different genetic backgrounds account for this variability.

Our first goal was to understand if the *Scn1a* truncating mutation (that causes the channel loss of function and is usually associated to DS) *per se* can be responsible for the cognitive phenotype observed in DS mice, as suggested by other recent studies (Han

et al., 2012a; Ito et al., 2013). We first used the *Scn1a*$^{+/-}$ mouse model in the 129 background. As detailed in the introduction (I-Chapter 4-2.3), the *Scn1a*$^{+/-}$-129 mice do not present spontaneous seizures and exhibit a survival rate comparable to WT littermates (Rubinstein et al., 2015d; Yu et al., 2006a). Due to its mild phenotype (no mortality, no epileptic activity) in presence of a truncation mutation, and its sensibility to SIH, this DS model was ideal to address our question. We observed that *Scn1a* $^{+/-}$-129 mice displayed similar performance to WT littermates in the MWM and the CFC tasks. *Rubinstein* and colleagues showed similar results in the CFC (Rubinstein et al., 2015d). Together, these results indicate that the mutation *per se* in this *Scn1a* mutant mouse is not sufficient to induce cognitive problems.

The main observation arguing against a role of this truncation mutation *per se* in the cognitive outcome in DS is the lack of behavioral phenotype observed in the DS-129 mice. These mice do not show spontaneous seizures activity, which could suggest that without the presence of epileptic seizures, the DS mice will not develop comorbidities. However, we do not know the effects of the genetic modifiers in the 129 background that could compensate for the $Na_V1.1$ loss of function in this model, so the role of seizures had to be addressed separately.

Klassen et al., showed one control patient (no epileptic or behavioral manifestations) carrying a severe missense mutation (associated with severe DS phenotype) (Klassen et al., 2011). Similarly, truncating mutations have been detected in patients with mild phenotypes comparable to the ones found in GEFS+ patients (Jiang et al., 2016; Takaori et al., 2017). The mechanisms underlying phenotypic heterogeneity within patients are not known. It may, however, involve variable expressivity of the single causative gene (mosaicism), modifying genes (i.e. other voltage-gated channel genes) or epigenetic factors.

Cognitive deficits and autistic-like behavior were reported before by *Han et al., 2012* and *Ito et al., 2013* in the *Scn1a*$^{+/-}$ in the C57BL/6J background. Due to high frequency of spontaneous seizures and important mortality level in this model (see **FIGURE 10**), it is hard to dissociate between the role of seizures and mutation *per se* in these mutant mice. Also it is hard to assume that the 20% surviving animals (the more resilients), on which the behavior analysis was performed, are representative of the total colony. As explained above, the *Scn1a*$^{+/-}$ mutation in the 129 background confers a mild phenotype in the mouse model. This mouse model would have been ideal to understand our question regarding the role of seizures when induced in these mice with the SIH, but

the low breeding performance led us to choose the B6:129 F1 background, which allowed for better breeding. This model did not therefore behave as we expected, according to the previous publications with this model (Kalume et al., 2007b; Yu et al., 2006a). It was previously reported in *Yu et al. 2006* that the *Scn1a* mutant mice resulting from mixed B6 and 129 background crossings had an intermediate phenotype (same mutant as used in our study). The authors report that these animals show 40% mortality at post-natal week 16, however, they have used the 2nd and 3rd generations, while we used the 1st generation and had no mortality (0%) in these animals when comparing the same age. The different generations could have explained the phenotype because of the genetic variability observed in generations 2 or 3. *Kalume et al* 2007 used the F1 generation (as used by us in this study) and reported subtle signs of ataxia at P21 in *Scn1a*$^{+/-}$ mice. Before our study, behavior abnormalities were not further explored in this mixed B6:129 genetic background.

Consistent with the absence of mortality in the *Scn1a*$^{+/-}$B6:129 mice used in our work, the behavioral and cognitive phenotypes in adulthood were normal. The *Scn1a*$^{+/-}$ B6:129 that were not submitted to SIH had normal activity in the openfield as well as normal circadian cycle in the actimeter. They also displayed normal spatial memory and working memory. We could not conclude on the state of sociability skills because the WT controls did not behave as expected. We would need to repeat this experiment to conclude. Another important parameter missing in our study with *Scn1a*$^{+/-}$ B6:129 mice is the analysis of the epileptic history at early-age by ECoG that could be correlated to the adult behavioral/cognitive phenotype. We, however, did not perform this experiment and it has never been reported by others in this genetic background before.

As in our study the *Scn1a*$^{+/-}$-B6:129 mice present a similar cognitive phenotype to the WT, this strongly suggests that cognitive deficits in adulthood are not related to the mutation *per se*. These data are in contrast to the previous report using the *Scn1a*$^{+/-}$ in the B6 background, where seizure frequency is very high and not controlled (Han et al., 2012c; Ito et al., 2013). Also, it is known that the *Scn1a*$^{+/-}$ mice have a seizure onset at P20-21 and high seizure intensity at their fourth week of life that tend to regress (Kalume et al., 2013), but no one has studied the later epileptic phenotype in these models. As we could not test the effect of seizures on the *Scn1a*$^{+/-}$ mutant mice in the 129 background (low breeding performance) nor the B6:129 (high mortality in the SIH protocol, described in next section), we used the *Scn1a*$^{RH/+}$ mutant mice (GEFS+ model)

in the 129:B6 background presenting a mild phenotype and sensibility to SIH (described in the next section).

We tested first the effect of the R1648H missense mutation *per se* on the behavioral and cognitive phenotypes in mice not submitted to SIH. We did not except behavioral abnormalities consistent with the favorable outcome as reported in the first human family carrying this mutation by (Escayg et al., 2000b). Yet, one patient has been described as having the same mutation and presenting DS (Depienne et al., 2010), suggesting that in particular cases this mutation could be associated to bad cognitive outcome. We observed that, in adulthood, the *Scn1a*$^{RH/+}$-129:B6 mice exhibited normal activity, social interaction and memory, similar to WT littermates.

Thus, when probing the *Scn1a*$^{+/-}$-B6:129 and the *Scn1a*$^{RH/+}$-129:B6 mice in a similar background, we evidence that neither the mild missense (*Scn1a*$^{RH/+}$) nor the truncation mutation (*Scn1a*$^{+/-}$) *per se* induced behavioral/cognitive deficits. *Sawyer et al. 2016* had previously studied the behavioral phenotype of the *Scn1a*$^{RH/+}$ mutant in the pure B6 background (I-Chapter 4-2.4.2 Table 7). They reported a slight increase in activity and mild spatial memory impairments, while the anxiety, the contextual fear conditioning, the sociability skills and the olfactory and visual abilities were normal. These subtle differences between this recent study and our results might be related to the difference in the genetic background. Indeed, as discussed before, pure B6 background can significantly impact the behavioral phenotype in *Scn1a* mutants (Yu et al., 2006b). All together, our results show that *Scn1a* mutations *per se* do not significantly contribute to cognitive and behavioral modifications in the mouse models carrying mild phenotypes. These data are arguing against the concept that DS could fully be explained as a channelopathy.

2. DS MICE DISPLAY SUSCEPTIBILITY TO HYPERTHERMIA INDUCED SEIZURES WITH HIGHER MORTALITY THAN GEFS+ MICE IN THE 10-DAYS PROTOCOL.

The protocol of repeated seizures induction by hyperthermia (SIH) in *Scn1a* models presented here has not yet been published elsewhere. There are several types of seizures induction in rodents, notably the two protocols of repeated seizures induction described in the introduction: hyperthermia-induced seizures and flurothyl-induced seizures. Other models of chemically (injection of piocarpine, kainate) or electrically (implantation of electrodes in the brain that are then electrically stimulated)-induced

seizures have been extensively reported as models of acute and long-lasting seizure induction more often classified into *SE* (i.e kainate, pilocarpine). As described in the introduction (I-Chapter 2-2.1), FS represent typical hallmarks of epilepsies associated to $Na_V1.1$ mutations. Indeed, GEFS+ and DS patients usually display a FS at disease onset and then febrile and afebrile seizures classified in different types. Therefore, the closest seizure induction protocol to FS is the hyperthermia-induced seizure protocol. For this reason, it was the model of choice for us to study the consequences of epileptic activity in early life in the *Scn1a* mutant models. To control for hyperthermia side-effects that could interfere with interpretation of our results, we systematically included a hyperthermia WT group (WT-HYP) in our study.

We faced two major concerns while setting up the protocol. The first concern was age of mice to be used at SIH onset. The second concern was the frequency of SIH episodes that could be clinically relevant without causing drastic mortality.

Regarding our first concern, data comparing rodent and human brain development are very limited. In addition, different brain regions develop at variable rates and chronological ages, in terms of neurogenesis, migration, connectivity and function, and these processes are not necessarily parallel in human and rodents. However, some studies show that P14-P16 in mice correspond to approximately 6 months in humans, and P21 corresponds to 1-2 years in humans (Avishai-Eliner et al., 2002; Dobbing and Sands, 1973; Gottlieb et al., 1977). To be closer to the earlier age at onset of seizures in patients (5 to 11 months of age on average) we could have chosen P14-15 as the age to start the SIH protocol. As described earlier, P14-15 WT rodents have been used as models of FS, with efficient induction of seizures by hyperthermia (Dubé et al., 2009). If we could induce seizures at P14 in WT as well as in *Scn1a* mutant mice, these WT + seizure group would have been an ideal control to test for combination of seizure ± *Scn1a* mutation on behavioral/cognitive outcome. Yet, for several reasons, we decided to start the SIH protocol later, at P21. First, Martin et al., 2010 induced seizures by hyperthermia in *Scn1a*$^{RH/+}$ mice and WT controls at P14. The mean temperature threshold for seizure in WT was 44°C and 43° in *Scn1a*$^{RH/+}$. The mice did not develop the typical GTC hyperthermic seizures, but only tonic hyperthermic seizures. The high temperature threshold and the lack of GTC hyperthermic seizures show the high resistance of the mice to hyperthermia-induced seizures at this age. Second, body temperature higher than 43°C is known to provoke brain injury (Burger and Fuhrman, 1964). Moreover, the previous results on the *Scn1a*$^{+/-}$ mouse model (in

the most severe background – B6) show that P17-18 mice do not show seizures under hyperthermia conditions to a maximum temperature of 42.5°C. The authors reported that the sensitivity to hyperthermia-induced seizures in *Scn1a*$^{+/-}$ mice coincides with the appearance of spontaneous seizures at P20-21 (Kalume et al., 2013; Oakley et al., 2009b). Finally, $Na_V1.1$ expression rising and $Na_V1.3$ failing in human and mice brain correspond to seizure onset in both human and mouse species at 5 months of age and P21, respectively, suggesting that the perfectly correlated timing of the channels expression could be a better indication to accurately target Na_V dysfunction-induced brain susceptibility (Cheah et al., 2013b). For all the reasons cited above, we chose to start the SIH protocol at P21.

Regarding our second concern, the average seizure frequency in DS patients is usually categorized from "daily or more" in the more severe periods to "yearly or less" when seizures tend to decrease. Patients can have several seizures per day. We first decided to induce 2 seizures per day for 10 days. Due to the very high mortality in the two mouse lines (data not shown), we decided to induce only one seizure per day for 10 days.

The *Scn1a*$^{+/-}$-129 mice were not tested in the SIH protocol due to the very low number of animals obtained from the breeding pairs. The *Scn1a*$^{+/-}$-B6:129, however, showed very high mortality (±70% after SIH protocol), leading to 30% of mice alive at P31. The high mortality was provoked by SIH and spontaneous seizures in the night during the 10 days of the protocol. The high mortality and increase in spontaneous seizure frequency (as seen in vehicle-treated *Scn1a*$^{+/-}$-B6:129 animals of the IV-Chapter 5-1- **FIGURE 44**, suggests that SIH brings this model closer to the *Scn1a*$^{+/-}$ B6 mice with severe phenotype reported previously (Kalume et al., 2013; Yu et al., 2006b). The observed phenomenon is very interesting. While it is possible that the genetic modifiers introduced by the 129 background allow for a mild phenotype (100% survival and no cognitive deficits) of the *Scn1a*$^{+/-}$–B6:129 model, our data suggest that the induction of repeated seizures by hyperthermia is enough to convert this into the more severe DS mouse model (like a model of *Scn1a*$^{+/-}$ in pure B6 background). Can the seizures episodes be the ON/OFF trigger to the severe phenotype observed in DS patients? While we meant to fully address this question, we unfortunately could not pursue our investigations in this model due to the high mortality observed in mice after SIH.

We therefore carried the final optimization of the SIH protocol on the *Scn1a*$^{RH/+}$ 129:B6 mice carrying the R1648H mutation present in the first identifies GEFS+ family

and in one DS patient. As discussed above, the model exhibited good sensitivity to seizures and presented a mild phenotype without SIH. The SIH protocol in this model conferred lower mortality rate at protocol day 10 (35 % mortality). In terms of seizure severity, the *Scn1a*$^{+/-}$ B6:129 mice reached the severity score 6 (for GTC seizure) at D2, while the *Scn1a*$^{RH/+}$ 129:B6 mice only reached this threshold at day 4. The temperature threshold to induce a seizure slightly increases until D3, possibly indicating that some compensations are taking place, and reaches a plateau from the following days to the end of the protocol.

Intriguingly, we also observed higher mortality in the WT-HYP control group from the *Scn1a*$^{+/-}$ B6:129 study than in the WT-HYP control group from the *Scn1a*$^{RH/+}$ 129:B6 study (92% survival and 72% survival, respectively). This difference could have interfered with the interpretation of our results if we had succeeded in comparing both sets of data in these two models after SIH (not done because of high mortality of *Scn1a*$^{+/-}$ B6:129 group after SIH). This different outcome of the WT-HYP group after SIH could be related to the fact that the two lines result from different breeding pairs, even if both bred on 50:50 129/B6 mixed background,. Indeed, *Scn1a*$^{+/-}$- B6:129 mice were always born from a WT B6 mother, which generally harbors large litters but provide little care leading to P21 pups rather weak and small in size. By contrast, *Scn1a*$^{RH/+}$-129:B6 mice were always born from a WT 129 mother, which generally harbor small litters but provide better care than B6 mothers resulting in bigger/stronger pups at P21. These differences in size of litters and maternal behavior displayed by B6 and 129 mothers have been reported previously (Champagne et al., 2007). Thus this apparently trivial difference in the breeding strategy we adopted in the two models, resulting in P21 pups with slightly different developmental profiles, could very well account for the increased death toll observed in WT-HYP in the B6 background (Banbury, 1997). Yet, we did not observe the occurrence of spontaneous seizures in these WT-HYP mice, so we do not think that death was caused by seizures *per se* provoked by SIH. Others causes of death might be associated with the negative consequences of hyperthermia on brain function, as inflammation (Mcilvoy, 2005). We did not try to pinpoint the accurate cause of death in these WT-HYP mice.

Together, the results of the SIH protocol survival rates suggest that this protocol induced more severe consequences in mice presenting the complete loss of the function (*Scn1a*$^{+/-}$ mice) than in the mice with reduced $Na_v1.1$ function (*Scn1a*$^{RH/+}$ mice). Also, it is likely that the type of *Scn1a* mutation confers a differential modulatory effect on the

seizure severity induced by SIH. Indeed, it is possible that seizures acting on a brain with a severe $Na_v1.1$ mutation confer a worst survival outcome than seizures acting on a brain carrying a milder $Na_v1.1$ mutation. These data thus reveal the complexity of the question addressed in this study, suggesting that both epileptic history and underlying genetic profile intervene in phenotypic outcomes.

3. LONG-TERM EFFECTS OF THE 10-DAYS SEIZURES INDUCTION BY HYPERTHERMIA PROTOCOL IN *SCN1A*$^{RH/+}$-129:B6 MICE.

The behavioral and cognitive testing was done using the *Scn1a*$^{RH/+}$-129:B6 mice submitted to SIH and respective controls. We did not proceed to the behavioral testing in *Scn1a*$^{+/-}$-B6:129 mice due to the low number of animals remaining after the SIH protocol.

3.1 *"Seizures beget seizures" in Scn1a* $^{RH/+}$ *mice*

We first wanted to clarify the epileptic profile of the *Scn1a*$^{RH/+}$ controls and test whether the SIH protocol changes the epileptic severity in this model. After the SIH protocol, the animals were implanted for ECoG recordings (P34-35). *Martin et al, 2010* reported the presence of few spontaneous seizures in the *Scn1a*$^{RH/+}$ in pure B6 background (out of 14 mice aged 3-5 months they reported that two exhibited spontaneous seizures). We did not observe any GTC seizures in the 4 control *Scn1a*$^{RH/+}$ mice tested between 1-3 months of age. Lack of observed seizures in our conditions might be justified by the introduction of 50% of the129 genetic background that has been described in the *Scn1a*$^{+/-}$ to promote a milder phenotype or by the low number of animals tested. It is also possible that these *Scn1a*$^{RH/+}$ -129:B6 mice harbor milder ECoG abnormalities that were not detected with our analysis. All the *Scn1a*$^{RH/+}$ submitted to our SIH protocol, however, developed spontaneous GTCs, which persisted until end of ECoG recordings (3 months of age). Previous literature supports the notion that appearance of spontaneous seizures subsequent to seizure induction is generally correlated to the intensity/duration of the induced seizures and to the age at which these are induced in the rodent brain. Indeed, induction of seizures using kainate led to spontaneous seizures in adult rats, while rats submitted to the same seizures at early age did not develop spontaneous seizures (Stafstrom et al., 1993). Also, in the adult mouse

brain, repeated seizures induction using flurothyl led to appearance of spontaneous seizures that then tended to remit after one month (Kadiyala et al., 2016). Concerning early ages, studies have previously shown that induction of one prolonged FS (~24 minutes) in immature rats, led to appearance of spontaneous seizures in 37% of the animals at later ages (Dubé et al., 2006). The results regarding outcome of short-lasting febrile/flurothyl-induced seizures at early age on spontaneous seizure appearance are more controversial and many studies show that these short-lasting protocols do not cause the appearance of spontaneous seizures (Bender et al., 2004a; Liu et al., 1999). In our model, we clearly show that a short-lasting (once a day, less than 1 minute) but repeated SIH protocol at early-age triggers the appearance of GTCs, worsening the epileptic severity in our model. While it is a very controversial notion in the epilepsy scientific community, we thus observed that "*seizures beget seizures*" in the *Scn1a*$^{RH/+}$ mouse model.

3.2 *SIH does not induce neuronal death in Scn1a*$^{RH/+}$*mutant mouse*

Long-lasting seizure episodes as pilocarpine or kainate-induced *SE* have been associated to important neuronal death in the hippocampus in mature rats (Deshpande et al., 2008; Kim et al., 2011, 2015; Wang et al., 2015; Williams et al., 2009). However the same seizures in young rats before postnatal day (P18) are less likely to cause cell death or recurrent epileptic activity (Albala et al., 1984; Mlsna and Koh, 2013; Sperber et al., 1991; Stafstrom et al., 1992). Our immunohistochemical investigation, performed in collaboration with Dr. Frassoni in Milan, showed that SIH in *Scn1a*$^{RH/+}$-129:B6 mice does not induce neuronal death nor important cytoarchitectural changes in the hippocampus. The results are consistent with previous findings in *Scn1a* mutant mouse models. Indeed, There was no evidence of neuronal death in hippocampi of the *Scn1a*$^{+/-}$ mouse model in pure B6 background, a model known to exhibit intense spontaneous epileptic seizure activity, (Yu et al., 2006b). Moreover, repeated flurothyl-induced seizures do no cause neuronal death (Liu et al., 1999) and similarly repeated or prolonged FS have not been associated to neuronal death (Bender et al., 2004b) in WT rodents.

3.3 *Increased firing properties of DG granule cells after SIH in* *Scn1a*$^{RH/+}$ *mice*

The DG is seen as the first stage or "gate" into the trisynaptic circuit of the hippocampus, leading to an increased focus in this sub-region of the hippocampus by the epilepsy research (Dudek and Sutula, 2007). Sustained firing of GABAergic inhibitory interneurons is critical to the 'gate-keeper' function of the DG in filtering neocortical and entorhinal excitatory inputs that converge into the CA3 region (Buhl et al., 1994; Lothman et al., 1992). Yet, while most of the hippocampus-related research in *Scn1a* models focuses on the hippocampal CA1 area, the pathological consequence of *Scn1a* dysfunction in the DG has been largely disregarded.

In human temporal lobe epilepsy, GABAergic neuronal cell loss and reduced inhibition of granule cells in the DG are associated with enhanced susceptibility to seizures (de Lanerolle et al., 1989). The loss of seizure-sensitive neuronal populations can critically alter the balance of excitation and inhibition in the hippocampus. However, whether hyperthermia-induced seizures or short-lasting repeated seizures induction (that are not associated with neuronal loss) cause DG damage has been less studied. Early-life FS have been associated to similar abnormalities in DG granule cells (Kwak et al., 2008). *Koyama et al. 2012* showed that after a prolonged FS, there was the aberrant migration of neonatal-generated granule cells and altered GABA receptors signaling (Koyama et al., 2012). In a similar experiment, *Swijen et al, 2012* showed reduced inhibitory currents in the DG 10 days after the FS event (Swijsen et al., 2012). Interestingly the DG filter was shown to be disrupted (impaired synaptic integration and increased excitability) 10 days following the FS seizure event but not later (Pathak et al., 2007).

Following recurrent seizures (i.e. flurothyl-induced seizures), important synaptic reorganization and impaired neurogenesis of DG granule cells have been observed (Holmes et al., 1998; McCabe et al., 2001). The previous studies indicate that FS or recurrent seizures events *per se* can be related to the abnormal properties of the DG. However, recently, a study correlated the *Scn1a*-associated phenotype with DG abnormalities. Indeed, *Tsai et al, 2015* reported the first study using *Scn1a* models in which the DG properties where investigated. The authors observed that, while at 4 weeks of age the *Scn1a*$^{E1099X/+}$ in a mixed 129:B6 background mice (model of DS) had a substantial reduction in $Na_V1.1$-expressing neurons in CA1, CA3 and DG, at 3 weeks of

age (representing the critical epileptic period), there was a specific reduction of $Na_V1.1$-expressing neurons in the DG but not in other hippocampal areas (CA1 and CA3) when compared to WT littermates. The number of GABAergic interneurons was unchanged in any areas. Also, the electrophysiological properties in the DG PV+ GABAergic neurons were altered in the *Scn1a*$^{E1099X/+}$ mice (altered action potential kinetics, reduced excitability, and fewer spontaneous inhibitory currents). In addition to these functional deficits, they observed morphological abnormalities of DG granule cells.

In light of this literature regarding DG in epilepsy, we thus decided to investigate the effects of repeated SIH in both CA1 and DG function in our *Scn1a*$^{RH/+}$-129:B6 mice at P60 and correlate these with behavioral abnormalities. We only analysed the firing properties of the excitatory neurons, because of the difficulty in the identification of the interneurons without markage ((GAD-67)-GFP). They present high variability of types/shapes and organization within the hippocampus. However, it would have been very relevant to analyse them due to their main role in *Scn1a* models physiopathology. The firing properties of the pyramidal cells of the CA1 region of the hippocampus were similar in the four groups (WT and *Scn1a*$^{RH/+}$ control and submitted to hyperthermia). By contrast, *Scn1a*$^{RH/+}$ mice submitted to the SIH protocol exhibited a strong increase in firing frequency in DG granule cells compared to other groups. These data clearly revealed that SIH produces an increase in the excitability of the "gate" region of the hippocampus. Thus, it is possible that the increase in DG firing frequency observed in the *Scn1a*$^{RH/+}$ after SIH underlies the impairment in the spatial memory task we observed in these mice. Direct causality cannot, however, be proven with our study. The exact role of the DG in subserving memory processes has been controversial for many years. Recently it has been shown that the DG might be associated to spatial pattern separation (dissociation between similar contexts) in tasks like the eight-arm radial maze (Gilbert et al., 2001; Kesner and Rolls, 2015). However, the majority of the studies published correlate a decrease in firing frequency with DG-related memory problems. Blocking DG granule cells have been correlated with impaired hippocampal-dependent memory aquisition and maintenance (Lassalle et al., 2000; Lee and Kesner, 2004; Madroñal et al., 2016). Also, impaired synaptic transmission and excitability in the DG have been associated to hippocampus-dependent memory deficits (Morice et al., 2013). We observed an opposite effect, characterized by increased excitability in DG granule cells. However, it is possible that this excitation in

the DG, characterized by an excitation/inhibition imbalance results in abnormal sensory information reception and impaired memory formation within the hippocampus.

Still, as described previously, DS patients show visual-spatial memory deficits indicating that the hippocampus functions might be altered in the patients (Chieffo et al., 2011c) and animal models showed that seizure generation might initiate in the hippocampus in the *Scn1a*$^{+/-}$ mouse model (Liautard et al., 2013). Thus, the alteration of DG excitation profile we observed is in line with these previous observations.

3.4 *The behavioral phenotypes observed in Scn1a*$^{RH/+}$*-129:B6 mice after SIH correlate with Scn1a*$^{+/-}$ *DS mouse models*

For the behavioral and cognitive assessment following the SIH protocol in *Scn1a*$^{RH/+}$ mutant mice, we wanted to evaluate the largest panel of behavior and cognitive parameters, perturbations of which are well described in DS patients. As described in the introduction (I-Chapter 3-page 27), DS patients present neurological, cognitive and psychiatric/behavioral abnormalities. The main observations pointed out through the numerous DS clinical studies are the neurological problems: ataxia, lack of motor coordination, crouch gait; the behavioral problems: hyperactivity and social interaction problems; and the cognitive problems: language delay, visual deficits, attention deficits, working memory and visual-spatial memory deficits.

- No major motor/visual impairment in *Scn1a*$^{RH/+}$ after SIH

We did not extensively address the neurological problems. However, through the different behavioral tasks tested we were able to record and analyse the global locomotor activity and speed in different contexts (openfield, actimeter, MWM, social interaction test) and, there were no signs of ataxia or nor important abnormalities in their posture and motor coordination. The only assessment of motor coordination and visual function was done during the MWM task, when mice were submitted to the cue task training. The cue task was done during two days with four trials per day, just before the spatial training. The escape strategy was exclusively based on the swim speed and visual integrity, as all the animals could identify the platform location marked with a flag. We observed that the *Scn1a*$^{RH/+}$ -SIH displayed higher latency to find the platform on the first day, but rapidly normalized their performance on the second day. Similarly,

they swam as fast as the three other groups on the second day (see **TABLE 12)**. These results thus indicate that, during this cue task, the *Scn1a*$^{RH/+}$-SIH mice took longer to understand the escape rule. They surprisingly showed lower average speed in the D1 of the cue task, and normalized by D2 where they swam as fast as the three other groups. Yet, as their performance normalized rapidly, we can conclude that they do not exhibit important motor or visual problems following the SIH protocol.

In the other tasks (openfield, social interaction), the Scn1a$^{RH/+}$-SIH mice travelled longer distances and with higher speed on average than the other 3 groups indicating that they are definitely not affected by major motor problems. *Kalume et al, 2007* observed a motor impairment in the P13-P21 *Scn1a*$^{-/-}$ and a mild motor dyscoordination in *Scn1a*$^{+/-}$ mice, which they correlated with $Na_V1.1$ loss of function observed in the cerebellar purkinje interneurons. In patients, cerebellar dysfunctionhas also been suggested to justify the motor impairment, language delay, attention-deficits and working-memory problems observed in DS (Battaglia et al., 2013). Our *Scn1a*$^{RH/+}$ mice submitted to SIH in early life do not show overt signs of important cerebellar impairment at 2 months of age, indicating that SIH might not cause long-lasting behavioral effects on this area. Similarly to our work, *Ito et al. 2013* did not detect motor impairment in *Scn1a*$^{RX/+}$ mice (DS model) using the foot-print test and rotarod at 9 weeks of age (Ito et al., 2013). Visual dysfunction is another major characteristic in DS patients. Yet, we observed normal performance of the Scn1a$^{RH/+}$ -SIH mice on the D2 of the cue task, arguing against major alterations in visual function after SIH. However, this task cannot detect slight visual deficits, which could be addressed using more specific techniques as tests for visual attention, optomotor function, infrared photorefraction (Abdeljalil et al., 2005; Fitzpatrick et al., 2017; Schaeffel, 2008).

- Hyperactivity but no anxiety profile following SIH in *Scn1a*$^{RH/+}$

The development of behavioral abnormalities was the most obvious observation made in *Scn1a*$^{RH/+}$ mice following recurrent seizure activity. Hyperactivity was evident as measured by the distance travelled in the openfield and during the habituation phase in the three-chamber social interaction. The same increase in activity was reported in DS mouse models in the openfield (Han et al., 2012c; Ito et al., 2013). We confirmed the novelty-associetd hyperactivity by measuring the circadian activity at D1 in the actimeter. Interestingly, we observed that this increased activity was particularly present

when the mice were first exposed to the actimeter (mainly first 24 hours), i.e. when confronted to a novel environment, but their activity normalized after habituation. This novelty-associated reaction was also observed in *Scn1a*$^{RX/+}$ mice (model of DS), while in a familiar environment these mice tended to exhibit lower activity than WT littermates (Ito et al., 2013). Together, these data confirm that SIH induces a hyperactive profile in our GEFS+ mouse model, mimicking a phenotype observed in DS mouse models and DS patients. More specifically, the hyperactivity observed in different tasks seems to be exacerbated in new environments which highlits the neophobia present in these mice, probably related to a higher anxiety profile or increased impulsive and risk-taking behavior. In the openfield (by measure of time in the center), we observed that the *Scn1a*$^{RH/+}$ did not present higher anxiety levels that the three other groups. As said before the openfield measure of anxiety alone is not sufficient to detect anxiety levels, we thus tested the animals in the dark-light paradigm. Again the anxiety levels were unchanged in the *Scn1a*$^{RH/+}$ with SIH. So in conclusion, we observed that the *Scn1a*$^{RH/+}$ submitted to SIH mice had a normal anxiety level when compared to the three other groups, and even a tendency for lower anxiety levels in the dark-light. The results were not in accordance with the study of *Han et al, 2012* who showed increased activity in the openfield and elevated-plus maze test. The results in the *Scn1a*$^{RX/+}$ by *Ito et al, 2013* were not clear because they show an increase in anxiety in the openfield (contrasting to our study) but a decrease in anxiety in the elevated-plus maze (similar to our study even if not significant for our study **FIGURE 36**). The tendency for a decrease in anxiety ans high activity can be associated to an increase in impulsivity and risk-taking in the *Scn1a*$^{RH/+}$-SIH mice. These measures could have been assessed using the five-choice serial test however due the low number of animals that we always had, we could not optimize the technique (*reviewed in* Dent and Isles, 2014).

- *Scn1a*$^{RH/+}$-SIH mice had an increase in stereotyped behavior

In addition to the hyperactivity, we observed, in the openfield test, an increase in the number of body rotations and rearing events specifically in the *Scn1a*$^{RH/+}$ –SIH group. These measures are considered as stereotyped behaviors, motor responses that are repetitive, invariant, and seemingly without purpose or goal in rodents (Kelley, 2001). Similarly, *Han et al, 2012* reported an increase in the number of body rotations and an increase in grooming time in the *Scn1a*$^{+/-}$-B6 mice. In addition to the repetitive

behavior, we observed that the *Scn1a*$^{RH/+}$ had an impairment in social interaction after experiencing SIH. Both measures are associated to measures of the autistic-like spectrum (Berkvens et al., 2015). Again the social impairment is a typical characteristic observed in DS mouse models (Han et al., 2012c; Ito et al., 2013). *Han et al, 2012*, stressed the fact that the *Scn1a*$^{+/-}$ presented an autistic-like behavior. However, whether or not DS patients are autistic is controversial. Clinical studies suggest that the autistic traits are not complete in DS patients and their difficulties in socializing might be due to their motor problems and language impairment (Li et al., 2011; Villeneuve et al., 2014; Wolff et al., 2006b). Again, these data suggest that SIH in early life is sufficient to turn a GEFS+ phenotype (neither stereotyped behaviors nor impairments in social interations) into a more severe DS phenotype with these autistic-like traits. These traits have been associated to PFC dysfunction, however more recently cerebellar function has also been correlated to these types of behavioral alterations through the cerebellum-PFC projections (Cupolillo et al., 2016; Wang et al., 2014). Thus, these two structures could be implicated in the phenotypes observed. Instead of autistic-like behavior, the phenotype observed, repetitive behaviors with hyperactivity can also be correlated to a spectrum of attention-deficit hyperactivity disorder (Leo and Gainetdinov, 2013). More analysis would have been required to address this issue.

- *Scn1a*$^{RH/+}$-SIH mice had working and spatial memory impairment

Regarding cognitive deficits, we tested the effects of SIH on long-term spatial memory. We observed an impairment in spatial learning and long-term memory in the MWM task, confirming that hippocampal function is importantly affected after SIH protocol in *Scn1a*$^{RH/+}$ mice. Again, the results were in accordance with the findings in the DS mouse models reported previously (Han et al., 2012c; Ito et al., 2013). Concerning CFC, *Han et al. 2012* reported lower freezing in *Scn1a*$^{+/-}$:B6 mice when compared to controls, demonstrating contextual-fear memory impairment. At present, we cannot conclude on our results obtained in the CFC. We observed lower freezing in the *Scn1a*$^{RH/+}$-SIH mice, but this trend was not significantly different from the other groups, although the number of mice per group was already consequent. The lack o memory impairment in the CFC task, after seeing changes in the spatial memory tasks, can be associated with the participation of different complementar structures in addition to the hippocampus in the memory tasks. The spatial memory in the MWM task, is

known to involve the hippocampus and upper cortical areas (Tse et al., 2011), whereas the CFC recruits the hippocampus and subcortical areas like the hippocampus and the amygdala (Phillips and LeDoux, 1992).

Finally, we tested the prefrontal cortex integrity using a working memory task. We observed that the *Scn1a*$^{RH/+}$-SIH mice exhibit lower working memory capacities and never reach the performance level of the other three groups. The two published studies using DS mouse models have not tested PFC dependent memory tasks so a comparison to a DS phenotype in this task is not possible. However, in DS patients, working memory problems have been reported in the majority of cases (Chieffo et al., 2011c; Ragona et al., 2011a). The results obtained in the behavioral/cognitive tasks in the *Scn1a*$^{RH/+}$-SIH mouse model are summarized in **TABLE 14** and compared to the results published in the DS mouse models. All together, the results clearly illustrate that the repeated SIH induction at early-age in a mild *Scn1a*$^{RH/+}$ model induces long-lasting behavioral/cognitive defects similar to those observed in the DS mouse models presenting severe phenotypes.

TABLE 14. SIH CONVERTS A MILD *SCN1A* MOUSE MODEL INTO A SEVERE *SCN1A* MOUSE MODEL.
Results observed in the battery of behavioral/cognitive tasks after SIH in the *Scn1a*$^{RH/+}$ mouse and comparison to the results published in DS mouse models with severe phenotype.

			Previous studies with DS mouse models (2-5 months)	
Study	OUR study (2-4 months)		*Han et al. 2012, Kalume et al. 2007*	*Ito et al. 2012*
Mouse model	***Scn1a*$^{RH/+}$ - 129:B6 -control** (Martin et al.2010)	***Scn1a*$^{RH/+}$ - 129:B6 -SIH** (Martin et al.2010)	***Scn1a*$^{+/-}$ - B6** (Yu et al.2006)	***Scn1a*$^{RX/+}$ - B6** (Ogiwara et al. 2007)
MOTOR PROBLEMS	↔	↔	↑ (mild) at P21, *not tested later*	↔
VISUAL PROBLEMS	↔	↔	*Not tested*	*Not tested*
ACTIVITY Openfield	↔	↑	↑	↑
STEREOTYPED BEHAVIOR	↔	↑	↑	↑
ANXIETY Openfield	↔	↔	↑	↑
ANXIETY Other task	↔	↔	↑	↓
ACTIVITY Familiar environment	↔	↔	*Not tested*	↓
SOCIAL INTERACTION	↔	↓	↓	↓
SPATIAL MEMORY	↔	↓	↓	↓
WORKING MEMORY	↔	↓	*Not tested*	*Not tested*

4. THE MUTATION IS REQUIRED FOR THE SEIZURES EFFECTS (PRELIMINARY RESULTS)

After obtaining these very interesting results we were confronted with two main questions.

Firstly, the only group which had seizures among the 4 groups tested was the *Scn1a*$^{RH/+}$ -SIH mice. Could the repeated seizures induce the same behavioral and cognitive defects in the WT mice? In other words, is the *Scn1a*$^{RH/+}$ mutation required for the behavioral and cognitive effects observed in the *Scn1a*$^{RH/+}$ -SIH mice? This is an important point to address as result interpretation of our study will depend on its answer.

Secondly, in many publications, it has been stressed that the effects of the hyperthermia *per se* must be distinguished from those of the associated seizures (Bender

et al., 2004b; Dubé et al., 2009). The potential effects of hyperthermia may not be inconsequential and, in some other epileptic models, hyperthermia enhances seizure severity and neuronal loss induced by kainic acid (Liu et al., 1993). However, this is controversial and no worsening of kainate-induced seizures have also been reported following hyperthermia (Hamelin et al., 2014). Also, when extreme, hyperthermia can result in neuronal injury by itself (Germano et al., 1996). Considering the hyperthermia itself, we address this issue with the WT HYP group and we observed that, except for the spatial probe test, where the WT control are significantly better than the WT-HYP, the two groups did not differ in any of the other tasks tested. This slight decrease in memory strength in the MWM in the WT HYP mice might be due to the hyperthermia effects, however, this group still performed well in this task and considerably better than the *Scn1a*$^{RH/+}$-SIH group. Considering the *Scn1a*$^{RH/+}$ -SIH group, we do not know if the seizures effects are exacerbated by the hyperthermia itself.

To address these two important points, we thus organized an additional experiment in which:

1) Seizures where induced by flurothyl in hyperthermia treated WT animals to verify if seizures (worsened or not by hyperthermia) could cause long-lasting behavioral/cognitive alterations in WT mice;

2) Flurothyl seizures where induced in *Scn1a*$^{RH/+}$ mice in the absence of hyperthermia to test if we could also observe long-lasting changes in the *Scn1a*$^{RH/+}$ mice using a different seizure induction protocol.

We first optimized the flurothyl/hyperthermia seizure induction protocol in our lab to mimic as closely as possible the SIH protocol. Of note, in our hands, the seizures induced by this new protocol are very similar to SIH induced seizures (i.e. behavioral seizure phenotype – starting from head nodding, rearing and failing, forelimb clonus and progression to GTC seizures).This is an ongoing experiment. However, the first preliminary results indicate that the *Scn1a*$^{RH/+}$ with flurothyl induced seizures exhibit increased activity, lower sociability skills and poor memory performance, while WT littermates submitted to flurothyl-induced seizures/ hyperthermia remain cognitively and behaviorally intact **(FIGURE 43)**. The results suggest that repeated seizures are not sufficient to lead to important behavioral changes in the WT mice. If these results are confirmed, this would strongly support the hypothesis that it is the combination of early life epileptic activity + *SCN1A* mutation that is at the origin of behavioral/cognitive deficits in DS patients. Also, our first data suggest that, similarly to *Scn1a*$^{RH/+}$-SIH

mice, *Scn1a*$^{RH/+}$ mice submitted to flurothyl-induced seizures seem to display impaired behavioral and cognitive phenotypes. These results need to be confirmed but are very interesting because they suggest that, while a normal young WT brain is able to cope with the effect of repeated seizures, probably by somehow restoring homeostasis, an $Na_V1.1$-dysfonctional brain is not capable of coping with recurrent seizure activity (independent of type of induction protocol), leading to behavioral and cognitive abnormalities in adulthood.

5. IS DS A CHANNELOPATHY?

In our study, we observed that SIH, not only causes the appearance of subsequent spontaneous seizures, worsening the epileptic phenotype, but also importantly impairs the behavioral and cognitive functions in the *Scn1a*$^{RH/+}$ mice.

The works of *Han et al. 2012* and *Ito et al. 2013* show that the *Scn1a*$^{+/-}$ and the *Scn1a*$^{RX/+}$ mouse models in pure B6 background exhibit very severe epileptic and behavioral/cognitive phenotypes comparable to those observed in the DS patients. Given these behavioral abnormalities, the two studies did not dissociate the strong epileptic activity presented in these mice from the network abnormalities caused by the mutation *per se*. Neither group investigated the epileptic profile of the animals from early-age to the adulthood and during behavioral tasks.

With these results in *Scn1a*$^{+/-}$-B6 mice, Han et al. 2012 challenged the DS definition of EE, suggesting that DS phenotype might solely be due to the *SCNA1* gene mutation i.e. a channelopathy, when they rescued some of the behavioral impairments (CFC and social interaction deficits) with low-dose clonazepan without causing sedation. However, the animals used in this study resulted from the 20% survivors following recurrent spontaneous seizure activity. It is thus possible that these remaining mice represent a sub-population of the colony most resilient to the seizures, which could also be most receptive to pharmacotherapy. Moreover, benzodiazepines might be effective in reducing the seizures in DS but rapidly become ineffective and the cognitive deficits are not overcome via the use of benzodiazepines (Connolly, 2016; Genton et al., 2011; Inoue et al., 2015).

Using a knock-down model to selectively reduce the $Na_V1.1$ function without causing seizures, *Bender et al. 2013,2016* had shown network abnormalities (reduction of neurons that fired phase-locked to hippocampal theta oscillations and dysruption of

medial septal regulation of theta rhythm) correlated with memory deficits, arguing again for the notion that DS might actually rather be a channelopathy. However this knock-down strategy was not sufficient to cover the severe behavioral/cognitive/neurological abnormalities presented in DS patients, thus questioning the validity of this model as a through DS model.

To date, there has been a general consensus that epileptic activity cannot be excluded in accounting from the severity of the phenotype in DS (Guerrini and Striano, 2016; Guzzetta, 2011; Wolff et al., 2006b). And very recently, a study showed that age at seizure onset appears to predict outcome better than mutation type in DS patients carrying *SCN1A* gene muatations (Cetica et al., 2017). However, the correlation between epileptic activity and behavioral/cognitive phenotype has never been fully established (Nabbout et al., 2013; Villeneuve et al., 2014).

Considering the clinical studies, recent evidences point to a possible role of network dysfunction to cause the very early visual impairments observed in DS patients (arguing for the channelopathy theory). Indeed, the study proposed by *Ricci et al. 2015* comprises five DS cases, that are visually impaired early in life, but only one patient carries the *SCN1A* gene mutation. However, it is difficult to conclude on one patient diagnosis. Also, a similar progressive neurocognitive decline was observed in two children with DS, carrying de novo *SCN1A* truncations and different epileptic phenotype severity (Riva et al., 2009). *Passamonti et al.* 2015 shows a family with inherited transmission where all the members have visual problems, even one patient who carries the mutation, but never had seizures. However, this patient was tested at 74 years of age, and the visual problems could be a consequence of normal aging (Passamonti et al., 2015). No study thus far evaluated visual problems before the appearance of the first febrile/afebrile seizure. Therefore, it is possible that the visual impairment is the first behavioral consequence of seizures. Interestingly, however, visual deterioration has rarely been reported following a GTC event (Subash et al., 2010). In animal models, the visual-spatial memory is affected following neo-natal seizures in normal brains (Holmes et al., 1998; Neill et al., 1996). Also attention importantly influences visual perception (Sundberg et al., 2012) and attention deficits (associated with PFC dysfunction) are present in DS children at the onset.

Thus as some studies pointed the possible role of the *SCN1A* gene mutation *per se* in generating the behavioral and cognitive impairment in DS, it was important to address the question in the opposite way i.e. could we exclude seizures as aggravating

factors in disease progression. Our data presented here strongly argument against this possibility. Thus, we propose that DS is probably not only due to the effect of *SCN1A* mutations on network dysfunction *per se*, arguing against DS as a channelopathy. We argue that *SCN1A* mutations set the developing brain into a fragile condition probably by altering network connection and synchronization upon which repeated seizures during early life will provoke irreversible network alterations at the basis of long-term behavioral and cognitive dysfunction. Thus, early life epileptic history is likely to play a major role in the progression of the disease.

6. THE IMPORTANCE OF UNDERSTANDING THE ROLE OF SEIZURES FOR THE DEVELOPMENT OF ADEQUATE TREAMENTS.

The $Na_V1.1$ dysfunction, by rendering the brain fragile to epileptic insults, has consequences in behavioral and cognitive phenotypes in DS. Indeed, it is clear from our study that the lack of **N**$a_V1.1$ causes the appearance of spontaneous seizures in mouse models associated with hyper-sensitivity to hyperthermia-induced seizures. Some studies show that more severe missense mutations (impacting changes in aminoacids polarity – inducing higher Grantham Score) and truncating mutations might be associated to earlier onset of seizures in DS (Brunklaus et al., 2014; Zuberi et al., 2011). However the mutation severities *per se* have not been successfully correlated with the behavioral and cognitive abnormalities in DS (Ishii et al., 2017; Jiang et al., 2016; Takaori et al., 2017).

We observe that seizures aggravate the epileptic and cognitive phenotypes in the *Scn1a*$^{RH/+}$ mice carrying a missense mutation inducing a DS phenotype. One possibility is that seizures might have more severe consequences for cognition and behavior in patients carrying more severe mutations (we saw for example that the same SIH protocols induce higher mortality in animals presenting a truncation mutation than a missense mutation). *Ishii, et. al 2016* suggested that the missense *vs.* truncation mutations in DS might have independent ways to induce cognitive deficits. Truncation mutations were associated with a more rapid rate of cognitive decline, regardless of age at seizure onset, while the age at seizure onset was a predictor for the rate of cognitive decline for missense mutations (Ishii et al., 2016).Yet, the fact that the mutations found in DS can occasionally cause GEFS+ if present only in some neurons (Depienne et al., 2006; Gennaro et al., 2006; Marini et al., 2006) and that mutations present in GEFS+

can cause DS (Depienne et al., 2010), as it is the case for the R1648H mutation, show the limit between the clinical dissociation of GEFS+ and DS with respect to mutation type. Also, it reveals that DS and GEFS+ share major features, including FS, sensitivity to hyperthermic seizures and polymorphous seizure types. Thus, these observations fit well with our current data, demonstrating that DS disease could be a severe end of GEFS+ (Scheffer et al., 2001; Singh et al., 2001; Veggiotti et al., 2001; Wallace et al., 2003). The R1648H mutation was found in GEFS+ patients and in one DS patient, suggesting that factors other than the mutation type account for the severity of the phenotype. Thus, our study is the reflect of a clinical observation associated to the R1648H mutation that confers two different phenotypes in the presence or absence of epileptic activity. Indeed, our results clearly show that early life repeated seizures worsen behavioral and cognitive phenotypes in the *Scn1a*$^{RH/+}$, thus transforming a mild GEFS+ model into a severe DS mouse model (schematized in **FIGURE 46**). Overall, this work stresses the importance of treating the early life epileptic seizures for a better outcome in DS patients.

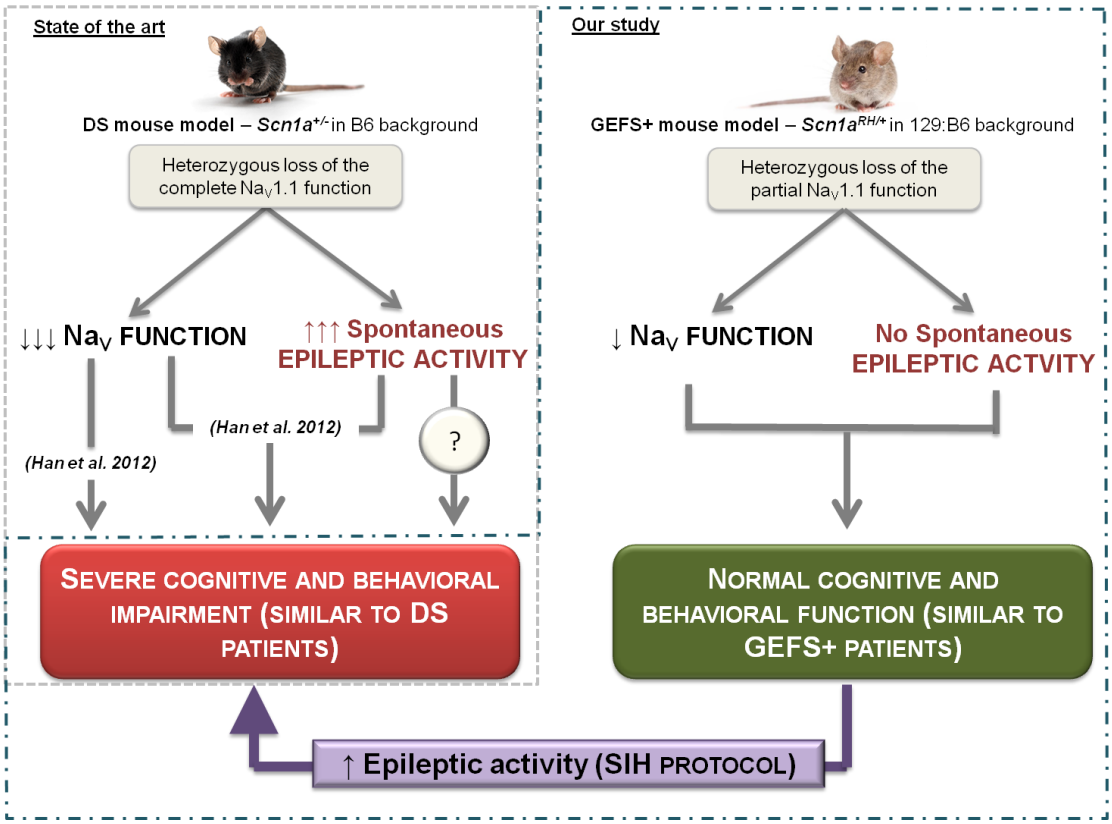

FIGURE 46. SCHEMATIC ILLUSTRATION OF THE STATE OF THE ART KNOWLEDGE AFTER OUR STUDY. The role of epileptic activity and $Na_V1.1$ dysfunction in contributing to the cognitive and behavioral phenotype in the DS mouse model (Left). The partial loss of the $Na_V1.1$ channel function and no spontaneous epileptic activity do not induce behavioral and cogntitive changes in the *Scn1a*$^{RH/+}$ mice, but when challenged with early life SIH, is converted into the phenotype observed in DS mouse models.

Conclusion and Perspectives

VI- CONCLUSION AND PERSPECTIVES

SCN1A gene mutations, encoding for $Na_V1.1$, are associated to a large spectrum of epileptic disorders. GEFS+, the milder syndrome, is usually caused by mild missense mutations. The patients present seizures with no cognitive deficits and in general, respond well to therapy. DS, the most severe disease of the spectrum, is a drug-resistant EE. GEFS+ and DS share common mutations and the distinction between the two is sometimes blurred. The cause of the cognitive decline in DS has never been proven clinically, questioning the definition of EE. In particular, the definition of DS as an EE has recently been challenged by experimental studies using animal models. In these studies, it has been suggested that the mutation *per se*, irrespective of epileptic history, causes the cognitive deficits in DS, thus proposing DS as a genetic channelopathy.

Understanding the origin of cognitive impairment in DS and other EE is crucial for a better quality of treatment and daily life of patients and caregivers. The type of mutation in the *SCN1A* gene is an important predictor of the seizure onset and development of epilepsy in DS patients. However, the strong epileptic activity might play a role in worsening the phenotype and in the appearance of the behavioral and cognitive comorbidities in DS.

The main goal of our work was to study the effect of repeated seizures induced by hyperthermia to the cognitive and behavioral phenotypes in mouse models carrying *Scn1a* gene mutations observed in DS patients or in GEFS+ patients, but which display little phenotypes in terms of spontaneous epileptic activity. Using the $Scn1a^{RH/+}$ mice (mouse model carrying a missense mutation that causes GEFS+ and DS in one patient), we disclosed an important role of early life seizures in the appearance of subsequent behavioral and cognitive phenotypes in adulthood. The results clearly indicate that early life seizures can change a mild phenotype (similar to the one found in GEFS+ patients) into a severe form (closer to DS patients), by increasing spontaneous seizure occurrence and inducing important behavioral and cognitive abnormalities. We observed that the same seizure induction protocol did not perturb WT animals. Finally, we observed specific alterations in DG neuron function in the $Scn1a^{RH/+}$ mice submitted to this seizure induction protocol. These results indicate that a developing brain carrying the $Scn1a^{RH/+}$ mutation, when submitted to repeated early life seizures, is not able to cope with seizures effects, thus developing DG neuron network abnormalities and additional

spontaneous seizures. These alterations change brain function inducing long-lasting behavioral and cognitive changes.

Our findings indicate a negative role of early life epileptic seizures in the progression/worsening of cognitive deficits in *Scn1a* mutant mice. It is therefore important to develop treatments that can completely block the seizures in the patients in order to expect better outcomes.

In terms of perspectives, the main perspective for now is to complete the behavioral analysis in the flurothyl-induced seizures as it represents an important control of our experiment. Flurothyl-induced seizures are also currently being induced in WT and *Scn1a*$^{RH/+}$ mice to investigate the development of spontaneous seizures using ECoG recordings and the electrophysiological properties of DG granule cells to complete our study.

We also need to complete the electrophysiological analysis by investigating the interneurons' properties in CA1 and DG areas of the hippocampus in the *Scn1a*$^{RH/+}$SIH and control mice, as play a key role in *Scn1a* mouse models neuropathology.

Later on, it would have been interesting to investigate if there is an age-dependent effect of seizures to the phenotype (e.g. Induce SIH at earlier age P17-P18 and later age P30 or P60).

Another interesting investigation would have been to use the severe DS mouse model in pure B6 background and block the spontaneous seizures from the very onset (probably with stiripentol+clonazepan (Inoue et al., 2015) or fenfluramine (Ceulemans et al., 2016; Schoonjans et al., 2017)) to evaluate if the animals still display behavioral abnormalities at later ages.

Considering the long-term future perspective, it consists in understanding why and how early life seizures can produce a severe phenotype in a model that was previously normal. Understanding the cellular and molecular mechanisms implicated in this conversion will provide new research avenues for innovative treatment therapies.

Bibliography

VII- BIBLIOGRAPHY

Abdeljalil, J., Hamid, M., Abdel-Mouttalib, O., Stéphane, R., Raymond, R., Johan, A., José, S., Pierre, C., and Serge, P. (2005). The optomotor response: a robust first-line visual screening method for mice. Vision Res. *45*, 1439–1446.

Acha, J., Pérez, A., Davidson, D.J., and Carreiras, M. (2015). Cognitive characterization of children with Dravet syndrome: A neurodevelopmental perspective. Child Neuropsychol. *21*, 693–715.

Acsády, L., and Káli, S. (2007). Models, structure, function: the transformation of cortical signals in the dentate gyrus. Prog. Brain Res. *163*, 577–599.

Adolphs, R., Tranel, D., and Buchanan, T.W. (2005). Amygdala damage impairs emotional memory for gist but not details of complex stimuli. Nat. Neurosci. *8*, 512–518.

Akiyama, M., Kobayashi, K., Yoshinaga, H., and Ohtsuka, Y. (2010). A long-term follow-up study of Dravet syndrome up to adulthood. Epilepsia *51*, 1043–1052.

Akiyama, M., Kobayashi, K., and Ohtsuka, Y. (2012). Dravet syndrome: a genetic epileptic disorder. Acta Med. Okayama *66*, 369–376.

Albala, B.J., Moshé, S.L., and Okada, R. (1984). Kainic-acid-induced seizures: a developmental study. Brain Res. *315*, 139–148.

Alheim, K., and Bartfai, T. (1998). The interleukin-1 system: receptors, ligands, and ICE in the brain and their involvement in the fever response. Ann. N. Y. Acad. Sci. *840*, 51–58.

Allen Hauser, W., and Lee, J.R. (2002). Do seizures beget seizures? B.-P. in B. Research, ed. (Elsevier), pp. 215–219.

Amaral, D.G., Scharfman, H.E., and Lavenex, P. (2007). The dentate gyrus: fundamental neuroanatomical organization (dentate gyrus for dummies). Prog. Brain Res. *163*, 3–22.

Anagnostaras, S.G., Maren, S., and Fanselow, M.S. (1999). Temporally graded retrograde amnesia of contextual fear after hippocampal damage in rats: within-subjects examination. J. Neurosci. Off. J. Soc. Neurosci. *19*, 1106–1114.

Andreollo, N.A., Santos, E.F. dos, Araújo, M.R., and Lopes, L.R. (2012). Rat's age versus human's age: what is the relationship? Arq. Bras. Cir. Dig. ABCD Braz. Arch. Dig. Surg. *25*, 49–51.

Annegers, J.F., Hauser, W.A., Shirts, S.B., and Kurland, L.T. (1987). Factors prognostic of unprovoked seizures after febrile convulsions. N. Engl. J. Med. *316*, 493–498.

Annesi, G., Gambardella, A., Carrideo, S., Incorpora, G., Labate, A., Pasqua, A.A., Civitelli, D., Polizzi, A., Annesi, F., Spadafora, P., et al. (2003). Two novel SCN1A missense mutations in generalized epilepsy with febrile seizures plus. Epilepsia *44*, 1257–1258.

Aram, J.A., and Lodge, D. (1987). Epileptiform activity induced by alkalosis in rat neocortical slices: block by antagonists of N-methyl-D-aspartate. Neurosci. Lett. *83*, 345–350.

Asarnow, R.F., LoPresti, C., Guthrie, D., Elliott, T., Cynn, V., Shields, W.D., Shewmon, D.A., Sankar, R., and Peacock, W.J. (1997). Developmental outcomes in children receiving resection surgery for medically intractable infantile spasms. Dev. Med. Child Neurol. *39*, 430–440.

Avanzini, G., Depaulis, A., Tassinari, A., and de Curtis, M. (2013). Do seizures and epileptic activity worsen epilepsy and deteriorate cognitive function? Epilepsia *54 Suppl 8*, 14–21.

Avishai-Eliner, S., Brunson, K.L., Sandman, C.A., and Baram, T.Z. (2002). Stressed-out, or in (utero)? Trends Neurosci. *25*, 518–524.

Baddeley, A. (1996). The fractionation of working memory. Proc. Natl. Acad. Sci. U. S. A. *93*, 13468–13472.

Baddeley, A., and Warrington, E.K. (1970). Amnesia and the distinction between long- and short-term memory. 176–189.

Bailet, L.L., and Turk, W.R. (2000). The impact of childhood epilepsy on neurocognitive and behavioral performance: a prospective longitudinal study. Epilepsia *41*, 426–431.

Balakrishnan, V., Srinivasan, G., and von Gersdorff, H. (2010). Post-tetanic potentiation involves the presynaptic binding of calcium to calmodulin. J. Gen. Physiol. *136*, 243–245.

Balestrino, M., and Somjen, G.G. (1988). Concentration of carbon dioxide, interstitial pH and synaptic transmission in hippocampal formation of the rat. J. Physiol. *396*, 247–266.

Banbury (1997). Mutant mice and neuroscience: recommendations concerning genetic background. Banbury Conference on genetic background in mice. Neuron *19*, 755–759.

Baram, T.Z., Gerth, A., and Schultz, L. (1997). Febrile seizures: an appropriate-aged model suitable for long-term studies. Brain Res. Dev. Brain Res. *98*, 265–270.

Barry, J.M., and Holmes, G.L. (2016). Why Are Children With Epileptic Encephalopathies Encephalopathic? J. Child Neurol. *31*, 1495–1504.

Battaglia, D., Chieffo, D., Siracusano, R., Waure, C., Brogna, C., Ranalli, D., Contaldo, I., Tortorella, G., Dravet, C., Mercuri, E., et al. (2013). Cognitive decline in Dravet syndrome: is there a cerebellar role? Epilepsy Res *106*, 211–221.

Battaglia, D., Ricci, D., Chieffo, D., and Guzzetta, F. (2016). Outlining a core neuropsychological phenotype for Dravet syndrome. Epilepsy Res. *120*, 91–97.

Baulac, S., Gourfinkel-An, I., Nabbout, R., Huberfeld, G., Serratosa, J., Leguern, E., and Baulac, M. (2004). Fever, genes, and epilepsy. Lancet Neurol. *3*, 421–430.

Baxendale, S., and Thompson, P. (2016). The new approach to epilepsy classification: Cognition and behavior in adult epilepsy syndromes. Epilepsy Behav. *64, Part A*, 253–256.

Ben-Ari, Y., Crepel, V., and Represa, A. (2008). Seizures beget seizures in temporal lobe epilepsies: the boomerang effects of newly formed aberrant kainatergic synapses. Epilepsy Curr. *8*, 68–72.

Bender, A.C., Natola, H., Ndong, C., Holmes, G.L., Scott, R.C., and Lenck-Santini, P.-P. (2013). Focal Scn1a knockdown induces cognitive impairment without seizures. Neurobiol. Dis. *54*, 297–307.

Bender, A.C., Luikart, B.W., and Lenck-Santini, P.-P. (2016). Cognitive Deficits Associated with Nav1.1 Alterations: Involvement of Neuronal Firing Dynamics and Oscillations. PloS One *11*, e0151538.

Bender, R.A., Dubé, C., Gonzalez-Vega, R., Mina, E.W., and Baram, T.Z. (2003). Mossy fiber plasticity and enhanced hippocampal excitability, without hippocampal cell loss or altered neurogenesis, in an animal model of prolonged febrile seizures. Hippocampus *13*, 399–412.

Bender, R.A., Dubé, C., and Baram, T.Z. (2004a). Febrile Seizures and Mechanisms of Epileptogenesis: Insights from an Animal Model. Adv. Exp. Med. Biol. *548*, 213–225.

Bender, R.A., Dubé, C., and Baram, T.Z. (2004b). Febrile Seizures and Mechanisms of Epileptogenesis: Insights from an Animal Model. Adv. Exp. Med. Biol. *548*, 213–225.

Berg, A.T. (2016). New classification efforts in epilepsy: Opportunities for clinical neurosciences. Epilepsy Behav. EB *64*, 304–305.

Berg, A.T., and Shinnar, S. (1996). Unprovoked seizures in children with febrile seizures: short-term outcome. Neurology *47*, 562–568.

Berg, A.T., Berkovic, S.F., Brodie, M.J., Buchhalter, J., Cross, J.H., Van Emde Boas, W., Engel, J., French, J., Glauser, T.A., Mathern, G.W., et al. (2010). Revised terminology and concepts for organization of seizures and epilepsies: Report of the ILAE Commission on Classification and Terminology, 2005–2009. Epilepsia *51*, 676–685.

Berkvens, J.J., Veugen, I., Veendrick-Meekes, M.J., Snoeijen-Schouwenaars, F.M., Schelhaas, H.J., Willemsen, M.H., Tan, I.Y., and Aldenkamp, A.P. (2015). Autism and behavior in adult patients with Dravet syndrome (DS). Epilepsy Behav *47*, 11–16.

Bliss, T.V., and Collingridge, G.L. (1993). A synaptic model of memory: long-term potentiation in the hippocampus. Nature *361*, 31–39.

Bliss, T.V., and Lomo, T. (1973). Long-lasting potentiation of synaptic transmission in the dentate area of the anaesthetized rabbit following stimulation of the perforant path. J. Physiol. *232*, 331–356.

Blume, W.T., Lüders, H.O., Mizrahi, E., Tassinari, C., van Emde Boas, W., and Engel, J. (2001). Glossary of descriptive terminology for ictal semiology: report of the ILAE task force on classification and terminology. Epilepsia *42*, 1212–1218.

Bo, T., Jiang, Y., Cao, H., Wang, J., and Wu, X. (2004). Long-term effects of seizures in neonatal rats on spatial learning ability and N-methyl-D-aspartate receptor expression in the brain. Brain Res. Dev. Brain Res. *152*, 137–142.

Brown, N.J., Berkovic, S.F., and Scheffer, I.E. (2007). Vaccination, seizures and "vaccine damage." Curr. Opin. Neurol. *20*, 181–187.

Browning, R.A. (1985). Role of the brain-stem reticular formation in tonic-clonic seizures: lesion and pharmacological studies. Fed. Proc. *44*, 2425–2431.

Brunklaus, A., Ellis, R., Reavey, E., Semsarian, C., and Zuberi, S.M. (2014). Genotype phenotype associations across the voltage-gated sodium channel family. J. Med. Genet. *51*, 650–658.

Brunklaus, A., Ellis, R., Stewart, H., Aylett, S., Reavey, E., Jefferson, R., Jain, R., Chakraborty, S., Jayawant, S., and Zuberi, S.M. (2015). Homozygous mutations in the SCN1A gene associated with genetic epilepsy with febrile seizures plus and Dravet syndrome in 2 families. Eur. J. Paediatr. Neurol. *19*, 484–488.

Buhl, E.H., Halasy, K., and Somogyi, P. (1994). Diverse sources of hippocampal unitary inhibitory postsynaptic potentials and the number of synaptic release sites. Nature *368*, 823–828.

Buoni, S., Orrico, A., Galli, L., Zannolli, R., Burroni, L., Hayek, J., Fois, A., and Sorrentino, V. (2006). SCN1A (2528delG) novel truncating mutation with benign outcome of severe myoclonic epilepsy of infancy. Neurology *66*, 606–607.

Bureau, M., and Dalla Bernardina, B. (2011). Electroencephalographic characteristics of Dravet syndrome. Epilepsia *52 Suppl 2*, 13–23.

Burger, F.J., and Fuhrman, F.A. (1964). EVIDENCE OF INJURY BY HEAT IN MAMMALIAN TISSUES. Am. J. Physiol. *206*, 1057–1061.

Camfield, P., and Camfield, C. (2015). Febrile seizures and genetic epilepsy with febrile seizures plus (GEFS+). Epileptic Disord. Int. Epilepsy J. Videotape *17*, 124–133.

Caraballo, R.H., and Fejerman, N. (2006). Dravet syndrome: a study of 53 patients. Epilepsy Res. *70 Suppl 1*, S231-238.

Caraballo, R., Vaccarezza, M., Cersósimo, R., Rios, V., Soraru, A., Arroyo, H., Agosta, G., Escobal, N., Demartini, M., Maxit, C., et al. (2011). Long-term follow-up of the ketogenic diet for refractory epilepsy: multicenter Argentinean experience in 216 pediatric patients. Seizure *20*, 640–645.

Cartmell, T., Luheshi, G.N., and Rothwell, N.J. (1999). Brain sites of action of endogenous interleukin-1 in the febrile response to localized inflammation in the rat. J. Physiol. *518 (Pt 2)*, 585–594.

Catarino, C.B., Liu, J.Y.W., Liagkouras, I., Gibbons, V.S., Labrum, R.W., Ellis, R., Woodward, C., Davis, M.B., Smith, S.J., Cross, J.H., et al. (2011). Dravet syndrome as epileptic encephalopathy: evidence from long-term course and neuropathology. Brain J. Neurol. *134*, 2982–3010.

Catterall, W.A. (1995). Structure and function of voltage-gated ion channels. Annu. Rev. Biochem. *64*, 493–531.

Catterall, W.A. (2014). Sodium channels, inherited epilepsy, and antiepileptic drugs. Annu. Rev. Pharmacol. Toxicol. *54*, 317–338.

Cersósimo, R.O., Bartuluchi, M., Fortini, S., Soraru, A., Pomata, H., and Caraballo, R.H. (2011). Vagus nerve stimulation: effectiveness and tolerability in 64 paediatric patients with refractory epilepsies. Epileptic Disord. Int. Epilepsy J. Videotape *13*, 382–388.

Cetica, V., Chiari, S., Mei, D., Parrini, E., Grisotto, L., Marini, C., Pucatti, D., Ferrari, A., Sicca, F., Specchio, N., et al. (2017). Clinical and genetic factors predicting Dravet syndrome in infants with SCN1A mutations. Neurology.

Ceulemans, B. (2011). Overall management of patients with Dravet syndrome. Dev. Med. Child Neurol. *53 Suppl 2*, 19–23.

Ceulemans, B., Schoonjans, A.-S., Marchau, F., Paelinck, B.P., and Lagae, L. (2016). Five-year extended follow-up status of 10 patients with Dravet syndrome treated with fenfluramine. Epilepsia *57*, e129-134.

Chabardès, S., Kahane, P., Minotti, L., Koudsie, A., Hirsch, E., and Benabid, A.-L. (2002). Deep brain stimulation in epilepsy with particular reference to the subthalamic nucleus. Epileptic Disord. Int. Epilepsy J. Videotape *4 Suppl 3*, S83-93.

Champagne, F.A., Curley, J.P., Keverne, E.B., and Bateson, P.P.G. (2007). Natural variations in postpartum maternal care in inbred and outbred mice. Physiol. Behav. *91*, 325–334.

Chang, Y.-C., Huang, A.-M., Kuo, Y.-M., Wang, S.-T., Chang, Y.-Y., and Huang, C.-C. (2003). Febrile seizures impair memory and cAMP response-element binding protein activation. Ann. Neurol. *54*, 706–718.

Cheah, C.S., Yu, F.H., Westenbroek, R.E., Kalume, F.K., Oakley, J.C., Potter, G.B., Rubenstein, J.L., and Catterall, W.A. (2012). Specific deletion of NaV1.1 sodium channels in inhibitory interneurons causes seizures and premature death in a mouse model of Dravet syndrome. Proc. Natl. Acad. Sci. U. S. A. *109*, 14646–14651.

Cheah, C.S., Westenbroek, R.E., Roden, W.H., Kalume, F., Oakley, J.C., Jansen, L.A., and Catterall, W.A. (2013a). Correlations in timing of sodium channel expression, epilepsy, and sudden death in Dravet syndrome. Channels *7*, 468–472.

Cheah, C.S., Westenbroek, R.E., Roden, W.H., Kalume, F., Oakley, J.C., Jansen, L.A., and Catterall, W.A. (2013b). Correlations in timing of sodium channel expression, epilepsy, and sudden death in Dravet syndrome. Channels Austin Tex *7*, 468–472.

Chieffo, D., Ricci, D., Baranello, G., Martinelli, D., Veredice, C., Lettori, D., Battaglia, D., Dravet, C., Mercuri, E., and Guzzetta, F. (2011a). Early development in Dravet syndrome; visual function impairment precedes cognitive decline. Epilepsy Res *93*, 73–79.

Chieffo, D., Battaglia, D., Lettori, D., Del Re, M., Brogna, C., Dravet, C., Mercuri, E., and Guzzetta, F. (2011b). Neuropsychological development in children with Dravet syndrome. Epilepsy Res *95*, 86–93.

Chieffo, D., Ricci, D., Baranello, G., Martinelli, D., Veredice, C., Lettori, D., Battaglia, D., Dravet, C., Mercuri, E., and Guzzetta, F. (2011c). Early development in Dravet syndrome; visual function impairment precedes cognitive decline. Epilepsy Res. *93*, 73–79.

Chipaux, M., Villeneuve, N., Sabouraud, P., Desguerre, I., Boddaert, N., Depienne, C., Chiron, C., Dulac, O., and Nabbout, R. (2010). Unusual consequences of status epilepticus in Dravet syndrome. Seizure *19*, 190–194.

Chiron, C., Marchand, M.C., Tran, A., Rey, E., d'Athis, P., Vincent, J., Dulac, O., and Pons, G. (2000). Stiripentol in severe myoclonic epilepsy in infancy: a randomised placebo-controlled syndrome-dedicated trial. STICLO study group. Lancet Lond. Engl. *356*, 1638–1642.

Claes, L., Del-Favero, J., Ceulemans, B., Lagae, L., Van Broeckhoven, C., and De Jonghe, P. (2001). De novo mutations in the sodium-channel gene SCN1A cause severe myoclonic epilepsy of infancy. Am. J. Hum. Genet. *68*, 1327–1332.

Claes, L.R.F., Deprez, L., Suls, A., Baets, J., Smets, K., Van Dyck, T., Deconinck, T., Jordanova, A., and De Jonghe, P. (2009). The SCN1A variant database: a novel research and diagnostic tool. Hum. Mutat. *30*, E904-920.

Clark, K., Squire, R.F., Merrikhi, Y., and Noudoost, B. (2015). Visual attention: Linking prefrontal sources to neuronal and behavioral correlates. Prog. Neurobiol. *132*, 59–80.

Colino, A., Muñoz, J., and Vara, H. (2002). [Short term synaptic plasticity]. Rev. Neurol. *34*, 593–599.

Connolly, M.B. (2016). Dravet Syndrome: Diagnosis and Long-Term Course. Can. J. Neurol. Sci. J. Can. Sci. Neurol. *43 Suppl 3*, S3-8.

Cossette, P. (2010). Channelopathies and juvenile myoclonic epilepsy. Epilepsia *51 Suppl 1*, 30–32.

Crawley, J.N., Evers, J.R., and Paul, S.M. (1992). Polyamines inhibit N-methyl-d-aspartate antagonist-induced darting behavior in the rat prefrontal cortex. Brain Res. *586*, 6–11.

Cross, J.H., and Guerrini, R. (2013). The epileptic encephalopathies. Handb. Clin. Neurol. *111*, 619–626.

Cupolillo, D., Hoxha, E., Faralli, A., De Luca, A., Rossi, F., Tempia, F., and Carulli, D. (2016). Autistic-Like Traits and Cerebellar Dysfunction in Purkinje Cell PTEN Knock-Out Mice. Neuropsychopharmacol. Off. Publ. Am. Coll. Neuropsychopharmacol. *41*, 1457–1466.

Dalla Bernardina, B., Capovilla, G., Gattoni, M.B., Colamaria, V., Bondavalli, S., and Bureau, M. (1982). [Severe infant myoclonic epilepsy (author's transl)]. Rev. Electroencephalogr. Neurophysiol. Clin. *12*, 21–25.

De Liso, P., Chemaly, N., Laschet, J., Barnerias, C., Hully, M., Leunen, D., Desguerre, I., Chiron, C., Dulac, O., and Nabbout, R. (2016). Patients with dravet syndrome in the era of stiripentol: A French cohort cross-sectional study. Epilepsy Res. *125*, 42–46.

Deng, W., Aimone, J.B., and Gage, F.H. (2010). New neurons and new memories: how does adult hippocampal neurogenesis affect learning and memory? Nat. Rev. Neurosci. *11*, 339–350.

Dent, C.L., and Isles, A.R. (2014). An overview of measuring impulsive behavior in mice. Curr. Protoc. Mouse Biol. *4*, 35–45.

Depienne, C., Arzimanoglou, A., Trouillard, O., Fedirko, E., Baulac, S., Saint-Martin, C., Ruberg, M., Dravet, C., Nabbout, R., Baulac, M., et al. (2006). Parental mosaicism can cause recurrent transmission of SCN1A mutations associated with severe myoclonic epilepsy of infancy. Hum. Mutat. *27*, 389.

Depienne, C., Bouteiller, D., Keren, B., Cheuret, E., Poirier, K., Trouillard, O., Benyahia, B., Quelin, C., Carpentier, W., Julia, S., et al. (2009). Sporadic infantile epileptic encephalopathy caused by mutations in PCDH19 resembles Dravet syndrome but mainly affects females. PLoS Genet. *5*, e1000381.

Depienne, C., Trouillard, O., Gourfinkel-An, I., Saint-Martin, C., Bouteiller, D., Graber, D., Barthez-Carpentier, M.A., Gautier, A., Villeneuve, N., Dravet, C., et al. (2010). Mechanisms for variable expressivity of inherited SCN1A mutations causing Dravet syndrome. J Med Genet *47*, 404–410.

Deshpande, L.S., Lou, J.K., Mian, A., Blair, R.E., Sombati, S., Attkisson, E., and DeLorenzo, R.J. (2008). Time course and mechanism of hippocampal neuronal death in an in vitro model of status epilepticus: role of NMDA receptor activation and NMDA dependent calcium entry. Eur. J. Pharmacol. *583*, 73–83.

Dhamija, R., Erickson, M.K., St Louis, E.K., Wirrell, E., and Kotagal, S. (2014). Sleep abnormalities in children with Dravet syndrome. Pediatr. Neurol. *50*, 474–478.

Dobbing, J., and Sands, J. (1973). Quantitative growth and development of human brain. Arch. Dis. Child. *48*, 757–767.

Dravet, C. (2014). Terminology and prognosis of Dravet syndrome. Epilepsia *55*, 942–943.

Dravet, C., and Guerrini, R. (2011). Dravet Syndrome (éditions John LibbeyEurotext).

Dravet, C., Bureau, M., Oguni, H., Fukuyama, Y., and Cokar, O. (2005). Severe myoclonic epilepsy in infancy: Dravet syndrome. Adv Neurol *95*, 71–102.

Dube, C., Chen, K., Eghbal-Ahmadi, M., Brunson, K., Soltesz, I., and Baram, T.Z. (2000). Prolonged febrile seizures in the immature rat model enhance hippocampal excitability long term. Ann. Neurol. *47*, 336–344.

Dubé, C., Vezzani, A., Behrens, M., Bartfai, T., and Baram, T.Z. (2005). Interleukin-1beta contributes to the generation of experimental febrile seizures. Ann. Neurol. *57*, 152–155.

Dubé, C., Richichi, C., Bender, R.A., Chung, G., Litt, B., and Baram, T.Z. (2006). Temporal lobe epilepsy after experimental prolonged febrile seizures: prospective analysis. Brain J. Neurol. *129*, 911–922.

Dubé, C.M., Zhou, J.-L., Hamamura, M., Zhao, Q., Ring, A., Abrahams, J., McIntyre, K., Nalcioglu, O., Shatskih, T., Baram, T.Z., et al. (2009). Cognitive dysfunction after experimental febrile seizures. Exp. Neurol. *215*, 167–177.

Dubé, C.M., Ravizza, T., Hamamura, M., Zha, Q., Keebaugh, A., Fok, K., Andres, A.L., Nalcioglu, O., Obenaus, A., Vezzani, A., et al. (2010). Epileptogenesis provoked by prolonged experimental febrile seizures: mechanisms and biomarkers. J. Neurosci. Off. J. Soc. Neurosci. *30*, 7484–7494.

Dubé, C.M., McClelland, S., Choy, M., Brewster, A.L., Noam, Y., and Baram, T.Z. (2012). Fever, febrile seizures and epileptogenesis. In Jasper's Basic Mechanisms of the Epilepsies, J.L. Noebels, M. Avoli, M.A. Rogawski, R.W. Olsen, and A.V. Delgado-Escueta, eds. (Bethesda (MD): National Center for Biotechnology Information (US)), p.

Dudek, F.E., and Sutula, T.P. (2007). Epileptogenesis in the dentate gyrus: a critical perspective. In Progress in Brain Research, H.E. Scharfman, ed. (Elsevier), pp. 755–773.

Duflocq, A., Le Bras, B., Bullier, E., Couraud, F., and Davenne, M. (2008). Nav1.1 is predominantly expressed in nodes of Ranvier and axon initial segments. Mol. Cell. Neurosci. *39*, 180–192.

Dutton, S.B., Makinson, C.D., Papale, L.A., Shankar, A., Balakrishnan, B., Nakazawa, K., and Escayg, A. (2013). Preferential inactivation of Scn1a in parvalbumin interneurons increases seizure susceptibility. Neurobiol. Dis. *49*, 211–220.

Eichenbaum, H. (2001). The hippocampus and declarative memory: cognitive mechanisms and neural codes. Behav. Brain Res. *127*, 199–207.

Ellenberg, J.H., and Nelson, K.B. (1978). Febrile seizures and later intellectual performance. Arch. Neurol. *35*, 17–21.

Escayg, A., and Goldin, A.L. (2010). Sodium channel SCN1A and epilepsy: mutations and mechanisms. Epilepsia *51*, 1650–1658.

Escayg, A., MacDonald, B.T., Meisler, M.H., Baulac, S., Huberfeld, G., An-Gourfinkel, I., Brice, A., LeGuern, E., Moulard, B., Chaigne, D., et al. (2000a). Mutations of SCN1A, encoding a neuronal sodium channel, in two families with GEFS+2. Nat. Genet. *24*, 343–345.

Escayg, A., De Waard, M., Lee, D.D., Bichet, D., Wolf, P., Mayer, T., Johnston, J., Baloh, R., Sander, T., and Meisler, M.H. (2000b). Coding and noncoding variation of the human calcium-channel beta4-subunit gene CACNB4 in patients with idiopathic generalized epilepsy and episodic ataxia. Am. J. Hum. Genet. *66*, 1531–1539.

Estacion, M., O'Brien, J.E., Conravey, A., Hammer, M.F., Waxman, S.G., Dib-Hajj, S.D., and Meisler, M.H. (2014). A novel de novo mutation of SCN8A (Nav1.6) with enhanced channel activation in a child with epileptic encephalopathy. Neurobiol. Dis. *69*, 117–123.

Etchamendy, N., Desmedt, A., Cortes-Torrea, C., Marighetto, A., and Jaffard, R. (2003). Hippocampal lesions and discrimination performance of mice in the radial maze: sparing or impairment depending on the representational demands of the task. Hippocampus *13*, 197–211.

Feng, B., Tang, Y.-S., Chen, B., Dai, Y.-J., Xu, C.-L., Xu, Z.-H., Zhang, X.-N., Zhang, S.-H., Hu, W.-W., and Chen, Z. (2014). Dysfunction of thermoregulation contributes to the generation of hyperthermia-induced seizures. Neurosci. Lett. *581*, 129–134.

Fewell, J.E., and Wong, V.H. (2002). Interleukin-1beta-induced fever does not alter the ability of 5- to 6-day-old rat pups to autoresuscitate from hypoxia-induced apnoea. Exp. Physiol. *87*, 17–24.

Fink, M. (2014). The seizure, not electricity, is essential in convulsive therapy: the flurothyl experience. J. ECT *30*, 91–93.

Fisher, J.L. (2011). The effects of stiripentol on GABA(A) receptors. Epilepsia *52 Suppl 2*, 76–78.

Fisher, R.S., and Wu, J. (2002). Chapter 16 - Basic Electrophysiology of Febrile Seizures A2 - Baram, Tallie Z. In Febrile Seizures, S. Shinnar, ed. (San Diego: Academic Press), pp. 231–247.

Fisher, F., Cross, H., and French Jacqueline A. (2016). Operational Classification of Seizure Types by the International League Against Epilepsy.

Fisher, R.S., Acevedo, C., Arzimanoglou, A., Bogacz, A., Cross, J.H., Elger, C.E., Engel, J., Forsgren, L., French, J.A., Glynn, M., et al. (2014). ILAE official report: a practical clinical definition of epilepsy. Epilepsia *55*, 475–482.

Fiske, S.T. (1993). Controlling other people. The impact of power on stereotyping. Am. Psychol. *48*, 621–628.

Fitzpatrick, C.M., Caballero-Puntiverio, M., Gether, U., Habekost, T., Bundesen, C., Vangkilde, S., Woldbye, D.P.D., Andreasen, J.T., and Petersen, A. (2017). Theory of Visual Attention (TVA) applied to mice in the 5-choice serial reaction time task. Psychopharmacology (Berl.) *234*, 845–855.

Frankel, W.N. (2009). Genetics of complex neurological disease: challenges and opportunities for modeling epilepsy in mice and rats. Trends Genet. TIG *25*, 361–367.

Fujiwara, T., Watanabe, M., Takahashi, Y., Higashi, T., Yagi, K., and Seino, M. (1992). Long-term course of childhood epilepsy with intractable grand mal seizures. Jpn. J. Psychiatry Neurol. *46*, 297–302.

Fulton, S.P., Van Poppel, K., McGregor, A.L., Mudigoudar, B., and Wheless, J.W. (2017). Vagus Nerve Stimulation in Intractable Epilepsy Associated With SCN1A Gene Abnormalities. J. Child Neurol. 0883073816687221.

Fuster, J.M. (2004). Patricia Shoer Goldman-Rakic (1937-2003). Am. Psychol. *59*, 559–560.

Gaily, E., Anttonen, A.-K., Valanne, L., Liukkonen, E., Träskelin, A.-L., Polvi, A., Lommi, M., Muona, M., Eriksson, K., and Lehesjoki, A.-E. (2013). Dravet syndrome: new potential genetic modifiers, imaging abnormalities, and ictal findings. Epilepsia *54*, 1577–1585.

Gatti, S., Beck, J., Fantuzzi, G., Bartfai, T., and Dinarello, C.A. (2002). Effect of interleukin-18 on mouse core body temperature. Am. J. Physiol. Regul. Integr. Comp. Physiol. *282*, R702-709.

Gennaro, E., Santorelli, F.M., Bertini, E., Buti, D., Gaggero, R., Gobbi, G., Lini, M., Granata, T., Freri, E., Parmeggiani, A., et al. (2006). Somatic and germline mosaicisms in severe myoclonic epilepsy of infancy. Biochem. Biophys. Res. Commun. *341*, 489–493.

Genton, P., Velizarova, R., and Dravet, C. (2011). Dravet syndrome: the long-term outcome. Epilepsia *52 Suppl 2*, 44–49.

Germano, I.M., Zhang, Y.F., Sperber, E.F., and Moshé, S.L. (1996). Neuronal migration disorders increase susceptibility to hyperthermia-induced seizures in developing rats. Epilepsia *37*, 902–910.

Gilbert, P.E., Kesner, R.P., and Lee, I. (2001). Dissociating hippocampal subregions: double dissociation between dentate gyrus and CA1. Hippocampus *11*, 626–636.

Gitiaux, C., Chemaly, N., Quijano-Roy, S., Barnerias, C., Desguerre, I., Hully, M., Chiron, C., Dulac, O., and Nabbout, R. (2016). Motor neuropathy contributes to crouching in patients with Dravet syndrome. Neurology *87*, 277–281.

Goldin, A.L. (1999). Diversity of mammalian voltage-gated sodium channels. Ann. N. Y. Acad. Sci. *868*, 38–50.

Gong, B., Rhodes, K.J., Bekele-Arcuri, Z., and Trimmer, J.S. (1999). Type I and type II Na(+) channel alpha-subunit polypeptides exhibit distinct spatial and temporal patterning, and association with auxiliary subunits in rat brain. J. Comp. Neurol. *412*, 342–352.

Gordon, D., Merrick, D., Auld, V., Dunn, R., Goldin, A.L., Davidson, N., and Catterall, W.A. (1987). Tissue-specific expression of the RI and RII sodium channel subtypes. Proc. Natl. Acad. Sci. U. S. A. *84*, 8682–8686.

Gottlieb, A., Keydar, I., and Epstein, H.T. (1977). Rodent brain growth stages: an analytical review. Biol. Neonate *32*, 166–176.

Gottwald, B., Mihajlovic, Z., Wilde, B., and Mehdorn, H.M. (2003). Does the cerebellum contribute to specific aspects of attention? Neuropsychologia *41*, 1452–1460.

Gowers, W. (1881). Epilepsy and other chronic convulsive disorders. J ChurchillLondon.

Grant, A.C., and Vazquez, B. (2005). A Case of Extended Spectrum GEFS+. Epilepsia *46*, 39–40.

Grantham, R. (1974). Amino acid difference formula to help explain protein evolution. Science *185*, 862–864.

Grill, M.F., and Ng, Y.-T. (2013). "Simple febrile seizures plus (SFS +)": More than one febrile seizure within 24 hours is usually okay. Epilepsy Behav. *27*, 472–476.

Guerrini, R., and Striano, P. (2016). Dravet syndrome: Not just epilepsy. Neurology *87*, 245–246.

Guerrini, R., Dravet, C., Genton, P., Belmonte, A., Kaminska, A., and Dulac, O. (1998). Lamotrigine and seizure aggravation in severe myoclonic epilepsy. Epilepsia *39*, 508–512.

Guerrini, R., Cellini, E., Mei, D., Metitieri, T., Petrelli, C., Pucatti, D., Marini, C., and Zamponi, N. (2010). Variable epilepsy phenotypes associated with a familial intragenic deletion of the SCN1A gene. Epilepsia *51*, 2474–2477.

Guillemain, I., Kahane, P., and Depaulis, A. (2012). Animal models to study aetiopathology of epilepsy: what are the features to model? Epileptic. Disord. *14*, 217–225.

Guzzetta, F. (2011). Cognitive and behavioral characteristics of children with Dravet syndrome: an overview. Epilepsia *52 Suppl 2*, 35–38.

Hamelin, S., Pouyatos, B., Khalaf-Nazzal, R., Chabrol, T., Francis, F., David, O., and Depaulis, A. (2014). Long-term modifications of epileptogenesis and hippocampal rhythms after prolonged hyperthermic seizures in the mouse. Neurobiol. Dis. *69*, 156–168.

Han, S., Tai, C., Westenbroek, R.E., Yu, F.H., Cheah, C.S., Potter, G.B., Rubenstein, J.L., Scheuer, T., de la Iglesia, H.O., and Catterall, W.A. (2012a). Autistic-like behaviour in Scn1a+/- mice and rescue by enhanced GABA-mediated neurotransmission. Nature *489*, 385–390.

Han, S., Tai, C., Westenbroek, R.E., Yu, F.H., Cheah, C.S., Potter, G.B., Rubenstein, J.L., Scheuer, T., de la Iglesia, H.O., and Catterall, W.A. (2012b). Autistic-like behaviour in Scn1a+/- mice and rescue by enhanced GABA-mediated neurotransmission. Nature *489*, 385–390.

Han, S., Tai, C., Westenbroek, R.E., Yu, F.H., Cheah, C.S., Potter, G.B., Rubenstein, J.L., Scheuer, T., de la Iglesia, H.O., and Catterall, W.A. (2012c). Autistic-like behaviour in Scn1a+/- mice and rescue by enhanced GABA-mediated neurotransmission. Nature *489*, 385–390.

Hashimoto, Y., Araki, H., Suemaru, K., and Gomita, Y. (2006). Effects of drugs acting on the GABA-benzodiazepine receptor complex on flurothyl-induced seizures in Mongolian gerbils. Eur. J. Pharmacol. *536*, 241–247.

Hawkins, N.A., Zachwieja, N.J., Miller, A.R., Anderson, L.L., and Kearney, J.A. (2016). Fine Mapping of a Dravet Syndrome Modifier Locus on Mouse Chromosome 5 and Candidate Gene Analysis by RNA-Seq. PLoS Genet. *12*, e1006398.

Hedrich, U.B.S., Liautard, C., Kirschenbaum, D., Pofahl, M., Lavigne, J., Liu, Y., Theiss, S., Slotta, J., Escayg, A., Dihné, M., et al. (2014). Impaired action potential initiation in GABAergic interneurons causes hyperexcitable networks in an epileptic mouse model carrying a human Na(V)1.1 mutation. J. Neurosci. Off. J. Soc. Neurosci. *34*, 14874–14889.

Heida, J.G., and Pittman, Q.J. (2005). Causal links between brain cytokines and experimental febrile convulsions in the rat. Epilepsia *46*, 1906–1913.

Henze, D.A., Wittner, L., and Buzsáki, G. (2002). Single granule cells reliably discharge targets in the hippocampal CA3 network in vivo. Nat. Neurosci. *5*, 790–795.

Hermann, B.P., Seidenberg, M., and Bell, B. (2002). The neurodevelopmental impact of childhood onset temporal lobe epilepsy on brain structure and function and the risk of progressive cognitive effects. Prog. Brain Res. *135*, 429–438.

Hernan, A.E., Holmes, G.L., Isaev, D., Scott, R.C., and Isaeva, E. (2013). Altered short-term plasticity in the prefrontal cortex after early life seizures. Neurobiol. Dis. *50*, 120–126.

Hesdorffer, D.C., Tomson, T., Benn, E., Sander, J.W., Nilsson, L., Langan, Y., Walczak, T.S., Beghi, E., Brodie, M.J., Hauser, A., et al. (2011). Combined analysis of risk factors for SUDEP. Epilepsia *52*, 1150–1159.

Hille, B. (2001). Ion channels of excitable membranes (Sinauer Sunderland).

Hodgkin, A.L., and Huxley, A.F. (1952). The dual effect of membrane potential on sodium conductance in the giant axon of Loligo. J. Physiol. *116*, 497–506.

Holmes, G.L. (2009). The long-term effects of neonatal seizures. Clin. Perinatol. *36*, 901–914, vii–viii.

Holmes, G.L. (2015). Cognitive impairment in epilepsy: the role of network abnormalities. Epileptic Disord. Int. Epilepsy J. Videotape *17*, 101–116.

Holmes, G.L., Gairsa, J.L., Chevassus-Au-Louis, N., and Ben-Ari, Y. (1998). Consequences of neonatal seizures in the rat: morphological and behavioral effects. Ann. Neurol. *44*, 845–857.

Howell, K.B., McMahon, J.M., Carvill, G.L., Tambunan, D., Mackay, M.T., Rodriguez-Casero, V., Webster, R., Clark, D., Freeman, J.L., Calvert, S., et al. (2015). SCN2A encephalopathy. Neurology *85*, 958–966.

Huang, L., Cilio, M.R., Silveira, D.C., McCabe, B.K., Sogawa, Y., Stafstrom, C.E., and Holmes, G.L. (1999). Long-term effects of neonatal seizures: a behavioral, electrophysiological, and histological study. Brain Res. Dev. Brain Res. *118*, 99–107.

Inoue, Y., Ohtsuka, Y., and STP-1 Study Group (2015). Long-term safety and efficacy of stiripentol for the treatment of Dravet syndrome: A multicenter, open-label study in Japan. Epilepsy Res. *113*, 90–97.

Isaeva, E., Isaev, D., Khazipov, R., and Holmes, G.L. (2009). Long-term suppression of GABAergic activity by neonatal seizures in rat somatosensory cortex. Epilepsy Res. *87*, 286–289.

Isaeva, E., Isaev, D., Savrasova, A., Khazipov, R., and Holmes, G.L. (2010). Recurrent neonatal seizures result in long-term increases in neuronal network excitability in the rat neocortex. Eur. J. Neurosci. *31*, 1446–1455.

Isaeva, E., Isaev, D., and Holmes, G.L. (2013). Alteration of synaptic plasticity by neonatal seizures in rat somatosensory cortex. Epilepsy Res. *106*, 280–283.

Ishii, A., Watkins, J.C., Chen, D., Hirose, S., and Hammer, M.F. (2016). Clinical implications of SCN1A missense and truncation variants in a large Japanese cohort with Dravet syndrome. Epilepsia.

Ishii, A., Watkins, J.C., Chen, D., Hirose, S., and Hammer, M.F. (2017). Clinical implications of SCN1A missense and truncation variants in a large Japanese cohort with Dravet syndrome. Epilepsia *58*, 282–290.

Ito, S., Ogiwara, I., Yamada, K., Miyamoto, H., Hensch, T.K., Osawa, M., and Yamakawa, K. (2013). Mouse with Nav1.1 haploinsufficiency, a model for Dravet syndrome, exhibits lowered sociability and learning impairment. Neurobiol. Dis. *49*, 29–40.

Jansen, F.E., Sadleir, L.G., Harkin, L.A., Vadlamudi, L., McMahon, J.M., Mulley, J.C., Scheffer, I.E., and Berkovic, S.F. (2006). Severe myoclonic epilepsy of infancy (Dravet syndrome): recognition and diagnosis in adults. Neurology *67*, 2224–2226.

Jehi, L., Wyllie, E., and Devinsky, O. (2015). Epileptic encephalopathies: Optimizing seizure control and developmental outcome. Epilepsia *56*, 1486–1489.

Jiang, P., Shen, J., Yu, Y., Jiang, L., Xu, J., Xu, L., Yu, H., and Gao, F. (2016). Dravet syndrome with favourable cognitive and behavioral development due to a novel SCN1A frameshift mutation. Clin. Neurol. Neurosurg. *146*, 144–146.

Kadiyala, S.B., Yannix, J.Q., Nalwalk, J.W., Papandrea, D., Beyer, B.S., Herron, B.J., and Ferland, R.J. (2016). Eight Flurothyl-Induced Generalized Seizures Lead to the Rapid Evolution of Spontaneous Seizures in Mice: A Model of Epileptogenesis with Seizure Remission. J. Neurosci. Off. J. Soc. Neurosci. *36*, 7485–7496.

Kalume, F., Yu, F.H., Westenbroek, R.E., Scheuer, T., and Catterall, W.A. (2007a). Reduced sodium current in Purkinje neurons from Nav1.1 mutant mice: implications for ataxia in severe myoclonic epilepsy in infancy. J. Neurosci. Off. J. Soc. Neurosci. *27*, 11065–11074.

Kalume, F., Yu, F.H., Westenbroek, R.E., Scheuer, T., and Catterall, W.A. (2007b). Reduced sodium current in Purkinje neurons from Nav1.1 mutant mice: implications for ataxia in severe myoclonic epilepsy in infancy. J. Neurosci. Off. J. Soc. Neurosci. *27*, 11065–11074.

Kalume, F., Westenbroek, R.E., Cheah, C.S., Yu, F.H., Oakley, J.C., Scheuer, T., and Catterall, W.A. (2013). Sudden unexpected death in a mouse model of Dravet syndrome. J. Clin. Invest. *123*, 1798–1808.

Kalume, F., Oakley, J.C., Westenbroek, R.E., Gile, J., de la Iglesia, H.O., Scheuer, T., and Catterall, W.A. (2015). Sleep impairment and reduced interneuron excitability in a mouse model of Dravet Syndrome. Neurobiol. Dis. *77*, 141–154.

Kambouris, M., Thevenon, J., Soldatos, A., Cox, A., Stephen, J., Ben-Omran, T., Al-Sarraj, Y., Boulos, H., Bone, W., Mullikin, J.C., et al. (2016). Biallelic SCN10A mutations in neuromuscular disease and epileptic encephalopathy. Ann. Clin. Transl. Neurol. *4*, 26–35.

Kang, D.H., Heo, R.W., Yi, C.-O., Kim, H., Choi, C.H., and Roh, G.S. (2015). High-fat diet-induced obesity exacerbates kainic acid-induced hippocampal cell death. BMC Neurosci. *16*, 72.

Karnam, H.B., Zhao, Q., Shatskikh, T., and Holmes, G.L. (2009a). Effect of age on cognitive sequelae following early life seizures in rats. Epilepsy Res. *85*, 221–230.

Karnam, H.B., Zhou, J.-L., Huang, L.-T., Zhao, Q., Shatskikh, T., and Holmes, G.L. (2009b). Early life seizures cause long-standing impairment of the hippocampal map. Exp. Neurol. *217*, 378–387.

Karoly, P.J., Nurse, E.S., Freestone, D.R., Ung, H., Cook, M.J., and Boston, R. (2017). Bursts of seizures in long-term recordings of human focal epilepsy. Epilepsia.

Kassaï, B., Chiron, C., Augier, S., Cucherat, M., Rey, E., Gueyffier, F., Guerrini, R., Vincent, J., Dulac, O., and Pons, G. (2008). Severe myoclonic epilepsy in infancy: a systematic review and a meta-analysis of individual patient data. Epilepsia *49*, 343–348.

Kelley, A.E. (2001). Measurement of rodent stereotyped behavior. Curr. Protoc. Neurosci. *Chapter 8*, Unit 8.8.

Kepecs, A., and Fishell, G. (2014). Interneuron Cell Types: Fit to form and formed to fit. Nature *505*, 318.

Kesner, R.P., and Churchwell, J.C. (2011). An analysis of rat prefrontal cortex in mediating executive function. Neurobiol. Learn. Mem. *96*, 417–431.

Kesner, R.P., and Rolls, E.T. (2015). A computational theory of hippocampal function, and tests of the theory: new developments. Neurosci. Biobehav. Rev. *48*, 92–147.

Kim, B.-S., Kim, M.-Y., and Leem, Y.-H. (2011). Hippocampal neuronal death induced by kainic acid and restraint stress is suppressed by exercise. Neuroscience *194*, 291–301.

Kim, J.H., Lee, D.W., Choi, B.Y., Sohn, M., Lee, S.H., Choi, H.C., Song, H.K., and Suh, S.W. (2015). Cytidine 5'-diphosphocholine (CDP-choline) adversely effects on pilocarpine seizure-induced hippocampal neuronal death. Brain Res *1595*, 156–165.

Klassen, T., Davis, C., Goldman, A., Burgess, D., Chen, T., Wheeler, D., McPherson, J., Bourquin, T., Lewis, L., Villasana, D., et al. (2011). Exome sequencing of ion channel genes reveals complex profiles confounding personal risk assessment in epilepsy. Cell *145*, 1036–1048.

Kleen, J.K., Sesqué, A., Wu, E.X., Miller, F.A., Hernan, A.E., Holmes, G.L., and Scott, R.C. (2011). Early-life seizures produce lasting alterations in the structure and function of the prefrontal cortex. Epilepsy Behav. EB *22*, 214–219.

Knowlton, B.J., Mangels, J.A., and Squire, L.R. (1996). A neostriatal habit learning system in humans. Science *273*, 1399–1402.

Kole, M.H.P., and Stuart, G.J. (2012). Signal processing in the axon initial segment. Neuron *73*, 235–247.

Korff, C., Laux, L., Kelley, K., Goldstein, J., Koh, S., and Nordli, D. (2007). Dravet syndrome (severe myoclonic epilepsy in infancy): a retrospective study of 16 patients. J. Child Neurol. *22*, 185–194.

Koyama, R., Tao, K., Sasaki, T., Ichikawa, J., Miyamoto, D., Muramatsu, R., Matsuki, N., and Ikegaya, Y. (2012). GABAergic excitation after febrile seizures induces ectopic granule cells and adult epilepsy. Nat. Med. *18*, 1271–1278.

Kwak, S.-E., Kim, J.-E., Kim, S.C., Kwon, O.-S., Choi, S.-Y., and Kang, T.-C. (2008). Hyperthermic seizure induces persistent alteration in excitability of the dentate gyrus in immature rats. Brain Res. *1216*, 1–15.

Lai, H.C., and Jan, L.Y. (2006). The distribution and targeting of neuronal voltage-gated ion channels. Nat. Rev. Neurosci. *7*, 548–562.

de Lanerolle, N.C., Kim, J.H., Robbins, R.J., and Spencer, D.D. (1989). Hippocampal interneuron loss and plasticity in human temporal lobe epilepsy. Brain Res. *495*, 387–395.

Lassalle, J.M., Bataille, T., and Halley, H. (2000). Reversible inactivation of the hippocampal mossy fiber synapses in mice impairs spatial learning, but neither consolidation nor memory retrieval, in the Morris navigation task. Neurobiol. Learn. Mem. *73*, 243–257.

Laux, L., and Blackford, R. (2013). The ketogenic diet in Dravet syndrome. J. Child Neurol. *28*, 1041–1044.

Lee, I., and Kesner, R.P. (2004). Encoding versus retrieval of spatial memory: double dissociation between the dentate gyrus and the perforant path inputs into CA3 in the dorsal hippocampus. Hippocampus *14*, 66–76.

Lee, Y.-J., Lee, J.S., Kang, H.-C., Kim, D.-S., Shim, K.-W., Eom, S., and Kim, H.D. (2014). Outcomes of epilepsy surgery in childhood-onset epileptic encephalopathy. Brain Dev. *36*, 496–504.

Lemmens, E.M.P., Aendekerk, B., Schijns, O.E.M.G., Blokland, A., Beuls, E.A.M., and Hoogland, G. (2009). Long-term behavioral outcome after early-life hyperthermia-induced seizures. Epilepsy Behav. EB *14*, 309–315.

Leo, D., and Gainetdinov, R.R. (2013). Transgenic mouse models for ADHD. Cell Tissue Res. *354*, 259–271.

Li, B.-M., Liu, X.-R., Yi, Y.-H., Deng, Y.-H., Su, T., Zou, X., and Liao, W.-P. (2011). Autism in Dravet syndrome: prevalence, features, and relationship to the clinical characteristics of epilepsy and mental retardation. Epilepsy Behav. EB *21*, 291–295.

Liautard, C., Scalmani, P., Carriero, G., de Curtis, M., Franceschetti, S., and Mantegazza, M. (2013). Hippocampal hyperexcitability and specific epileptiform activity in a mouse model of Dravet syndrome. Epilepsia *54*, 1251–1261.

Liu, Z., Gatt, A., Mikati, M., and Holmes, G.L. (1993). Effect of temperature on kainic acid-induced seizures. Brain Res. *631*, 51–58.

Liu, Z., Yang, Y., Silveira, D.C., Sarkisian, M.R., Tandon, P., Huang, L.T., Stafstrom, C.E., and Holmes, G.L. (1999). Consequences of recurrent seizures during early brain development. Neuroscience *92*, 1443–1454.

Lossin, C. (2009). A catalog of SCN1A variants. Brain Dev. *31*, 114–130.

Lothman, E.W., Stringer, J.L., and Bertram, E.H. (1992). The dentate gyrus as a control point for seizures in the hippocampus and beyond. Epilepsy Res. Suppl. *7*, 301–313.

Macrae, C.N., and Bodenhausen, G.V. (2000). Social cognition: thinking categorically about others. Annu. Rev. Psychol. *51*, 93–120.

Madroñal, N., Delgado-García, J.M., Fernández-Guizán, A., Chatterjee, J., Köhn, M., Mattucci, C., Jain, A., Tsetsenis, T., Illarionova, A., Grinevich, V., et al. (2016). Rapid erasure of hippocampal memory following inhibition of dentate gyrus granule cells. Nat. Commun. *7*.

Mahoney, K., Moore, S.J., Buckley, D., Alam, M., Parfrey, P., Penney, S., Merner, N., Hodgkinson, K., and Young, T.-L. (2009). Variable neurologic phenotype in a GEFS+ family with a novel mutation in SCN1A. Seizure *18*, 492–497.

Makinson, C.D., Dutt, K., Lin, F., Papale, L.A., Shankar, A., Barela, A.J., Liu, R., Goldin, A.L., and Escayg, A. (2016). An Scn1a epilepsy mutation in Scn8a alters seizure susceptibility and behavior. Exp. Neurol. *275 Pt 1*, 46–58.

Malcolmson, J., Kleyner, R., Tegay, D., Adams, W., Ward, K., Coppinger, J., Nelson, L., Meisler, M.H., Wang, K., Robison, R., et al. (2016). SCN8A mutation in a child presenting with seizures and developmental delays. Cold Spring Harb. Mol. Case Stud. *2*.

Mantegazza, M., and Catterall, W.A. (2012). Voltage-Gated Na+ Channels: Structure, Function, and Pathophysiology. In Jasper's Basic Mechanisms of the Epilepsies, J.L. Noebels, M. Avoli, M.A. Rogawski, R.W. Olsen, and A.V. Delgado-Escueta, eds. (Bethesda (MD)), p.

Mantegazza, M., Gambardella, A., Rusconi, R., Schiavon, E., Annesi, F., Cassulini, R.R., Labate, A., Carrideo, S., Chifari, R., Canevini, M.P., et al. (2005). Identification of an Nav1.1 sodium channel (SCN1A) loss-of-function mutation associated with familial simple febrile seizures. Proc. Natl. Acad. Sci. U. S. A. *102*, 18177–18182.

Marini, C., Mei, D., Helen Cross, J., and Guerrini, R. (2006). Mosaic SCN1A mutation in familial severe myoclonic epilepsy of infancy. Epilepsia *47*, 1737–1740.

Marini, C., Scheffer, I.E., Nabbout, R., Mei, D., Cox, K., Dibbens, L.M., McMahon, J.M., Iona, X., Carpintero, R.S., Elia, M., et al. (2009). SCN1A duplications and deletions detected in Dravet syndrome: implications for molecular diagnosis. Epilepsia *50*, 1670–1678.

Martin, M.S., Tang, B., Papale, L.A., Yu, F.H., Catterall, W.A., and Escayg, A. (2007). The voltage-gated sodium channel Scn8a is a genetic modifier of severe myoclonic epilepsy of infancy. Hum. Mol. Genet. *16*, 2892–2899.

Martin, M.S., Dutt, K., Papale, L.A., Dubé, C.M., Dutton, S.B., de Haan, G., Shankar, A., Tufik, S., Meisler, M.H., Baram, T.Z., et al. (2010a). Altered function of the SCN1A voltage-gated sodium channel leads to gamma-aminobutyric acid-ergic (GABAergic) interneuron abnormalities. J. Biol. Chem. *285*, 9823–9834.

Martin, M.S., Dutt, K., Papale, L.A., Dubé, C.M., Dutton, S.B., de Haan, G., Shankar, A., Tufik, S., Meisler, M.H., Baram, T.Z., et al. (2010b). Altered function of the SCN1A voltage-gated sodium channel leads to gamma-aminobutyric acid-ergic (GABAergic) interneuron abnormalities. J. Biol. Chem. *285*, 9823–9834.

Mashimo, T., Ohmori, I., Ouchida, M., Ohno, Y., Tsurumi, T., Miki, T., Wakamori, M., Ishihara, S., Yoshida, T., Takizawa, A., et al. (2010). A missense mutation of the gene encoding voltage-dependent sodium channel (Nav1.1) confers susceptibility to febrile seizures in rats. J. Neurosci. Off. J. Soc. Neurosci. *30*, 5744–5753.

Matsuzaka, T., Baba, H., Matsuo, A., Tsuru, A., Moriuchi, H., Tanaka, S., and Kawasaki, C. (2001). Developmental assessment-based surgical intervention for intractable epilepsies in infants and young children. Epilepsia *42 Suppl 6*, 9–12.

McCabe, B.K., Silveira, D.C., Cilio, M.R., Cha, B.H., Liu, X., Sogawa, Y., and Holmes, G.L. (2001). Reduced neurogenesis after neonatal seizures. J. Neurosci. Off. J. Soc. Neurosci. *21*, 2094–2103.

McClelland, S., Dubé, C.M., Yang, J., and Baram, T.Z. (2011). Epileptogenesis after prolonged febrile seizures: mechanisms, biomarkers and therapeutic opportunities. Neurosci. Lett. *497*, 155–162.

Mcilvoy, L.H. (2005). The effect of hypothermia and hyperthermia on acute brain injury. AACN Clin. Issues *16*, 488–500.

Meisler, M.H., and Kearney, J.A. (2005). Sodium channel mutations in epilepsy and other neurological disorders. J. Clin. Invest. *115*, 2010.

Meisler, M.H., Kearney, J., Escayg, A., MacDonald, B.T., and Sprunger, L.K. (2001). Sodium channels and neurological disease: insights from Scn8a mutations in the mouse. Neurosci. Rev. J. Bringing Neurobiol. Neurol. Psychiatry *7*, 136–145.

Messner, D.J., and Catterall, W.A. (1985). The sodium channel from rat brain. Separation and characterization of subunits. J. Biol. Chem. *260*, 10597–10604.

Miller, A.R., Hawkins, N.A., McCollom, C.E., and Kearney, J.A. (2014). Mapping genetic modifiers of survival in a mouse model of Dravet syndrome. Genes Brain Behav. *13*, 163–172.

Misra, S.N., Kahlig, K.M., and George, A.L. (2008). Impaired NaV1.2 Function and Reduced Cell Surface Expression in Benign Familial Neonatal-Infantile Seizures. Epilepsia *49*, 1535–1545.

Mistry, A.M., Thompson, C.H., Miller, A.R., Vanoye, C.G., George, A.L., and Kearney, J.A. (2014). Strain- and Age-dependent Hippocampal Neuron Sodium Currents Correlate with Epilepsy Severity in Dravet Syndrome Mice. Neurobiol. Dis. *65*, 1–11.

Mitchell, J.P., Macrae, C.N., and Banaji, M.R. (2006). Dissociable medial prefrontal contributions to judgments of similar and dissimilar others. Neuron *50*, 655–663.

Mlsna, L.M., and Koh, S. (2013). Maturation-dependent behavioral deficits and cell injury in developing animals during the subacute postictal period. Epilepsy Behav. EB *29*, 190–197.

Morgan, K., Stevens, E.B., Shah, B., Cox, P.J., Dixon, A.K., Lee, K., Pinnock, R.D., Hughes, J., Richardson, P.J., Mizuguchi, K., et al. (2000). beta 3: an additional auxiliary subunit of the voltage-sensitive sodium channel that modulates channel gating with distinct kinetics. Proc. Natl. Acad. Sci. U. S. A. *97*, 2308–2313.

Morice, E., Farley, S., Poirier, R., Dallerac, G., Chagneau, C., Pannetier, S., Hanauer, A., Davis, S., Vaillend, C., and Laroche, S. (2013). Defective synaptic transmission and structure in the dentate gyrus and selective fear memory impairment in the Rsk2 mutant mouse model of Coffin-Lowry syndrome. Neurobiol. Dis. *58*, 156–168.

Moroni, R.F., Inverardi, F., Regondi, M.C., Panzica, F., Spreafico, R., and Frassoni, C. (2008). Altered spatial distribution of PV-cortical cells and dysmorphic neurons in the somatosensory cortex of BCNU-treated rat model of cortical dysplasia. Epilepsia *49*, 872–887.

Morris, R.G., Anderson, E., Lynch, G.S., and Baudry, M. (1986). Selective impairment of learning and blockade of long-term potentiation by an N-methyl-D-aspartate receptor antagonist, AP5. Nature *319*, 774–776.

Mula, M., and Sander, J.W. (2016). Psychosocial aspects of epilepsy: a wider approach. BJPsych Open *2*, 270–274.

Mulley, J.C., Scheffer, I.E., Petrou, S., Dibbens, L.M., Berkovic, S.F., and Harkin, L.A. (2005). SCN1A mutations and epilepsy. Hum. Mutat. *25*, 535–542.

Myers, K.A., Burgess, R., Afawi, Z., Damiano, J.A., Berkovic, S.F., Hildebrand, M.S., and Scheffer, I.E. (2017). De novo SCN1A pathogenic variants in the GEFS+ spectrum: Not always a familial syndrome. Epilepsia.

Nabbout, R., Gennaro, E., Dalla Bernardina, B., Dulac, O., Madia, F., Bertini, E., Capovilla, G., Chiron, C., Cristofori, G., Elia, M., et al. (2003). Spectrum of SCN1A mutations in severe myoclonic epilepsy of infancy. Neurology *60*, 1961–1967.

Nabbout, R., Copioli, C., Chipaux, M., Chemaly, N., Desguerre, I., Dulac, O., and Chiron, C. (2011). Ketogenic diet also benefits Dravet syndrome patients receiving stiripentol: a prospective pilot study. Epilepsia *52*, e54-57.

Nabbout, R., Chemaly, N., Chipaux, M., Barcia, G., Bouis, C., Dubouch, C., Leunen, D., Jambaqué, I., Dulac, O., Dellatolas, G., et al. (2013). Encephalopathy in children with Dravet syndrome is not a pure consequence of epilepsy. Orphanet J. Rare Dis. *8*, 176.

Nagao, S., and Kitazawa, H. (2008). [Role of the cerebellum in the acquisition and consolidation of motor memory]. Brain Nerve Shinkei Kenkyu No Shinpo *60*, 783–790.

Nashef, L. (1997). Sudden unexpected death in epilepsy: terminology and definitions. Epilepsia *38*, S6-8.

Neill, J.C., Liu, Z., Sarkisian, M., Tandon, P., Yang, Y., Stafstrom, C.E., and Holmes, G.L. (1996). Recurrent seizures in immature rats: effect on auditory and visual discrimination. Brain Res. Dev. Brain Res. *95*, 283–292.

Neves, G., Cooke, S.F., and Bliss, T.V.P. (2008). Synaptic plasticity, memory and the hippocampus: a neural network approach to causality. Nat. Rev. Neurosci. *9*, 65–75.

Nieto-Barrera, M., Lillo, M.M., Rodríguez-Collado, C., Candau, R., and Correa, A. (2000). [Severe myoclonic epilepsy in childhood. Epidemiologic analytical study]. Rev. Neurol. *30*, 620–624.

Nishimura, M., Gu, X., and Swann, J.W. (2011). Seizures in early life suppress hippocampal dendrite growth while impairing spatial learning. Neurobiol. Dis. *44*, 205–214.

Notenboom, R.G.E., Ramakers, G.M.J., Kamal, A., Spruijt, B.M., and de Graan, P.N.E. (2010). Long-lasting modulation of synaptic plasticity in rat hippocampus after early-life complex febrile seizures. Eur. J. Neurosci. *32*, 749–758.

Oakley, J.C., Kalume, F., Yu, F.H., Scheuer, T., and Catterall, W.A. (2009a). Temperature- and age-dependent seizures in a mouse model of severe myoclonic epilepsy in infancy. Proc. Natl. Acad. Sci. U. S. A. *106*, 3994–3999.

Oakley, J.C., Kalume, F., Yu, F.H., Scheuer, T., and Catterall, W.A. (2009b). Temperature- and age-dependent seizures in a mouse model of severe myoclonic epilepsy in infancy. Proc. Natl. Acad. Sci. U. S. A. *106*, 3994–3999.

O'Connell, B.K., Gloss, D., and Devinsk, O. (2017). Cannabinoids in treatment-resistant epilepsy: A review. Epilepsy Behav. EB.

Ogino, T., Ohtsuka, Y., Yamatogi, Y., Oka, E., and Ohtahara, S. (1989). The epileptic syndrome sharing common characteristics during early childhood with severe myoclonic epilepsy in infancy. Jpn. J. Psychiatry Neurol. *43*, 479–481.

Ogiwara, I., Miyamoto, H., Morita, N., Atapour, N., Mazaki, E., Inoue, I., Takeuchi, T., Itohara, S., Yanagawa, Y., Obata, K., et al. (2007). Nav1.1 localizes to axons of parvalbumin-positive inhibitory interneurons: a circuit basis for epileptic seizures in mice carrying an Scn1a gene mutation. J. Neurosci. Off. J. Soc. Neurosci. *27*, 5903–5914.

Ogiwara, I., Ito, K., Sawaishi, Y., Osaka, H., Mazaki, E., Inoue, I., Montal, M., Hashikawa, T., Shike, T., Fujiwara, T., et al. (2009). De novo mutations of voltage-gated sodium channel αII gene SCN2A in intractable epilepsies. Neurology *73*, 1046–1053.

Ogiwara, I., Iwasato, T., Miyamoto, H., Iwata, R., Yamagata, T., Mazaki, E., Yanagawa, Y., Tamamaki, N., Hensch, T.K., Itohara, S., et al. (2013). Nav1.1 haploinsufficiency in excitatory neurons ameliorates seizure-associated sudden death in a mouse model of Dravet syndrome. Hum. Mol. Genet. *22*, 4784–4804.

Oguni, H., Hayashi, K., Awaya, Y., Fukuyama, Y., and Osawa, M. (2001). Severe myoclonic epilepsy in infants--a review based on the Tokyo Women's Medical University series of 84 cases. Brain Dev. *23*, 736–748.

Ohmori, I., Ouchida, M., Miki, T., Mimaki, N., Kiyonaka, S., Nishiki, T., Tomizawa, K., Mori, Y., and Matsui, H. (2008). A CACNB4 mutation shows that altered Ca(v)2.1 function may be a genetic modifier of severe myoclonic epilepsy in infancy. Neurobiol. Dis. *32*, 349–354.

Ohmori, I., Ouchida, M., Kobayashi, K., Jitsumori, Y., Mori, A., Michiue, H., Nishiki, T., Ohtsuka, Y., and Matsui, H. (2013). CACNA1A variants may modify the epileptic phenotype of Dravet syndrome. Neurobiol. Dis. *50*, 209–217.

Ohmori, I., Kawakami, N., Liu, S., Wang, H., Miyazaki, I., Asanuma, M., Michiue, H., Matsui, H., Mashimo, T., and Ouchida, M. (2014). Methylphenidate improves learning impairments and hyperthermia-induced seizures caused by an Scn1a mutation. Epilepsia *55*, 1558–1567.

Ohno, Y., Ishihara, S., Mashimo, T., Sofue, N., Shimizu, S., Imaoku, T., Tsurumi, T., Sasa, M., and Serikawa, T. (2011). Scn1a missense mutation causes limbic hyperexcitability and vulnerability to experimental febrile seizures. Neurobiol. Dis. *41*, 261–269.

O'Keefe, J., Burgess, N., Donnett, J.G., Jeffery, K.J., and Maguire, E.A. (1998). Place cells, navigational accuracy, and the human hippocampus. Philos. Trans. R. Soc. Lond. B. Biol. Sci. *353*, 1333–1340.

Olivieri, G., Battaglia, D., Chieffo, D., Rubbino, R., Ranalli, D., Contaldo, I., Dravet, C., Mercuri, E., and Guzzetta, F. (2016). Cognitive-behavioral profiles in teenagers with Dravet syndrome. Brain Dev.

Olton, D.S., and Samuelson, R.J. (1976). Remembrance of places passed: Spatial memory in rats. J. Exp. Psychol. Anim. Behav. Process. *2*, 97–116.

Osaka, H., Ogiwara, I., Mazaki, E., Okamura, N., Yamashita, S., Iai, M., Yamada, M., Kurosawa, K., Iwamoto, H., Yasui-Furukori, N., et al. (2007). Patients with a sodium channel alpha 1 gene mutation show wide phenotypic variation. Epilepsy Res. *75*, 46–51.

Papale, L.A., Makinson, C.D., Christopher Ehlen, J., Tufik, S., Decker, M.J., Paul, K.N., and Escayg, A. (2013). Altered sleep regulation in a mouse model of SCN1A-derived genetic epilepsy with febrile seizures plus (GEFS+). Epilepsia *54*, 625–634.

Parihar, R., and Ganesh, S. (2013). The SCN1A gene variants and epileptic encephalopathies. J. Hum. Genet. *58*, 573–580.

Passamonti, C., Petrelli, C., Mei, D., Foschi, N., Guerrini, R., Provinciali, L., and Zamponi, N. (2015). A novel inherited SCN1A mutation associated with different neuropsychological phenotypes: is there a common core deficit? Epilepsy Behav. EB *43*, 89–92.

Pathak, H.R., Weissinger, F., Terunuma, M., Carlson, G.C., Hsu, F.-C., Moss, S.J., and Coulter, D.A. (2007). Disrupted dentate granule cell chloride regulation enhances synaptic excitability during development of temporal lobe epilepsy. J. Neurosci. Off. J. Soc. Neurosci. *27*, 14012–14022.

Petilla Interneuron Nomenclature Group, Ascoli, G.A., Alonso-Nanclares, L., Anderson, S.A., Barrionuevo, G., Benavides-Piccione, R., Burkhalter, A., Buzsáki, G., Cauli, B., Defelipe, J., et al. (2008). Petilla terminology: nomenclature of features of GABAergic interneurons of the cerebral cortex. Nat. Rev. Neurosci. *9*, 557–568.

Phillips, R.G., and LeDoux, J.E. (1992). Differential contribution of amygdala and hippocampus to cued and contextual fear conditioning. Behav. Neurosci. *106*, 274–285.

Pineda-Trujillo, N., Carrizosa, J., Cornejo, W., Arias, W., Franco, C., Cabrera, D., Bedoya, G., and Ruíz-Linares, A. (2005). A novel SCN1A mutation associated with severe GEFS+ in a large South American pedigree. Seizure *14*, 123–128.

Porter, R. (2003). Madness: A Brief History (Oxford, New York: Oxford University Press).

Press, C.A., Knupp, K.G., and Chapman, K.E. (2015). Parental reporting of response to oral cannabis extracts for treatment of refractory epilepsy. Epilepsy Behav. EB *45*, 49–52.

Prut, L., and Belzung, C. (2003). The open field as a paradigm to measure the effects of drugs on anxiety-like behaviors: a review. Eur. J. Pharmacol. *463*, 3–33.

Purcell, R.H., Papale, L.A., Makinson, C.D., Sawyer, N.T., Schroeder, J.P., Escayg, A., and Weinshenker, D. (2013). Effects of an epilepsy-causing mutation in the SCN1A sodium channel gene on cocaine-induced seizure susceptibility in mice. Psychopharmacology (Berl.) *228*, 263–270.

Quinn, R. (2005). Comparing rat's to human's age: how old is my rat in people years? Nutr. Burbank Los Angel. Cty. Calif *21*, 775–777.

Ragona, F., Brazzo, D., De Giorgi, I., Morbi, M., Freri, E., Teutonico, F., Gennaro, E., Zara, F., Binelli, S., Veggiotti, P., et al. (2010). Dravet syndrome: early clinical manifestations and cognitive outcome in 37 Italian patients. Brain Dev. *32*, 71–77.

Ragona, F., Granata, T., Dalla Bernardina, B., Offredi, F., Darra, F., Battaglia, D., Morbi, M., Brazzo, D., Cappelletti, S., Chieffo, D., et al. (2011a). Cognitive development in Dravet syndrome: a retrospective, multicenter study of 26 patients. Epilepsia *52*, 386–392.

Ragona, F., Granata, T., Dalla Bernardina, B., Offredi, F., Darra, F., Battaglia, D., Morbi, M., Brazzo, D., Cappelletti, S., Chieffo, D., et al. (2011b). Cognitive development in Dravet syndrome: a retrospective, multicenter study of 26 patients. Epilepsia *52*, 386–392.

Rajab, E., Abdeen, Z., Hassan, Z., Alsaffar, Y., Mandeel, M., Al Shawaaf, F., Al-Ansari, S., and Kamal, A. (2014). Cognitive performance and convulsion risk after experimentally-induced febrile-seizures in rat. Int. J. Dev. Neurosci. Off. J. Int. Soc. Dev. Neurosci. *34*, 19–23.

Reilly, C., Atkinson, P., Das, K.B., Chin, R.F.M., Aylett, S.E., Burch, V., Gillberg, C., Scott, R.C., and Neville, B.G.R. (2015). Cognition in school-aged children with "active" epilepsy: A population-based study. J. Clin. Exp. Neuropsychol. *37*, 429–438.

Reynolds, E.H. (2002). Introduction: epilepsy in the world. Epilepsia *43 Suppl 6*, 1–3.

Ricci, D., Chieffo, D., Battaglia, D., Brogna, C., Contaldo, I., De Clemente, V., Losito, E., Dravet, C., Mercuri, E., and Guzzetta, F. (2015). A prospective longitudinal study on visuo-cognitive development in Dravet syndrome: Is there a "dorsal stream vulnerability"? Epilepsy Res *109*, 57–64.

Richmond, C.A. (2003). The role of arginine vasopressin in thermoregulation during fever. J. Neurosci. Nurs. J. Am. Assoc. Neurosci. Nurses *35*, 281–286.

Rilstone, J.J., Coelho, F.M., Minassian, B.A., and Andrade, D.M. (2012). Dravet syndrome: seizure control and gait in adults with different SCN1A mutations. Epilepsia *53*, 1421–1428.

Riva, D., Vago, C., Pantaleoni, C., Bulgheroni, S., Mantegazza, M., and Franceschetti, S. (2009). Progressive neurocognitive decline in two children with Dravet syndrome, de novo SCN1A truncations and different epileptic phenotypes. Am. J. Med. Genet. A. *149A*, 2339–2345.

Romijn, H.J., Hofman, M.A., and Gramsbergen, A. (1991). At what age is the developing cerebral cortex of the rat comparable to that of the full-term newborn human baby? Early Hum. Dev. *26*, 61–67.

Rubinstein, M., Westenbroek, R.E., Yu, F.H., Jones, C.J., Scheuer, T., and Catterall, W.A. (2015a). Genetic background modulates impaired excitability of inhibitory neurons in a mouse model of Dravet syndrome. Neurobiol. Dis. *73*, 106–117.

Rubinstein, M., Han, S., Tai, C., Westenbroek, R.E., Hunker, A., Scheuer, T., and Catterall, W.A. (2015b). Dissecting the phenotypes of Dravet syndrome by gene deletion. Brain J. Neurol. *138*, 2219–2233.

Rubinstein, M., Westenbroek, R.E., Yu, F.H., Jones, C.J., Scheuer, T., and Catterall, W.A. (2015c). Genetic background modulates impaired excitability of inhibitory neurons in a mouse model of Dravet syndrome. Neurobiol. Dis. *73*, 106–117.

Rubinstein, M., Westenbroek, R.E., Yu, F.H., Jones, C.J., Scheuer, T., and Catterall, W.A. (2015d). Genetic background modulates impaired excitability of inhibitory neurons in a mouse model of Dravet syndrome. Neurobiol. Dis. *73*, 106–117.

Rusconi, R., Scalmani, P., Cassulini, R.R., Giunti, G., Gambardella, A., Franceschetti, S., Annesi, G., Wanke, E., and Mantegazza, M. (2007). Modulatory proteins can rescue a trafficking defective epileptogenic Nav1.1 Na+ channel mutant. J. Neurosci. Off. J. Soc. Neurosci. *27*, 11037–11046.

Rusconi, R., Combi, R., Cestèle, S., Grioni, D., Franceschetti, S., Dalprà, L., and Mantegazza, M. (2009). A rescuable folding defective Nav1.1 (SCN1A) sodium channel mutant causes GEFS+: common mechanism in Nav1.1 related epilepsies? Hum. Mutat. *30*, E747-760.

Sankar, R., and Mazarati, A. (2012). Neurobiology of Depression as a Comorbidity of Epilepsy. In Jasper's Basic Mechanisms of the Epilepsies, J.L. Noebels, M. Avoli, M.A. Rogawski, R.W. Olsen, and A.V. Delgado-Escueta, eds. (Bethesda (MD): National Center for Biotechnology Information (US)), p.

Sawyer, N.T., Helvig, A.W., Makinson, C.D., Decker, M.J., Neigh, G.N., and Escayg, A. (2016). Scn1a dysfunction alters behavior but not the effect of stress on seizure response. Genes Brain Behav. *15*, 335–347.

Schaeffel, F. (2008). Test systems for measuring ocular parameters and visual function in mice. Front. Biosci. J. Virtual Libr. *13*, 4904–4911.

Scheffer, I.E. (2015). Vaccination Triggers, Rather Than Causes, Seizures. Epilepsy Curr. *15*, 335–337.

Scheffer, I.E., and Berkovic, S.F. (1997). Generalized epilepsy with febrile seizures plus. A genetic disorder with heterogeneous clinical phenotypes. Brain J. Neurol. *120 (Pt 3)*, 479–490.

Scheffer, I.E., Wallace, R., Mulley, J.C., and Berkovic, S.F. (2001). Clinical and molecular genetics of myoclonic-astatic epilepsy and severe myoclonic epilepsy in infancy (Dravet syndrome). Brain Dev. *23*, 732–735.

Scheffer, I.E., French, J., Hirsch, E., Jain, S., Mathern, G.W., Moshé, S.L., Perucca, E., Tomson, T., Wiebe, S., Zhang, Y.-H., et al. (2016). Classification of the epilepsies: New concepts for discussion and debate—Special report of the ILAE Classification Task Force of the Commission for Classification and Terminology. Epilepsia Open *1*, 37–44.

Schoonjans, A., Paelinck, B.P., Marchau, F., Gunning, B., Gammaitoni, A., Galer, B.S., Lagae, L., and Ceulemans, B. (2017). Low-dose fenfluramine significantly reduces seizure frequency in Dravet syndrome: a prospective study of a new cohort of patients. Eur. J. Neurol. *24*, 309–314.

Schuchmann, S., Schmitz, D., Rivera, C., Vanhatalo, S., Salmen, B., Mackie, K., Sipilä, S.T., Voipio, J., and Kaila, K. (2006). Experimental febrile seizures are precipitated by a hyperthermia-induced respiratory alkalosis. Nat. Med. *12*, 817–823.

Schuchmann, S., Hauck, S., Henning, S., Grüters-Kieslich, A., Vanhatalo, S., Schmitz, D., and Kaila, K. (2011). Respiratory alkalosis in children with febrile seizures. Epilepsia *52*, 1949–1955.

Scoville, W.B., and Milner, B. (1957). Loss of recent memory after bilateral hippocampal lesions. J. Neurol. Neurosurg. Psychiatry *20*, 11–21.

Shinnar, S., and Pellock, J.M. (2002). Update on the epidemiology and prognosis of pediatric epilepsy. J. Child Neurol. *17 Suppl 1*, S4-17.

Sillanpää, M., Suominen, S., Rautava, P., and Aromaa, M. (2011). Academic and social success in adolescents with previous febrile seizures. Seizure *20*, 326–330.

Singh, N.A., Pappas, C., Dahle, E.J., Claes, L.R.F., Pruess, T.H., De Jonghe, P., Thompson, J., Dixon, M., Gurnett, C., Peiffer, A., et al. (2009). A role of SCN9A in human epilepsies, as a cause of febrile seizures and as a potential modifier of Dravet syndrome. PLoS Genet. *5*, e1000649.

Singh, R., Scheffer, I.E., Crossland, K., and Berkovic, S.F. (1999). Generalized epilepsy with febrile seizures plus: a common childhood-onset genetic epilepsy syndrome. Ann. Neurol. *45*, 75–81.

Singh, R., Andermann, E., Whitehouse, W.P., Harvey, A.S., Keene, D.L., Seni, M.H., Crossland, K.M., Andermann, F., Berkovic, S.F., and Scheffer, I.E. (2001). Severe myoclonic epilepsy of infancy: extended spectrum of GEFS+? Epilepsia *42*, 837–844.

Sowers, L.P., Massey, C.A., Gehlbach, B.K., Granner, M.A., and Richerson, G.B. (2013). Sudden unexpected death in epilepsy: fatal post-ictal respiratory and arousal mechanisms. Respir. Physiol. Neurobiol. *189*, 315–323.

Sperber, E.F., Haas, K.Z., Stanton, P.K., and Moshé, S.L. (1991). Resistance of the immature hippocampus to seizure-induced synaptic reorganization. Brain Res. Dev. Brain Res. *60*, 88–93.

Squire, L.R. (1992). Memory and the hippocampus: a synthesis from findings with rats, monkeys, and humans. Psychol. Rev. *99*, 195–231.

Squire, L.R., and Knowlton, B.J. (1995). Learning about categories in the absence of memory. Proc. Natl. Acad. Sci. U. S. A. *92*, 12470–12474.

Stafstrom, C.E., Thompson, J.L., and Holmes, G.L. (1992). Kainic acid seizures in the developing brain: status epilepticus and spontaneous recurrent seizures. Brain Res. Dev. Brain Res. *65*, 227–236.

Stafstrom, C.E., Chronopoulos, A., Thurber, S., Thompson, J.L., and Holmes, G.L. (1993). Age-dependent cognitive and behavioral deficits after kainic acid seizures. Epilepsia *34*, 420–432.

Subash, M., Sheth, H.G., Saihan, Z., and Plant, G.T. (2010). Transient visual loss after seizures. Clin. Experiment. Ophthalmol. *38*, 734–735.

Sugawara, T., Mazaki–Miyazaki, E., Ito, M., Nagafuji, H., Fukuma, G., Mitsudome, A., Wada, K., Kaneko, S., Hirose, S., and Yamakawa, K. (2001). Nav1.1 mutations cause febrile seizures associated with afebrile partial seizures. Neurology *57*, 703–705.

Sugawara, T., Mazaki-Miyazaki, E., Fukushima, K., Shimomura, J., Fujiwara, T., Hamano, S., Inoue, Y., and Yamakawa, K. (2002). Frequent mutations of SCN1A in severe myoclonic epilepsy in infancy. Neurology *58*, 1122–1124.

Suls, A., Velizarova, R., Yordanova, I., Deprez, L., Van Dyck, T., Wauters, J., Guergueltcheva, V., Claes, L.R.F., Kremensky, I., Jordanova, A., et al. (2010). Four generations of epilepsy caused by an inherited microdeletion of the SCN1A gene. Neurology *75*, 72–76.

Sundberg, K.A., Mitchell, J.F., Gawne, T.J., and Reynolds, J.H. (2012). Attention influences single unit and local field potential response latencies in visual cortical area V4. J. Neurosci. Off. J. Soc. Neurosci. *32*, 16040–16050.

Swijsen, A., Avila, A., Brône, B., Janssen, D., Hoogland, G., and Rigo, J.-M. (2012). Experimental early-life febrile seizures induce changes in GABA(A) R-mediated neurotransmission in the dentate gyrus. Epilepsia *53*, 1968–1977.

Tai, C., Abe, Y., Westenbroek, R.E., Scheuer, T., and Catterall, W.A. (2014). Impaired excitability of somatostatin- and parvalbumin-expressing cortical interneurons in a mouse model of Dravet syndrome. Proc. Natl. Acad. Sci. U. S. A. *111*, E3139-3148.

Takaori, T., Kumakura, A., Ishii, A., Hirose, S., and Hata, D. (2017). Two mild cases of Dravet syndrome with truncating mutation of SCN1A. Brain Dev. *39*, 72–74.

Takayama, R., Fujiwara, T., Shigematsu, H., Imai, K., Takahashi, Y., Yamakawa, K., and Inoue, Y. (2014). Long-term course of Dravet syndrome: a study from an epilepsy center in Japan. Epilepsia *55*, 528–538.

Tao, K., Ichikawa, J., Matsuki, N., Ikegaya, Y., and Koyama, R. (2016). Experimental febrile seizures induce age-dependent structural plasticity and improve memory in mice. Neuroscience *318*, 34–44.

Thomas, E.A., Hawkins, R.J., Richards, K.L., Xu, R., Gazina, E.V., and Petrou, S. (2009). Heat opens axon initial segment sodium channels: a febrile seizure mechanism? Ann. Neurol. *66*, 219–226.

Thurman, D.J., Beghi, E., Begley, C.E., Berg, A.T., Buchhalter, J.R., Ding, D., Hesdorffer, D.C., Hauser, W.A., Kazis, L., Kobau, R., et al. (2011). Standards for epidemiologic studies and surveillance of epilepsy. Epilepsia *52 Suppl 7*, 2–26.

Treves, A., Tashiro, A., Witter, M.P., and Moser, E.I. (2008). What is the mammalian dentate gyrus good for? Neuroscience *154*, 1155–1172.

Tsai, M.-S., Lee, M.-L., Chang, C.-Y., Fan, H.-H., Yu, I.-S., Chen, Y.-T., You, J.-Y., Chen, C.-Y., Chang, F.-C., Hsiao, J.H., et al. (2015). Functional and structural deficits of the dentate gyrus network coincide with emerging spontaneous seizures in an Scn1a mutant Dravet Syndrome model during development. Neurobiol. Dis. *77*, 35–48.

Tse, D., Takeuchi, T., Kakeyama, M., Kajii, Y., Okuno, H., Tohyama, C., Bito, H., and Morris, R.G.M. (2011). Schema-dependent gene activation and memory encoding in neocortex. Science *333*, 891–895.

Tulving, E. (2002). Episodic memory: from mind to brain. Annu. Rev. Psychol. *53*, 1–25.

Tuncer, F.N., Gormez, Z., Calik, M., Altiokka Uzun, G., Sagiroglu, M.S., Yuceturk, B., Yuksel, B., Baykan, B., Bebek, N., Iscan, A., et al. (2015). A clinical variant in SCN1A inherited from a mosaic father cosegregates with a novel variant to cause Dravet syndrome in a consanguineous family. Epilepsy Res. *113*, 5–10.

Vanoye, C.G., Gurnett, C.A., Holland, K.D., George, A.L., and Kearney, J.A. (2014). Novel SCN3A Variants Associated with Focal Epilepsy in Children. Neurobiol. Dis. *62*.

Veggiotti, P., Cardinali, S., Montalenti, E., Gatti, A., and Lanzi, G. (2001). Generalized epilepsy with febrile seizures plus and severe myoclonic epilepsy in infancy: a case report of two Italian families. Epileptic Disord. Int. Epilepsy J. Videotape *3*, 29–32.

Velíšková, J., Miller, A.M., Nunes, M.L., and Brown, L.L. (2005). Regional neural activity within the substantia nigra during peri-ictal flurothyl generalized seizure stages. Neurobiol. Dis. *20*, 752–759.

Vestergaard, M., and Christensen, J. (2009). Register-based studies on febrile seizures in Denmark. Brain Dev. *31*, 372–377.

Villeneuve, N., Laguitton, V., Viellard, M., Lepine, A., Chabrol, B., Dravet, C., and Milh, M. (2014). Cognitive and adaptive evaluation of 21 consecutive patients with Dravet syndrome. Epilepsy Behav *31*, 143–148.

Volkers, L., Kahlig, K.M., Verbeek, N.E., Das, J.H.G., van Kempen, M.J.A., Stroink, H., Augustijn, P., van Nieuwenhuizen, O., Lindhout, D., George, A.L., et al. (2011). Nav 1.1 dysfunction in genetic epilepsy with febrile seizures-plus or Dravet syndrome. Eur. J. Neurosci. *34*, 1268–1275.

Voronin, L.L. (1982). [Prolonged post-tetanic potentiation in hippocampus]. Usp. Fiziol. Nauk *13*, 45–73.

Wallace, R.H., Wang, D.W., Singh, R., Scheffer, I.E., George, A.L., Phillips, H.A., Saar, K., Reis, A., Johnson, E.W., Sutherland, G.R., et al. (1998). Febrile seizures and generalized epilepsy associated with a mutation in the Na+-channel beta1 subunit gene SCN1B. Nat. Genet. *19*, 366–370.

Wallace, R.H., Hodgson, B.L., Grinton, B.E., Gardiner, R.M., Robinson, R., Rodriguez-Casero, V., Sadleir, L., Morgan, J., Harkin, L.A., Dibbens, L.M., et al. (2003). Sodium channel alpha1-subunit mutations in severe myoclonic epilepsy of infancy and infantile spasms. Neurology *61*, 765–769.

Wang, C., Xie, N., Wang, Y., Li, Y., Ge, X., and Wang, M. (2015). Role of the Mitochondrial Calcium Uniporter in Rat Hippocampal Neuronal Death After Pilocarpine-Induced Status Epilepticus. Neurochem. Res. *40*, 1739–1746.

Wang, P.J., Fan, P.C., Lee, W.T., Young, C., Huang, C.C., and Shen, Y.Z. (1996). Severe myoclonic epilepsy in infancy: evolution of electroencephalographic and clinical features. Zhonghua Minguo Xiao Er Ke Yi Xue Hui Za Zhi J. Zhonghua Minguo Xiao Er Ke Yi Xue Hui *37*, 428–432.

Wang, S.S.-H., Kloth, A.D., and Badura, A. (2014). The cerebellum, sensitive periods, and autism. Neuron *83*, 518–532.

Wei, S.-H., and Lee, W.-T. (2015). Comorbidity of childhood epilepsy. J. Formos. Med. Assoc. Taiwan Yi Zhi *114*, 1031–1038.

Westenbroek, R.E., Merrick, D.K., and Catterall, W.A. (1989). Differential subcellular localization of the RI and RII Na+ channel subtypes in central neurons. Neuron *3*, 695–704.

Whelan, H., Harmelink, M., Chou, E., Sallowm, D., Khan, N., Patil, R., Sannagowdara, K., Kim, J.H., Chen, W.L., Khalil, S., et al. (2017). Complex febrile seizures-A systematic review. Dis.--Mon. DM.

Whitaker, W.R., Faull, R.L., Waldvogel, H.J., Plumpton, C.J., Emson, P.C., and Clare, J.J. (2001). Comparative distribution of voltage-gated sodium channel proteins in human brain. Brain Res. Mol. Brain Res. *88*, 37–53.

Whitlock, J.R., Heynen, A.J., Shuler, M.G., and Bear, M.F. (2006). Learning induces long-term potentiation in the hippocampus. Science *313*, 1093–1097.

Williams, P.A., White, A.M., Clark, S., Ferraro, D.J., Swiercz, W., Staley, K.J., and Dudek, F.E. (2009). Development of spontaneous recurrent seizures after kainate-induced status epilepticus. J. Neurosci. Off. J. Soc. Neurosci. *29*, 2103–2112.

Willis, T., and Pordage, S. (1681). An essay of the pathology of the brain and nervous stock: in which convulsive diseases are treated of (London: Printed by J.B. for T. Dring ...).

Wilson, J.V., and Reynolds, E.H. (1990). Texts and documents. Translation and analysis of a cuneiform text forming part of a Babylonian treatise on epilepsy. Med. Hist. *34*, 185–198.

Wirrell, E.C. (2016). Treatment of Dravet Syndrome. Can. J. Neurol. Sci. J. Can. Sci. Neurol. *43 Suppl 3*, S13-18.

Wolff, M., Casse-Perrot, C., and Dravet, C. (2006a). Severe myoclonic epilepsy of infants (Dravet syndrome): natural history and neuropsychological findings. Epilepsia *47 Suppl 2*, 45–48.

Wolff, M., Cassé-Perrot, C., and Dravet, C. (2006b). Severe myoclonic epilepsy of infants (Dravet syndrome): natural history and neuropsychological findings. Epilepsia *47 Suppl 2*, 45–48.

Wu, Y.W., Sullivan, J., McDaniel, S.S., Meisler, M.H., Walsh, E.M., Li, S.X., and Kuzniewicz, M.W. (2015). Incidence of Dravet Syndrome in a US Population. Pediatrics *136*, e1310-1315.

Xiong, Y., Zhou, H., and Zhang, L. (2014). Influences of hyperthermia-induced seizures on learning, memory and phosphorylative state of CaMKIIα in rat hippocampus. Brain Res. *1557*, 190–200.

Yagoubi, N., Jomni, Y., and Sakly, M. (2015). Hyperthermia-Induced Febrile Seizures Have Moderate and Transient Effects on Spatial Learning in Immature Rats. Behav. Neurol. *2015*, 924303.

Yakoub, M., Dulac, O., Jambaqué, I., Chiron, C., and Plouin, P. (1992). Early diagnosis of severe myoclonic epilepsy in infancy. Brain Dev. *14*, 299–303.

Yu, F.H., Westenbroek, R.E., Silos-Santiago, I., McCormick, K.A., Lawson, D., Ge, P., Ferriera, H., Lilly, J., DiStefano, P.S., Catterall, W.A., et al. (2003). Sodium channel beta4, a new disulfide-linked auxiliary subunit with similarity to beta2. J. Neurosci. Off. J. Soc. Neurosci. *23*, 7577–7585.

Yu, F.H., Mantegazza, M., Westenbroek, R.E., Robbins, C.A., Kalume, F., Burton, K.A., Spain, W.J., McKnight, G.S., Scheuer, T., and Catterall, W.A. (2006a). Reduced sodium current in GABAergic interneurons in a mouse model of severe myoclonic epilepsy in infancy. Nat. Neurosci. *9*, 1142–1149.

Yu, F.H., Mantegazza, M., Westenbroek, R.E., Robbins, C.A., Kalume, F., Burton, K.A., Spain, W.J., McKnight, G.S., Scheuer, T., and Catterall, W.A. (2006b). Reduced sodium current in GABAergic interneurons in a mouse model of severe myoclonic epilepsy in infancy. Nat Neurosci *9*, 1142–1149.

Zamponi, N., Passamonti, C., Cappanera, S., and Petrelli, C. (2011). Clinical course of young patients with Dravet syndrome after vagal nerve stimulation. Eur. J. Paediatr. Neurol. EJPN Off. J. Eur. Paediatr. Neurol. Soc. *15*, 8–14.

Zanchin, G. (1992). Considerations on “the sacred disease” by Hippocrates. J. Hist. Neurosci. *1*, 91–95.

Zhou, J.-L., Shatskikh, T.N., Liu, X., and Holmes, G.L. (2007). Impaired single cell firing and long-term potentiation parallels memory impairment following recurrent seizures. Eur. J. Neurosci. *25*, 3667–3677.

Zuberi, S.M., Brunklaus, A., Birch, R., Reavey, E., Duncan, J., and Forbes, G.H. (2011). Genotype-phenotype associations in SCN1A-related epilepsies. Neurology *76*, 594–600.

Zucker, R.S., and Regehr, W.G. (2002). Short-term synaptic plasticity. Annu. Rev. Physiol. *64*, 355–405.

Statistic Tables

VIII- STATISTIC TABLES

1. RESULTS – CHAPTER 1 – *SCN1A*$^{+/-}$-129 MICE AND *SCN1A*$^{+/-}$-B6:129

RESULTS Chapter 1- Phenotypic characterization of Scn1a+/--129 (DS model)

Morris Water Maze (MWM)

Mouse model and genetic backgroun	Experiment	Measurment	Protocol phase	Genotype	treatment/ protocol	average	S.E.M	# values/slices/cells	# animals	Statistical test	Source of variation	F(DFn,DFd) / t (dF) value/U/χ^2/H	p value	Comparision	post hoc test	t(dF) value / q(dF) value	p value	Figure
Scn1a+/-129	MWM	CUE TASK - latency	D1	WT	-	33.250	4.343	24	12	Two-Way RM ANOVA	Interaction	F (1, 90) = 0,3028	0.5835	WT: D1 vs. D2	Sidak's	t(90)=4,276	**< 0,0001**	21A
			D2			13.010	2.576	24	12		Day	F (1, 90) = 25,89	< 0,0001					
			D1	Scn1a+/-	-	29.850	4.376	20	10		Genotype	F (1, 90) = 0,1317	0.7176	Scn1a+/-: D1 vs. D2		t(90)=3,018	**0.0066**	
			D2			13.560	3.351	20	10									
	MWM	CUE TASK - latency	D1	WT	-	33.250	4.343	24	12	Two-Way RM ANOVA	Interaction	F (1, 90) = 0,3028	0.5835	D1: WT vs. Scn1a+/-	Sidak's	t(180)=0,6392	0.773	21A
				Scn1a+/-		29.850	4.376	24	12		Day	F (1, 90) = 25,89	< 0,0001					
			D2	WT	-	13.010	2.576	20	10		Genotype	F (1, 90) = 0,1317	0.7176	D2: WT vs. Scn1a+/-		t(180)=0,1039	0.9932	
				Scn1a+/-		13.560	3.351	20	10									
	MWM	SPATIAL-latency	D1	WT	-	54.931	4.540	48	12	Two-Way RM ANOVA	Interaction	F (3, 258) = 0,1529	0.9278	WT: D1 vs. D2	Tuckey's	t(258)=1,436	0.4779	21A
			D2			47.485	4.591	48	12					WT: D1 vs.D3		t(258)=4,666	**< 0,0001**	
			D3			30.742	3.780	48	12		Day	F (3, 258) = 29,10	< 0,0001	WT: D1 vs. D4		t(258)=5,761	**< 0,0001**	
									12					WT: D2 vs. D3		t(258)=3,23	**0.0076**	
			D4			25.063	3.064	48	12		Genotype	F (1, 86) = 1,413	0.2378	WT: D2 vs. D4		t(258)=4,325	**0.0001**	
									12					WT: D3 vs. D4		t(258)=1,095	0.6926	
			D1	Scn1a+/-	-	53.220	5.239	40	10	Two-Way RM ANOVA	Interaction	F (3, 258) = 0,1529	0.9278	Scn1a+/-:D1 vs. D2	Tuckey's	t(258)=1,754	0.298	21A
			D2			43.258	5.022	40	10					Scn1a+/-:D1 vs.D3		t(258)=5,169	**< 0,0001**	
			D3			23.865	3.269	40	10		Day	F (3, 258) = 29,10	< 0,0001	Scn1a+/-:D1 vs. D4		t(258)=5,615	**< 0,0001**	
									10					Scn1a+/-:D2 vs. D3		t(258)=3,415	**0.0041**	
			D4			21.330	2.659	40	10		Genotype	F (1, 86) = 1,413	0.2378	Scn1a+/-:D2 vs. D4		t(258)=3,861	**0.0008**	
									10					Scn1a+/-:D3 vs. D4		t(258)=0,4464	0.9703	
	MWM	SPATIAL-latency	D1	WT	-	54.931	4.540	48	12	Two-Way RM ANOVA	Interaction	F (3, 258) = 0,1529	0.9278	D1: WT vs. Scn1a+/-	Tuckey's	t(344)= 0,2922	0.9972	21A
				Scn1a+/-	-	53.220	5.239	40	10									
			D2	WT	-	47.485	4.591	48	12		Day	F (3, 258) = 29,10	< 0,0001	D2: WT vs. Scn1a+/-		t(344)=0,722	0.9215	
				Scn1a+/-	-	43.258	5.022	40	10									
			D3	WT	-	30.742	3.780	48	12					D3: WT vs. Scn1a+/-		t(344)=1,174	0.6682	
				Scn1a+/-	-	23.865	3.269	40	10		Genotype	F (1, 86) = 1,413	0.2378					
			D4	WT	-	25.063	3.064	48	12					D4: WT vs. Scn1a+/-		t(344)=0,6374	0.9488	
				Scn1a+/-	-	21.330	2.659	40	10									
	MWM	Presence in quadrant (%)	Probe test	WT: LEFT	-	25.916	3.690	12	12	RM-Two Way ANOVA	Interaction	F (3, 60) = 4,144	0.0098	WT vs. Scn1a+/-+/-: LEFT	Sidak's	t(80)=2,613	**0.0422**	21B
				WT: TARGET	-	35.223	3.559	12	12					WT vs. Scn1a+/-+/-: TARGET		t(80)=2,395	0.0738	
				WT: RIGHT	-	19.126	3.189	12	12		Quadrant	F (3, 60) = 22,75	< 0,0001	WT vs. Scn1a+/- +/-:RIGHT		t(80)=1,861	0.2405	
				WT: OPPOSITE	-	11.029	2.281	12	12									
				Scn1a+/-: LEFT	-	13.335	1.489	10	10									
				Scn1a+/-: TARGET	-	46.751	5.036	10	10									
				Scn1a+/-: RIGHT	-	28.084	3.812	10	10		Genotype	F (1, 20) = 2,126	0.1603	WT vs. Scn1a+/- +/-: OPPOSITE		t(80)=0,479	0.9819	
				Scn1a+/-: OPPOSITE	-	8.723	3.031	10	10									
	MWM	Presence in quadrant (%)	Probe test	WT: LEFT	-	25.916	3.690	12	12	RM-Two Way ANOVA	Interaction	F (3, 60) = 4,144	0.0098	WT: LEFT vs. TARGET	Sidak's	t(60)=1,792	0.3866	21B
				Scn1a+/-: LEFT	-	13.335	1.489	10	10					WT: TARGET vs. RIGHT		t(60)=3,099	**0.0176**	
				WT: TARGET	-	35.223	3.559	12	12					WT: TARGET vs. OPPOSITE		t(60)=4,658	**0.0001**	
				Scn1a+/-: TARGET	-	46.751	5.036	10	10		Quadrant	F (3, 60) = 22,75	< 0,0001					
				WT: RIGHT	-	19.126	3.189	12	12					Scn1a+/-: LEFT vs. TARGET		t(60)=5,873	**< 0,0001**	
				Scn1a+/-: RIGHT	-	28.084	3.812	10	10									
				WT: OPPOSITE	-	11.029	2.281	12	12		Genotype	F (1, 20) = 2,126	0.1603	Scn1a+/-: TARGET vs. RIGHT		t(60)=3,281	**0.0103**	
				Scn1a+/-: OPPOSITE	-	8.723	3.031	10	10					Scn1a+/-: TARGET vs. OPPOSITE		t(60)=6,683	**< 0,0001**	
	MWM	Target quadrant:Difference to chance level	Probe test	WT	-	35.223	3.559	12	12	One sample t-test	-	t(11)=2,873	0.0152	-	-	-	-	21B
				Chance level	-	25.000	-	-	-		-							
				Nav 1.1 KO +/-	-	46.751	5.036	10	10		-	t(9)=4,319	0.0019	-	-	-	-	
				Chance level	-	25.000	-	-	-		-							

Contextual Fear-Conditioning (CFC)

Mouse model and genetic	Experiment	Measurment	Protocol phase	Genotype	treatment /protocol	average	S.E.M	# values/slices/cells	# animals	Statistical test	Source of variation	F(DFn,DFd) / t (dF) value/U/χ^2/H	p value	Comparision	post hoc test	t(dF) value / q(dF)	p value	Figure
Scn1a+/-129	CFC	Freezing %	1 shock	WT	-	29,530	8,770	6	6	Mann-Withney test	-	U=21,50	0,7799	-	-	-	-	22
				Scn1a+/-	-	32,230	7,362	8	8		-			-	-	-	-	
		Freezing %	3 shocks	WT	-	43,010	9,192	9	9	Unpaired two-tailed t-test	-	t(14)=0,038	0,9695	-	-	-	-	
				Scn1a+/-	-	42,470	10,340	7	7		-			-	-	-	-	

Contextual Fear Conditioning																		
Mouse model and genetic	Experiment	Measurment	Protocol phase	Genotype	treatment /protocol	average	S.E.M	# values/slices/cells	# animals	Statistical test	Source of variation	F(DFn,DFd) / t (dF) value/U/χ^2/H	p value	Comparision	post hoc test	t(dF) value / q(dF) value	p value	Figure
Scn1a+/– B6:129	Contextual Fear Conditioni	**Freezing %**	**Conditioning 3 shocks**	WT	-	75,330	4,540	-	12	Unpaired two-tailed t-test	-	t(20)=09533	0,925	-	-	-	-	**27**
				Scn1a+/-	-	74,790	2,819	-	10		-			-	-	-	-	

Three-chamber social																		
Mouse model and genetic	Experiment	Measurment	Protocol phase	Genotype	treatment /protocol	average	S.E.M	# values/slices/cells	# animals	Statistical test	Source of variation	F(DFn,DFd) / t (dF) value/U/χ^2/H	p value	Comparision	post hoc test	t(dF) value / q(dF) value	p value	Figure
Scn1a+/–B6:129	**Three chamber social interactio test**	**Distance travelled (m)**	**Habituation phase**	WT	-	25,040	1,248	12	12	Unpaired two-tailed t-test	-	t(20)=0,7283	0,4749	-	-	-	-	**25A**
				Scn1a+/-	-	26,560	1,731	10	10		-			-	-	-	-	
		Average speed (m/s)	**Habituation phase**	WT	-	0,042	0,002	12	12	Unpaired two-tailed t-test	-	t(20)=0,7597	0,4653	-	-	-	-	**25B**
				Scn1a+/-	-	0,044	0,003	10	10		-			-	-	-	-	
		Time in the room (s)	**Habituation phase**	C1:WT	-	167,800	14,390	12	12	Two-way ANOVA	Interaction	F (2, 40) = 2,114	0,1341	**WT:** C1 vs. Center	Tuckey's	t(40)=3,605	**0,0026**	**25C**
				C:WT	-	240,000	12,030	12	12					**WT:** C1 vs. C2		t(40)=1,127	0,605	
				C2:WT	-	190,400	15,380	12	12		Chamber	F (2, 40) = 14,15	< 0,0001	**WT:** Center vs. C2		t(40)=2,478	0,0517	
				C1: Scn1a+/-	-	192,700	9,190	10	10					**Scn1a+/-:** C1 vs. Center	Tuckey's	t(40)=2,614	**0,0372**	
				C: Scn1a+/-	-	250,000	8,510	10	10		Genotype	F (1, 20) = 2,034	0,1692	**Scn1a+/-**: C1 vs. C2		t(40)=1,648	0,2884	
				C2: Scn1a+/-	-	156,600	6,930	10	10					**Scn1a+/-**: Center vs. C2		t(40)=4,262	**0,0004**	
		Interaction time (s)	**Sociability phase**	EC: WT	-	92,218	10,069	11	11	RM-Two Way ANOVA	Interaction	F (1, 20) = 0,4825	0,4953	**EC - M:** WT	Sidak's	t(18)=2,303	0,0668	**25D**
				M:WT	-	136,046	13,254	11	11		Genotype	F (1, 20) = 4,335	0,0504					
				EC:Scn1a+/-	-	118,067	9,197	9	9		Cage	F (1, 20) = 2,429	0,1348	**EC - M:** Scn1a+/-		t(18)=1,138	0,5404	
				M: Scn1a+/-	-	142,000	18,660	9	9									
		Interaction time (s)	**Social Novelty phase**	familiar mouse: WT	-	49,836	7,939	11	11	RM-Two Way ANOVA	Interaction	F (1, 18) = 0,4089	0,5306	**fM - nM:** WT	Sidak's	t(18)=2,789	**0,0243**	**25E**
				novel mouse: WT	-	87,273	9,653	11	11		Genotype	F (1, 18) = 2,990	0,1009					
				miliar mouse: Scn1a+	-	62,656	6,549	9	9		Cage	F (1, 18) = 19,19	0,0004	**fM - nM:** Scn1a+/-		t(18)=3,385	**0,0066**	
				ovel mouse: Scn1a+	-	112,889	16,492	9	9									

Morriw Water Maze

Mouse model and genetic	Experiment	Measurment	Protocol phase	Genotype	treatment /protocol	average	S.E.M	# values/slices/cells	# animals	Statistical test	Source of variation	F(DFn,DFd) / t (dF) value/U/χ^2/H	p value	Comparision	post hoc test	t(dF) value / q(dF) value	p value	Figure
Scn1a+/-B6.129	Morris Water Maze	Latency to find the cued platform (s)	Cue task 1	WT	-	23,540	3,927	48	12	Two-Way RM ANOVA	Interaction	F (1, 86) = 0,0800	0,7779	WT: Cue task 1 vs. Cue task 2	Sidak's	t(86)=5,045	**< 0,0001**	**26A**
			Cue task 2		-	2,652	0,272	48	12									
			Cue task 1	Scn1a+/-	-	23,790	4,838	40	10		Cue task Day	F (1, 86) = 42,51	< 0,0001	Scn1a+/-: Cue task 1 vs. Cue task 2	Sidak's	t(86)=4,223	**0,0001**	
			Cue task 2		-	4,640	0,980	40	10		Genotype	F (1, 86) = 0,1250	0,7245					
	Morris Water Maze	Latency to find the cued platform (s)	Cue task1	WT	-	23,540	3,927	48	12	Two-Way RM ANOVA	Interaction	F (1, 86) = 0,0800	0,7779	Cue task 1: WT vs. Scn1a+/-	Sidak's	t(172)=0,056	0,998	**26A**
				Scn1a+/-	-	23,790	4,838	40	10									
			Cue task 2	WT	-	2,652	0,272	48	12		Cue task Day	F (1, 86) = 42,51	< 0,0001	Cue task 2: WT vs. Scn1a+/-	Sidak's	t(172)=0,87	0,8794	**26A**
				Scn1a+/-	-	4,640	0,980	10	40		Genotype	F (1, 86) = 0,1250	0,7245					
	Morris Water Maze	Latency to find the hidden platform (s)	Training 1	WT	-	31,631	4,972	48	12	Two-Way RM ANOVA	Interaction	F (3, 258) = 0,773	0,5097	WT: Training 1 vs. Training 2	Sidak's	t(258)=5,925	**< 0,0001**	**26A**
			Training 2		-	9,240	2,288	48	12					WT: Training 1 vs. Training 3		t(258)=6,444	**< 0,0001**	
			Training 3		-	7,277	1,008	48	12		Training Day	F (3, 258) = 27,22	< 0,0001	WT: Training 1 vs. Training 4		t(258)=6,267	**< 0,0001**	
														WT: Training 2 vs. Training 3		t(258)=0,5193	0,9961	
			Training 4		-	7,946	1,754	48	12		Genotype	(1, 86) = 0,00192	0,9651	WT: Training 2 vs. Training 4		t(258)=0,3423	0,9996	
														WT: Training 3 vs. Training 4		t(258)=0,177	> 0,9999	
			Training 1	Scn1a+/-	-	27,195	4,827	40	10		Interaction	F (3, 258) = 0,773	0,5097	Scn1a+/-: Training 1 vs. Training 2		t(258)=4,042	**0,0004**	
			Training 2		-	10,460	1,545	40	10					Scn1a+/-:Training 1 vs. Training 3		t(258)=3,894	**0,0008**	
			Training 3		-	11,073	1,756	40	10		Training Day	F (3, 258) = 27,22	< 0,0001	Scn1a+/-:Training 1 vs. Training 4		t(258)=4,882	**< 0,0001**	
														Scn1a+/-:Training 2 vs. Training 3		t(258)=0,148	> 0,9999	
			Training 4		-	6,985	1,160	40	10		Genotype	(1, 86) = 0,00192	0,9651	Scn1a+/-:Training 2 vs. Training 4		t(258)=0,8394	0,9543	
														Scn1a+/-:Training 3 vs. Training 4		t(258)=0,9874	0,9049	
	Morris Water Maze	Latency to find the hidden platform	Training 1	WT	-	31,631	4,972	48	12	Two-Way RM ANOVA	Interaction	F (3, 258) = 0,773	0,5097	Training 1: WT vs. Scn1a+/-	Sidak's	t(344)=1,092	0,7244	**26A**
				Scn1a+/-	-	27,195	4,827	40	10									
			Training 2	WT	-	9,240	2,288	48	12		Training Day	F (3, 258) = 27,22	< 0,0001	Training 2: WT vs. Scn1a+/-		t(344)=0,3005	0,9969	
				Scn1a+/-	-	10,460	1,545	40	10									
			Training 3	WT	-	7,277	1,008	48	12					Training 3: WT vs. Scn1a+/-		t(344)=0,9345	0,8223	
				Scn1a+/-	-	11,073	1,756	40	10									
			Training 4	WT	-	7,946	1,754	48	12		Genotype	(1, 86) = 0,00192	0,9651	Training 4: WT vs. Scn1a+/-		t(344)=0,2366	0,9988	
				Scn1a+/-	-	6,985	1,160	40	10									
	Morris Water Maze	Presence in quadrant (%) Quadrant discriminatio n by group	Probe test	WT: LEFT	-	21,930	3,385	12	12	RM-Two Way ANOVA	Interaction	F (3, 60) = 1,610	0,1965	WT: LEFT vs. TARGET	Sidak's	t(60)=4,12	**0,0007**	**26B**
				WT: TARGET	-	40,260	3,795	12	12					WT: TARGET vs. RIGHT		t(60)=3,137	**0,0158**	
				WT: RIGHT	-	26,310	2,558	12	12					WT: TARGET vs. OPPOSITE		t(60)=6,486	**<0,0001**	
				WT: OPPOSITE	-	11,400	1,813	12	12		Quadrant	F (3, 60) = 24,41	< 0,0001	Scn1a+/- LEFT vs. TARGET		t(60)=5,015	**<0,0001**	
				Scn1a+/-: LEFT	-	14,230	1,906	10	10					Scn1a+/- TARGET vs. RIGHT		t(60)=1,566	0,5439	
				Scn1a+/-: TARGET	-	38,680	2,917	10	10									
				Scn1a+/-: RIGHT	-	31,050	3,485	10	10		Genotype	F (1, 20) = 0,5451	0,4689	Scn1a+/- TARGET vs. OPPOSITE		t(60)=4,657	**0,0001**	
				Scn1a+/-: OPPOSITE	-	15,980	1,607	10	10									
	Morris Water Maze	Presence in quadrant (%) Quadrant discriminatio n between the groups	Probe test	WT: LEFT	-	21,930	3,385	12	12	RM-Two Way ANOVA	Interaction	F (3, 60) = 1,610	0,1965	WT vs. Scn1a+/-: LEFT	Sidak's	t(80)=1,904	0,2209	**26B**
				Scn1a+/-: LEFT	-	14,230	1,906	10	10									
				WT: TARGET	-	40,260	3,795	12	12					WT vs. Scn1a+/-: TARGET		t(80)=0,3912	0,9915	
				Scn1a+/-: TARGET	-	38,680	2,917	10	10		Quadrant	F (3, 60) = 24,41	< 0,0001					
				WT: RIGHT	-	26,310	2,558	12	12					WT vs.Scn1a+/-:RIGHT		t(80)=1,174	0,6733	
				Scn1a+/-: RIGHT	-	31,050	3,485	10	10									
				WT: OPPOSITE	-	11,400	1,813	12	12		Genotype	F (1, 20) = 0,5451	0,4689	WT vs. Scn1a+/-: OPPOSITE		t(80)=1,133	0,7013	
				Scn1a+/- OPPOSITE	-	15,980	1,607	10	10									
	Morris Water Maze	Target quadrant:Difference to chance level	Probe test	WT	-	40,260	3,795	12	12	One sample t-test	-	t(11)=4,022	0,002	-	-	-	-	**26B**
				Chance level	-	25	-				-							
				Scn1a+/-	-	38,680	2,917	10	10		-	t (9)=4,690	0,0011	-	-	-	-	
				Chance level	-	25	-				-							
	Morris Water Maze	Number of platform crosses	Probe test	WT	-	10,330	0,742	12	12	Mann Whitney test	-	U=10,5	0,8332	-	-	-	-	**26B**
				Nav 1.1 KO +/-	-	9,700	0,746	10	10									

Contextual Fear Conditioning

Mouse model and genetic	Experiment	Measurment	Protocol phase	Genotype	treatment /protocol	average	S.E.M	# values/slices/cells	# animals	Statistical test	Source of variation	F(DFn,DFd) / t (dF) value/U/χ^2/H	p value	Comparision	post hoc test	t(dF) value / q(dF) value	p value	Figure
Scn1a+/-B6.129	Contextual Fear Conditioni	Freezing %	Conditioning 3 shocks	WT	-	75,330	4,540	-	12	Unpaired two-tailed t-test	-	t(20)=09533	0,925	-	-	-	-	27
				Scn1a+/-	-	74,790	2,819	-	10		-			-	-	-	-	

Radial Maze																		
Mouse model and genetic	Experiment	Measurment	Protocol phase	Genotype	treatment/protocol	average	S.E.M	# values/slices/cells	# animals	Statistical test	Source of variation	F(DFn,DFd) / t (dF) value/U/χ^2/H	p value	Comparision	post hoc test	t(dF) value / q(dF) value	p value	Figure
Scn1a+/-B6:129	Radial Maze	Number of correct choices	D1	WT	-	2.917	0.260	12	12	Two-Way RM ANOVA	Interaction	F (11, 220) = 0,1394	0.9995	**D1:** WT vs. Scn1a+/-	Sidak's	t(240)=0,031	> 0,9999	28
				Scn1a+/-	-	2.900	0.314	10	10									
			D2	WT	-	3.917	0.379	12	12					**D2:** WT vs. Scn1a+/-		t(240)=0,218	> 0,9999	
				Scn1a+/-	-	3.800	0.327	10	10									
			D3	WT	-	3.333	0.396	12	12					**D3:**WT vs. Scn1a+/-		t(240)=0,311	> 0,9999	
				Scn1a+/-	-	3.500	0.401	10	10									
			D4	WT	-	3.833	0.423	12	12					**D4:**WT vs. Scn1a+/-		t(240)=0,435	> 0,9999	
				Scn1a+/-	-	3.600	0.371	10	10									
			D5	WT	-	3.667	0.256	12	12		Training Day	F (11, 220) = 13,69	< 0,0001	**D5:**WT vs. Scn1a+/-		t(240)=0,249	> 0,9999	
				Scn1a+/-	-	3.800	0.359	10	10									
			D6	WT	-	3.750	0.429	12	12					**D6**:WT vs. Scn1a+/-		t(240)=0,093	> 0,9999	
				Scn1a+/-	-	3.800	0.359	10	10									
			D7	WT	-	4.083	0.468	12	12					**D7:**WT vs. Scn1a+/-		t(240)=0,591	> 0,9999	
				Scn1a+/-	-	4.400	0.267	10	10									
			D8	WT	-	5.000	0.389	12	12					**D8:**WT vs. Scn1a+/-		t(240)=0,186	> 0,9999	
				Scn1a+/-	-	5.100	0.407	10	10									
			D9	WT	-	5.250	0.524	12	12		Genotype	F (1, 20) = 0,2325	0.6349	**D9:**WT vs. Scn1a+/-		t(240)=0,093	> 0,9999	
				Scn1a+/-	-	5.200	0.359	10	10									
			D10	WT	-	5.167	0.386	12	12					**D10**:WT vs. Scn1a+/-		t(240)=0,809	0.9985	
				Scn1a+/-	-	5.600	0.400	10	10									
			D11	WT	-	5.583	0.288	12	12					**D11:**WT vs. Scn1a+/-		t(240)=0,591	> 0,9999	
				Scn1a+/-	-	5.900	0.407	10	10									
			D12	WT	-	5.500	0.359	12	12					**D12:**WT vs. Scn1a+/-		t(240)=0,186	> 0,9999	
				Scn1a+/-	-	5.600	0.267	10	10									
Scn1a+/-B6:129	Radial Maze	Differences to chance level	D1	WT	-	2.917	0.260	12	12	One sample t-test	D1 : WT vs. Chance level	t(11)=2,244	0.0463	-	-	-	-	28
			D2	WT	-	3.917	0.379	12	12		D2 : WT vs. Chance level	t(11)=1,101	0.2945	-	-	-	-	
			D3	WT	-	3.333	0.396	12	12		D3 : WT vs. Chance level	t(11)=0,4212	0.6817	-	-	-	-	
			D4	WT	-	3.833	0.423	12	12		D4 : WT vs. Chance level	t(11)=0,7872	0.4478	-	-	-	-	
			D5	WT	-	3.667	0.256	12	12		D5 : WT vs. Chance level	t(11)=0,6504	0.5288	-	-	-	-	
			D6	WT	-	3.750	0.429	12	12		D6 : WT vs. Chance level	t(11)=0,5833	0.5715	-	-	-	-	
			D7	WT	-	4.083	0.468	12	12		D7 : WT vs. Chance level	t(11)=1,246	0.2385	-	-	-	-	
			D8	WT	-	5.000	0.389	12	12		D8 : WT vs. Chance level	t(11)=3,854	0.0027	-	-	-	-	
			D9	WT	-	5.250	0.524	12	12		D9 : WT vs. Chance level	t(11)=3,339	0.0066	-	-	-	-	
			D10	WT	-	5.167	0.386	12	12		D10 : WT vs. Chance level	t(11)=4,318	0.0012	-	-	-	-	
			D11	WT	-	5.583	0.288	12	12		D11 : WT vs. Chance level	t(11)=7,244	< 0,0001	-	-	-	-	
			D12	WT	-	5.500	0.359	12	12		D12 : WT vs. Chance level	t(11)=5,573	0.0002	-	-	-	-	
			Chance level		-	3.500	-	-	-									
			D1	Scn1a+/-	-	2.900	0.314	10	10		D1 : Scn1a+/- vs. Chance level	t(9)=1,908	0.0887	-	-	-	-	28
			D2	Scn1a+/-	-	3.800	0.327	10	10		D2 : Scn1a+/- vs. Chance level	t(9)=0,9186	0.3823	-	-	-	-	
			D3	Scn1a+/-	-	3.500	0.401	10	10		D3 : Scn1a+/- vs. Chance level	t(9)=0,0	1	-	-	-	-	
			D4	Scn1a+/-	-	3.600	0.371	10	10		D4 : Scn1a+/- vs. Chance level	t(9)=0,2694	0.7937	-	-	-	-	
			D5	Scn1a+/-	-	3.800	0.359	10	10		D5 : Scn1a+/- vs. Chance level	t(9)=0,8356	0.425	-	-	-	-	
			D6	Scn1a+/-	-	3.800	0.359	10	10		D6 : Scn1a+/-vs. Chance level	t(9)=0,8356	0.425	-	-	-	-	
			D7	Scn1a+/-	-	4.400	0.267	10	10		D7 : Scn1a+/- vs. Chance level	t(9)=3,375	0.0082	-	-	-	-	
			D8	Scn1a+/-	-	5.100	0.407	10	10		D8 : Scn1a+/- vs. Chance level	t(9)=3,932	0.0034	-	-	-	-	
			D9	Scn1a+/-	-	5.200	0.359	10	10		D9 : Scn1a+/- vs. Chance level	(9)t=4,735	0.0011	-	-	-	-	
			D10	Scn1a+/-	-	5.600	0.400	10	10		D10 : Scn1a+/- vs. Chance level	t(9)=5,250	0.0005	-	-	-	-	
			D11	Scn1a+/-	-	5.900	0.407	10	10		D11 : Scn1a+/-vs. Chance level	t(9)=5,898	0.0002	-	-	-	-	
			D12	Scn1a+/-	-	5.600	0.267	10	10		D12 : Scn1a+/- vs. Chance level	t(9)=7,875	< 0,0001	-	-	-	-	
			Chance level		-	3.500	-	-	-									

RESULTS Chapter 2- Seizures induction by hyperthermia (SIH) in *Scn1a*$^{+/-}$-B6:129 and *Scn1a*$^{RH/+}$-129:B6 mouse models																			
Seizures Induced by hyperthermia (SIH) in *Scn1a*$^{+/-}$-B6:129																			
Mouse model and	Experiment	Measurment	Protocol phase	Genotype	treatment /protocol	average	S.E.M	# values/slices/cells	# animals	Statistical test	Source of variation	F(DFn,DFd) / t (dF) value/U/χ^2/H	p value	Comparision	post hoc test	t(dF) value / q(dF)	p value	Figure
Scn1a+/-B6:129	**Seizures Induction by hyperthermia**	**Survival curve comparision**	**Survival percentage at day 10**	WT	-	100,000	-	12	12	Log-rank (Mantel-Cox) test	Curve comparision	χ^2(3)=17,52	0,0001	-	-	-	-	**29A**
				Scn1a+/-	-	100,000	-	10	10									
				WT	hyperthermi	72,720	13,428	11	11									
				Scn1a+/-	SIH	36,769	12,800	13	13									
Scn1a+/-B6:129	**Seizures Induction by hyperthermia**	**Temperature threshold for seizure induction**	D1	Scn1a+/-	SIH	41,173	0,106	11	11	Kruskal-Wallis test	Differences between protocol days	H(10)=18,38	0,031	1 vs. 2	Dunn's	-	> 0,9999	**29B**
			D2			41,320	0,213	10	10					1 vs. 3		-	> 0,9999	
			D3			40,122	0,514	9	9					1 vs. 4		-	0,624	
			D4			40,017	0,481	6	6					1 vs. 5		-	> 0,9999	
			D5			40,717	0,257	6	6					1 vs. 6		-	0,6634	
			D6			40,240	0,385	5	5					1 vs. 7		-	> 0,9999	
			D7			40,350	0,328	4	4					1 vs. 8		-	> 0,9999	
			D8			41,160	0,308	5	5					1 vs. 9		-	> 0,9999	
			D9			40,925	0,439	4	4					1 vs. 10		-	0,7633	
			D10			41,900	0,058	3	3									
Scn1a+/-B6:129	**Seizures Induction by hyperthermia**	**Seizure severity caracterization**	D1	Scn1a+/-	SIH	5,091	0,091	11	11	Kruskal-Wallis test	Differences between protocol days	H(10)=39,29	< 0,0001	1 vs. 2	Dunn's	-	**0,0004**	**29C**
			D2			5,900	0,100	10	10					1 vs. 3		-	**< 0,0001**	
			D3			6,000	0,000	9	9					1 vs. 4		-	**< 0,0001**	
			D4			6,167	0,167	6	6					1 vs. 5		-	**0,0007**	
			D5			6,000	0,000	6	6					1 vs. 6		-	**0,0018**	
			D6			6,000	0,000	5	5					1 vs. 7		-	**0,009**	
			D7			6,000	0,408	4	4					1 vs. 8		-	**0,0018**	
			D8			6,000	0,000	5	5					1 vs. 9		-	**0,0002**	
			D9			6,250	0,250	4	4					1 vs. 10		-	**0,0189**	
			D10			6,000	0,000	3	3									

Seizures Induced by hyperthermia (SIH) in *Scn1a*$^{RH/+}$-129:B6																				
Mouse model and	Experiment	Measurment	Protocol phase	Genotype	treatment /protocol	average	S.E.M	# values/slices/cells	# animals	Statistical test	Source of variation	F(DFn,DFd) / t (dF) value/U/χ^2/H	p value	Comparision	post hoc test	t(dF) value / q(dF)	p value	Figure
Scn1a$^{RH/+}$-129:B6	**Seizures induction by hyperthermia**	**Survival curve comparision**	**Survival percentage at day 10**	WT	-	100,000	-	20	20	Log-rank (Mantel-Cox) test	Curve comparision	χ^2(3)=27,19	< 0,0001	-	-	-	-	**30A**
				Scn1a $^{RH/+}$	-	100,000	-	20	20									
				WT	hyperthermi	92,063	3,406	33	33									
				Scn1a $^{RH/+}$	SIH	65,079	6,006	63	63									
Scn1aRH/+-129:B6	**Seizures Induction by hyperthermia**	**Temperature threshold for seizure induction**	D1	*Scn1a* $^{RH/+}$	SIH	41,632	0,049	63	63	Kruskal-Wallis test	Differences between protocol days	H(10)=69,98	< 0,0001	1 vs. 2	Dunn's	-	**0,0092**	**30B**
			D2			41,918	0,057	56	56					1 vs. 3		-	**0,0001**	
			D3			42,042	0,048	57	57					1 vs. 4		-	> 0,9999	
			D4			41,475	0,168	53	53					1 vs. 5		-	> 0,9999	
			D5			41,486	0,130	50	50					1 vs. 6		-	> 0,9999	
			D6			41,298	0,147	48	48					1 vs. 7		-	> 0,9999	
			D7			41,292	0,108	48	48					1 vs. 8		-	0,8898	
			D8			41,200	0,132	45	45					1 vs. 9		-	0,7714	
			D9			41,240	0,120	43	43					1 vs. 10		-	> 0,9999	
			D10			41,605	0,116	41	41									
Scn1aRH/+-129:B6	**Seizures Induction by hyperthermia**	**Seizure severity caracterization**	D1	*Scn1a* $^{RH/+}$	SIH	4,804	0,059	46	46	Kruskal-Wallis test	Differences between protocol days	H(10)=227,7	< 0,0001	1 vs. 2	Dunn's	-	0,968	**30C**
			D2			5,093	0,056	43	43					1 vs. 3		-	**< 0,0001**	
			D3			5,581	0,089	43	43					1 vs. 4		-	**< 0,0001**	
			D4			5,925	0,066	40	40					1 vs. 5		-	**< 0,0001**	
			D5			5,865	0,079	37	37					1 vs. 6		-	**< 0,0001**	
			D6			6,059	0,041	34	34					1 vs. 7		-	**< 0,0001**	
			D7			5,971	0,029	34	34					1 vs. 8		-	**< 0,0001**	
			D8			6,030	0,030	33	33					1 vs. 9		-	**< 0,0001**	
			D9			6,032	0,032	31	31					1 vs. 10		-	**< 0,0001**	
			D10			5,929	0,071	28	28									

3. RESULTS – CHAPTER 3 – *SCN1A*$^{RH/+}$-SIH

RESULTS Chapter 3- Long-term effects of the 10-days seizures induction by hyperthermia protocol in *Scn1a*$^{RH/+}$-129:B6 mice																		
Spontaneous seizure analysis in Scn1aRH/+ -129:B6																		
Mouse model and genetic background	Experiment	Measurment	Protocol phase	Genotype	treatment/protocol	average	S.E.M	# values/slices/cells	# animals	Statistical test	Source of variation	F(DFn,DFd) / t (dF) value/U/χ^2/H	p value	Comparision	post hoc test	t(dF) value / q(dF) value	p value	Figure
Scn1aRH/+-129:B6	Spontaneous Seizure Activity	Number of spontaneous seizures	Post SIH week 1	*Scn1a* $^{RH/+}$	-	0.00	0.00	4	4	Multiple T-test	Holm-Sidak correction for multiple comparision	t(13)=1,370	0.193622	-	-	-	-	31C
				Scn1a $^{RH/+}$	SIH	0.40	0.17	11	11					-	-	-	-	
			Post SIH week 2	*Scn1a* $^{RH/+}$	-	0.00	0.00	4	4			t(9)=8,412	**< 0,0001**	-	-	-	-	
				Scn1a $^{RH/+}$	SIH	1.03	0.09	7	7					-	-	-	-	
			Post SIH week 3	*Scn1a* $^{RH/+}$	-	0.00	0.00	4	4			t(12)=2,570	**0.0245105**	-	-	-	-	
				Scn1a $^{RH/+}$	SIH	0.89	0.21	10	10					-	-	-	-	
			Post SIH week 4	*Scn1a* $^{RH/+}$	-	0.00	0.00	4	4			t(10)=5,466	**0.0002744**	-	-	-	-	
				Scn1a $^{RH/+}$	SIH	0.70	0.09	8	8					-	-	-	-	
			Post SIH week 5	*Scn1a* $^{RH/+}$	-	0.00	0.00	4	4			t(10)=3,217	**0.0092105**	-	-	-	-	
				Scn1a $^{RH/+}$	SIH	0.56	0.12	8	8					-	-	-	-	
			Post SIH week 6	*Scn1a* $^{RH/+}$	-	0.00	0.00	4	4			t(12)=2,458	**0.0301598**	-	-	-	-	
				Scn1a $^{RH/+}$	SIH	0.51	0.13	10	10					-	-	-	-	
			Post SIH week 7	*Scn1a* $^{RH/+}$	-	0.00	0.00	4	4			t(9)=3,688	**0.0050108**	-	-	-	-	
				Scn1a $^{RH/+}$	SIH	0.64	0.13	7	7					-	-	-	-	
			Post SIH week 8	*Scn1a* $^{RH/+}$	-	0.00	0.00	3	3			t(8)=2,290	0.0512169	-	-	-	-	
				Scn1a $^{RH/+}$	SIH	0.63	0.17	7	7					-	-	-	-	
			Post SIH week 9	*Scn1a* $^{RH/+}$	-	0.00	0.00	3	3			t(5)=2,206	0.078416	-	-	-	-	
				Scn1a $^{RH/+}$	SIH	0.55	0.21	4	4					-	-	-	-	
			Post SIH week 10	*Scn1a* $^{RH/+}$	-	0.00	0.00	3	3			t(5)=4,225	**0.0082818**	-	-	-	-	
				Scn1a $^{RH/+}$	SIH	0.75	0.15	4	4					-	-	-	-	

Long-term potentiation in CA1 area of the hippocampus in Scn1aRH/+ -129:B6

Mouse model and genetic background	Experiment	Measurment	Protocol phase	Genotype	treatment/protocol	average	S.E.M	# values/slices/cells	# animals	Statistical test	Source of variation	F(DFn,DFd) / t (dF) value/U/χ^2/H	p value	Comparision	post hoc test	t(dF) value / q(dF) value	p value	Figure
Scn1aRH/+-129:B6	1x HFS-LTP	fEPSP slope (% baseline)	1st minute PTP	WT	-	202.61	9.79	14	7	RM Two-way ANOVA	Interaction	F (237, 3792) = 1.841	< 0.0001	WT control vs. *Scn1a*$^{RH/+}$ control	Sidak's	t(3840)=1.471	0.5996	33A
				Scn1a$^{RH/+}$	-	215.63	9.50	11	8					WT control vs. WT HYP		t(3840)=1.58	0.5168	
				WT	HYP	215.73	11.52	14	8					*Scn1a*$^{RH/+}$ control vs. *Scn1a*$^{RH/+}$ SIH		t(3840)=4.915	**< 0.0001**	
				Scn1a$^{RH/+}$	SIH	259.85	20.28	13	8					WT HYP vs. *Scn1a*$^{RH/+}$ SIH		t(3840)=5.216	**< 0.0001**	
			2nd minute PTP	WT	-	192.56	10.77	14	7					WT control vs. *Scn1a*$^{RH/+}$ control		t(3840)=3.57	**0.0022**	
				Scn1a$^{RH/+}$	-	224.15	12.66	11	8					WT control vs. WT HYP		t(3840)=2.962	**0.0183**	
				WT	HYP	217.16	12.75	14	8					*Scn1a*$^{RH/+}$ control vs. *Scn1a*$^{RH/+}$ SIH		t(3840)=2.826	**0.0281**	
				Scn1a$^{RH/+}$	SIH	249.58	25.66	13	8					WT HYP vs. *Scn1a*$^{RH/+}$ SIH		t(3840)=3.833	**0.0008**	
			3rd minute PTP	WT	-	166.06	5.91	14	7		Time	F (79, 3792) = 133.9	< 0.0001	WT control vs. *Scn1a*$^{RH/+}$ control		t(3840)=2.514	0.0698	
				Scn1a$^{RH/+}$	-	188.31	8.92	11	8					WT control vs. WT HYP		t(3840)=1.956	0.2674	
				WT	HYP	182.30	9.45	14	8					*Scn1a*$^{RH/+}$ control vs. *Scn1a*$^{RH/+}$ SIH		t(3840)=2.277	0.1296	
				Scn1a$^{RH/+}$	SIH	208.79	21.24	13	8					WT HYP vs. *Scn1a*$^{RH/+}$ SIH		t(3840)=3.132	**0.0105**	
			4th minute PTP	WT	-	153.78	4.79	14	7					WT control vs. *Scn1a*$^{RH/+}$ control		t(3840)=2.409	0.0924	
				Scn1a$^{RH/+}$	-	175.11	7.44	11	8					WT control vs. WT HYP		t(3840)=1.581	0.5163	
				WT	HYP	166.91	7.77	14	8		Group (Treatment-genotype)	F (3, 48) = 2.736	0.0537	*Scn1a*$^{RH/+}$ control vs. *Scn1a*$^{RH/+}$ SIH		t(3840)=1.958	0.2665	
				Scn1a$^{RH/+}$	SIH	192.72	17.57	13	8					WT HYP vs. *Scn1a*$^{RH/+}$ SIH		t(3840)=3.051	**0.0137**	
			5th minute PTP	WT	-	147.60	4.60	14	7					WT control vs. *Scn1a*$^{RH/+}$ control		t(3840)=1.792	0.3661	
				Scn1a$^{RH/+}$	-	163.46	6.23	11	8					WT control vs. WT HYP		t(3840)=1.364	0.6795	
				WT	HYP	158.93	8.02	14	8					*Scn1a*$^{RH/+}$ control vs. *Scn1a*$^{RH/+}$ SIH		t(3840)=2.121	0.1874	
				Scn1a$^{RH/+}$	SIH	182.55	15.89	13	8					WT HYP vs. *Scn1a*$^{RH/+}$ SIH		t(3840)=2.792	**0.0311**	
Scn1aRH/+-129:B6	1x HFS-LTP	fEPSP slope (% baseline)	last 15 minutes	WT	-	117.91	5.31	14	7	Two-way ANOVA	Interaction	F (1, 48) = 0,03241	0.8579	WT control vs. WT HYP	Tuckey's	q(48)=1,669	0.6419	33B
				Scn1a$^{RH/+}$	-	124.72	4.24	11	8					WT control vs. *Scn1a*$^{RH/+}$ control		q(48)=1,086	0.8684	
				WT	HYP	127.91	6.58	13	8		Genotype	F (1, 48) = 0,8656	0.3568	*Scn1a*$^{RH/+}$ control vs. *Scn1a*$^{RH/+}$ SIH		q(48)=1,244	0.8155	
				Scn1a$^{RH/+}$	SIH	132.51	7.17	14	8		Treatment	F (1, 48) = 2,107	0.1532	WT HYP vs. *Scn1a*$^{RH/+}$ SIH		q(48)=0,7678	0.948	
	4x HFS-LTP	fEPSP slope (% baseline)	last 15 minutes	WT	-	149.79	8.42	14	8	Two-way ANOVA	Interaction	F (1, 54) = 0,4493	0.5055	WT control vs. WT HYP	Tuckey's	q(54)=0,7188	0.9568	33D
				Scn1a$^{RH/+}$	-	140.59	7.77	14	8					WT control vs. *Scn1a*$^{RH/+}$ control		q(54)=1,112	0.8603	
				WT	HYP	155.64	9.06	15	8		Genotype	F (1, 54) = 0,2123	0.6468	*Scn1a*$^{RH/+}$ control vs. *Scn1a*$^{RH/+}$ SIH		q(54)=2,059	0.4706	
				Scn1a$^{RH/+}$	SIH	157.35	7.11	15	8		Treatment	F (1, 54) = 1,930	0.1705	WT HYP vs. *Scn1a*$^{RH/+}$ SIH		q(54)=0,2132	0.9988	

Paired-pulse ratio in CA1 area of the hippocampus in Scn1aRH/+ -129:B6																			
Mouse model and genetic background	Experiment	Measurment	Protocol phase	Genotype	treatment/protocol	average	S.E.M	# values/slices/cells	# animals	Statistical test	Source of variation	F(DFn,DFd) / t (dF) value/U/χ^2/H	p value	Comparision	post hoc test	t(dF) value / q(dF) value	p value	Figure
Scn1aRH/+-129B6	PPR	(P2/P1)	50 ms ISI	WT	-	1.579	0.053	12	5	Two-way ANOVA	Interaction	F (1, 43) = 2,566	0.1165	WT control vs. WT HYP	Tuckey's	q(43)=0,6265	0.9706	33E
				Scn1a$^{RH/+}$	-	1.510	0.045	11	4					WT control vs. *Scn1a*$^{RH/+}$ control		q(43)=1,370	0.7676	
				WT	HYP	1.548	0.032	12	5		Treatment	F (1, 43) = 0,9651	0.3314	*Scn1a*$^{RH/+}$ control vs. *Scn1a*$^{RH/+}$ SIH		q(43)=2,556	0.2839	
				Scn1a$^{RH/+}$	SIH	1.639	0.062	12	4		Genotype	F (1, 43) = 0,04681	0.8297	WT HYP vs. *Scn1a*$^{RH/+}$ SIH		q(43)=1,839	0.5678	
			100 ms ISI	WT	-	1.473	0.047	12	6	Two-way ANOVA	Interaction	F (1, 43) = 2,108	0.1538	WT control vs. WT HYP	Tuckey's	q(43)=0,4022	0.9919	
				Scn1a$^{RH/+}$	-	1.457	0.021	12	6					WT control vs. *Scn1a*$^{RH/+}$ control		q(43)=0,4208	0.9907	
				WT	HYP	1.488	0.039	12	5		Treatment	F (1, 43) = 3,421	0.0712	*Scn1a*$^{RH/+}$ control vs. *Scn1a*$^{RH/+}$ SIH		q(43)=3,266	0.1118	
				Scn1a$^{RH/+}$	SIH	1.584	0.044	11	5		Genotype	F (1, 43) = 1,073	0.306	WT HYP vs. *Scn1a*$^{RH/+}$ SIH		q(43)=2,461	0.3161	
			150 ms ISI	WT	-	1.380	0.030	12	6	Two-way ANOVA	Interaction	F (1, 44) = 10,87	0.0019	WT control vs. WT HYP	Tuckey's	q(44)=1,578	0.6817	
				Scn1a$^{RH/+}$	-	1.313	0.010	12	7					WT control vs. *Scn1a*$^{RH/+}$ control		q(44)=2,466	0.3138	
				WT	HYP	1.338	0.024	12	5		Treatment	F (1, 44) = 2,951	0.0928	*Scn1a*$^{RH/+}$ control vs. *Scn1a*$^{RH/+}$ SIH		q(44)=5,014	**0.005**	
				Scn1a$^{RH/+}$	SIH	1.450	0.037	12	5		Genotype	F (1, 44) = 0,6886	0.4111	WT HYP vs. *Scn1a*$^{RH/+}$ SIH		q(44)=4,126	**0.0274**	
			200 ms ISI	WT	-	1.256	0.025	13	7	Two-way ANOVA	Interaction	F (1, 43) = 0,5365	0.4679	WT control vs. WT HYP	Tuckey's	q(43)=0,4675	0.9874	
				Scn1a$^{RH/+}$	-	1.252	0.026	12	6					WT control vs. *Scn1a*$^{RH/+}$ control		q(43)=0,1419	0.9996	
				WT	HYP	1.269	0.033	12	6		Treatment	F (1, 43) = 1,402	0.2429	*Scn1a*$^{RH/+}$ control vs. *Scn1a*$^{RH/+}$ SIH		q(43)=1,855	0.5606	
				Scn1a$^{RH/+}$	SIH	1.308	0.032	10	6		Genotype	F (1, 43) = 0,3546	0.5547	WT HYP vs. *Scn1a*$^{RH/+}$ SIH		q(43)=1,285	0.8002	
			250 ms ISI	WT	-	1.210	0.021	12	7	Two-way ANOVA	Interaction	F (1, 41) = 11,25	0.0017	WT control vs. WT HYP	Tuckey's	q(41)=2,008	0.4946	
				Scn1a$^{RH/+}$	-	1.175	0.019	11	7					WT control vs. *Scn1a*$^{RH/+}$ control		q(41)=1,641	0.6548	
				WT	HYP	1.168	0.021	12	6		Treatment	F (1, 41) = 2,005	0.1643	*Scn1a*$^{RH/+}$ control vs. *Scn1a*$^{RH/+}$ SIH		q(41)=4,617	**0.0114**	
				Scn1a$^{RH/+}$	SIH	1.280	0.028	10	7		Genotype	F (1, 41) = 3,009	0.0903	WT HYP vs. *Scn1a*$^{RH/+}$ SIH		q(41)=5,026	**0.0052**	
			300 ms ISI	WT	-	1.132	0.014	12	5	Two-way ANOVA	Interaction	F (1, 44) = 7,730	0.008	WT control vs. WT HYP	Tuckey's	q(44)=0,1466	0.9996	
				Scn1a$^{RH/+}$	-	1.116	0.015	11	7					WT control vs. *Scn1a*$^{RH/+}$ control		q(44)=0,9341	0.9113	
				WT	HYP	1.130	0.012	13	7		Treatment	F (1, 44) = 6,953	0.0115	*Scn1a*$^{RH/+}$ control vs. *Scn1a*$^{RH/+}$ SIH		q(44)=5,307	**0.0028**	
				Scn1a$^{RH/+}$	SIH	1.204	0.022	12	7		Genotype	F (1, 44) = 3,338	0.0745	WT HYP vs. *Scn1a*$^{RH/+}$ SIH		q(44)=4,707	**0.0093**	
			350 ms ISI	WT	-	1.103	0.021	12	8	Two-way ANOVA	Interaction	F (1, 42) = 3,678	0.0619	WT control vs. WT HYP	Tuckey's	q(42)=0,3697	0.9936	
				Scn1a$^{RH/+}$	-	1.101	0.017	11	6					WT control vs. *Scn1a*$^{RH/+}$ control		q(42)=0,08919	> 0,9999	
				WT	HYP	1.110	0.015	12	6		Treatment	F (1, 42) = 5,196	0.0278	*Scn1a*$^{RH/+}$ control vs. *Scn1a*$^{RH/+}$ SIH		q(42)=4,109	**0.0287**	
				Scn1a$^{RH/+}$	SIH	1.180	0.021	11	8		Genotype	F (1, 42) = 3,344	0.0746	WT HYP vs. *Scn1a*$^{RH/+}$ SIH		q(42)=3,746	0.0531	
			400 ms ISI	WT	-	1.088	0.019	12	7	Two-way ANOVA	Interaction	F (1, 41) = 9,940	0.003	WT control vs. WT HYP	Tuckey's	q(41)=1,117	0.8587	
				Scn1a$^{RH/+}$	-	1.065	0.011	11	7					WT control vs. *Scn1a*$^{RH/+}$ control		q(41)=1,454	0.7341	
				WT	HYP	1.105	0.016	11	6		Treatment	F (1, 41) = 18,13	0.0001	*Scn1a*$^{RH/+}$ control vs. *Scn1a*$^{RH/+}$ SIH		q(41)=7,333	**< 0,0001**	
				Scn1a$^{RH/+}$	SIH	1.183	0.016	11	7		Genotype	F (1, 41) = 2,939	0.094	WT HYP vs. *Scn1a*$^{RH/+}$ SIH		q(41)=4,816	**0.0078**	
			450 ms ISI	WT	-	1.065	0.021	12	7	Two-way ANOVA	Interaction	F (1, 45) = 0,3963	0.5322	WT control vs. WT HYP	Tuckey's	q(45)=2,642	0.2562	
				Scn1a$^{RH/+}$	-	1.069	0.018	11	5					WT control vs. *Scn1a*$^{RH/+}$ control		q(45)=0,2418	0.9982	
				WT	HYP	1.111	0.014	12	5		Treatment	F (1, 45) = 10,82	0.002	*Scn1a*$^{RH/+}$ control vs. *Scn1a*$^{RH/+}$ SIH		q(45)=3,944	**0.0374**	
				Scn1a$^{RH/+}$	SIH	1.137	0.017	14	7		Genotype	F (1, 45) = 0,7715	0.3844	WT HYP vs. *Scn1a*$^{RH/+}$ SIH		q(45)=1,555	0.6918	
			500 ms ISI	WT	-	1.054	0.017	12	5	Two-way ANOVA	Interaction	F (1, 44) = 5,443	0.0243	WT control vs. WT HYP	Tuckey's	q(44)=1,988	0.5025	
				Scn1a$^{RH/+}$	-	1.047	0.014	11	6					WT control vs. *Scn1a*$^{RH/+}$ control		q(44)=0,4376	0.9896	
				WT	HYP	1.085	0.011	12	5		Treatment	F (1, 44) = 18,64	< 0,0001	*Scn1a*$^{RH/+}$ control vs. *Scn1a*$^{RH/+}$ SIH		q(44)=6,639	**0.0001**	
				Scn1a$^{RH/+}$	SIH	1.150	0.018	13	8		Genotype	F (1, 44) = 3,559	0.0658	WT HYP vs. *Scn1a*$^{RH/+}$ SIH		q(44)=4,311	**0.0196**	

Excitability in DG area of the hippocampus in Scn1aRH/+ -129:B6																				
Mouse model and genetic background	Experiment	Measurment	Protocol phase	Genotype	treatment/protocol	average	S.E.M	# values/slices/cells	# animals	Statistical test	Source of variation	F(DFn,DFd) / t (dF) value/U/χ^2/H	p value	Comparision	post hoc test	t(dF) value / q(dF) value	p value	Figure
Scn1aRH/+-129:B6	Frequency in DG granular cells	Number of action potentials	0	WT	-	0.00	0.00	13	3	Two-way ANOVA	Interaction	F (87, 1247) = 1,774	< 0,0001	WT control vs. *Scn1a*$^{RH/+}$ control	Tuckey's	q(1290)=0	> 0,9999	34 B
				Scn1a$^{RH/+}$	-	0.00	0.00	12	3					WT control vs. WT HYP		q(1290)=0	> 0,9999	
				WT	HYP	0.00	0.00	12	4					*Scn1a*$^{RH/+}$ control vs. *Scn1a*$^{RH/+}$ SIH		q(1290)=0,077	> 0,9999	
				Scn1a$^{RH/+}$	SIH	0.30	0.21	10	4					WT HYP vs. *Scn1a*$^{RH/+}$ SIH		q(1290)=0,077	> 0,9999	
			20	WT	-	1.85	0.82	13	3					WT control vs. *Scn1a*$^{RH/+}$ control	Tuckey's	q(1290)=0,02658	> 0,9999	
				Scn1a$^{RH/+}$	-	1.75	1.22	12	3					WT control vs. WT HYP		q(1290)=0,1116	0.9998	
				WT	HYP	2.25	0.99	12	4					*Scn1a*$^{RH/+}$ control vs. *Scn1a*$^{RH/+}$ SIH		q(1290)=1,305	0.7927	
				Scn1a$^{RH/+}$	SIH	6.80	1.53	10	4					WT HYP vs. *Scn1a*$^{RH/+}$ SIH		q(1290)=1,176	0.8395	
			40	WT	-	5.31	1.46	13	3					WT control vs. *Scn1a*$^{RH/+}$ control	Tuckey's	q(1290)=0,4536	0.9886	
				Scn1a$^{RH/+}$	-	3.67	1.52	12	3					WT control vs. WT HYP		q(1290)=0,01595	> 0,9999	
				WT	HYP	5.25	1.60	12	4					*Scn1a*$^{RH/+}$ control vs. *Scn1a*$^{RH/+}$ SIH		q(1290)=2,154	0.4241	
				Scn1a$^{RH/+}$	SIH	12.00	2.44	10	4					WT HYP vs. *Scn1a*$^{RH/+}$ SIH		q(1290)=1,744	0.6056	
			60	WT	-	8.23	1.86	13	3					WT control vs. *Scn1a*$^{RH/+}$ control	Tuckey's	q(1290)=0,7087	0.9588	
				Scn1a$^{RH/+}$	-	5.67	1.70	12	3					WT control vs. WT HYP		q(1290)=0,01772	> 0,9999	
				WT	HYP	8.17	2.08	12	4					*Scn1a*$^{RH/+}$ control vs. *Scn1a*$^{RH/+}$ SIH		q(1290)=2,722	0.2181	
				Scn1a$^{RH/+}$	SIH	16.20	2.99	10	4					WT HYP vs. *Scn1a*$^{RH/+}$ SIH		q(1290)=2,076	0.4573	
			80	WT	-	11.00	2.10	13	3					WT control vs. *Scn1a*$^{RH/+}$ control	Tuckey's	q(1290)=0,8522	0.9312	
				Scn1a$^{RH/+}$	-	7.92	1.94	12	3					WT control vs. WT HYP		q(1290)=0,1612	0.9995	
				WT	HYP	11.58	2.44	12	4					*Scn1a*$^{RH/+}$ control vs. *Scn1a*$^{RH/+}$ SIH		q(1290)=3,252	0.0987	
				Scn1a$^{RH/+}$	SIH	20.50	3.43	10	4					WT HYP vs. *Scn1a*$^{RH/+}$ SIH		q(1290)=2,304	0.3624	
			100	WT	-	10.85	2.10	13	3					WT control vs. *Scn1a*$^{RH/+}$ control	Tuckey's	q(1290)=0,349	0.9947	
				Scn1a$^{RH/+}$	-	9.58	2.20	12	3					WT control vs. WT HYP		q(1290)=0,8948	0.9215	
				WT	HYP	14.08	2.98	12	4					*Scn1a*$^{RH/+}$ control vs. *Scn1a*$^{RH/+}$ SIH		q(1290)=4,191	**0.0164**	
				Scn1a$^{RH/+}$	SIH	25.80	3.97	10	4					WT HYP vs. *Scn1a*$^{RH/+}$ SIH		q(1290)=3,028	0.1408	
			120	WT	-	12.38	2.49	13	3					WT control vs. *Scn1a*$^{RH/+}$ control	Tuckey's	q(1290)=0,01417	> 0,9999	
				Scn1a$^{RH/+}$	-	12.33	2.47	12	3					WT control vs. WT HYP		q(1290)=1,091	0.8672	
				WT	HYP	16.33	3.57	12	4					*Scn1a*$^{RH/+}$ control vs. *Scn1a*$^{RH/+}$ SIH		q(1290)=4,385	**0.0106**	
				Scn1a$^{RH/+}$	SIH	29.30	4.38	10	4					WT HYP vs. *Scn1a*$^{RH/+}$ SIH		q(1290)=3,351	0.0836	
			140	WT	-	14.23	3.12	13	3					WT control vs. *Scn1a*$^{RH/+}$ control	Tuckey's	q(1290)=0,1099	0.9998	
				Scn1a$^{RH/+}$	-	13.83	2.70	12	3					WT control vs. WT HYP		q(1290)=0,7424	0.9531	
				WT	HYP	16.92	3.14	12	4					*Scn1a*$^{RH/+}$ control vs. *Scn1a*$^{RH/+}$ SIH		q(1290)=4,772	**0.0042**	
				Scn1a$^{RH/+}$	SIH	32.30	4.85	10	4					WT HYP vs. *Scn1a*$^{RH/+}$ SIH		q(1290)=3,975	**0.0258**	
			160	WT	-	14.62	3.00	13	3		Treatment	F (29, 1247) = 27,58	< 0,0001	WT control vs. *Scn1a*$^{RH/+}$ control	Tuckey's	q(1290)=0,4057	0.9918	
				Scn1a$^{RH/+}$	-	16.08	2.92	12	3					WT control vs. WT HYP		q(1290)=0,6821	0.963	
				WT	HYP	17.08	3.10	12	4					*Scn1a*$^{RH/+}$ control vs. *Scn1a*$^{RH/+}$ SIH		q(1290)=5,328	**0.001**	
				Scn1a$^{RH/+}$	SIH	36.70	5.01	10	4					WT HYP vs. *Scn1a*$^{RH/+}$ SIH		q(1290)=5,069	**0.002**	
			180	WT	-	17.00	3.42	13	3					WT control vs. *Scn1a*$^{RH/+}$ control	Tuckey's	q(1290)=0,1843	0.9992	
				Scn1a$^{RH/+}$	-	17.67	3.11	12	3					WT control vs. WT HYP		q(1290)=0,4837	0.9862	
				WT	HYP	18.75	3.61	12	4					*Scn1a*$^{RH/+}$ control vs. *Scn1a*$^{RH/+}$ SIH		q(1290)=5,642	**0.0004**	
				Scn1a$^{RH/+}$	SIH	39.50	5.05	10	4					WT HYP vs. *Scn1a*$^{RH/+}$ SIH		q(1290)=5,362	**0.0009**	
			200	WT	-	18.46	3.74	13	3					WT control vs. *Scn1a*$^{RH/+}$ control	Tuckey's	q(1290)=0,0567	> 0,9999	
				Scn1a$^{RH/+}$	-	18.67	2.85	12	3					WT control vs. WT HYP		q(1290)=0,1506	0.9996	
				WT	HYP	17.92	3.66	12	4					*Scn1a*$^{RH/+}$ control vs. *Scn1a*$^{RH/+}$ SIH		q(1290)=6,056	**0.0001**	
				Scn1a$^{RH/+}$	SIH	42.10	4.90	10	4					WT HYP vs. *Scn1a*$^{RH/+}$ SIH		q(1290)=6,249	**< 0,0001**	
			220	WT	-	19.08	3.90	13	3					WT control vs. *Scn1a*$^{RH/+}$ control	Tuckey's	q(1290)=0,14	0.9997	
				Scn1a$^{RH/+}$	-	19.58	2.75	12	3					WT control vs. WT HYP		q(1290)=0,1134	0.9998	
				WT	HYP	18.67	4.11	12	4					*Scn1a*$^{RH/+}$ control vs. *Scn1a*$^{RH/+}$ SIH		q(1290)=6,336	**< 0,0001**	
				Scn1a$^{RH/+}$	SIH	44.10	4.91	10	4					WT HYP vs. *Scn1a*$^{RH/+}$ SIH		q(1290)=6,572	**< 0,0001**	
			240	WT	-	18.62	3.53	13	3					WT control vs. *Scn1a*$^{RH/+}$ control	Tuckey's	q(1290)=0,6821	0.963	
				Scn1a$^{RH/+}$	-	21.08	2.62	12	3					WT control vs. WT HYP		q(1290)=0,815	0.9392	
				WT	HYP	15.67	3.80	12	4					*Scn1a*$^{RH/+}$ control vs. *Scn1a*$^{RH/+}$ SIH		q(1290)=6,051	**0.0001**	
				Scn1a$^{RH/+}$	SIH	44.50	5.12	10	4					WT HYP vs. *Scn1a*$^{RH/+}$ SIH		q(1290)=7,451	**< 0,0001**	
			260	WT	-	16.46	3.22	13	3					WT control vs. *Scn1a*$^{RH/+}$ control	Tuckey's	q(1290)=1,485	0.72	
				Scn1a$^{RH/+}$	-	21.83	2.50	12	3					WT control vs. WT HYP		q(1290)=0,2658	0.9976	
				WT	HYP	15.50	4.22	12	4					*Scn1a*$^{RH/+}$ control vs. *Scn1a*$^{RH/+}$ SIH		q(1290)=5,16	**0.0016**	
				Scn1a$^{RH/+}$	SIH	41.80	5.35	10	4					WT HYP vs. *Scn1a*$^{RH/+}$ SIH		q(1290)=6,796	**< 0,0001**	
			280	WT	-	16.85	3.52	13	3					WT control vs. *Scn1a*$^{RH/+}$ control	Tuckey's	q(1290)=1,448	0.7356	
				Scn1a$^{RH/+}$	-	22.08	2.67	12	3					WT control vs. WT HYP		q(1290)=0,3721	0.9936	
				WT	HYP	15.50	4.72	12	4					*Scn1a*$^{RH/+}$ control vs. *Scn1a*$^{RH/+}$ SIH		q(1290)=5,147	**0.0016**	
				Scn1a$^{RH/+}$	SIH	42.00	6.36	10	4					WT HYP vs. *Scn1a*$^{RH/+}$ SIH		q(1290)=6,848	**< 0,0001**	
			300	WT	-	16.15	3.53	13	3					WT control vs. *Scn1a*$^{RH/+}$ control	Tuckey's	q(1290)=1,224	0.8225	
				Scn1a$^{RH/+}$	-	20.58	2.97	12	3					WT control vs. WT HYP		q(1290)=0,2959	0.9968	
				WT	HYP	15.08	4.59	12	4					*Scn1a*$^{RH/+}$ control vs. *Scn1a*$^{RH/+}$ SIH		q(1290)=4,94	**0.0028**	
				Scn1a$^{RH/+}$	SIH	39.70	7.02	10	4					WT HYP vs. *Scn1a*$^{RH/+}$ SIH		q(1290)=6,361	**< 0,0001**	
			320	WT	-	16.85	3.85	13	3					WT control vs. *Scn1a*$^{RH/+}$ control	Tuckey's	q(1290)=0,8257	0.937	
				Scn1a$^{RH/+}$	-	19.83	3.16	12	3					WT control vs. WT HYP		q(1290)=0,6024	0.974	
				WT	HYP	14.67	4.47	12	4					*Scn1a*$^{RH/+}$ control vs. *Scn1a*$^{RH/+}$ SIH		q(1290)=5,134	**0.0017**	
				Scn1a$^{RH/+}$	SIH	39.70	7.69	10	4					WT HYP vs. *Scn1a*$^{RH/+}$ SIH		q(1290)=6,469	**< 0,0001**	
			340	WT	-	15.54	3.53	13	3					WT control vs. *Scn1a*$^{RH/+}$ control	Tuckey's	q(1290)=0,9568	0.906	
				Scn1a$^{RH/+}$	-	19.00	3.33	12	3					WT control vs. WT HYP		q(1290)=0,0567	> 0,9999	
				WT	HYP	15.33	4.99	12	4					*Scn1a*$^{RH/+}$ control vs. *Scn1a*$^{RH/+}$ SIH		q(1290)=5,117	**0.0018**	
				Scn1a$^{RH/+}$	SIH	38.80	8.12	10	4					WT HYP vs. *Scn1a*$^{RH/+}$ SIH		q(1290)=6,064	**0.0001**	

Mouse model and genetic background	Experiment	Measurement	Protocol phase	Genotype	treatment/protocol	average	S.E.M	# values/slices/cells	# animals	Statistical test	Source of variation	F(DFn,DFd) / t (dF) value/U/χ²/H	p value	Comparision	post hoc test	t(dF) value / q(dF) value	p value	Figure
			360	WT	-	16.77	4.17	13	3					WT control vs. $Scn1a^{RH/+}$ control	Tuckey's	q(1290)=0,1329	0.9997	
				$Scn1a^{RH/+}$	-	17.25	3.56	12	3					WT control vs. WT HYP		q(1290)=0,8345	0.9351	
				WT	HYP	13.75	4.41	12	4					$Scn1a^{RH/+}$ control vs. $Scn1a^{RH/+}$ SIH		q(1290)=5,285	**0.0011**	
				$Scn1a^{RH/+}$	SIH	37.70	8.70	10	4					WT HYP vs. $Scn1a^{RH/+}$ SIH		q(1290)=6,189	**< 0,0001**	
			380	WT	-	15.00	3.91	13	3					WT control vs. $Scn1a^{RH/+}$ control	Tuckey's	q(1290)=0,5989	0.9745	
				$Scn1a^{RH/+}$	-	17.17	3.77	12	3					WT control vs. WT HYP		q(1290)=0,8292	0.9362	
				WT	HYP	12.00	3.93	12	4					$Scn1a^{RH/+}$ control vs. $Scn1a^{RH/+}$ SIH		q(1290)=3,911	**0.0294**	
				$Scn1a^{RH/+}$	SIH	32.30	8.37	10	4					WT HYP vs. $Scn1a^{RH/+}$ SIH		q(1290)=5,246	**0.0012**	
			400	WT	-	13.23	3.77	13	3					WT control vs. $Scn1a^{RH/+}$ control	Tuckey's	q(1290)=0,6272	0.9709	
				$Scn1a^{RH/+}$	-	15.50	3.80	12	3					WT control vs. WT HYP		q(1290)=0,5014	0.9847	
				WT	HYP	11.42	3.57	12	4					$Scn1a^{RH/+}$ control vs. $Scn1a^{RH/+}$ SIH		q(1290)=4,057	**0.0218**	
				$Scn1a^{RH/+}$	SIH	31.20	8.40	10	4					WT HYP vs. $Scn1a^{RH/+}$ SIH		q(1290)=5,112	**0.0018**	
			420	WT	-	10.92	3.08	13	3					WT control vs. $Scn1a^{RH/+}$ control	Tuckey's	q(1290)=0,8274	0.9366	
				$Scn1a^{RH/+}$	-	13.92	3.87	12	3					WT control vs. WT HYP		q(1290)=0,4624	0.9879	
				WT	HYP	9.25	2.66	12	4					$Scn1a^{RH/+}$ control vs. $Scn1a^{RH/+}$ SIH		q(1290)=3,743	**0.041**	
				$Scn1a^{RH/+}$	SIH	28.40	7.97	10	4					WT HYP vs. $Scn1a^{RH/+}$ SIH		q(1290)=4,949	**0.0027**	
			440	WT	-	9.69	2.89	13	3					WT control vs. $Scn1a^{RH/+}$ control	Tuckey's	q(1290)=1,122	0.8576	
				$Scn1a^{RH/+}$	-	13.75	3.92	12	3					WT control vs. WT HYP		q(1290)=0,652	0.9675	
				WT	HYP	7.33	2.46	12	4					$Scn1a^{RH/+}$ control vs. $Scn1a^{RH/+}$ SIH		q(1290)=3,088	0.1283	
				$Scn1a^{RH/+}$	SIH	25.70	7.48	10	4					WT HYP vs. $Scn1a^{RH/+}$ SIH		q(1290)=4,746	**0.0045**	
			460	WT	-	7.54	2.39	13	3					WT control vs. $Scn1a^{RH/+}$ control	Tuckey's	q(1290)=1,51	0.7095	
				$Scn1a^{RH/+}$	-	13.00	3.68	12	3					WT control vs. WT HYP		q(1290)=0,010	> 0,9999	
				WT	HYP	7.50	2.75	12	4					$Scn1a^{RH/+}$ control vs. $Scn1a^{RH/+}$ SIH		q(1290)=2,429	0.3148	
				$Scn1a^{RH/+}$	SIH	22.40	7.23	10	4		Genotype	F (3, 43) = 8,369	0.0002	WT HYP vs. $Scn1a^{RH/+}$ SIH		q(1290)=3,85	**0.0332**	
			480	WT	-	6.77	1.91	13	3					WT control vs. $Scn1a^{RH/+}$ control	Tuckey's	q(1290)=1,63	0.6569	
				$Scn1a^{RH/+}$	-	12.67	3.93	12	3					WT control vs. WT HYP		q(1290)=0,1329	0.9997	
				WT	HYP	7.25	2.81	12	4					$Scn1a^{RH/+}$ control vs. $Scn1a^{RH/+}$ SIH		q(1290)=2,024	0.4799	
				$Scn1a^{RH/+}$	SIH	20.50	6.30	10	4					WT HYP vs. $Scn1a^{RH/+}$ SIH		q(1290)=3,424	0.0736	
			500	WT	-	5.69	1.59	13	3					WT control vs. $Scn1a^{RH/+}$ control	Tuckey's	q(1290)=1,237	0.8181	
				$Scn1a^{RH/+}$	-	10.17	3.24	12	3					WT control vs. WT HYP		q(1290)=0,1541	0.9995	
				WT	HYP	6.25	2.54	12	4					$Scn1a^{RH/+}$ control vs. $Scn1a^{RH/+}$ SIH		q(1290)=2,309	0.3607	
				$Scn1a^{RH/+}$	SIH	19.10	6.20	10	4					WT HYP vs. $Scn1a^{RH/+}$ SIH		q(1290)=3,321	0.0879	
			520	WT	-	5.08	1.54	13	3					WT control vs. $Scn1a^{RH/+}$ control	Tuckey's	q(1290)=1,084	0.8694	
				$Scn1a^{RH/+}$	-	9.00	2.96	12	3					WT control vs. WT HYP		q(1290)=0,3242	0.9958	
				WT	HYP	6.25	2.93	12	4					$Scn1a^{RH/+}$ control vs. $Scn1a^{RH/+}$ SIH		q(1290)=1,68	0.6347	
				$Scn1a^{RH/+}$	SIH	15.50	5.57	10	4					WT HYP vs. $Scn1a^{RH/+}$ SIH		q(1290)=2,39	0.3292	
			540	WT	-	4.85	1.31	13	3					WT control vs. $Scn1a^{RH/+}$ control	Tuckey's	q(1290)=0,8717	0.9269	
				$Scn1a^{RH/+}$	-	8.00	2.82	12	3					WT control vs. WT HYP		q(1290)=0,2268	0.9985	
				WT	HYP	5.67	2.42	12	4					$Scn1a^{RH/+}$ control vs. $Scn1a^{RH/+}$ SIH		q(1290)=1,628	0.6578	
				$Scn1a^{RH/+}$	SIH	14.30	6.43	10	4					WT HYP vs. $Scn1a^{RH/+}$ SIH		q(1290)=2,231	0.3918	
			560	WT	-	4.77	1.29	13	3					WT control vs. $Scn1a^{RH/+}$ control	Tuckey's	q(1290)=0,8009	0.9421	
				$Scn1a^{RH/+}$	-	7.67	2.72	12	3					WT control vs. WT HYP		q(1290)=0,06378	> 0,9999	
				WT	HYP	5.00	2.29	12	4					$Scn1a^{RH/+}$ control vs. $Scn1a^{RH/+}$ SIH		q(1290)=1,559	0.6881	
				$Scn1a^{RH/+}$	SIH	13.70	6.43	10	4					WT HYP vs. $Scn1a^{RH/+}$ SIH		q(1290)=2,248	0.3848	
			580	WT	-	4.15	1.05	13	3					WT control vs. $Scn1a^{RH/+}$ control	Tuckey's	q(1290)=0,8327	0.9355	
				$Scn1a^{RH/+}$	-	7.17	2.74	12	3					WT control vs. WT HYP		q(1290)=0,01949	> 0,9999	
				WT	HYP	4.08	1.61	12	4					$Scn1a^{RH/+}$ control vs. $Scn1a^{RH/+}$ SIH		q(1290)=1,533	0.6993	
				$Scn1a^{RH/+}$	SIH	13.10	6.42	10	4					WT HYP vs. $Scn1a^{RH/+}$ SIH		q(1290)=2,33	0.3523	

Openfield in Scn1aRH/+ -129:B6

Mouse model and genetic background	Experiment	Measurement	Protocol phase	Genotype	treatment/protocol	average	S.E.M	# values/slices/cells	# animals	Statistical test	Source of variation	F(DFn,DFd) / t (dF) value/U/χ²/H	p value	Comparision	post hoc test	t(dF) value / q(dF) value	p value	Figure
Scn1aRH/+-129:B6	Openfield	Locomotor Activity	Distance travelled (m)	WT	-	17.375	1.012	19	19	Two-way ANOVA	Interaction	F (1, 64) = 15,13	0.0002	WT control vs. $Scn1a^{RH/+}$ control	Tuckey's	q(64)=2,064	0.4676	35B
				$Scn1a^{RH/+}$	-	20.946	1.338	22	22					WT control vs. WT HYP		q(64)=2,749	0.2203	
				WT	HYP	22.841	1.808	13	13		Treatment	F (1, 64) = 45,01	< 0,0001	$Scn1a^{RH/+}$ control vs. $Scn1a^{RH/+}$ SIH		q(64)=10,88	**< 0,0001**	
				$Scn1a^{RH/+}$	SIH	41.498	3.492	14	14		Genotype	F (1, 64) = 32,85	< 0,0001	WT HYP vs. $Scn1a^{RH/+}$ SIH		q(64)=8,768	**< 0,0001**	
			Average speed (m/s)	WT	-	0.029	0.002	19	19	Two-way ANOVA	Interaction	F (1, 64) = 15,58	0.0002	WT control vs. $Scn1a^{RH/+}$ control	Tuckey's	q(64)=62,033	0.4808	35A
				$Scn1a^{RH/+}$	-	0.035	0.002	22	22					WT control vs. WT HYP		q(64)=2,762	0.2167	
				WT	HYP	0.038	0.003	13	13		Treatment	F (1, 64) = 45,97	< 0,0001	$Scn1a^{RH/+}$ control vs. $Scn1a^{RH/+}$ SIH		q(64)=11,01	**< 0,0001**	
				$Scn1a^{RH/+}$	SIH	0.069	0.006	14	14		Genotype	F (1, 64) = 33,20	< 0,0001	WT HYP vs. $Scn1a^{RH/+}$ SIH		q(64)=8,849	**< 0,0001**	
		Stereotyped behavior	Rotations of the animal's body	WT	-	20.632	1.575	19	19	Two-way ANOVA	Interaction	F (1, 64) = 3,460	0.0675	WT control vs. $Scn1a^{RH/+}$ control	Tuckey's	q(64)=1,463	0.7298	35E
				$Scn1a^{RH/+}$	-	23.364	1.244	22	22					WT control vs. WT HYP		q(64)=1,928	0.5266	
				WT	HYP	24.769	1.680	13	13		Treatment	F (1, 64) = 14,73	0.0003	$Scn1a^{RH/+}$ control vs. $Scn1a^{RH/+}$ SIH		q(64)=5,85	**0.0006**	
				$Scn1a^{RH/+}$	SIH	35.286	3.739	14	14		Genotype	F (1, 64) = 10,02	0.0024	WT HYP vs. $Scn1a^{RH/+}$ SIH		q(64)=4,58	**0.01**	
			Rearing episodes	WT	-	26.385	5.112	13	13	Two-way ANOVA	Interaction	F (1, 47) = 9,191	0.0039	WT control vs. $Scn1a^{RH/+}$ control	Tuckey's	q(47)=1,145	0.8495	35F
				$Scn1a^{RH/+}$	-	33.500	4.350	16	16					WT control vs. WT HYP		q(47)=2,118	0.4472	
				WT	HYP	40.818	7.499	11	11		Treatment	F (1, 47) = 27,00	< 0,0001	$Scn1a^{RH/+}$ control vs. $Scn1a^{RH/+}$ SIH		q(47)=8,419	**< 0,0001**	
				$Scn1a^{RH/+}$	SIH	88.364	10.098	11	11		Genotype	F (1, 47) = 16,80	0.0002	WT HYP vs. $Scn1a^{RH/+}$ SIH		q(47)=6,702	**0.0001**	
		Anxiety	Distance in the center (m)/total distance(m)	WT	-	0.162	0.020	18	18	Two-way ANOVA	Interaction	F (1, 64) = 1,020	0.3164	WT control vs. $Scn1a^{RH/+}$ control	Tuckey's	q(64)=1,244	0.8155	35C
				$Scn1a^{RH/+}$	-	0.181	0.014	23	23					WT control vs. WT HYP		q(64)=0,2553	0.9979	
				WT	HYP	0.158	0.018	13	13		Treatment	F (1, 64) = 1,623	0.2072	$Scn1a^{RH/+}$ control vs. $Scn1a^{RH/+}$ SIH		q(64)=2,37	0.3449	
				$Scn1a^{RH/+}$	SIH	0.142	0.013	14	14		Genotype	F (1, 64) = 0,01061	0.9183	WT HYP vs. $Scn1a^{RH/+}$ SIH		q(64)=0,8281	0.9361	

Dark-light in Scn1aRH/+ -129:B6																			
Mouse model and genetic background	Experiment	Measurment	Protocol phase	Genotype	treatment/protocol	average	S.E.M	# values/slices/cells	# animals	Statistical test	Source of variation	F(DFn,DFd) / t (dF) value/U/χ^2/H	p value	Comparision	post hoc test	t(dF) value / q(dF) value	p value	Figure
Scn1aRH/+-129:B6	Dark-light box	Anxiety	% Time in the light compartment	WT	-	4.621	2.049	8	8	Two-way ANOVA	Interaction	F (1, 40) = 2,982	0.0919	WT control vs. *Scn1a*$^{RH/+}$ control	Tuckey's	q(40)=2,893	0.1887	36A
				Scn1a$^{RH/+}$	-	13.343	3.374	10	10					WT control vs. WT HYP		q(40)=2,945	0.1764	
				WT	HYP	13.031	2.347	13	13		Treatment	F (1, 40) = 1,725	0.1965	*Scn1a*$^{RH/+}$ control vs. *Scn1a*$^{RH/+}$ SIH		q(40)=0,4277	0.9902	
				Scn1a$^{RH/+}$	SIH	12.200	2.671	13	13		Genotype	F (1, 40) = 2,035	0.1615	WT HYP vs. *Scn1a*$^{RH/+}$ SIH		q(40)=0,3332	0.9953	
		Anxiety	Number of entries in the light compartment	WT	-	2.875	0.833	8	8	Two-way ANOVA	Interaction	F (1, 40) = 6,042	0.0184	WT control vs. *Scn1a*$^{RH/+}$ control	Tuckey's	q(40)=2,042	0.4802	36B
				Scn1a$^{RH/+}$	-	7.100	1.616	10	10					WT control vs. WT HYP		q(40)=5,181	**0.0039**	
				WT	HYP	6.538	1.169	13	13		Treatment	F (1, 40) = 8,361	0.0062	*Scn1a*$^{RH/+}$ control vs. *Scn1a*$^{RH/+}$ SIH		q(40)=0,4486	0.9888	
				Scn1a$^{RH/+}$	SIH	7.923	1.579	13	13		Genotype	F (1, 40) = 0,05405	0.8174	WT HYP vs. *Scn1a*$^{RH/+}$ SIH		q(40)=2,985	0.1671	

ACTIMETER in Scn1aRH/+ -129:B6																		
Mouse model and genetic background	Experiment	Measurment	Protocol phase	Genotype	treatment/protocol	average	S.E.M	# values/slices/cells	# animals	Statistical test	Source of variation	F(DFn,DFd) / t (dF) value/U/χ^2/H	p value	Comparision	post hoc test	t(dF) value / q(dF) value	p value	Figure
Scn1aRH/+-129:B6	Actimeter	Vertical activity (number of rearing episodes) 12-hour fraction of time	D1	WT	-	11.378	2.046	5	5	RM-Two Way ANOVA	Interaction	F (15, 135) = 3,210	0.0002	D1:WT control vs. WT HYP	Tuckey's	q(162)=1,201	0.9519	37C
				Scn1a$^{RH/+}$	-	16.495	4.277	8	8					D1:WT control vs. *Scn1a*$^{RH/+}$ control		q(162)=1,636	0.8207	
				WT	HYP	18.198	3.381	9	9					D1:WT HYP vs. *Scn1a*$^{RH/+}$ SIH		q(162)=7,625	**< 0,0001**	
				Scn1a$^{RH/+}$	SIH	44.186	8.787	9	9					D1:Scn1a$^{RH/+}$ control vs. *Scn1a*$^{RH/+}$ SIH		q(162)=7,376	**< 0,0001**	
			N1	WT	-	8.933	0.994	5	5					N1:WT control vs. WT HYP	Tuckey's	q(162)=1,306	0.9293	
				Scn1a$^{RH/+}$	-	14.500	2.054	8	8					N1:WT control vs. *Scn1a*$^{RH/+}$ control		q(162)=2,182	0.5508	
				WT	HYP	18.028	2.064	9	9					N1:WT HYP vs. *Scn1a*$^{RH/+}$ SIH		q(162)=4,996	**0.0032**	
				Scn1a$^{RH/+}$	SIH	32.644	8.853	9	9					N1:Scn1a$^{RH/+}$ control vs. *Scn1a*$^{RH/+}$ SIH		q(162)=4,148	**0.0228**	
			D2	WT	-	1.467	0.346	5	5		Group (Treatment-genotype)	F (3, 27) = 6,318	0.0022	D2:WT control vs. WT HYP	Tuckey's	q(162)=0,2853	> 0,9999	
				Scn1a$^{RH/+}$	-	2.682	0.583	8	8					D2:WT control vs. *Scn1a*$^{RH/+}$ control		q(162)=0,4933	0.9996	
				WT	HYP	3.523	0.749	9	9					D2:WT HYP vs. *Scn1a*$^{RH/+}$ SIH		q(162)=0,7185	0.9966	
				Scn1a$^{RH/+}$	SIH	5.292	1.631	9	9					D2:Scn1a$^{RH/+}$ control vs. *Scn1a*$^{RH/+}$ SIH		q(162)=0,502	0.9995	
			N2	WT	-	8.883	1.512	5	5					N2:WT control vs. WT HYP	Tuckey's	q(162)=0,8329	0.9924	
				Scn1a$^{RH/+}$	-	12.432	1.509	8	8					N2:WT control vs. *Scn1a*$^{RH/+}$ control		q(162)=2,371	0.4525	
				WT	HYP	18.769	3.980	9	9					N2:WT HYP vs. *Scn1a*$^{RH/+}$ SIH		q(162)=3,308	0.1172	
				Scn1a$^{RH/+}$	SIH	24.444	4.954	9	9					N2:Scn1a$^{RH/+}$ control vs. *Scn1a*$^{RH/+}$ SIH		q(162)=1,611	0.8308	
			D3	WT	-	1.583	0.433	5	5		Time	F (5, 135) = 24,76	< 0,0001	D3:WT control vs. WT HYP	Tuckey's	0.3032	> 0,9999	
				Scn1a$^{RH/+}$	-	2.875	0.326	8	8					D3:WT control vs. *Scn1a*$^{RH/+}$ control		0.5897	0.9989	
				WT	HYP	4.042	0.620	9	9					D3:WT HYP vs. *Scn1a*$^{RH/+}$ SIH		q(162)=0,02932	> 0,9999	
				Scn1a$^{RH/+}$	SIH	2.981	0.552	9	9					D3:Scn1a$^{RH/+}$ control vs. *Scn1a*$^{RH/+}$ SIH		q(162)=0,3009	> 0,9999	
			N3	WT	-	7.158	1.287	5	5					N3:WT control vs. WT HYP	Tuckey's	q(162)=1,083	0.9708	
				Scn1a$^{RH/+}$	-	11.771	1.119	8	8					N3:WT control vs. *Scn1a*$^{RH/+}$ control		q(162)=1,339	0.9211	
				WT	HYP	12.741	1.942	9	9					N3:WT HYP vs. *Scn1a*$^{RH/+}$ SIH		q(162)=1,813	0.741	
				Scn1a$^{RH/+}$	SIH	18.356	2.967	9	9					N3:Scn1a$^{RH/+}$ control vs. *Scn1a*$^{RH/+}$ SIH		q(162)=1,594	0.8376	

Three-chamber social interaction test in Scn1aRH/+ -129:B6																		
Mouse model and genetic background	Experiment	Measurment	Protocol phase	Genotype	treatment/protocol	average	S.E.M	# values/slices/cells	# animals	Statistical test	Source of variation	F(DFn,DFd) / t (dF) value/U/χ^2/H	p value	Comparision	post hoc test	t(dF) value / q(dF) value	p value	Figure
Scn1aRH/+-129:B6	Three chamber social interactio test	Distance travelled (m)	Habituation phase	WT	-	20.718	1.470	13	13	Two-way ANOVA	Interaction	F (1, 59) = 4,910	0.0306	WT control vs. WT HYP	Tuckey's	q(59)=0,5149	0.9833	38C
				Scn1a$^{RH/+}$	-	26.629	1.373	16	16		Treatment	F (1, 59) = 7,535	0.008	WT control vs. *Scn1a*$^{RH/+}$ control		q(59)=2,685	0.2398	
				WT	HYP	21.909	1.530	17	17		Genotype	F (1, 59) = 25,12	< 0,0001	WT HYP vs. *Scn1a*$^{RH/+}$ SIH		q(59)=7,555	**< 0,0001**	
				Scn1a$^{RH/+}$	SIH	37.617	3.314	16	16					Scn1a$^{RH/+}$ control vs. *Scn1a*$^{RH/+}$ SIH		q(59)=5,106	**0.0034**	
		Average speed (m/s)	Habituation phase	WT	-	0.035	0.002	13	13	Two-way ANOVA	Interaction	F (1, 58) = 5,256	0.0255	WT control vs. WT HYP	Tuckey's	q(59)=0,5149	0.9833	38B
				Scn1a$^{RH/+}$	-	0.044	0.002	16	16		Treatment	F (1, 58) = 8,120	0.006	WT control vs. *Scn1a*$^{RH/+}$ control		q(59)=2,685	0.2398	
				WT	HYP	0.036	0.003	17	17		Genotype	F (1, 58) = 25,59	< 0,0001	WT HYP vs. *Scn1a*$^{RH/+}$ SIH		q(59)=7,555	**< 0,0001**	
				Scn1a$^{RH/+}$	SIH	0.062	0.005	17	17					Scn1a$^{RH/+}$ control vs. *Scn1a*$^{RH/+}$ SIH		q(59)=5,106	**0.0034**	
		Time in the chamber (s)	Habituation phase	**C1:**WT	-	124.985	17.737	13	13	RM- Two way ANOVA	Interaction	F (6, 177) = 3,213	0.0051	WT control: C1 vs. C2	Sidak's	t(177)=1,605	0.2957	38A
				C:WT	-	302.292	33.575	13	13									
				C2:WT	-	169.739	21.850	13	13									
				C1: *Scn1a*$^{RH/+}$	-	173.400	17.391	16	16		Chamber	F (2, 177) = 46,72	< 0,0001	*Scn1a*$^{RH/+}$ control : C1 vs. C2		t(177)=0,1912	0.9965	
				C: *Scn1a*$^{RH/+}$	-	254.125	21.591	16	16									
				C2: *Scn1a*$^{RH/+}$	-	168.594	11.535	16	16									
				C1:WT	HYP	146.712	13.545	17	17					WT HYP: C1 vs. C2		t(177)=0,2212	0.9947	
				C:WT	HYP	292.965	25.432	17	17									
				C2:WT	HYP	152.106	15.605	17	17		Group (Treatment-genotype)	F (3, 177) = 0,005712	0.9994					
				C1: *Scn1a*$^{RH/+}$	SIH	178.712	10.768	17	17					*Scn1a*$^{RH/+}$ SIH: C1 vs. C2		t(177)=0,4147	0.9669	
				C: *Scn1a*$^{RH/+}$	SIH	226.194	10.895	17	17									
				C2: *Scn1a*$^{RH/+}$	SIH	188.824	9.170	17	17									
		Interaction time (s)	Sociability phase	**EC:**WT	-	111.170	12.998	10	10	RM- Two way ANOVA	Interaction	F (3, 102) = 1,941	0.1277	WT control: EC vs. M	Sidak's	t(102)=2,570	**0.0457**	38D
				M:WT	-	167.830	20.922	10	10									
				EC: *Scn1a*$^{RH/+}$	-	96.100	9.994	15	15		Cage	F (1, 102) = 15,79	0.0001	Scn1aRH/+ control : EC vs. M		t(102)=2,707	**0.0314**	
				M: *Scn1a*$^{RH/+}$	-	144.840	12.114	15	15									
				EC:WT	HYP	112.444	9.542	16	16					WT HYP: EC vs. M		t(102)=2,741	**0.0286**	
				M:WT	HYP	160.219	11.413	16	16		Group (Treatment-genotype)	F (3, 102) = 1,468	0.2277					
				EC: *Scn1a*$^{RH/+}$	SIH	147.471	18.404	14	14					Scn1aRH/+ SIH: EC vs. M		t(102)=0,069	> 0,9999	
				M: *Scn1a*$^{RH/+}$	SIH	146.186	12.129	14	14									
		Average speed (m/s)	Sociability phase	WT	-	0.038	0.002	10	10	Two-way ANOVA	Interaction	F (1, 51) = 0,4221	0.5188	WT control vs. WT HYP	Tuckey's	q(51)=1,381	0.7633	not shown
				Scn1a$^{RH/+}$	-	0.045	0.003	15	15		Treatment	F (1, 51) = 4,350	0.042	WT control vs. *Scn1a*$^{RH/+}$ control		q(51)=1,666	0.6431	
				WT	HYP	0.043	0.002	16	16		Genotype	F (1, 51) = 5,782	0.0199	WT HYP vs. *Scn1a*$^{RH/+}$ SIH		q(51)=2,854	0.1949	
				Scn1a$^{RH/+}$	SIH	0.055	0.006	14	14					Scn1a$^{RH/+}$ control vs. *Scn1a*$^{RH/+}$ SIH		q(51)=3,235	0.1143	
		Interaction time (s)	Social Novelty phase	**fM:**WT	-	80.500	9.741	10	10	RM- Two way ANOVA	Interaction	F (3, 102) = 1,905	0.1335	WT control: fM vs. nM	Sidak's	t(102)=2,540	**0.0495**	38E
				nM:WT	-	117.360	9.051	10	10									
				fM: *Scn1a*$^{RH/+}$	-	68.007	6.451	15	15		Cage	F (1, 102) = 17,38	< 0,0001	Scn1aRH/+ control : fM vs. nM		t(102)=2,953	**0.0155**	
				nM: *Scn1a*$^{RH/+}$	-	103.000	7.704	15	15									
				fM:WT	HYP	68.325	5.244	16	16					WT HYP: fM vs. nM		t(102)=2,824	**0.0226**	
				nM:WT	HYP	100.725	6.523	16	16		Group (Treatment-genotype)	F (3, 102) = 2,157	0.0977					
				fM: *Scn1a*$^{RH/+}$	SIH	101.679	12.268	14	14					Scn1aRH/+ SIH: fM vs. nM		t(102)=0,05357	> 0,9999	
				nM: *Scn1a*$^{RH/+}$	SIH	102.336	11.979	14	14									
		Average speed (m/s)	Social Novelty phase	WT	-	0.050	0.008	10	10	Two-way ANOVA	Interaction	F (1, 51) = 6,241	0.0157	WT control vs. WT HYP	Tuckey's	q(51)=2,689	0.2402	not shown
				Scn1a$^{RH/+}$	-	0.041	0.003	15	15		Treatment	F (1, 51) = 0,08887	0.7668	WT control vs. *Scn1a*$^{RH/+}$ control		q(51)=1,994	0.4993	
				WT	HYP	0.039	0.002	16	16		Genotype	F (1, 51) = 0,1591	0.6916	WT HYP vs. *Scn1a*$^{RH/+}$ SIH		q(51)=2,295	0.3751	
				Scn1a$^{RH/+}$	SIH	0.050	0.003	14	14					Scn1a$^{RH/+}$ control vs. *Scn1a*$^{RH/+}$ SIH		q(51)=3,069	0.1454	

Morris Water Mazein Scn1aRH/+ -129:B6																			
Mouse model and genetic background	Experiment	Measurment	Protocol phase	Genotype	treatment/protocol	average	S.E.M	# values/slices/cells	# animals	Statistical test	Source of variation	F(DFn,DFd) / t (dF) value/U/χ^2/H	p value	Comparision	post hoc test	t(dF) value / q(dF) value	p value	Figure
	Morris Water Maze	Latency to find the cued platform (s) - CUE TASK	D1	WT	-	17.554	2.501	76	19	Two-Way RM ANOVA	Interaction	F (3, 336) = 2,259	0.0814	WT control : Cue task 1 vs. Cue task 2	Sidak's	t(336)=4,163	**0.0002**	39A
			D2			5.293	0.683	76	19									
			D1	WT	HYP	16.296	2.391	92	23					WT HYP: Cue task 1 vs. Cue task 2	Sidak's	t(336)=3,736	**0.0009**	
			D2			6.296	0.910	92	23		Cue task Day	F (1, 336) = 101,8	< 0,0001					
			D1	Scn1aRH/+	-	17.810	2.353	88	22					Scn1aRH/+ control : Cue task 1 vs. Cue task 2	Sidak's	t(336)=5,242	**< 0,0001**	
			D2			3.463	0.332	88	22									
			D1	Scn1aRH/+	SIH	29.068	3.569	84	21		Group (Treatment-genotype)	F (3, 336) = 7,057	0.0001	Scn1aRH/+ SIH: Cue task 1 vs. Cue task 2	Sidak's	t(336)=7,042	**< 0,0001**	
			D2			9.340	1.617	84	21									
	Morris Water Maze	Latency to find the cued platform (s) - CUE TASK	D1	WT	-	17.554	2.501	76	19	Two-Way RM ANOVA	Interaction	F (3, 336) = 2,259	0.0814	Cue task 1: WT control vs. WT HYP	Tuckey's	q(672)=0,6033	0.9739	39A
				Scn1aRH/+	-	17.810	2.353	88	22					Cue task 1:WT control vs. *Scn1a*$^{RH/+}$ control		q(672)=0,08600	> 0,9999	
				WT	HYP	16.296	2.391	92	23					Cue task 1: WT HYP vs. *Scn1a*$^{RH/+}$ SIH		q(672)=6,290	**< 0,0001**	
				Scn1aRH/+	SIH	29.068	3.569	84	21		Cue task Day	F (1, 336) = 101,8	< 0,0001	Cue task 1: *Scn1a*$^{RH/+}$ control vs. *Scn1a*$^{RH/+}$ SIH		q(672)=5,485	**0.0007**	
			D2	WT	-	5.293	0.683	76	19					Cue task 2: WT control vs. WT HYP		q(672)=0,4805	0.9865	
				Scn1aRH/+	-	3.463	0.332	88	22		Group (Treatment-genotype)	F (3, 336) = 7,057	0.0001	Cue task 2:WT control vs. *Scn1a*$^{RH/+}$ control		q(672)=0,6144	0.6144	
				WT	HYP	6.296	0.910	92	23					Cue task 2: WT HYP vs. *Scn1a*$^{RH/+}$ SIH		q(672)=1,499	0.7138	
				Scn1aRH/+	SIH	9.340	1.617	84	21					Cue task 2: *Scn1a*$^{RH/+}$ control vs. *Scn1a*$^{RH/+}$ SIH		q(672)=2,864	0.1798	
	Morris Water Maze	Average speed (m/s) CUETASK	D1	WT	-	0.128	0.006	76	19	Two-Way RM ANOVA	Interaction	F (3, 336) = 0,5145	0.6726	Cue task 1: WT control vs. WT HYP	Tuckey's	q(672)=0,8557	0.9305	Table 12
				Scn1aRH/+	-	0.132	0.006	88	22		Cue task Day	F (1, 336) = 5,212	0.0231	Cue task 1:WT control vs. *Scn1a*$^{RH/+}$ control		q(672)=0,5562	0.1121	
				WT	HYP	0.134	0.006	92	23		Seizures	F (3, 336) = 4,919	0.0023	Cue task 1: WT HYP vs. *Scn1a*$^{RH/+}$ SIH		q(672)=4,211	**0.0159**	
				Scn1aRH/+	SIH	0.104	0.006	84	21					Cue task 1: *Scn1a*$^{RH/+}$ control vs. *Scn1a*$^{RH/+}$ SIH		q(672)=3,867	**0.0324**	
			D2	WT	-	0.146	0.009	76	19	Two-Way RM ANOVA	Interaction	F (3, 336) = 0,5145	0.6726	Cue task 2: WT control vs. WT HYP	Tuckey's	q(672)=1,016	0.8897	
				Scn1aRH/+	-	0.138	0.008	88	22		Cue task Day	F (1, 336) = 5,212	0.0231	Cue task 2:WT control vs. *Scn1a*$^{RH/+}$ control		q(672)=1,068	0.8745	
				WT	HYP	0.138	0.009	92	23		Group (Treatment-genotype)	F (3, 336) = 4,919	0.0023	Cue task 2: WT HYP vs. *Scn1a*$^{RH/+}$ SIH		q(672)=2,460	0.3039	
				Scn1aRH/+	SIH	0.121	0.007	84	21					Cue task 2: *Scn1a*$^{RH/+}$ control vs. *Scn1a*$^{RH/+}$ SIH		q(672)=2,370	0.3371	
	Morris Water Maze	Distance travelled (m) - CUETASK	D1	WT	-	2.970763	0.4965251	76	19	Two-Way RM ANOVA	Interaction	F (3, 332) = 0,7880	0.5013	Cue task 1: WT control vs. WT HYP	Tuckey's	q(664)=0,7936	0.9435	Table 13
				Scn1aRH/+	-	2.653614	0.3747214	88	22		Cue task Day	F (1, 332) = 57,91	< 0,0001	Cue task 1:WT control vs. *Scn1a*$^{RH/+}$ control		q(664)=0,7803	0.9461	
				WT	HYP	2.644679	0.4470432	84	23		Seizures	F (3, 332) = 4,410	0.0047	Cue task 1: WT HYP vs. *Scn1a*$^{RH/+}$ SIH		q(664)=4,279	**0.0137**	
				Scn1aRH/+	SIH	4.338921	0.6543971	88	21					Cue task 1: *Scn1a*$^{RH/+}$ control vs. *Scn1a*$^{RH/+}$ SIH		q(664)=4,307	**0.0129**	
			D2	WT	-	1.223474	0.2069968	76	19	Two-Way RM ANOVA	Interaction	F (3, 332) = 0,7880	0.5013	Cue task 2: WT control vs. WT HYP	Tuckey's	q(664)=0,3639	0.994	
				Scn1aRH/+	-	0.5581932	0.075622	88	22		Cue task Day	F (1, 332) = 57,91	< 0,0001	Cue task 2:WT control vs. *Scn1a*$^{RH/+}$ control		q(664)=1,637	0.654	
				WT	HYP	1.073941	0.2038943	84	23		Group (Treatment-genotype)	F (3, 332) = 4,410	0.0047	Cue task 2: WT HYP vs. *Scn1a*$^{RH/+}$ SIH		q(664)=1,62	0.6616	
				Scn1aRH/+	SIH	1.715159	0.3986418	88	21					Cue task 2: *Scn1a*$^{RH/+}$ control vs. *Scn1a*$^{RH/+}$ SIH		q(664)=2,957	0.1571	
	Morris Water Maze	Latency to find the hidden platform (s) - Spatial learning	D1	WT	-	32.04473	3.67175	76	19	Two-Way RM ANOVA	Interaction	F (9, 1008) = 1,063	0.3877	WT: Training 1 vs. Training 2	Tuckey's	q(1008)=9,827	**< 0,0001**	39A
			D2			8.242105	0.8416948	76	19					WT: Training 1 vs. Training 3		q(1008)=10,24	**< 0,0001**	
			D3			7.247368	1.002153	76	19					WT: Training 1 vs. Training 4		q(1008)=9,948	**< 0,0001**	
														WT: Training 2 vs. Training 3		q(1008)=0,4107	0.9915	
			D4			7.948684	1.358431	76	19					WT: Training 2 vs. Training 4		q(1008)=0,1211	0.9998	
														WT: Training 3 vs. Training 4		q(1008)=0,2896	0.997	
			D1	WT	HYP	32.22717	3.422416	92	23					WT HYP: Training 1 vs. Training 2		q(1008)=9,399	**< 0,0001**	
			D2			11.53696	1.807323	92	23					WT HYP: Training 1 vs. Training 3		q(1008)=10,77	**< 0,0001**	
			D3			8.513043	1.087739	92	23					WT HYP: Training 1 vs. Training 4		q(1008)=11,46	**< 0,0001**	
											Training Day	F (3, 1008) = 117,0	< 0,0001	WT HYP: Training 2 vs. Training 3		q(1008)=1,374	0.7658	
			D4			6.998913	1.016919	92	23					WT HYP: Training 2 vs. Training 4		q(1008)=2,061	0.4637	
														WT HYP: Training 3 vs. Training 4		q(1008)=0,6878	0.9621	
			D1	Scn1aRH/+	-	29.22955	3.296376	88	22					*Scn1a*$^{RH/+}$ control: Training 1 vs. Training 2	Tuckey's	q(1008)=7,948	**< 0,0001**	
			D2			11.33977	1.36383	88	22					*Scn1a*$^{RH/+}$ control: Training 1 vs. Training 3		q(1008)=9,127	**< 0,0001**	
			D3			8.685227	1.229834	88	22					*Scn1a*$^{RH/+}$ control: Training 1 vs. Training 4		q(1008)=10,2	**< 0,0001**	
														Scn1a$^{RH/+}$ control: Training 2 vs. Training 3		q(1008)=1,179	0.8383	
			D4			6.267045	0.7822427	88	22					*Scn1a*$^{RH/+}$ control: Training 2 vs. Training 4		q(1008)=2,254	0.3827	
														Scn1a$^{RH/+}$ control: Training 3 vs. Training 4		q(1008)=1,074	0.8725	
			D1	Scn1aRH/+	SIH	57.88572	3.629017	84	21		Group (Treatment-genotype)	F (3, 336) = 55,50	< 0,0001	*Scn1a*$^{RH/+}$ SIH: Training 1 vs. Training 2	Tuckey's	q(1008)=12,54	**< 0,0001**	
			D2			28.98571	3.359673	84	21					*Scn1a*$^{RH/+}$ SIH: Training 1 vs. Training 3		q(1008)=13,56	**< 0,0001**	
			D3			26.64881	3.134997	84	21					*Scn1a*$^{RH/+}$ SIH: Training 1 vs. Training 4		q(1008)=14,02	**< 0,0001**	
														Scn1a$^{RH/+}$ SIH: Training 2 vs. Training 3		q(1008)=1,014	0.8903	
			D4			25.59524	3.211734	84	21					*Scn1a*$^{RH/+}$ SIH: Training 2 vs. Training 4		q(1008)=1,472	0.7256	
														Scn1a$^{RH/+}$ SIH: Training 3 vs. Training 4		q(1008)=0,4573	0.9883	

Scn1aRH/+-129/B6	Morris Water Maze	Latency to find the hidden platform (s)	t1-D1	**WT**	-	67,88421	6,222804	19	19	Two-Way RM ANOVA	Interaction	F (9, 246) = 1,007	P = 0,4351	Trial 1: WT control vs. WT HYP	Tuckey's	q(328)=1,16	0.845	**39B**
				Scn1aRH/+	-	64	6,950537	22	22		Trial	F (3, 246) = 58,27	P < 0,0001	Trial 1: WT control vs. *Scn1a*$^{RH/+}$ control		q(328)=0,6534	0.9672	
				WT	HYP	61,06087	6,284087	23	23		Seizures	F (3, 82) = 15,95	P < 0,0001	Trial 1: WT HYP vs. *Scn1a*$^{RH/+}$ SIH		q(328)=3,356	0.0844	
				Scn1aRH/+	SIH	80,05454	4,602327	22	22					Trial 1: Scn1a$^{RH/+}$ control vs. *Scn1a*$^{RH/+}$ SIH		q(328)=2,805	0.1962	
	Morris Water Maze	Latency to find the hidden platform (s)	t1-D1	**WT**	-	67,88421	6,222804	19	19	Two-Way RM ANOVA	Interaction	F (9, 246) = 1,007	P = 0,4351	WT control: Trial1 vs.Trial 2	Tuckey's	q(246)=6,789	**< 0,0001**	**39B**
			t2-D1			27,94737	7,072909	19	19									
			t1-D1	**Scn1aRH/+**	-	64	6,950537	22	22					Scn1aRH/+ control : Trial1 vs.Trial 2		q(246)=7,257	**< 0,0001**	
			t2-D1			24,32727	5,898617	22	22		Trial	F (3, 246) = 58,27	P < 0,0001					
			t1-D1	**WT**	HYP	61,06087	6,284087	23	23					WT HYP : Trial1 vs.Trial 2		q(246)=5,400	**0.001**	
			t2-D1			32,18696	7,241072	23	23									
			t1-D1	**Scn1aRH/+**	SIH	80,05454	4,602327	22	22		Group (Treatment-genotype)	F (3, 82) = 15,95	P < 0,0001	Scn1aRH/+ SIH: Trial1 vs.Trial 2		q(246)=4,468	**0.0096**	
			t2-D1			55,62727	7,725384	22	22									
	Morris Water Maze	Latency to find the hidden platform - SPATIAL LEARNING	D1	**WT**	-	32,04473	3,67175	76	19	Two-Way RM ANOVA	Interaction	F (9, 1008) = 1,063	0.3877	**Training 1:** WT control vs. WT HYP	Tuckey's	q(1344)=0,07479	> 0,9999	**39A**
				Scn1aRH/+	-	32,22717	3,422416	92	23					**Training 1:** WT control vs. *Scn1a*$^{RH/+}$ control		q(1344)=1,142	0.8508	
				WT	HYP	29,22955	3,296376	88	22					**Training 1:** WT HYP vs. *Scn1a*$^{RH/+}$ SIH		q(1344)=10,8	**< 0,0001**	
				Scn1aRH/+	SIH	57,88572	3,629017	84	21					**Training 1:** Scn1a$^{RH/+}$ control vs. *Scn1a*$^{RH/+}$ SIH		q(1344)=11,94	**< 0,0001**	
			D2	**WT**	-	8,242105	0,8416948	76	19					**Training 2:** WT control vs. WT HYP	Tuckey's	q(1344)=1,351	0.775	
				Scn1aRH/+	-	11,53696	1,807323	92	23					**Training 2:** WT control vs. *Scn1a*$^{RH/+}$ control		q(1344)=1,257	0.8107	
				WT	HYP	11,33977	1,36383	88	22		Training Day	F (3, 1008) = 117,0	< 0,0001	**Training 2:** WT HYP vs. *Scn1a*$^{RH/+}$ SIH		q(1344)=7,347	**< 0,0001**	
				Scn1aRH/+	SIH	28,98571	3,359673	84	21					**Training 2:** Scn1a$^{RH/+}$ control vs. *Scn1a*$^{RH/+}$ SIH		q(1344)=7,351	**< 0,0001**	
			D3	**WT**	-	7,247368	1,002153	76	19					**Training 3:** WT control vs. WT HYP	Tuckey's	q(1344)=0,5188	0.9831	
				Scn1aRH/+	-	8,513043	1,087739	92	23					**Training 3:**WT control vs. *Scn1a*$^{RH/+}$ control		q(1344)=0,5834	0.9763	
				WT	HYP	8,685227	1,229834	88	22					**Training 3:**WT HYP vs. *Scn1a*$^{RH/+}$ SIH		q(1344)=7,636	**< 0,0001**	
				Scn1aRH/+	SIH	26,64881	3,134997	84	21		Group (Treatment-genotype)	F (3, 336) = 55,50	< 0,0001	**Training 3:** Scn1a$^{RH/+}$ control vs. *Scn1a*$^{RH/+}$ SIH		q(1344)=7,483	**< 0,0001**	
			D4	**WT**	-	7,948684	1,358431	76	19					**Training 4:** WT control vs. WT HYP	Tuckey's	q(1344)=0,3893	0.9927	
				Scn1aRH/+	-	6,998913	1,016919	92	23					**Training 4:** WT control vs. *Scn1a*$^{RH/+}$ control		q(1344)=0,6824	0.963	
				WT	HYP	6,267045	0,7822427	88	22					**Training 4:** WT HYP vs. *Scn1a*$^{RH/+}$ SIH		q(1344)=7,83	**< 0,0001**	
				Scn1aRH/+	SIH	25,59524	3,211734	84	21					**Training 4:** Scn1a$^{RH/+}$ control vs. *Scn1a*$^{RH/+}$ SIH		q(1344)=8,051	**< 0,0001**	
	Morris Water Maze	Average speed (m/s)	D1	WT	-	0,1731	0,0064	76	19	Two-Way RM ANOVA	Interaction	F (9, 972) = 1,543	0.1281	Training 1: WT control vs. WT HYP	Tuckey's	q(1296)=1,406	0.7528	**Table 12**
				Scn1aRH/+	-	0,1573	0,0058	88	22					Training 1: WT control vs. *Scn1a*$^{RH/+}$ control		q(1296)=2,347	0.3455	
				WT	HYP	0,1634	0,0069	80	20					Training 1: WT HYP vs. *Scn1a*$^{RH/+}$ SIH		q(1296)=4,189	**0.0164**	
				Scn1aRH/+	SIH	0,1915	0,0056	84	21					Training 1: Scn1a$^{RH/+}$ control vs. *Scn1a*$^{RH/+}$ SIH		q(1296)=5,224	**0.0013**	
			D2	WT	-	0,1398	0,0066	76	19					Training 2: WT control vs. WT HYP	Tuckey's	q(1296)=0,6093	0.9732	
				Scn1aRH/+	-	0,1388	0,0061	88	22					Training 2: WT control vs. *Scn1a*$^{RH/+}$ control		q(1296)=0,1489	0.9996	
				WT	HYP	0,1440	0,0078	80	20		Training Day	F (3, 972) = 17,11	< 0,0001	Training 2: WT HYP vs. *Scn1a*$^{RH/+}$ SIH		q(1296)=3,484	0.0662	
				Scn1aRH/+	SIH	0,1673	0,0063	84	21					Training 2: Scn1a$^{RH/+}$ control vs. *Scn1a*$^{RH/+}$ SIH		q(1296)=4,361	**0.0112**	
			D3	WT	-	0,1197	0,0073	76	19					Training 3: WT control vs. WT HYP	Tuckey's	q(1296)=4,268	**0.0138**	
				Scn1aRH/+	-	0,1390	0,0067	88	22					Training 3:WT control vs. *Scn1a*$^{RH/+}$ control		q(1296)=2,881	0.175	
				WT	HYP	0,1490	0,0079	80	20					Training 3:WT HYP vs. *Scn1a*$^{RH/+}$ SIH		q(1296)=3,127	0.1207	
				Scn1aRH/+	SIH	0,1699	0,0062	84	21					Training 3: Scn1a$^{RH/+}$ control vs. *Scn1a*$^{RH/+}$ SIH		q(1296)=4,727	**0.0047**	
			D4	WT	-	0,1255	0,0065	76	19		Group (Treatment-genotype)	F (3, 324) = 20,77	< 0,0001	Training 4: WT control vs. WT HYP	Tuckey's	q(1296)=2,341	0.3479	
				Scn1aRH/+	-	0,1299	0,0073	88	22					Training 4: WT control vs. *Scn1a*$^{RH/+}$ control		q(1296)=0,6571	0.9667	
				WT	HYP	0,1416	0,0076	80	20					Training 4: WT HYP vs. *Scn1a*$^{RH/+}$ SIH		q(1296)=4,775	**0.0042**	
				Scn1aRH/+	SIH	0,1735	0,0057	84	21					Training 4: Scn1a$^{RH/+}$ control vs. *Scn1a*$^{RH/+}$ SIH		q(1296)=6,674	**< 0,0001**	
	Morris Water Maze	Distance travelled (m)	D1	WT	-	6,460737	0,7937213	76	19	Two-Way RM ANOVA	Interaction	F (9, 1020) = 0,8253	0.5928	Training 1: WT control vs. WT HYP	Tuckey's	q(1296)=0,4226	0.9907	**Table 13**
				Scn1aRH/+	-	5,556216	0,6823414	88	22					Training 1: WT control vs. *Scn1a*$^{RH/+}$ control		q(1296)=1,65	0.6481	
				WT	HYP	6,23138	0,6989641	80	20					Training 1: WT HYP vs. *Scn1a*$^{RH/+}$ SIH		q(1296)=10,46	**< 0,0001**	
				Scn1aRH/+	SIH	11,68935	0,8374145	84	21					Training 1: Scn1a$^{RH/+}$ control vs. *Scn1a*$^{RH/+}$ SIH		q(1296)=11,62	**< 0,0001**	
			D2	WT	-	1,315329	0,1638174	76	19					Training 2: WT control vs. WT HYP	Tuckey's	q(1296)=1,384	0.7616	
				Scn1aRH/+	-	1,921886	0,2769157	88	22					Training 2: WT control vs. *Scn1a*$^{RH/+}$ control		q(1296)=1,106	0.8625	
				WT	HYP	2,066435	0,364425	80	20		Training Day	F (3, 1020) = 99,83	< 0,0001	Training 2: WT HYP vs. *Scn1a*$^{RH/+}$ SIH		q(1296)=7,731	**< 0,0001**	
				Scn1aRH/+	SIH	6,10242	0,7526377	84	21					Training 2: Scn1a$^{RH/+}$ control vs. *Scn1a*$^{RH/+}$ SIH		q(1296)=7,921	**< 0,0001**	
			D3	WT	-	1,139329	0,2044359	76	19					Training 3: WT control vs. WT HYP	Tuckey's	q(1296)=0,8549	0.9307	
				Scn1aRH/+	-	1,435739	0,2222679	88	22					Training 3:WT control vs. *Scn1a*$^{RH/+}$ control		q(1296)=0,5407	0.981	
				WT	HYP	1,603261	0,2461549	80	20					Training 3:WT HYP vs. *Scn1a*$^{RH/+}$ SIH		q(1296)=8,188	**< 0,0001**	
				Scn1aRH/+	SIH	5,877432	0,7365466	84	21					Training 3: Scn1a$^{RH/+}$ control vs. *Scn1a*$^{RH/+}$ SIH		q(1296)=8,416	**< 0,0001**	
			D4	WT	-	1,295526	0,2833215	76	19		Group (Treatment-genotype)	F (3, 340) = 54,81	< 0,0001	Training 4: WT control vs. WT HYP	Tuckey's	q(1296)=0,1389	0.9997	
				Scn1aRH/+	-	1,025261	0,1717624	88	22					Training 4: WT control vs. *Scn1a*$^{RH/+}$ control		q(1296)=0,493	0.9855	
				WT	HYP	1,22013	0,2120321	80	20					Training 4: WT HYP vs. *Scn1a*$^{RH/+}$ SIH		q(1296)=7,513	**< 0,0001**	

	Morris Water Maze	Presence in quadrant (%)	Probe test	WT: LEFT	-	17.11351	1.590523	19	19	RM-Two Way ANOVA	Interaction	F (9, 243) = 6,353	< 0,0001	WT: LEFT vs. TARGET	Sidak's	q(243)=14,33	**< 0,0001**	**39C**
				WT: TARGET		56.76281	3.567275	19	19					WT: TARGET vs. RIGHT		q(243)=14,91	**< 0,0001**	
				WT: RIGHT		15.52632	2.157894	19	19					WT: TARGET vs. OPPOSITE		q(243)=16,72	**< 0,0001**	
				WT: OPPOSITE		10.5	2.111683	19	19									
				WT: LEFT	HYP	24.55077	2.435804	23	23					WT HYP: LEFT vs. TARGET	Sidak's	q(243)=10,46	**< 0,0001**	
				WT: TARGET		50.85536	2.845297	23	23		Quadrant	F (3, 243) = 166,1	< 0,0001	WT HYP: TARGET vs. RIGHT		q(243)=14,58	**< 0,0001**	
				WT: RIGHT		14.20072	1.664953	23	23					WT HYP: TARGET vs. OPPOSITE		q(243)=16,23	**< 0,0001**	
				WT: OPPOSITE		10.05507	1.590904	23	23									
				Scn1aRH/+: LEFT	-	19.53106	1.379024	22	22					Scn1aRH/+: LEFT vs. TARGET	Sidak's	q(243)=13,82	**< 0,0001**	
				Scn1aRH/+: TARGET		55.06091	3.040268	22	22					Scn1aRH/+: TARGET vs. RIGHT		q(243)=15,49	**< 0,0001**	
				Scn1aRH/+: RIGHT		15.24242	2.271501	22	22					Scn1aRH/+: TARGET vs. OPPOSITE		q(243)=17,52	**< 0,0001**	
				Scn1aRH/+: OPPOSITE		10.03061	1.408996	22	22									
				Scn1aRH/+: LEFT	SIH	26.3889	2.395459	21	21		Group (Treatment-genotype)	F (3, 81) = 1,820	0.15	Scn1aRH/+ SIH: LEFT vs. TARGET	Sidak's	q(243)=3,55	0.0608	
				Scn1aRH/+: TARGET		35.73079	2.968656	21	21					Scn1aRH/+ SIH: TARGET vs. RIGHT		q(243)=6,508	**< 0,0001**	
				Scn1aRH/+: RIGHT		18.60619	1.648541	21	21					Scn1aRH/+SIH : TARGET vs. OPPOSITE		q(243)=6,356	**< 0,0001**	
				Scn1aRH/+: OPPOSITE		19.00603	1.901427	21	21									
	Morris Water Maze	Presence in quadrant (%)	Probe test	WT: TARGET	-	56.76281	3.567275	19	19	RM-Two Way ANOVA	Interaction	F (9, 243) = 6,353	< 0,0001	Target: WT control vs. WT HYP	Tuckey's	q(324)=2,58	0.3488	**39C**
				Scn1aRH/+: TARGET	-	50.85536	2.845297	23	23		Quadrant	F (3, 243) = 166,1	< 0,0001	Target: WT control vs. *Scn1a*$^{RH/+}$ control		q(324)=0,7359	0.9961	
				WT: TARGET	HYP	55.06091	3.040268	22	22		Group (Treatment-genotype)	F (3, 81) = 1,820	0.15	Target: WT HYP vs. *Scn1a*$^{RH/+}$ SIH		q(324)=6,786	**< 0,0001**	
				Scn1aRH/+: TARGET	SIH	35.73079	2.968656	21	21					Target: Scn1a$^{RH/+}$ control vs. *Scn1a*$^{RH/+}$ SIH		q(324)=8,58	**< 0,0001**	
	Morris Water Maze	Target quadrant/Difference to chance level	Probe test	WT	-	56.76281	3.567275	19	19	One sample t-test	-	t(18)=8,904	< 0,0001	-	-	-	-	**39C**
				Chance level		25.000					-							
				WT	HYP	55.06091	3.040268	22	22		-	t(22)=9,087	< 0,0001	-	-	-	-	
				Chance level		25.000					-							
				Scn1aRH/+	-	50.85536	2.845297	23	23		-	t(21)=9,888	< 0,0001	-	-	-	-	
				Chance level		25.000					-							
				Scn1aRH/+	SIH	35.73079	2.968656	21	21		-	t(20)=3,615	0.0017	-	-	-	-	
				Chance level		25.000					-							
	Morris Water Maze	Number of platform crosses	Probe test	WT	-	13.737	0.908	19	19	Two-Way ANOVA	Interaction	F (1, 81) = 8,504	0.0046	WT control vs. WT HYP	Tuckey's	q(81)=2,722	0.2259	**39D**
				Scn1aRH/+	-	13.182	0.755	22	22		Treatment	F (1, 81) = 32,03	< 0,0001	WT control vs. *Scn1a*$^{RH/+}$ control		q(81)=0,626	0.9709	
				WT	HYP	11.348	1.055	23	23		Genotype	F (1, 81) = 12,63	0.0006	WT HYP vs. *Scn1a*$^{RH/+}$ SIH		q(81)=6,593	**< 0,0001**	
				Scn1aRH/+	SIH	5.714	0.673	21	21					Scn1a$^{RH/+}$ control vs. *Scn1a*$^{RH/+}$ SIH		q(81)=8,646	**< 0,0001**	

Contextual-fear conditioningin Scn1aRH/+ -129:B6																	
Mouse model and genetic background	Experiment	Measurment	Protocol phase	Genotype	treatment/protocol	average	S.E.M	# values/slices/cells	# animals	Statistical test	Source of variation	F(DFn,DFd) / t (dF) value/U/χ^2/H	p value	Comparision	post hoc test	t(dF) value / q(dF) value	p value	**Figure**
Scn1aRH/+-129:B6	**Contextual Fear Conditioning**	**Freezing %**	CONDITIONING	WT	-	21.09296	3.291269	18	18	Two-Way ANOVA	Interaction	F (1, 63) = 0,2228	0.6385	WT control vs. WT HYP	Tuckey's	q(63)=1,237	0.818	**40A**
				Scn1aRH/+	-	11.52091	2.292139	22	22		Treatment	F (1, 63) = 0,6443	0.4252	WT control vs. *Scn1a*$^{RH/+}$ control		q(63)=3,373	0.0904	
				WT	HYP	17.07436	4.300251	13	13		Genotype	F (1, 63) = 6,576	0.0127	WT HYP vs. *Scn1a*$^{RH/+}$ SIH		q(63)=0,3415	0.995	
				Scn1aRH/+	SIH	10.47857	2.789497	14	14					Scn1a$^{RH/+}$ control vs. *Scn1a*$^{RH/+}$ SIH		q(63)=1,918	0.5311	
			TEST	WT	-	75.07111	4.162738	18	18	Two-Way ANOVA	Interaction	F (1, 64) = 0,1338	0.7157	WT control vs. WT HYP	Tuckey's	q(63)=1,633	0.4939	**40B**
				Scn1aRH/+	-	56.56424	4.336703	22	22		Treatment	F (1, 64) = 7,673	0.0073	WT control vs. *Scn1a*$^{RH/+}$ control		q(63)=2,422	0.1048	
				WT	HYP	60.77692	7.499846	13	13		Genotype	F (1, 64) = 12,10	0.0009	WT HYP vs. *Scn1a*$^{RH/+}$ SIH		q(63)=2,316	0.1345	
				Scn1aRH/+	SIH	37.91956	8.232697	15	15					Scn1a$^{RH/+}$ control vs. *Scn1a*$^{RH/+}$ SIH		q(63)=2,509	0.0848	

Radial Maze in Scn1aRH/+ -129:B6																		
Mouse model and genetic background	Experiment	Measurment	Protocol phase	Genotype	treatment/protocol	average	S.E.M	# values/slices/cells	# animals	Statistical test	Source of variation	F(DFn,DFd) / t (dF) value/U/χ^2/H	p value	Comparision	post hoc test	t(dF) value / q(dF) value	p value	Figure
Scn1aRH/+-129:B6	Radial Maze	Number of correct choices	D1	WT	-	3.308	0.1748	13	13	Two-Way RM ANOVA	Interaction	F (27, 540) = 1,922	0.0038	WT control vs. WT HYP	Tuckey's	q(600)=1,833	0.5658	41
				Scn1aRH/+	-	3.5	0.3416	16	16					WT control vs. *Scn1a*$^{RH/+}$ control		q(600)=0,549	0.9801	
				WT	HYP	3.941	0.2496	17	17					WT HYP vs. *Scn1a*$^{RH/+}$ SIH		q(600)=2,967	0.155	
				Scn1aRH/+	SIH	3	0.2915	18	18					Scn1a$^{RH/+}$ control vs. *Scn1a*$^{RH/+}$ SIH		q(600)=1,551	0.6916	
			D2	WT	-	3.692	0.5705	13	13					WT control vs. WT HYP	Tuckey's	q(600)=1,492	0.7168	
				Scn1aRH/+	-	3.875	0.3276	16	16					WT control vs. *Scn1a*$^{RH/+}$ control		q(600)=0,5216	0.9829	
				WT	HYP	3.176	0.2743	17	17					WT HYP vs. *Scn1a*$^{RH/+}$ SIH		q(600)=1,895	0.5376	
				Scn1aRH/+	SIH	3.778	0.2977	18	18					Scn1a$^{RH/+}$ control vs. *Scn1a*$^{RH/+}$ SIH		q(600)=0,3016	0.9966	
			D3	WT	-	3.923	0.2878	13	13					WT control vs. WT HYP	Tuckey's	q(600)=1,65	0.6483	
				Scn1aRH/+	-	4	0.3873	16	16					WT control vs. *Scn1a*$^{RH/+}$ control		q(600)=0,2196	0.9987	
				WT	HYP	3.353	0.2704	17	17					WT HYP vs. *Scn1a*$^{RH/+}$ SIH		q(600)=0,2369	0.9983	
				Scn1aRH/+	SIH	3.278	0.2532	18	18					Scn1a$^{RH/+}$ control vs. *Scn1a*$^{RH/+}$ SIH		q(600)=2,241	0.3883	
			D4	WT	-	3.231	0.3608	13	13		Training Day	F (9, 540) = 18,75	< 0,0001	WT control vs. WT HYP	Tuckey's	q(600)=2,736	0.2146	
				Scn1aRH/+	-	3.5	0.2739	16	16					WT control vs. *Scn1a*$^{RH/+}$ control		q(600)=0,7686	0.9483	
				WT	HYP	4.176	0.2606	17	17					WT HYP vs. *Scn1a*$^{RH/+}$ SIH		q(600)=0,206	0.9989	
				Scn1aRH/+	SIH	4.111	0.3223	18	18					Scn1a$^{RH/+}$ control vs. *Scn1a*$^{RH/+}$ SIH		q(600)=1,896	0.5373	
			D5	WT	-	3.846	0.3553	13	13					WT control vs. WT HYP	Tuckey's	q(600)=0,7462	0.9524	
				Scn1aRH/+	-	3.438	0.3648	16	16					WT control vs. *Scn1a*$^{RH/+}$ control		q(600)=1,167	0.8426	
				WT	HYP	3.588	0.3644	17	17					WT HYP vs. *Scn1a*$^{RH/+}$ SIH		q(600)=1,154	0.847	
				Scn1aRH/+	SIH	3.222	0.384	18	18					Scn1a$^{RH/+}$ control vs. *Scn1a*$^{RH/+}$ SIH		q(600)=0,6679	0.9651	
			D6	WT	-	3.077	0.5122	13	13					WT control vs. WT HYP	Tuckey's	q(600)=2,501	0.2898	
				Scn1aRH/+	-	4	0.3651	16	16					WT control vs. *Scn1a*$^{RH/+}$ control		q(600)=2,635	0.245	
				WT	HYP	3.941	0.3685	17	17					WT HYP vs. *Scn1a*$^{RH/+}$ SIH		q(600)=1,916	0.5284	
				Scn1aRH/+	SIH	3.333	0.2425	18	18					Scn1a$^{RH/+}$ control vs. *Scn1a*$^{RH/+}$ SIH		q(600)=2,068	0.4609	
			D7	WT	-	4	0.4385	13	13					WT control vs. WT HYP	Tuckey's	q(600)=2,893	0.1725	
				Scn1aRH/+	-	4.5	0.3291	16	16					WT control vs. *Scn1a*$^{RH/+}$ control		q(600)=1,427	0.744	
				WT	HYP	5	0.3835	17	17					WT HYP vs. *Scn1a*$^{RH/+}$ SIH		q(600)=3,502	0.0647	
				Scn1aRH/+	SIH	3.889	0.3419	18	18					Scn1a$^{RH/+}$ control vs. *Scn1a*$^{RH/+}$ SIH		q(600)=1,896	0.5373	
			D8	WT	-	4.923	0.3662	13	13		Group (Treatment-genotype)	F (3, 60) = 6,860	0.0005	WT control vs. WT HYP	Tuckey's	q(600)=0,05237	> 0,9999	
				Scn1aRH/+	-	4.813	0.3561	16	16					WT control vs. *Scn1a*$^{RH/+}$ control		q(600)=0,3157	0.9961	
				WT	HYP	4.941	0.3262	17	17					WT HYP vs. *Scn1a*$^{RH/+}$ SIH		q(600)=2,616	0.251	
				Scn1aRH/+	SIH	4.111	0.2668	18	18					Scn1a$^{RH/+}$ control vs. *Scn1a*$^{RH/+}$ SIH		q(600)=2,176	0.4149	
			D9	WT	-	5.538	0.2912	13	13					WT control vs. WT HYP	Tuckey's	q(600)=0,995	0.8957	
				Scn1aRH/+	-	5.375	0.301	16	16					WT control vs. *Scn1a*$^{RH/+}$ control		q(600)=0,4667	0.9876	
				WT	HYP	5.882	0.2556	17	17					WT HYP vs. *Scn1a*$^{RH/+}$ SIH		q(600)=6,459	**< 0,0001**	
				Scn1aRH/+	SIH	3.833	0.3547	18	18					Scn1a$^{RH/+}$ control vs. *Scn1a*$^{RH/+}$ SIH		q(600)=4,783	**0.0043**	
			D10	WT	-	5.769	0.3028	13	13					WT control vs. WT HYP	Tuckey's	q(600)=1,034	0.8845	
				Scn1aRH/+	-	5.813	0.3319	16	16					WT control vs. *Scn1a*$^{RH/+}$ control		q(600)=0,1235	0.9998	
				WT	HYP	5.412	0.3328	17	17					WT HYP vs. *Scn1a*$^{RH/+}$ SIH		q(600)=3,925	**0.029**	
				Scn1aRH/+	SIH	4.167	0.2712	18	18					Scn1a$^{RH/+}$ control vs. *Scn1a*$^{RH/+}$ SIH		q(600)=5,106	**0.0019**	
Scn1aRH/+-129:B6	Radial Maze	Differences to chance level	D1	WT	-	3.308	0.1748	13	13	One sample t-test	D1 : WT control vs. Chance level	t(12)=1,100	0.293	-	-	-	-	41
			D2	WT	-	3.692	0.5705	13	13		D2 : WT control vs. Chance level	t(12)=0,3371	0.7419	-	-	-	-	
			D3	WT	-	3.923	0.2878	13	13		D3 : WT control vs. Chance level	t(12)=1,470	0.1673	-	-	-	-	
			D4	WT	-	3.231	0.3608	13	13		D4 : WT control vs. Chance level	t(12)=0,7462	0.4699	-	-	-	-	
			D5	WT	-	3.846	0.3553	13	13		D5 : WT control vs. Chance level	t(12)=0,9743	0.3491	-	-	-	-	
			D6	WT	-	3.077	0.5122	13	13		D6 : WT control vs. Chance level	t(12)=0,8260	0.4249	-	-	-	-	
			D7	WT	-	4	0.4385	13	13		D7 : WT control vs. Chance level	t(12)=1,140	0.2765	-	-	-	-	
			D8	WT	-	4.923	0.3662	13	13		D8 : WT control vs. Chance level	t(12)=3,886	**0.0022**	-	-	-	-	
			D9	WT	-	5.538	0.2912	13	13		D9 : WT control vs. Chance level	t(12)=7,000	**< 0,0001**	-	-	-	-	
			D10	WT	-	5.769	0.3028	13	13		D10 : WT control vs. Chance level	t(12)=7,493	**< 0,0001**	-	-	-	-	
			Chance level			3.500												
			D1	Scn1aRH/+	-	3.5	0.3416	16	16	One sample t-test	D1 : Scn1aRH/+ control vs. Chance level	t(15)=0,0	1	-	-	-	-	
			D2	Scn1aRH/+	-	3.875	0.3276	16	16		D2 :Scn1aRH/+ control vs. Chance level	t(15)=1,145	0.2702	-	-	-	-	
			D3	Scn1aRH/+	-	4	0.3873	16	16		D3 :Scn1aRH/+ control vs. Chance level	t(15)=1,291	0.2162	-	-	-	-	
			D4	Scn1aRH/+	-	3.5	0.2739	16	16		D4 :Scn1aRH/+ control vs. Chance level	t(15)=0,0	1	-	-	-	-	
			D5	Scn1aRH/+	-	3.438	0.3648	16	16		D5 : Scn1aRH/+ control vs. Chance level	t(15)=0,1713	0.8663	-	-	-	-	
			D6	Scn1aRH/+	-	4	0.3651	16	16		D6 : Scn1aRH/+ control vs. Chance level	t(15)=1,369	0.1911	-	-	-	-	
			D7	Scn1aRH/+	-	4.5	0.3291	16	16		D7 : Scn1aRH/+ control vs. Chance level	t(15)=3,038	**0.0083**	-	-	-	-	
			D8	Scn1aRH/+	-	4.813	0.3561	16	16		D8 : Scn1aRH/+ control vs. Chance level	t(15)=3,686	**0.0022**	-	-	-	-	
			D9	Scn1aRH/+	-	5.375	0.301	16	16		D9 : Scn1aRH/+ control vs. Chance level	t(15)=6,228	**< 0,0001**	-	-	-	-	
			D10	Scn1aRH/+	-	5.813	0.3319	16	16		D10 : Scn1aRH/+ control vs. Chance level	t(15)=6,968	**< 0,0001**	-	-	-	-	
			Chance level			3.500												
			D1	WT	HYP	3.941	0.2496	17	17	One sample t-test	D1 : WT HYP vs. Chance level	t(16)=1,768	0.0962	-	-	-	-	
			D2	WT	HYP	3.176	0.2743	17	17		D2 : WT HYP vs. Chance level	t(16)=1,179	0.2555	-	-	-	-	
			D3	WT	HYP	3.353	0.2704	17	17		D3 : WT HYPvs. Chance level	t(16)=0,5439	0.594	-	-	-	-	
			D4	WT	HYP	4.176	0.2606	17	17		D4 : WT HYP vs. Chance level	t(16)=2,596	0.0195	-	-	-	-	
			D5	WT	HYP	3.588	0.3644	17	17		D5 : WT HYP vs. Chance level	t(16)=0,2421	0.8117	-	-	-	-	
			D6	WT	HYP	3.941	0.3685	17	17		D6 : WT HYP vs. Chance level	t(16)=1,197	0.2487	-	-	-	-	
			D7	WT	HYP	5	0.3835	17	17		D7 : WT HYP vs. Chance level	t(16)=3,912	**0.0012**	-	-	-	-	
			D8	WT	HYP	4.941	0.3262	17	17		D8 : WT HYP vs. Chance level	t(16)=4,418	**0.0004**	-	-	-	-	
			D9	WT	HYP	5.882	0.2556	17	17		D9 : WT HYP vs. Chance level	t(16)=9,322	**< 0,0001**	-	-	-	-	
			D10	WT	HYP	5.412	0.3328	17	17		D10 : WT HYP vs. Chance level	t(16)=5,745	**< 0,0001**	-	-	-	-	
			Chance level			3.500												
			D1	Scn1aRH/+	SIH	3	0.2915	18	18	One sample t-test	D1 : Scn1aRH/+ SIH vs. Chance level	t(17)=1,715	0.1045	-	-	-	-	
			D2	Scn1aRH/+	SIH	3.778	0.2977	18	18		D2 : Scn1aRH/+ SIH vs. Chance level	t(17)=0,9332	0.3638	-	-	-	-	
			D3	Scn1aRH/+	SIH	3.278	0.2532	18	18		D3 :Scn1aRH/+ SIHvs. Chance level	t(17)=0,8778	0.3923	-	-	-	-	
			D4	Scn1aRH/+	SIH	4.111	0.3223	18	18		D4 : Scn1aRH/+ SIHvs. Chance level	t(17)=1,896	0.075	-	-	-	-	
			D5	Scn1aRH/+	SIH	3.222	0.384	18	18		D5 : Scn1aRH/+ SIH vs. Chance level	t(17)=0,7235	0.4792	-	-	-	-	
			D6	Scn1aRH/+	SIH	3.333	0.2425	18	18		D6 : Scn1aRH/+ SIHvs. Chance level	t(17)=0,6872	0.5012	-	-	-	-	
			D7	Scn1aRH/+	SIH	3.889	0.3419	18	18		D7 :Scn1aRH/+ SIH vs. Chance level	t(17)=1,137	0.2712	-	-	-	-	
			D8	Scn1aRH/+	SIH	4.111	0.2668	18	18		D8 : Scn1aRH/+ SIH vs. Chance level	t(17)=2,291	**0.035**	-	-	-	-	
			D9	Scn1aRH/+	SIH	3.833	0.3547	18	18		D9 : Scn1aRH/+ SIH vs. Chance level	t(17)=0,9397	0.3605	-	-	-	-	
			D10	Scn1aRH/+	SIH	4.167	0.2712	18	18		D10 : Scn1aRH/+ SIH vs. Chance level	t(17)=2,459	**0.025**	-	-	-	-	
			Chance level			3.500												

4. RESULTS – CHAPTER 4 – *SCN1A*$^{RH/+}$ - FLUROTHYL

RESULTS Chapter 4- Role of flurothyl-induced seizure in cognitive/behavioral phenotypes in *Scn1a*$^{RH/+}$ - 129:B6.																	
Survival during the flurothyl-induced seizures																	
Mouse model and genetic background	Experiment	Measurment	Protocol phase	Genotype	treatment/protocol	average	S.E.M	# values/slices/cells	# animals	Statistical test	Source of variation	F(DFn,DFd) / t (dF) value/U/χ^2/H	p value	Comparision	post hoc test	t(dF) value / q(dF) value	p value	Figure
Scn1aRH/+ (F1-129:B6)	**Seizures Induction by Flurothyl**	**Survival curve comparision**	Survival percentage at day 10	WT	HYP+Flurothyl	88.235	7.814	17	17	Log-rank (Mantel-Cox) test	Curve comparision	$\chi^2(1)=3,149$	0.076	-	-	-	-	**42A**
				Scn1aRH/+	Flurothyl	61.538	13.493	13	13									

5. RESULTS – CHAPTER 5 – *SCN1A*$^{+/-}$ - DRUG X ADMINISTRATION

RESULTS Chapter 5-Collaborative work using Scn1a$^{+/-}$B6:129 (DS) mouse model																	
Survival curve and spontaneous seizure activity																	
Mouse model and genetic background	Experiment	Measurment	Protocol phase	Genotype	treatment/protocol	average	S.E.M	# values/slices/cells	# animals	Statistical test	Source of variation	F(DFn,DFd) / t (dF) value/U/χ^2/H	p value	Comparision	post hoc test	t(dF) value / q(dF) value	p value	Figure
Scn1a$^{+/-}$ B6:129	**SIH**	**Survival curve comparision**	D10	Scn1a+/- vehicle	-	14.286	7.636	21	21	Log-rank (Mantel-Cox) test	Curve comparision	$\chi^2(1)=8.968$	0.0027	-	-	-	-	44A
				Scn1a+/- SIH	-	57.143	10.799	21	21									
Scn1a+/- B6:129	**SIH**	**Temperature threshold for seizure induction**	D1	Scn1a+/- vehicle	Vehicle	40.744	0.206	16	16	Two-way ANOVA	Interaction	F (4, 96) = 1.317	0.2693	D1: Scn1a+/- vehicle vs. Scn1a+/- SIH	Sidak's	t(96)=1.147	0.7691	44B
				Scn1a+/- SIH	Drug	41.207	0.143	15	15									
			D2	Scn1a+/- vehicle	Vehicle	39.838	0.413	13	13					D2: Scn1a+/- vehicle vs. Scn1a+/- SIH		t(96)=2.324	0.1064	
				Scn1a+/- SIH	Drug	40.862	0.304	13	13		Day	F (4, 96) = 13.30	< 0.0001					
			D3	Scn1a+/- vehicle	Vehicle	38.813	0.402	8	8					D3:Scn1a+/- vehicle vs. Scn1a+/- SIH		t(96)=0.8874	0.9062	
				Scn1a+/- SIH	Drug	38.340	0.565	10	10									
			D4	Scn1a+/- vehicle	Vehicle	39.960	0.181	5	5					D4: Scn1a+/- vehicle vs. Scn1a+/- SIH		t(96)=0.05405	> 0.9999	
				Scn1a+/- SIH	Drug	39.927	0.395	11	11									
			D5	Scn1a+/- vehicle	Vehicle	40.220	0.240	5	5		Treatment	F (1, 96) = 0.9898	0.3223	D5: Scn1a+/- vehicle vs. Scn1a+/- SIH		t(96)=0.309	0.9992	
				Scn1a+/- SIH	Drug	40.410	0.311	10	10									
Scn1a+/- B6:129	**Spontaneous seizure frequency**	**Number of seizures**	D1	Scn1a+/- vehicle	Vehicle	0.8125	0.5261396	16	16	Two-way ANOVA	Interaction	F (9, 190) = 0.1969	0.9943	D1: Scn1a+/- vehicle vs. Scn1a+/- SIH	Sidak's	t(190)=1.355	0.8575	45
				Scn1a+/- SIH	Drug	0	0	15	15									
			N1	Scn1a+/- vehicle	Vehicle	0.375	0.375	16	16					N1: Scn1a+/- vehicle vs. Scn1a+/- SIH		t(190)=0.1807	> 0.9999	
				Scn1a+/- SIH	Drug	0.2666667	0.2666667	15	15									
			D2	Scn1a+/- vehicle	Vehicle	0.7333333	0.3304638	15	15					D2: Scn1a+/- vehicle vs. Scn1a+/- SIH		t(190)=0.7948	0.9962	
				Scn1a+/- SIH	Drug	0.2307692	0.1661728	13	13									
			N2	Scn1a+/- vehicle	Vehicle	2	0.5773503	12	12					N2: Scn1a+/- vehicle vs. Scn1a+/- SIH		t(190)=0.3455	> 0.9999	
				Scn1a+/- SIH	Drug	1.769231	0.7085001	13	13		Day	F (9, 190) = 5.620	< 0.0001					
			D3	Scn1a+/- vehicle	Vehicle	2.625	0.4604928	8	8					D3: Nav 1.1 KO+/- vehicle vs. Nav 1.1 KO+/- SIH		t(190)=0.731	0.9981	
				Scn1a+/- SIH	Drug	2.076923	0.7800521	13	13									
			N3	Scn1a+/- vehicle	Vehicle	2.833333	0.7031674	6	6					N3: Scn1a+/- vehicle vs. Scn1a+/- SIH		t(190)=0.9476	0.9854	
				Scn1a+/- SIH	Drug	2	0.6666667	9	9									
			D4	Scn1a+/- vehicle	Vehicle	2.2	0.3741657	5	5					D4: Scn1a+/- vehicle vs. Scn1a+/- SIH		t(190)=0.09551	> 0.9999	
				Scn1a+/- SIH	Drug	2.111111	0.5879447	9	9									
			N4	Scn1a+/- vehicle	Vehicle	2.4	0.5099019	5	5		Treatment	F (1, 190) = 5.337	0.022	N4: Scn1a+/- vehicle vs. Scn1a+/- SIH		t(190)=0.8485	0.9937	
				Scn1a+/- SIH	Drug	1.636364	0.5094155	11	11									
			D5	Scn1a+/- vehicle	Vehicle	2	0.7071068	5	5					D5: Scn1a+/- vehicle vs. Scn1a+/- SIH		t(190)=0.9848	0.9806	
				Scn1a+/- SIH	Drug	1.1	0.4582576	10	10									
			N5	Scn1a+/- vehicle	Vehicle	2.25	0.9464847	4	4					N5: Scn1a+/- vehicle vs. Scn1a+/-SIH		t(190)=0.9848	0.9669	
				Scn1a+/- SIH	Drug	1.2	0.3265986	10	10									

RÉSUMÉ

Les mutations du gène *SCN1A*, codant pour le canal sodique de type 1 potentiel-dépendant (Nav1.1), sont impliquées dans plusieurs formes d'épilepsie du nourrisson, comme le Syndrome de Dravet (SD), une épilepsie rare et pharmaco-résistante ou l'Epilepsie généralisée avec crises fébriles plus (GEFS+), une épilepsie plus légère. GEFS+ et SD sont associés à des crises épileptiques fébriles dès l'âge de 6 mois. Le SD constitue la forme la plus grave où l'on voit apparaitre des retards mentaux mais également des déficits moteurs, visuels, langagiers et mnésiques au cours de l'évolution de la maladie. L'impact des crises épileptiques au cours de la petite enfance sur ces déficits cognitifs n'est pas connu. Jusqu'à présent, le SD était considéré comme étant une encéphalopathie épileptique où les crises étaient les principales responsables du phénotype à l'âge adulte. Cependant, récemment, un rôle potentiel de la mutation dans les troubles cognitifs a été mis en évidence changeant a priori la définition de SD d'encéphalopathie épileptique à une canalopathie (Bender et al., 2013, 2016; Han et al., 2012a). Notre projet adresse la question suivante: Quel est le rôle des crises épileptiques répétées présentées par les enfants SD sur les fonctions cognitives à l'âge adulte? Pour cela nous avons utilisé un modèle murin de la maladie portant une mutation faux-sens du gène *Scn1a* (R1648H), et qui présente une pathologie très légère. Nous avons induit des crises épileptiques par hyperthermie à l'âge de 21 jours pendant 10 jours et testé les effets à long-terme sur ces animaux à l'âge adulte. Nos résultats révèlent que l'induction de crises épileptiques par hyperthermie induit une hyperactivité, des altérations dans les interactions sociales et des déficits en mémoire hippocampo-dépendante et cortex préfronto-dépendante. Ces modifications comportementales sont associées à des modifications de l'électrocorticogramme avec apparition de crises spontanées et à d'importantes modifications de l'excitabilité neuronale intrinsèque dans l'hippocampe. Même si le rôle possible du canal $Na_V1.1$ dans le dysfonctionnement neuronal et l'effet des crises répétées ne sont probablement pas mutuellement distinctes, l'induction de crises répétées à un jeune âge semble donc suffisante pour convertir un modèle léger portant la mutation du gène *Scn1a* en un modèle sévère. Ainsi nous avons mis en évidence que les crises épileptiques répétées pendant le développement ont un fort impact sur la fonction cérébrale et qu'il est donc capital de les prévenir afin de diminuer, voir de prévenir, ces déficits.